Universitat Autònoma de Barcelona

ApoE4 pathology in Alzheimer's disease from the perspective of organelle dysfunction in astrocytes

Raquel Larramona Arcas

Institut de Neurociències
Departament de Bioquímica i Biologia Molecular
Unitat de Bioquímica, Facultat de Medicina
Univesitat Autònoma de Barcelona

ApoE4 pathology in Alzheimer's disease from the perspective of organelle dysfunction in astrocytes

Raquel Larramona Arcas

PhD in Neurosciences
September 2018

Institut de Neurociències
Departament de Bioquímica i Biología Molecular
Unitat de Bioquímica, Facultat de Medicina
Univesitat Autònoma de Barcelona

ApoE4 pathology in Alzheimer's disease from the perspective of organelle dysfunction in astrocytes

Memoria de tesis doctoral presentada por Raquel Larramona Arcas para optar al título de doctora en neurociencias por el Institut de Neurociències de la Universitat Autònoma de Barcelona.
Trabajo realizado en el Departament de Bioquímica i Biologia Molecular y en el Institut de Neurociències de la Universitat Autònoma de Barcelona bajo la dirección de la Dra. Roser Masgrau Juanola y la Dra. Elena Galea Rodríguez de Velasco.

En Bellaterra, a 12 de Septiembre de 2018

Doctoranda — Directoras

Raquel Larramona Arcas — Dra. Roser Masgrau — Dra. Elena Galea

A mis padres,
A María,
A Guillermina y
A Vidallé.

Index

Abstract

Alzheimer's disease is the most common form of dementia in advanced ages affecting more than 40 million people around the world. It is a complex disease that affects not only neurons but also astrocytes. Apolipoprotein E4 (ApoE4) has been described as the most important genetic risk factor for the sporadic form of the disease and interestingly, astrocytes are its main secretors. The research about its pathogenic mechanisms has mainly focused on its extracellular role. On the contrary, we analysed the dysregulations that endogenous intracellular ApoE4 causes on astrocytes. We focused on 2 principal physiological processes altered in Alzheimer's disease: calcium signalling and mitochondrial functions. As cellular model, we used immortalized astrocytes that express human ApoE3 (non-associated with any pathology) or ApoE4. Using fluorescent calcium indicators and the technique of Calcium Imaging, we determined that ApoE4 astrocytes have altered calcium homeostasis as they have lower basal intracellular calcium levels but higher purinergic-induced calcium signals compared to ApoE3 astrocytes. A high V-ATPase activity, and hence, higher lysosomal calcium uptake in ApoE4 astrocytes explains these alterations. Moreover, lysosomal calcium release after purinergic receptor activation is followed by higher endoplasmic reticulum (ER) calcium mobilization in ApoE4 than in ApoE3 astrocytes. Extracellular calcium entry is similar in both cell types. Our studies also demonstrated that the lack of lipoproteins in the extracellular medium upregulates the magnitude of purinergic-elicited calcium responses in ApoE3 astrocytes, as extracellular calcium entry amplifies lysosomal calcium release. This feature is missing in ApoE4 astrocytes being the magnitude of calcium responses unaffected by extracellular lipoproteins. On the other hand, we described alterations in mitochondrial dynamics determined by real-time microscopy and fluorescent mitochondria labelling. In particular, ApoE4 cell mitochondria do not perform fission after inhibition of mitochondrial oxidative phosphorylation whereas ApoE3 astrocyte mitochondria perform it. In addition, ApoE4 astrocytes have increased mitochondrial motility, reduction of Parkin, a protein involved in mitophagy, and reduction in mitochondrial DNA content compared to ApoE3 astrocytes. In summary, we demonstrated, for the first time, that endogenous ApoE4 alters calcium signalling and mitochondrial functions in astrocytes. Taking into account that ApoE is expressed throughout the life of individuals, these astrocytic alterations might appear in the early stages of the Alzheimer's disease. In order to advance in the detection of such early phases of the pathology, and since cerebrospinal fluid proteins reflect the cellular function of brain cells, we next identified a group of astrocytic proteins present in the cerebrospinal

fluid related to Alzheimer's disease that we propose as a functional astrocytic signature for early stages of the disease. This signature is composed of S100B, ApoE, prostaglandin D2 synthetase, cystatin 3, integral membrane protein 2C and clusterin. Overall, endogenous ApoE4 alters astrocyte functions, a phenomenon that can contribute to Alzheimer's disease, but also, to its detection through cerebrospinal fluid biomarkers.

List of Abbreviations

qPCR	Quantitative real-time PCR
3xTg-AD	Triple transgenic mice of AD
Aβ	Amyloid β
Ach	Acetylcholine
AD	Alzheimer's disease
ADNI	Alzheimer's disease neuroimaging initiative
AM	Acetoxymethyl
ApoE	Apolipoprotein E
ApoE2	ApoE e2
ApoE3	ApoE e3
ApoE4	ApoE e4
ApoeR2	Apolipoprotein E receptor 2
APP	Amyloid precursor protein
ARN	Ribonucleic acid
ATP	Adenosine triphosphate
AUC	Area under the curve
AV	Autophagic vesicles
BMP4	Bone morphogenetic protein 4,
BOLD	Brain activity by blood oxygen level dependent
CaGeDB	Calcium Gene Database
CEPIA	Calcium-measuring organelle-entrapped protein indicator
CLU	Clusterin
CMA	Chaperone-mediated autophagy
CMRG	Cerebral metabolic rate for glucose
CNS	Central nervous system
CNTF	Ciliary neurotrophic factor
CSF	Cerebrospinal fluid
CST3	Cystatin C
D^2	Squared displacement
DDAH1	Dymethylarginine dimethylaminohydrolase 1
DNA	Deoxyribonucleic acid
DRP1	Dynamin-related protein 1

EFEMP1	EFG containing fibulin extracellular matrix protein 1
EGTA	Ethylene glycol-bis (2-aminoethylether)-N,N,N',N-tetraacetic acid
ER	Endoplasmic reticulum
FBLN1	Fibulin 1
FBS	Fetal bovine serum
FDG-PET	Fluorodeoxyglucose- positron emission tomography
fMRI	Functional magnetic resonance imaging
GECI	Genetically encoded calcium indicator
GFAP	Glial fibrillary acid protein
GPN	Gly-Phe ß-naphthylamide
HDL	High-density lipoproteins
HFIP	hexafluoroisopropanol
hLGDB	Human Lysosome Gene Database
HPR	Horseradish peroxidase
IP3	Inositol 1,4,5 triphosphate
IP3R	IP3 receptor
iPSC	Induced pluripotent stem cells
ITM2C	Integral membrane protein 2C
KIF5	Kinesin superfamily
Kir	Inward rectifier K^+ channel
LCAT	Lecithin cholesterol acyltransferase
LD	Lipid droplets
LDHB	Lactate dehydrogenase B
LDLR	Low-density lipoprotein receptor
LPC	Lysophosphatidylcholine
LPE	Lysophosphatidylethanolamine
LPL	Lysophospholipids
LRP1	LDLR-related protein 1
LTBP1	Latent transforming growth factor beta binding protein 1
LTP	Long-term potentiation
MAMs	Mitochondria associated ER-membranes
MCI	Mild cognitive impairment
MCTs	Monocarboxylate transporters

Mfn1	Mitofusin 1
Mfn2	Mitofusin 2
mtDNA	Mitochondrial DNA
NA	Noradrenaline
NAADP	Nicotinic acid adenine dinucleotide phosphate
NADP	Nicotinamide adenine dinucleotide phosphate
NCAN	Neurocan
NCX	Sodium-calcium exchanger
NFTs	Neurofibrillary tangles
NRCAM	Neural cell adhesion molecule 1
NRXN1	Neurexin1
oAβ	Oligomeric amyloid β
PAGE	Polyacrylamide gels electrophoresis
PAP	Peripheral astroglial processes
PC	Phosphatidylcholine
PCR	Polymerase chain reaction
PE	Phosphatidylethanolamine
PET	Positron emission tomography
PIB	Pittsburgh compound B
PL	Phospholipid
PLS-DA	Partial least square discriminant analysis
PMCA	Plasma membrane calcium ATPase
PPAR	Peroxisome proliferator-activated receptor
PRDX1	Peroxiredoxin 1
PS	Phosphatidylserine
PS1	Presenilin 1
PS2	Presenilin 2
PTGDS	Prostaglandin D2 synthase
ROI	Region of interest
ROS	Reactive oxygen species
RT	Room temperature
RXR	Retinoic X receptor
RyR	Ryanodine receptor
SDS	Sodium dodecyl sulphate

SEM	Standard error of the mean
SERCA	Sarco/endoplasmic reticulum calcium ATPase
SOCE	Store-operated calcium entry
SPARCL1	Sparc like 1
TauP	Hyperphosphorylated Tau
TBI	Traumatic brain injury
TPC	Two pore channels
TBS-T	Tris-buffer tween
V-ATPase	Vacuolar -ATPase
VLDL	Very low density lipoproteins
VLDLR	Very-low-density lipoprotein receptor

Introduction

1. Apolipoprotein E: Alzheimer's disease risk factor

1.1. Isoforms and protein structure

Apolipoprotein E (ApoE) is a 299 amino acid protein that in humans exists in 3 isoforms, ApoE ε2, ApoE ε3 and ApoE ε4 that differ in 1 single nucleotide. This polymorphism involves a modification in the amino acid sequence and the structure of the mature protein, that confers a different disease susceptibility to the carriers (Yamazaki et al. 2016) (figure I1A). Among them, the isoform ApoE ε3 (ApoE3) is the most common allele, as its frequency in the population ranges from 67 to 87%. Besides, it is not associated with any disease. The ApoE ε4 (ApoE4) isoform is associated with Alzheimer's disease (AD) and its allele frequency is from 10 to 20% in overall population, and reaches a 65% in AD population. The AD is a devastating neurodegenerative disease that is defined as the principal cause of dementia (Yamazaki et al. 2016). Finally, ApoE ε2 (ApoE2), with an allele frequency of around 7%, has a protective role against the AD (C. C. Liu et al. 2013). However, this isoform is also associated to a peripheral disease, type III hyperlipoproteinemia, since its sequence peculiarity compromises its binding to the ApoE receptors (Mahley 2016; Mahley, Huang, and Rall Jr. 1999). Focusing on the differences between ApoE3 and ApoE4, the nucleotide that changes

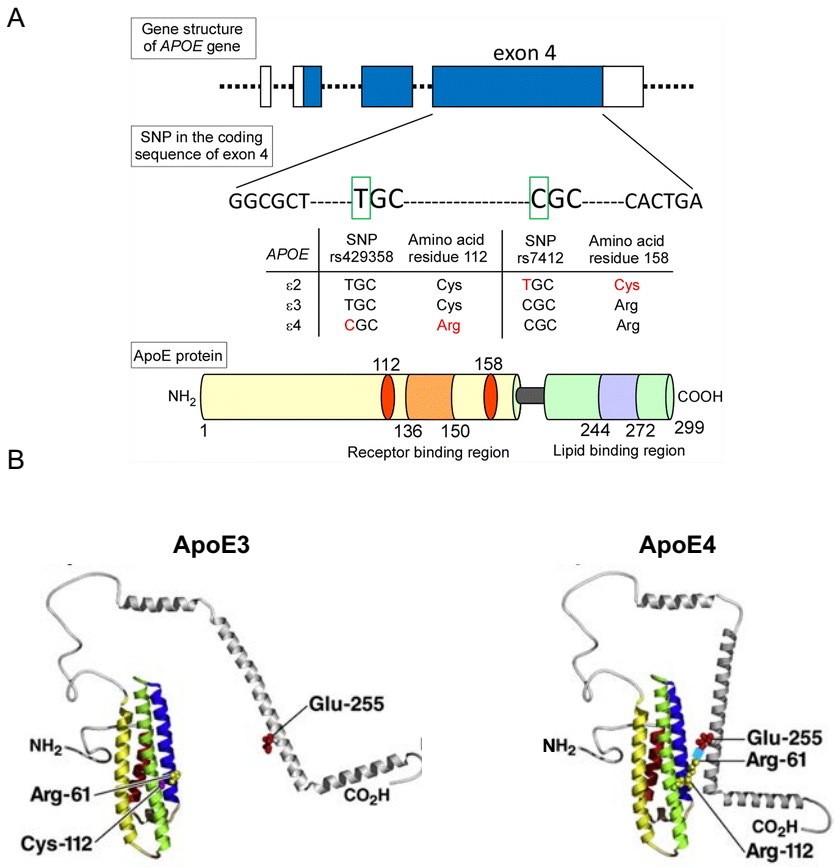

Figure I1: ApoE isoforms and structural differences. A) ApoE gene structure, polymorphism of ApoE isoforms and the different changes of the nucleotides and the amino acids of each isoform. Below, the protein domains of ApoE. Modified from Yamazaki et al. 2016. B) Different structure conformation of ApoE3 and ApoE4. Modified from Mahley and Huang 2012.

between them is found in exon 4, in which, thymine is substituted by a cytosine, thus, modifying the amino acid sequence from cysteine to arginine in the position 112 (Yamazaki et al. 2016) (Figure I1A). ApoE structure is divided into 2 structural domains, the lipid binding and the receptor binding that are connected by 20 or 30 amino acids. The lipid-binding domain, as its name indicates, bind to lipids and is the region affected by the amino acid substitution in the ApoE4 isoform. In ApoE3 isoform, cysteine 112 is close to glutamic acid 109 allowing the arginine 61 being close to both. However, the arginine 112 of ApoE4 forms a salt bridge with glutamic acid 109, causing a reorientation of arginine 61, that then, interacts through a salt bridge with glutamic acid 255 from the lipid binding region (Y. Huang and Mahley 2014) (figure I1B). Consequently, the conformation of ApoE4 is altered showing a glomerular form (Morrow et al. 2002). Since the principal difference between both isoforms is in the lipid-binding domain, the lipid union in the peripheral system is different, ApoE3 binds preferentially to phospholipid-rich high-density lipoproteins (HDL) while ApoE4 to triglycerides-rich very low-density lipoproteins (VLDL) (N. Zhong and Weisgraber 2009; Y. Huang and Mahley 2014).

1.2. Principal functions

ApoEs are regulators of lipid homeostasis since they form lipoproteins that transport cholesterol and other lipids around the body. These lipoproteins are not able to cross the blood-brain barrier, so they are not exchanged between the central nervous system (CNS) and peripheral blood system (Linton et al. 1991). Therefore, in the CNS they are produced and secreted by astrocytes. Lipoproteins are formed extracellularly as HDL-like particles whose principal function is to supply with lipids such as phospholipids and cholesterol to neurons and other cell types (C. C. Liu et al. 2013).

HDL-like particles are protein- and lipid-structures that travel extracellularly providing lipids to cells. In the CNS, the formation of these particles is mediated by ABCA1 and ABCG1 receptors, although the most studied is the first one. ABCA1 is a transmembrane receptor, which is transcriptionally controlled by the retinoic X receptor (RXR) family (that includes Liver X receptor) and the peroxisome proliferator-activated receptor (PPAR)(Koldamova, Fitz, and Lefterov 2014). Therefore, the ABCA1-mediated cholesterol efflux that forms the lipoproteins is potentiated by factors that are agonists of the RXR such as oxysterol in astrocytes. On the contrary, in neurons or microglia, the secretion of lipoproteins is restricted

to the injury or neurodegenerative processes (Uchihara et al. 1995; Xu et al. 2006; Mahley and Huang 2012; Yadong Huang and Mucke 2012).

The ABCA1 receptor requires ATP for binding lipids and cholesterol to ApoE particles (Hirsch-Reinshagen et al. 2004; Wahrle et al. 2004). In detail, cholesterol and lipids efflux from astrocytes to the ABCA1 receptor and subsequently, to ApoE, forming discoidal lipoproteins with unesterified cholesterol and phospholipids. Once these particles arrive at the cerebrospinal fluid (CSF), they have a spherical conformation and a cholesterol ester core. The changes of the conformation demonstrate that the lipoproteins suffer a maturation process due to secreted enzymes, such as lecithin cholesterol acyltransferase (LCAT) (Koch et al. 2001; C. Yu, Youmans, and LaDu 2010).

The ability of ApoE for binding lipids differs between the isoforms, being less effective the ApoE4 isoform (Mahley and Huang 2012). Despite the fact that ABCA1 could not be directly related as a risk factor to the AD (Yamazaki et al. 2016), some drugs have been used to increase its synthesis (Bexarotene) or its stability in the membrane (CS-6253) as a therapy due to its close relation to ApoE4 (Boehm-Cagan and Michaelson 2014; Koldamova, Fitz, and Lefterov 2014). Interestingly, both drugs showed cognitive improvement in animal models, although the translation to clinical trials did not have the expected success (Ghosal et al. 2016).

The endocytosis of the lipoproteins is mediated by the LDL receptor family, which is composed of the low-density lipoprotein receptor (LDLR), LDLR-related protein 1 (LRP1), very-low-density lipoprotein receptor (VLDLR), megalin (LRP2), apolipoprotein E receptor 2 (ApoeR2 or LRP8), LRP4, and LRP1b. In the CNS, ApoE in the lipoproteins binds to LDLR, LRP1, ApoER2 and VLDLR receptors (Holtzman, Herz, and Bu 2012; Lane-Donovan and Herz 2017) whose expression have been identified in neurons, astrocytes, microglia and oligodendrocytes (Fan et al. 2001). After binding to the receptor, the lipoprotein is endocytosed forming the endosome whose material is degraded through the fusion with a lysosome. Then the receptor can be recycled and turned back to the membrane, a process that is slower when ApoE4 is present (Heeren et al. 2004).

ApoE is also involved in synaptic pruning or long-term potentiation (LTP) (Chung et al. 2016; Lane-Donovan et al. 2016), which are essential processes for memory consolidation.

Memory processes are based on the formation of synapsis, and as Lane-Donovan et al. addressed, the lack of ApoE in the mouse brain causes synaptic deficits (Lane-Donovan et al. 2016). In this regard, ApoE is likely involved in these processes through its function as a lipid provider to neurons. Moreover, other authors described that the phagocytic activity of synaptosomes performed by astrocytes depends on ApoE isoform *in vitro* (Chung et al. 2016), underlining that ApoE could be involved in the synaptic control in different manners.

Remarkably, most of the ApoE4 research has been focused on the extracellular role of this protein but there is intracellular ApoE and so, it could participate in intracellular process. Moreover, not all the ApoE functions might be related to lipid transport. As an example, the study of Theendakara et al., in which they expressed ApoE endogenously and ascribed a new intracellular function to ApoE as a transcriptional factor. They found that ApoE can translocate to the nucleus and bind to double strand DNA of the gene promoter changing its expression (Theendakara et al. 2016).

In summary, ApoE participates in important processes of the CNS but not all its functions have been elucidated. In this context, this thesis provides important insights, as describes ApoE-regulated processes in astrocytes and its alterations by ApoE4 isoform.

1.3. ApoE4 is the principal genetic risk factor for sporadic AD

ApoE4 is the most important genetic risk factor for the late-onset AD (Strittmatter et al. 1993; Saunders et al. 1993; Corder et al. 1993). Clinical-, population- and community-based studies have associated this apolipoprotein to the disease since the 1990s (n.d 2010). Inheritance studies demonstrated that having 1 allele of the ApoE3 increases the risk of developing the disease four-fold whereas carrying 2 copies increases twelve-fold it (Raber, Huang, and Ashford 2004). Indeed, the onset of the disease in ApoE4 carriers is earlier than in ApoE2 or ApoE3 carriers (Spinney 2014), being more affected women at a specific range of age (Nyarko et

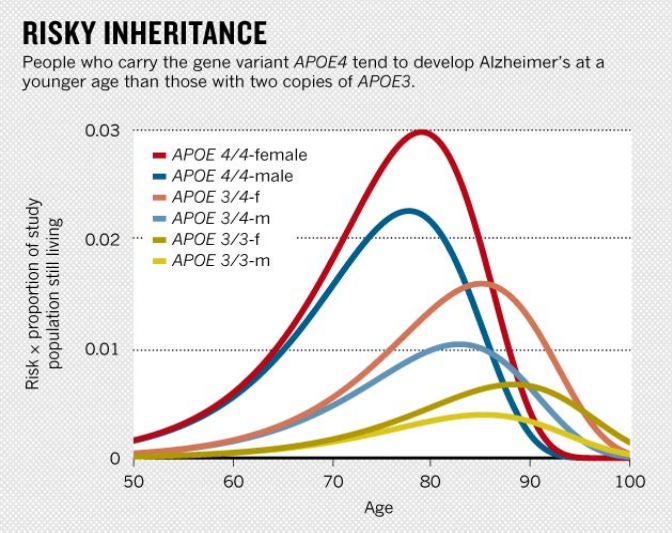

Figure I2: Risk to develop AD depending on ApoE isoform. From Spinney 2014.

al. 2018; Neu et al. 2017) (Figure I2). For instance, the measurement of brain activity by blood oxygen level dependent (BOLD) functional magnetic resonance imaging (fMRI) showed the alteration in the hippocampal function of ApoE4 carriers decades before any other remarkable dysfunction developed (Filippini et al. 2009). Furthermore, ApoE4 carriers with mild cognitive impairment (MCI), stage characterized by slight but measurable decline of cognitive abilities, show worse memory and development of functional activity tasks when compared to ApoE4 non-carriers with MCI (Farlow et al. 2004).

AD is the most prevalent form of dementia in older ages. The number of people suffering from dementia in 2016 was 46.8 million around the world and, more importantly, it is expected that this number will increase until 131.5 million people by 2050 (Prince et al. 2016). AD is a devastating disease that involves alterations of the brain parenchyma such as atrophy, ventricular enlargement, widened sulci and gyri shrinkage, among others (n.d. 2017) (figure I3). This disease exists in 2 different forms: the familiar and the sporadic type. The familiar form is characterized by mutations in the genes APP (amyloid precursor protein), PS1(presenilin 1) and PS2 (presenilin 2) and is developed at early ages whereas, the sporadic form appears in older ages and has no direct genetic mutation associated. (n.d. 2017).

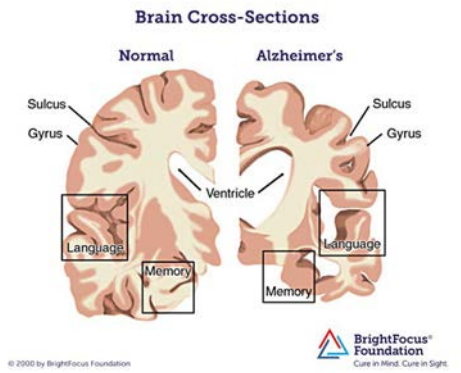

Figure I3: Alzheimer's disease phenotype and genetic risk factors. Comparison of a normal brain with an AD brain. The principal affected areas are framed. From the BrightFocus Foundation website.

The sporadic form has a long progression characterized by different stages: preclinical, prodromal or MCI and mild, moderate and severe dementia. The preclinical phase is the no symptomatic stage although some alterations start to appear in the brain parenchyma whereas in the prodromal stage, people suffer mild changes in memory and thinking (Staff 2018). Both phases are being studied in order to be able to diagnose AD in its early stages.

The principal hallmarks that distinguish AD from other dementias are the accumulation of extracellular amyloid β (Aβ) plaques and intracellular hyperphosphorylated Tau (TauP) accumulations. (Figure I4) However, there are other alterations that are potentially related to Aβ or TauP, such as neuronal death, synaptic loss, neurotransmitter decrease, astrogliosis, excitotoxicity, mitochondrial dysfunction, vascular damage, lipid metabolism alteration (n.d. 2017). Nowadays, the most popular explanation as the cause of sporadic AD is the amyloid cascade hypothesis, in which, the alterations evoked by amyloid β production and accumulation appear as the initial events of the disease. In brief, Aβ is the product of the APP cleavage by the β-secretase and γ-secretase, resulting in a fragment of 38 to 43 residues that oligomerizes and accumulates. In addition, these oligomers are considered the most toxic conformation of Aβ (Yadong Huang and Mucke 2012).

Nevertheless, the success of therapeutics drugs whose target is this peptide failed in the majority of cases. One of them is Solanezumab, an antibody targeting Aβ that did not reach the clinical benefit in patients that they expected (Abbott and Dolgin 2016). Thus, a depth investigation is needed to find the targets that cause or contribute to the disease.

1.4. Dysregulations caused by ApoE4 that contribute to AD pathology

1.4.1. Amyloid protein

Human data from different sources support the idea of an interrelationship between ApoE and Aβ (Morris et al. 2010; E. M. Reiman et al. 2009; Y. Y. Lim et al. 2018; Mecca et al. 2018). PIB (Pittsburgh compound B) measurements obtained by positron emission tomography (PET) to scan amyloid β deposition showed that ApoE4 carriers presented an increase in the deposition (Mecca et al. 2018; Morris et al. 2010). Moreover, ApoE4 carriers also manifest higher levels of fibrillar Aβ (E. M. Reiman et al. 2009). However, to date, there is not a unique and definite explanation of their relationship, in other words, it is not known if there is a cause-consequence connection between them or, alternatively, it is by chance. Even more, there

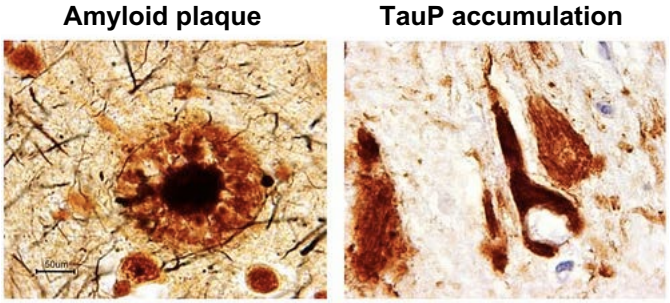

Figure I4: Alzheimer's disease principal hallmarks. Post-mortem identification of amyloid plaque and neurofibrillary tangle accumulation from hyperphosphorylated tau. From BigThink website.

are opposite results depending on the cellular model or technique used, that will be explained as follows.

The research about this question has been focused on the contribution of ApoE to diverse Aβ aspects such as amyloid plaque and fibrillar formation, clearance and metabolism, among others. Firstly, ApoE is involved in the formation of Aβ species demonstrated by the fact that human ApoE4 carriers have an increased number of Aβ oligomers (Hashimoto et al. 2012; Hudry et al. 2013). In addition, it has been established by *in vitro* infrared spectroscopy measurements, that the stability of the oligomers is higher in the presence of ApoE4 (Cerf et al. 2011).

Secondly, ApoE is an enhancing factor for the plaque deposition as it has been probed that the presence of mouse ApoE increases the amyloid β deposition and fibrillation in mice (K R Bales et al. 1999). Furthermore, the plaque formation acquires different characteristics depending on the ApoE isoform, being the plaques more compact when the human ApoE4 is present (Youmans et al. 2012). However, there is controversy over the amount of ApoE required and if it is directly or indirectly related to the plaque deposition. In one hand, authors using a transgenic mouse model with the human mutated APP which ApoE has been knocked out, found that the lack of murine ApoE expression diminished Aβ deposition (Kelly R Bales et al. 1997). Furthermore, using the same transgenic mouse model of the APP but in this case, expressing human ApoE3 or ApoE4 isoform, other authors discovered that increased levels of any human isoform of ApoE enhanced the deposition (Bien-Ly et al. 2012). On the other hand, the analysis of the distribution in different human brain areas confirmed the inverse correlation between ApoE and Aβ deposition suggesting that ApoE negatively impacts the deposition (Shinohara et al. 2013). In line with this, another study showed that treatment with Bexarotene (to increase ABCA1 expression and ApoE expression) decreased the extension of plaques and promoted a behavioural improvement (Cramer et al. 2012). However, other authors did not validate these results since they showed a no reduction of the plaque deposition (Fitz et al. 2013) and no behavioural improvement with the treatment (Fitz et al. 2013). Therefore, how the amount of ApoE affects plaque formations remains unclear.

Aβ deposition is also affected by the cell origin of ApoE, although the results obtained are contraries depending on the study. For instance, a comparison between the ApoE from

astrocytes and neurons showed that the latter promotes a e higher deposition (Van Dooren et al. 2006) but, a previous study did not find any alteration of deposition depending on the ApoE origin (Lesuisse et al. 2001).

Thirdly and finally, Aβ clearance is a crucial mechanism to eliminate it and ApoE has been proposed as a promoter of Aβ clearance (Yadong Huang and Mucke 2012). Specifically, ApoE has been related to the Aβ clearance in an isoform-dependent manner being the clearance of ApoE4 the less effective (Castellano et al. 2011). In addition, this clearance is negatively regulated by ApoE4 in astrocytes but not in microglia (S. D. Mulder et al. 2014).

One of the mechanisms proposed for the Aβ clearance, is that ApoE binds to Aβ to eliminate it through receptor binding and endocytosis. However, these results are unclear. Concretely, it was documented that the binding depends on the ApoE isoform, being this process more efficient with ApoE3 but faster with ApoE4 (LaDu et al. 1994). Nevertheless, Verghese et al. demonstrated that the interaction of ApoE with Aβ in solution or CSF is minimal (Verghese et al. 2013). Moreover, they indicated that ApoE competes with Aβ for receptor binding highlighting a receptor competition that could be affecting the clearance by endocytosis. This process could be representative of the situation taking place in astrocytes.

Another mechanism for ApoE promoting clearance of Aβ is through proteases activation. Proteases, which degrade Aβ, are more effective when ApoE is forming a complex with them (Russo et al. 1998). In addition, the degradation of Aβ also depends on the lipidation status of ApoE (Q. Jiang et al. 2008) that varies depending on the cell type that produces ApoE (Uchihara et al. 1995; Xu et al. 2006; Mahley and Huang 2012; Yadong Huang and Mucke 2012).

Overall, there is a clear participation of ApoE in the Aβ formation and clearance process. Furthermore, ApoE also regulates hallmarks and processes of the pathology different from Aβ. Some of them are summarized in the following sections. In these sense, in the present thesis, we have analysed the intracellular consequences of ApoE4 expression in astrocytes, the main producers of ApoE and also affected in AD, with the aim to elucidate how ApoE4 contributes to this pathology.

1.4.2. Tau hyperphosphorylation

Neurofibrillary tangles (NFTs) are the other main hallmarks of the AD. NFTs are intracellular aggregates of post-translational modified Tau protein, TauP (Yadong Huang and Mucke 2012). Tau is a microtubule-associated protein that stabilizes microtubules, so, its aggregation causes cytosolic alterations. Interestingly, some pieces of evidence suggest that ApoE4 is related to the increase in Tau hyperphosphorylation (Inbar et al. 2010; Shi et al. 2017; Cao et al. 2017; Antes et al. 2013). As an example, the levels of TauP in ApoE4-transgenic mice are increased even at three-month aged-animals, also pointing out that Tau alteration due to ApoE4 genotype, is an early pathogenic event (Shi et al. 2017). The mechanism behind ApoE4 and TauP increase is still not clear. Recently, Cao et al. described that the synaptojanin, a phosphoinositide phosphatase, is more expressed in ApoE4 targeted replacement mice, in which the mouse ApoE is replaced by one of the human ApoE isoforms. The expression of this synaptojanin affects the kinase GSK3β that consequently increases the phosphorylation of Tau (Cao et al. 2017). Thus, these results highlight that phospholipid metabolism has a relevant role in ApoE4 dysregulations. Furthermore, another mechanism has been described linking ApoE and TauP: the toxicity of ApoE fragments. In particular, ApoE can be fragmented by neuronal proteolysis in human and mouse brains (Chang et al. 2005). Transfecting neuronal cells with these fragments increase the NFT inclusions, and, even more, both proteins colocalize together and interact physically (Y. Huang et al. 2001). Indeed, the ApoE4 isoform is more susceptible to being proteolyzed than ApoE3, being a possible explanation to the differences seen among the genotypes regarding TauP alterations (Harris et al. 2003).

1.4.3. Brain metabolism

As mentioned above (section 1.1.), brain functions of ApoE4 individuals are affected even years before the first symptoms of AD appear. One of such alteration described in the ApoE4 carriers and AD patients is the hypometabolism of the brain (Brandon et al. 2018). For example, Liu et al. used ADNI (Alzheimer's disease neuroimaging initiative) data of brain metabolism measurements using positron emission tomography (PET) to compare the fluorodeoxyglucose consumption and obtaining a cerebral metabolic rate for glucose (CMRG). In other words, they used measurements of glucose consumption from specific areas such as the hippocampus and they demonstrated a lower CMRG in ApoE4 carriers (Y. Liu et al. 2016). In addition, other authors found that CMRG in ApoE4 carriers is diminished

in the precuneus, posterior cingulate, parietotemporal and frontal cortex and this correlation seems to be ApoE dose-dependent (Eric M Reiman et al. 2005).

The mechanism that triggers the hypometabolism is not fully understood, but some authors described metabolic pathways that are altered in the posterior cingulate of ApoE4 young adults (Perkins et al. 2016). Moreover, the mitochondria are the principal organelle that control metabolism, so, it is not surprising that this organelle exhibits a diminution in its activity measured by a reduction of Complex IV of the mitochondrial electron transport chain in post-mortem young ApoE4 individuals (Valla et al. 2010). The question of how ApoE4 is affecting mitochondrial function could be partially answered by looking at the fragments of ApoE. These fragments not only increase the TauP but also interact with complexes of the electron chain and difficult their function (Nakamura et al. 2009; Chang et al. 2005). Interestingly, this alteration has been described in neurons but not in astrocytes (Chen et al. 2011). However, other authors defend that apart from the involvement of ApoE4 on the hypometabolism, the hypometabolism is also correlated with Aβ deposits (Carbonell et al. 2016).

Not only neurons consume glucose, so since hypometabolism is a general feature of ApoE4 carriers, how other cells are contributing to this process is still unknown. In this context, being astrocytes the main ApoE4 source, the present thesis provides evidence to answer this important question by looking at principal mitochondrial processes such as metabolism and dynamics.

1.4.4. Lipid alterations of the AD

Lipid alterations have also been described in AD (Svennerholm and Gottfries 1994). Specifically, the quantity of cholesterol or sphingomyelins is altered in AD brains, and even, it has been demonstrated that the quantity of cholesterol appears as a regulator of Aβ production (Q. Liu and Zhang 2014). Moreover, the importance of lipids dysregulations in AD is also supported by the fact that ApoE is involved in lipid trafficking and the isoform E4 is an AD risk factor. Consequently, research about ApoE4 has been focused on cholesterol and lipid homeostasis.

Lipid transport controls several essential functions, for instance, neuronal plasticity. As an example, the cholesterol that is contained in HDL-like particles secreted by astrocytes is a

key factor for the synapsis formation (Mauch et al. 2001). Therefore, it is not surprising that the human ApoE4 targeted replacement mouse has deficiencies in dendritic arborization and synaptic activity (R. C. Klein et al. 2010), since ApoE4 isoform is less effective transporting cholesterol and lipids (Hamanaka et al. 2000; Mahley and Huang 2012). Certainly, human ApoE4 knock-in mice showed lower cholesterol and other lipids quantity in the whole brain than ApoE3 knock-in rodents (Hamanaka et al. 2000).

Based on these results, a general lipid reduction seems a feature of ApoE4 mice, although other data do not argue with it. It has been demonstrated that ApoE4 causes an increase in the mitochondria-associated ER membranes (MAMs) activity, increasing the phospholipid production in the fibroblasts treated with conditioned medium from astrocytes (Tambini et al. 2015). Taking into account both facts, the reduction in the brain lipids such as cholesterol or phospholipids and the increase in the MAMs activity, a possible explanation is that ApoE performs different functions related to lipids depending on the cell type and maybe in the brain region.

Interestingly, ApoE4 isoform not only modulates the amount of lipids, but also the saturation of fatty acid that composes membrane lipids. Thus, in the case of ApoE3 neuroblastoma cell line, the monounsaturated fatty acids increase more prominently than in ApoE4 neuroblastoma cell line whereas the polyunsaturated fatty acids are diminished in ApoE3 cells and remain unchanged in ApoE4 cells (Prasinou et al. 2017).

1.4.5. Endolysosomal pathway alterations

Aβ presence has been reported in all the different vesicles that form the endolysosomal pathway such as endosomes, late endosomes, autophagic vesicles and lysosomes (Whyte et al. 2017). These studies were performed predominantly in neurons, such as the one from Gowrishankar et al., where they found this Aβ accumulation in the axonal lysosomes as a defect in axonal transport (Gowrishankar et al. 2015). This transport impairment has also been described by Tammineni et al. They reported that lysosomes cannot return to the soma of neurons, affecting lysosomal degradative capacity due to the lack of their removal (Tammineni et al. 2017).

Additionally, autophagy has been implicated in AD pathology, since it is one of the processes that is activated to degrade amyloid proteins and TauP (Y. Wang et al. 2009; W. H. Yu et al.

2004). Autophagy is the process to degrade cellular components by englobing them in a 2 membrane autophagosome that, subsequently, is fused to a lysosome to degrade the englobed material. Autophagic vesicles are accumulated in neuronal cells of the AD mouse model PS1/APP and it is believe that this is affecting Aβ clearance due to the increase in the endocytosis to eliminate protein aggregations and the defects in lysosomal function (Whyte et al. 2017; Sanchez-Varo et al. 2012). Astrocytes that express ApoE4 display autophagy dysregulations, as it was uncovered by Simonovitch et al. (Simonovitch et al. 2016). Nevertheless, the causes and the consequences of autophagy in AD are not fully understood neither how it affects different cell types of the brain. Moreover, there is not an agreement about which is the correct therapeutic approach against the autophagic alterations contributing to AD.

1.5. ApoE4 dysregulations not necessarily associated to AD

Apart from the ApoE4 contribution to the principal phenomena described in AD, ApoE4 seems to induce alterations that per se might translate into cellular dysfunctions. Such dysfunctions possibly would be contributing to the AD, but not necessarily since not all the ApoE4 carriers will develop this disease. Besides, other pathologies have been related to ApoE4, for instance, ischemic stroke, vascular dementia, multiple sclerosis, Huntington disease or cerebral amyloid angiopathy, where carrying ApoE4 allele enhances the risk to develop them (Van Giau et al. 2015).

Remarkably, most of the ApoE4 research has been focused on the extracellular role of this protein regarding Aβ and only a few articles have examined the alterations caused by intracellular ApoE4 and even less, when the expression of ApoE is endogenous and not added exogenously to the cells. As an example, the previously mentioned study of Theendakara et al. have shown that ApoE4 regulates different genes than ApoE3 (Theendakara et al. 2016). Another example is the study of Brodbeck et al., that illustrated how the intracellular trafficking of ApoE4 in neurons is affected by its glomerular structure of the protein causing endoplasmic reticulum (ER) stress (Brodbeck et al. 2011). This finding has also been described in astrocytes, indicating a general dysfunction associated with the ApoE4 structure (N. Zhong, Ramaswamy, and Weisgraber 2009). There is also the autophagic impairment addressed in astrocytes (Simonovitch et al. 2016) or the mitochondrial toxicity of ApoE4 fragments in neurons and neuroblastoma cells but not in astrocytes (Chang et al. 2005).

It is important to underline that the ApoE4 affects differently to the cell types and that the research has been focused on neurons, underestimating the potential contribution of other cell types. For example, the study of Nuriel et al. described endolysosomal alterations in brain extracts that they believe are related to neurons (Nuriel et al. 2017). However, this tendency is changing in the last years with increasing interest in the field.

It is this lack of knowledge described, that prompted us to undertake the necessary study of the effects of ApoE4 in astrocytes. More concretely, we focused our research on intracellular alterations caused by endogenous expression of ApoE4. Therefore, the present study aims to clarify the mechanisms induced by ApoE4 that contribute to the development of AD but it can provide insights into other pathologies too.

1.6. A main question: is it a problem of quantity or gain of toxic function?

Considering the diverse functions caused by ApoE4, it is still unclear which is the most suitable therapeutic approach: to modulate ApoE expression or to "convert" ApoE4 to ApoE3 or ApoE2 by using small molecules, mimetic peptides or gene edition. These discrepancies in therapeutics are due to the contradictory data obtained in the studies that are summarized below.

One therapeutic approach is to increase the ApoE content since it has been shown that the amount of ApoE4 in the CSF is diminished in AD patients (Talwar et al. 2016). Furthermore, the data on plasma, CSF and brain tissues of ApoE4 targeted replacement mice also report a reduction in the ApoE4 levels (Riddell et al. 2008). Based on this rationale, one of the most promising drugs is Bexarotene which increases the ApoE levels and also its lipidation status. As it has been described in section 1.2. the mouse data with this treatment was promising, but, unfortunately, the human results did not illustrate any improvement.

Contrary to that, other authors support that the appropriated therapy is to decrease ApoE levels using specific antibodies (F. Liao et al. 2014). They demonstrated that ApoE antibodies slow the amyloid plaque formation improving the spatial learning performance in the water maze of animals from APP/PS1 mutation AD mouse model. In addition, they created an antibody that binds specifically to the non-lipidated form of ApoE, which they affirmed is aggregated with the amyloid plaques showing a decrease in the amyloid accumulation(Fan Liao et al. 2018). Evidently, a consensus about ApoE quantity that are therapeutically optimal

has not been achieved. Further investigation is needed to answer more consistently this question.

Interestingly, another therapeutic approach exists: to modify the structure of ApoE4. This approach was based on the hypothesis that ApoE4 acquire dysfunctional properties due to its structure. For instance, Wang et al. used a small molecule corrector in human iPSCs-derived neurons (inducing pluripotent stem cells-derived neurons) that decreased the fragmentation of ApoE and the hyperphosphorylation of Tau, avoiding the toxicity of some ApoE fragments (C. Wang et al. 2018). Another example is the injection of viral constructs of the ApoE2 isoform, that decrease the Aβ levels (Hudry et al. 2013). Notably, the viral injections that only infect astrocytes improve the binding of ApoE to cholesterol and consequently the lipid transport (Hu et al. 2015).

Although promising, whether the strategy of structural correction or the modulation of its levels is more appropriated is still to be determined since the deleterious effect of ApoE4 could be a combination of both, a low amount of ApoE and a dysfunction or toxicity derived for its glomerular structure, that even could be affecting cell types differentially. Therefore, deeper studies of the ApoE4 contribution to cellular functions and the AD has to be carried out.

2. Astrocytes as a key player in AD

2.1. Physiological function of astrocytes

Astrocytes are glial cells whose important implication in both brain physiology and pathology is still not completely revealed. Astrocytes are considered non-excitable cells in terms of membrane excitability, as they cannot perform action potentials. Their membrane potential is very negative (-80mV) and is created due to the permeability of ions, especially of potassium. Interestingly, although they do not perform action potentials, they can communicate with each other and with other cell types due to calcium transients (Alexei Verkhratsky and Nedergaard 2018). Therefore, calcium signalling is the basis of their excitability and hence, the inductor of the release of transmitters that will act on membrane receptors of other astrocytes or other cell types in the process called gliotransmission. Alternatively, astrocytes can also communicate with each other through gap junctions that allow the flux of calcium and other ions, seconds messengers and bioactive molecules. Owing

to their union by gap junctions, all astrocytes form a reticular network called syncytia. (Alexei Verkhratsky and Nedergaard 2018). Another characteristic is that they are territorial; in other words, each astrocyte has a determined non-overlapping domain (figure I5A). Furthermore, their structure *in vivo* is highly complex due to the ramifications of the processes (figure I5B) (Medvedev et al. 2014; Alexei Verkhratsky and Nedergaard 2018).

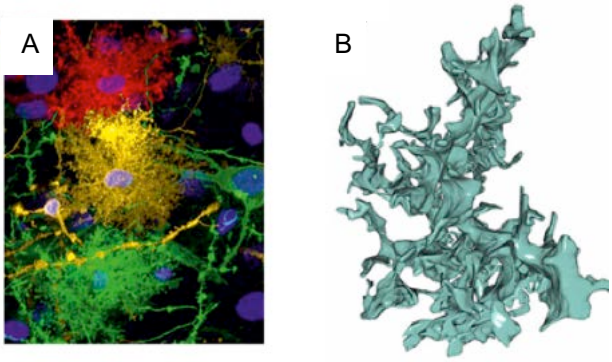

Figure I5: Astrocyte domain and structure. (A) Different astrocytes diolistically labelled. From Verkhratsky and Nedergaard 2018. (B) 3D reconstruction of a fragment of an *in vivo* mouse astrocyte. From Medvedev et al. 2014.

Astrocytes accomplish diverse functions, most of them carried out under the control of calcium signalling. Subsequently, the functions from adult astrocytes are briefly described (Alexei Verkhratsky and Parpura 2014).

- Brain ion homeostasis: astrocytes modulate the extracellular concentration of ions such as K^+, Cl^- and Ca^+ that have a restricted range to ensure the normal brain function. For example, astrocytes counteract the excess of potassium, by performing a potassium spatial buffering, which consists in the delivery of this ion in low-concentration regions of the astrocyte syncytia and even extruded to the bloodstream of extracellular areas also with lower concentration. This potassium buffering functions are mainly the cause of the very low membrane potential of astrocytes. This fact allows the inward-rectifier K^+ channel (Kir) uptake of potassium, in contrast to what is reported for other cells where Kir only acts forming outward currents (Kofuji and Newman 2004). Other example is the pH regulation that is carried out by the transport of protons through Na^+/H^+ exchanger and of bicarbonate through Na^+/ HCO_{3-} cotransporter

- Brain volume homeostasis: the transport of water is carried out by aquaporins. Aquaporin 4 is the astrocyte-specific water channel and is located at the endfeets near to Kir channels, underlining the coordination of water and potassium flux (Alexei Verkhratsky and Parpura 2014).

- Metabolic support to neurons: astrocytes uptake glucose and metabolize it mainly to lactate. Interestingly, it has been suggested that lactate is secreted by astrocytes and uptaked by neurons through monocarboxylate transporters (MCTs). Therefore, neurons can obtain ATP from lactate during increases in neuronal activity. This theory is known as the astrocyte-neuron lactate shuttle (Pellerin and Magistretti 2012). However, it is not universally accepted and some authors believe that increased metabolic in neurons after the neuronal activity is not related to the lactate secreted by astrocytes (Mason 2017).

- Brain lipid metabolism and transport: astrocytes control the production, metabolism and distribution of cholesterol and phospholipids through the secretion of HDL-like which are composed of ApoE, as it has been mentioned in previous sections (Pfrieger and Ungerer 2011).

- Antioxidant defence: the oxidative phosphorylation of neurons generates high amounts of reactive oxygen species (ROS). Therefore, neurons require antioxidant molecules to regulate that ROS production: the electron donor glutathione. To produce it, neurons need cysteine, glycine and glutamine, which are all provided by astrocytes. Neurons uptakes these molecules and generate glutathione to induce the detoxification of ROS (Bélanger, Allaman, and Magistretti 2011).

- Glutamate uptake: astrocytes control the concentration of glutamate in the synaptic cleft a function that is critical, as glutamate at high concentrations is cytotoxic and there is no extracellular enzymes for its degradation. The glutamate uptake is part of the cycle of glutamate/glutamine, where astrocytes uptake the glutamate that is metabolized to glutamine and released again to extracellular space. Then, neurons uptake the glutamine and synthetize glutamate. Moreover, glutamate in astrocytes can also be used as a substrate for the tricarboxylic cycle to obtain ATP (Alexei Verkhratsky and Nedergaard 2018).

- Synaptic process: astrocytes participate in the synapses in different manners. Interestingly, astrocytes are present in several synapses as a very thin peripheral astroglial processes (PAP) that cover them. This coverage differs depending on the brain region. For instance, 29-57% of excitatory synapses are enwrapped by PAP in

the neocortex, while in the somatosensory cortex the proportion is approximately 90% (Bernardinelli, Muller, and Nikonenko 2014). However, PAP are not only a structural part of the synapsis, they also promote the synapsis formation through the release of HDL-like particles that contain cholesterol and other lipids, as it mentioned before. Moreover, they are responsible of the maintenance and the removal of synapses (Alexei Verkhratsky and Nedergaard 2018). Interestingly, astrocytes play an active role in the release of gliotransmitters that acts directly on the rest of elements that form the synapses (Halassa and Haydon 2010). These gliotransmitters released could be glutamate, ATP, adenosine or GABA. Notably, astrocytes also arbour different neurotransmitters receptors, so, it is a bidirectional interaction with neurons. As a consequence, gliotransmission modulates LTP as it was addressed by Henneberger et al. in their study performed in the CA1 area of the hippocampus (Henneberger et al. 2010). Moreover, astrocyte-mediated ATP release also controls circadian rhythms that allow the awake and sleep cycles of the brain (Marpegan et al. 2011). Due to the involvement of astrocytes in synaptic transmission, a new term appeared, the tripartite synapse, which place astrocytes as main actors of the synaptic process. However, this concept is being revised since, for example, the timescale of the sensing and processing by astrocytes ranges from hundreds of milliseconds to minutes whereas this process in neurons takes place in the millisecond range (Savtchouk and Volterra 2018).

- Cerebral vascular regulation: brain vasculature is covered by astrocytic endfeets, forming the neurovascular unit, in where the release of vasoactive substances such as prostaglandin E_2 or epoxyeicosatrienoic acid from astrocytes regulates the contraction of blood vessels and subsequently, the brain flux of blood (Iadecola and Nedergaard 2007). The release of these substances is dependent on neuronal activity and carried out by astrocytes through their calcium oscillations (Bazargani and Attwell 2016).

In addition, astrocytes also have principal roles in CNS development and the neuronal guidance since the radial glia, a type of astrocytes, promotes the migration of the precursors. Interestingly, specialized astrocytes are also responsible for adult neurogenesis as they can migrate and differentiate to neurons in certain conditions (Kriegstein and Alvarez-Buylla 2009).

Having such a variety of functions, it is not surprising the wide heterogeneity of astrocytes. Accordingly, there are different types of astrocytes in mammals' brains that differ in their location, shape, structure, and probably, in their function. For example, depending on their location there exist fibrous (presents in the white matter), protoplasmic (from the grey matter), surface-associated (associated to cortical surfaces), velate (from a region of the brain densely packed) or perivascular astrocytes (near to blood vessels), among others. (Alexei Verkhratsky and Nedergaard 2018).

Indeed, the complexity of astrocytes increases in human brain as compared to other mammals. Human brain possesses unique astrocyte types, such as interlaminar astrocytes that are located in the upper cortical layer and with long processes; or varicose projection astrocytes that have a long projection without ramifications. Regarding human protoplasmic astrocytes, their domain volume is more prominent and they contain a higher amount of primary and peripheral processes than rat astrocytes (Oberheim et al. 2009). A fascinating finding that point out astrocytes not only as a homeostatic regulator but also as a principal player in high mental processes, was discovered in a mouse model whose astrocytes were replaced by human ones. The results demonstrated that this mouse has better synaptic plasticity, learning and faster calcium responses than control mice (Han et al. 2013).

2.2. Calcium signalling in astrocytes

As mentioned above, calcium signalling controls the principal functions of astrocytes. Specifically, the oscillations of this ion have been implicated directly in 2 processes, the gliotransmission (Araque et al. 2014) and the neurovascular coupling (Haydon 2006; Bazargani and Attwell 2016). Gliotransmission is the process by which astrocytes secrete transmitters (called gliotransmitters). It was first observed in cultured astrocytes and subsequently reported *in vivo* (Bezzi and Volterra 2001; Araque et al. 2014). Despite the huge amount of evidence for astrocyte to regulate synaptic transmission through gliotransmission some authors still question this process and defend that gliotransmission is caused by applying different techniques but does not occur in a physiological condition (Fiacco and McCarthy 2018).

Cultured models have shown that calcium wave is initiated by neurotransmitters such as glutamate (Cornell-Bell et al. 1990) or ATP (Anderson, Bergher, and Swanson 2003) and that this process can be depended on neuronal activity (Dani, Chernjavsky, and Smith 1992).

These results have also been supported by *in vivo* experiments where the astrocyte stimulation from noradrenergic projections of locus coeruleus (Ding et al. 2013) and cholinergic projections (Takata et al. 2011) evoked global calcium elevations. Transmitters activate receptors that in turn activate coordinated and precisely regulated intracellular pathways that involve several channels, pumps, receptors and calcium binding proteins from the plasmatic membrane, organelles and cytosol. All these components also control the basal calcium of astrocytes. Any change in the magnitude, shape (such as oscillation patter), spatial and temporal characteristics or the mechanism by which the calcium signalling takes places could change the consequences of this process (Alexei Verkhratsky and Nedergaard 2018).

Despite the variety of calcium signalling pathways, the central mechanism is the generation of second messengers, mainly inositol 1,4,5 triphosphate (IP3) (Islam 2012; Alexei

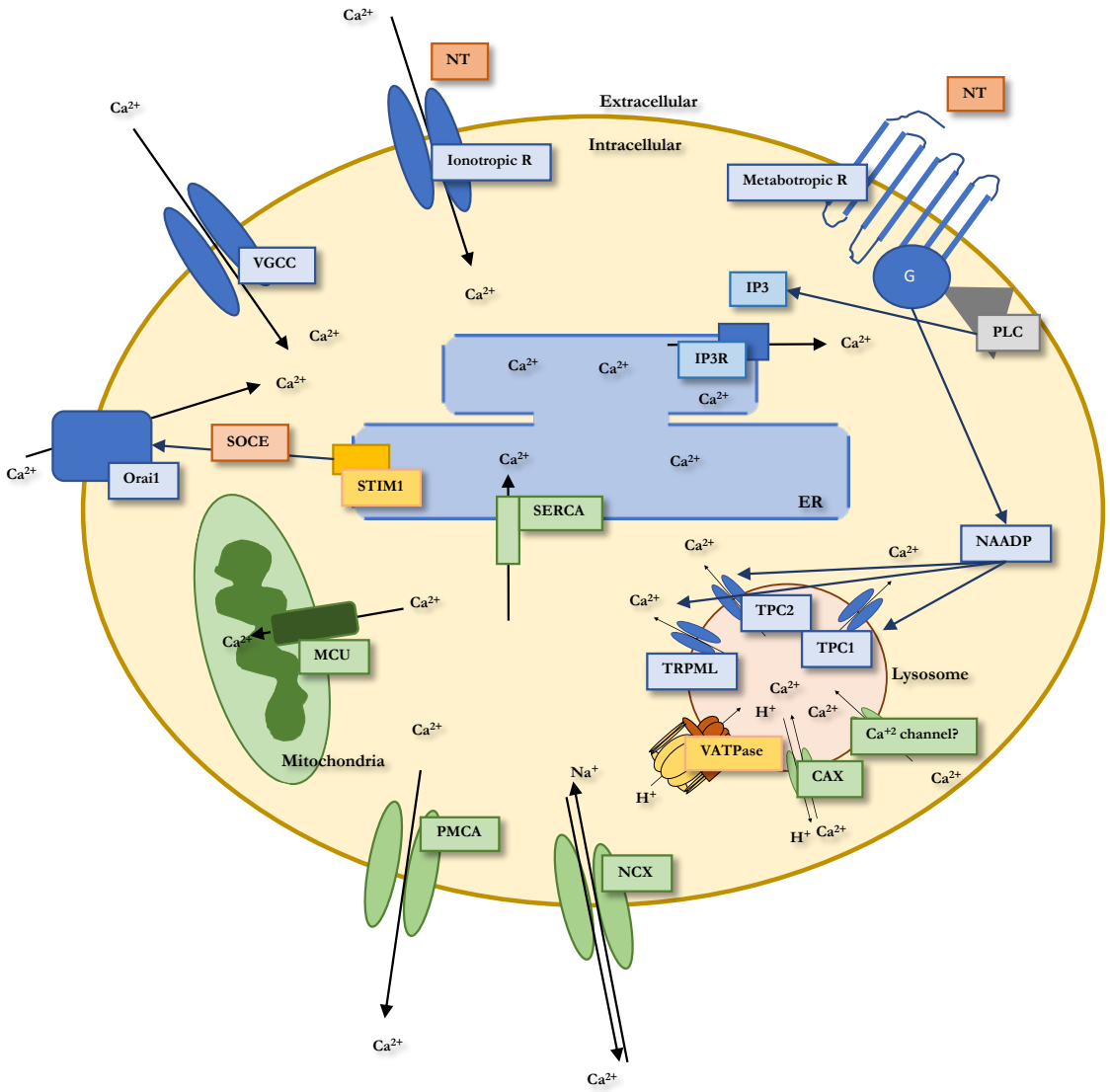

Figure I6: Principal calcium signalling pathways in astrocytes. In blue channels that increase cytosolic calcium and in green channels that decrease cytosolic calcium.

Verkhratsky and Nedergaard 2018). Phospholipase C activation promotes the hydrolysis of phosphatidylinositol 4,5-biphosphate into diacylglycerol and IP3. IP3 acts on the IP3 receptor (IP3R) in the (ER) that releases calcium into the cytosol (figure I6). Apart from IP3, this receptor is activated by calcium itself, amplifying the release of calcium and potentiating the generation of a global calcium increase necessary to calcium propagation and wave formation (Raffaello et al. 2016). There are 3 different IP3 receptors, being the subtype 2 the most predominant in astrocytes (Holtzclaw et al. 2002; Alexei Verkhratsky and Nedergaard 2018). IP3 also participates in the propagation of the calcium oscillations to nearby astrocytes rather than calcium per se (Allbritton, Meyer, and Stryer 1992). This is due to the transport of this molecule through the gap junctions (Charles 1998).

cADPR is a nucleotide that also acts on an ER receptor, the ryanodine receptor (RyR). This receptor shows similar activation as IP3R, being activated by its ligand but also by calcium per se. (Islam 2012). Nevertheless, some controversy exists around the contribution of this receptor to astrocytic calcium increase since hippocampal astrocytes do not display RyR activity (Beck et al. 2004). In cultured astrocytes, it has been described that RyR receptors are activated by bradykinin receptors but not by purinergic receptors (Barceló-Torns et al. 2011).

The other second messenger related to calcium signalling is nicotinic acid adenine dinucleotide phosphate (NAADP). It is a metabolite of pyridine nucleotide with a very similar structure to nicotinamide adenine dinucleotide phosphate (NADP). In many cell types, including astrocytes, it has been shown that mobilizes calcium from acidic organelles upon stimulation of particular receptors, such as purinergic (Barceló-Torns et al. 2011). Acid organelles are a heterogeneous population of vesicles, mainly related to lysosomes. For simplicity from now, we will refer to them as lysosomes. NAADP releases lysosomal calcium through NAADP receptors. The more accepted hypothesis is that its receptors are two-pore channels (TPC) from the endolysosomal compartment (Pereira et al. 2011) (figure I6). There are 2 types of this receptor: TPC1 and TPC2 that differ in their cellular localization, TPC2 is preferably located at lysosomes and TPC1 at endosomal compartment (Galione 2011) Remarkably, other studies has also proposed TRPML (Raffaello et al. 2016) or RyR (Gerasimenko 2006) as receptors for NAADP.

It has been proposed that NAADP plays a critical role in the initiation of calcium signalling since it evokes the initial calcium release that is amplified by the ER channels (Churchill and Galione 2001; Galione 2015). This mechanism has been discovered in sea urchin, a marine creature, in which, the initial calcium increase after stimulation is not abolished by thapsigargin (inhibitor of calcium entrance in the ER) whereas the calcium propagation disappears with that inhibitor (Churchill and Galione 2001). This is the proof that calcium released from lysosomes can be amplified converting calcium responses from local calcium to global. Furthermore, this mechanism has also been described in mammalian cells (Galione 2015).

Interestingly, the organelle source of calcium determinates the consequences of that calcium increase. For example, in the case of astrocytes, the lysosomal calcium release regulates cellular processes such as autophagy (Pereira et al. 2011). The mechanism behind this regulation has been indicated in other cell types. TFEB (transcription factor) is activated through this lysosomal calcium release and translocated to the nucleus to regulate autophagy-related genes (Medina et al. 2015).

Apart from intracellular calcium mobilization, calcium signals in astrocytes are also due to extracellular calcium entrance. An example is the activation of ionotropic receptors such as P2X or by the store-operated calcium entry (SOCE). SOCE is a mechanism triggered by the depletion of calcium in the ER. This depletion, in turn activates STIM proteins that bind and activate membrane channels such as Orai or TRPC leading to the calcium entrance (Islam 2012). In astrocytes, the expression of Orai channels it has been demonstrated in vitro (Moreno et al. 2012). Recently, it has been suggested that SOCE can also be triggered by lysosomal calcium release (Y. Jiang et al. 2018; Brailoiu and Brailoiu 2016) (figure I6).

Several organelles and the plasmatic membrane participate in returning intracellular calcium to the basal condition (Alexei Verkhratsky and Nedergaard 2018). In the plasmatic membrane there is the plasma membrane calcium ATPase (PMCA) and in the endoplasmic reticulum, the sarco/endoplasmic reticulum calcium ATPase (SERCA). Both are Ca^{2+}-ATPases. The first one releases calcium extracellularly and the second one introduces calcium in the ER (Islam 2012) (figure I6). Apart from these pumps, the plasmatic membrane possesses sodium-calcium exchanger (NCX), that exchange extracellular sodium for intracellular calcium. Mitochondria also uptake calcium, mainly though the MCU complex

that is it formed by different subunits and is inserted in the inner mitochondrial membrane. (Alexei Verkhratsky and Nedergaard 2018) (figure I6).

Lysosomal calcium uptake is suggested to be carried out by a secondary transport performed by the vacuolar (V)-ATPase and a calcium- proton exchanger (figure I6). The V-ATPase is a macro complex formed by 2 domains with different subunits: V0 that is inserted in lysosomal membrane and V1 that is faced to the cytosol. Both domains are coupled when this pump is active or uncouple when it is inactive (Forgac 2007). The ATPase promotes the entrance of protons to the lysosomal lumen using the ATP hydrolysis as fuel. In addition, a calcium-proton exchanger is needed in the lysosomal membrane to exchange the protons of lysosome for calcium. The molecular identity responsible of this transport has recently been described in vertebrate and named CAX (Melchionda et al. 2016). Moreover, some authors believe that there is another putative calcium channel that is performing the entrance of calcium to the lysosome independently of protons (Xiong and Zhu 2016) (figure I6).

Organelles communicate with each other and with the plasmatic membrane to elicit specific spatial-temporal patterns for each calcium response. The previously described SOCE is an illustration of that, but there are also interactions between the ER and the mitochondria and between the lysosomes and the ER. Regarding the ER and mitochondria, both organelles are connected by closed contact domain called MAMs, which allow the release from the ER directly to the mitochondria (Patergnani et al. 2011). With respect to the interaction between lysosomes and the ER, it has been demonstrated that both colocalize to evoke NAADP calcium release from lysosomes that act on the RyR in the area of contact (Kinnear et al. 2004; Aston et al. 2017).

In vivo, astrocytes have a complex morphology, being extremely branched cells. It has been described that processes and soma can use different calcium pathways since responses of both are heterogeneous (Bindocci et al. 2017). The principal source of calcium for the soma is the IP3R2 whereas for the processes, calcium is obtained extracellularly (Srinivasan et al. 2015; Rungta et al. 2016). Such specialized mechanism enables independent calcium signalling depending on the astrocyte area. Furthermore, soma Ca^{2+} transients are larger and longer whereas process transients localized in microdomains, are more frequent and faster (Volterra, Liaudet, and Savtchouk 2014).

Overall, calcium signalling controls astrocytic physiology and hence, it is complex and highly regulated. The disturbance of intracellular calcium signals can result in pathological conditions, as it will be explained in the context of the AD in section 2.5. In this context, this thesis contributes to the understanding of such alterations but with a new focuses, as place ApoE4 at the centre of the research.

2.3. Mitochondria of astrocytes

Astrocytic mitochondria have obtained minor attention since it was thought that astrocytic metabolism was not oxidative and hence, did not depend on this organelle. However, it has recently been described that many mitochondrial genes are significantly more expressed in astrocytes than in neurons (Lovatt et al. 2007). In addition, astrocytic mitochondria play an active role in fatty acid and amino acid metabolism in those cells (Eraso-Pichot et al. 2018) and, as mentioned in the previous section, they have an essential role in the buffering of calcium from the cytosol and in regulating the calcium signalling.

In addition, there are significant differences between neuronal and astrocytic mitochondria, for example, the latter tend to move slower than neuronal ones (Stephen et al. 2015). Recent work has reported that mitochondria are present in the fine astrocytic process *in vivo* where they contribute to local calcium buffering (Agarwal et al. 2017), glutamate metabolism (J. G. Jackson et al. 2014) and likely in ATP production (Joshua G. Jackson and Robinson 2018). To perform all these functions, astrocytic mitochondria might rely on their dynamics. Dynamics, which involve fusion and fission events and motility, control the mitochondrial morphology and location adapting the mitochondrial network to the metabolic needs and the cellular environment (Baker, Palmer, and Stojanovski 2014; van der Bliek, Shen, and Kawajiri 2013).

Mitochondrial fission ensures that the mitochondrial network attains the proper number of mitochondria. Furthermore, if there is a damaged mitochondrion, after a fission process, this mitochondrion will segregated to be degraded through mitophagy (a specific mitochondrial autophagy that will be described in the next section) (Baker, Palmer, and Stojanovski 2014; van der Bliek, Shen, and Kawajiri 2013). In astrocytes, it has been shown that this is a calcium-dependent process, with a reduction in mitochondrial length associated to calcium increase (Tan et al. 2011). The principal protein that mediates fission is the dynamin-related protein 1 (Drp1), a dynamin-related GTPase. This protein is affected by several post-

translational modifications that influence its fission activity, either activating or inhibiting it, such as phosphorylation, sumoylation or ubiquitination. When the protein is activated in the cytosol, it is recruited at the mitochondrial membrane through the action of Fis1, Mff, MiD49 or MiD51/MIEF1 and oligomerized (Loson et al. 2013). Then, Drp1 oligomers form a constrictive helix around the mitochondria which is progressively reduced until the total fission (Labrousse et al. 1999) (Figure I7A).

With respect to fusion, its main functions are to mediate the exchange of material between mitochondria such as the mitochondrial deoxyribonucleic acid (mtDNA) and to rescue partially damaged mitochondrion fusing to a healthy one (Baker, Palmer, and Stojanovski 2014; van der Bliek, Shen, and Kawajiri 2013). The main proteins that promote fusion are Opa1, Mitofusin 1 (Mfn1) and Mitofusin 2 (Mfn2), that are also dynamin-related GTPases. As mitochondria are formed by 2 membranes, 2 fusions take place at the same time. Opa1 promotes the fusion of the inner mitochondrial membrane while Mfn1 and Mfn2 are involved in the outer mitochondrial membrane fusion (Mishra and Chan 2016) (Figure I7B). Regarding astrocytes, mitochondrial fusion has been observed in astrocyte processes (Stephen et al. 2015). However, it seems that they have limited capacity to exchange material within the mitochondria of an individual cell (Waagepetersen et al. 2006) as it has been demonstrated by the mitochondrial heterogeneity inside the astrocytes. Both processes (fusion and fission) are precisely regulated and their unbalance is implicated in several diseases including neurodegenerative diseases (Devi 2006).

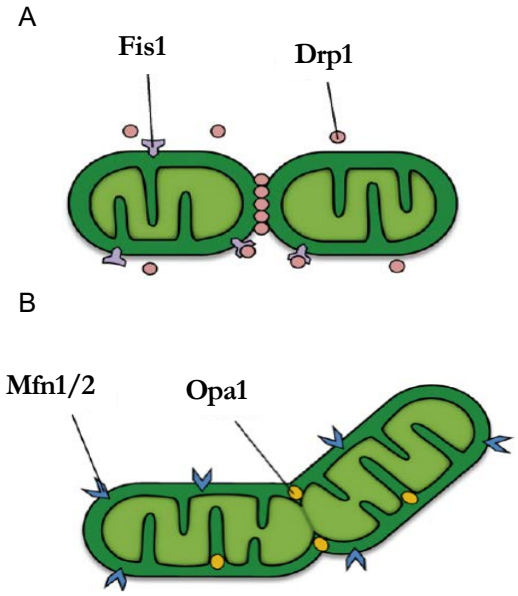

Figure I7: Principal proteins that participate in mitochondrial fission (A) and fusion (B) events. Modified from Kuzmicic et al. 2011.

Finally, mitochondria motility controls that a suitable location of mitochondria is reached, for example in places with a high energy requirement (Sheng and Cai 2012). In addition, a percentage of the mitochondria are stationary due to the specific energy or calcium buffering requirements. These mitochondria are anchored to the microtubules in neurons. One of the molecules that carries out this function is Syntaphilin, (Sheng and Cai 2012). Also, in

neurons, Miro promotes the localization of mitochondria in places with synaptic activity through its activation or inhibition by calcium. The mechanism by which synaptic activity or increases of exogenous glutamate affects mitochondrial motility is through the increase in calcium levels in neurons that stops mitochondria near to the synapsis (MacAskill et al. 2009). Similar results have been obtained in astrocyte mitochondria, where an increase in the calcium levels slows their movement (Tan et al. 2011; Stephen et al. 2015). Furthermore, glutamate uptake and calcium buffering in astrocytes have also been related to a diminution of the mitochondrial movement (J. G. Jackson and Robinson 2015; J. G. Jackson et al. 2014).

Mammals harbour 2 Miro isoforms, 1 and 2 that bind the mitochondria to an adaptor protein, Trak (that has 2 isoforms: 1 or 2). Finally, Trak attaches all the complex to the kif5 (kinesin superfamily) a motor protein that binds to the microtubules (Sheng and Cai 2012). However, Trak expression has not been found in astrocytes to date.

2.4. Astrocytes and lysosomes

Astrocytes secrete a variety of molecules to communicate with other cells in the brain: neurotransmitters and their precursors, hormones, metabolic substrates, antioxidant molecules, vasoactive factors, interleukins, ApoE and cholesterol to form HDL-like particles (A. Verkhratsky et al. 2016; Bezzi et al. 2004; Calegari et al. 1999; Z. Zhang et al. 2007; Kang et al. 2013; Lafon-Cazal et al. 2003; Choi et al. 2014). Most of these substances are released through the endosomal pathway, formed by a variety of vesicles; among which the lysosomes are found.

However, lysosomes do not only participate in exocytosis, but also they play a fundamental role in astrocyte calcium signalling (as previously explained) and in the digestion of different molecules that come from endocytosis, phagocytosis or autophagy processes. The digestion is carried out by lysosomal enzymes that break down all the biological polymers (Cooper 2000; Luzio, Pryor, and Bright 2007). They have a pH acidic (between 4.5 to 5) owing to the V-ATPase activity that uptakes protons from the cytosol using ATP (mentioned in 2.2. section) (Mellman, Fuchs, and Helenius 1960). All the enzymes contained in lysosomes are acid hydrolases, which can only degrade substrates inside of this organelle (Cooper 2000).
Autophagy is an essential homeostatic process that clearances abnormal proteins and other molecules such as lipids or entire organelles like mitochondria (Ward et al. 2016; Zare-Shahabadi et al. 2015). The role of autophagy in astrocytes has been demonstrated in models

of neurodegenerative disease, showing that autophagy dysfunction impairs astrocyte physiological functions (Di Malta et al. 2012). Lysosomes play a central role in this process since they provide related-enzymes and generate the adequate milieu to degrade the abnormal substrates. Remarkably, lysosomes participate in the different types of autophagy, from chaperone-mediated autophagy (CMA) where cytoplasmic proteins are delivered into the lysosome and degraded, to macroautophagy, where the autophagosome, a double membrane structure, engulfs and degrades cytosolic components or organelles through the fusion to a lysosome (Zare-Shahabadi et al. 2015).

Regarding mitophagy, this process is activated by the reduction of mitochondrial membrane potential. Mitochondria membrane potential is an important characteristic of mitochondria that allows them to perform their functions such as oxidative phosphorylation. This alteration promotes that Pink protein stays in the mitochondrial membrane, which phosphorylates and recruits Parkin, a ubiquitin ligase. Parkin binds ubiquitin to the substrates of the mitochondrial membrane tagging that mitochondrion for undergoing autophagy (Eiyama and Okamoto 2015). Regarding astrocyte mitophagy, it has been demonstrated the importance of these processes to regenerate their mitochondrial network upon a damage (Motori et al. 2013).

2.5. Principal astrocytic alterations in AD

Since astrocytes are complex cells that accomplish several and principal brain functions, it is not surprising that they are altered in several brain diseases. In the case of neurodegenerative disease, most of the research has been focused on neurons whereas studies conducted on other cell types aimed to study their impact on neurons.

In the case of AD, astrocytes undergo a morphological, molecular and functional change, acquiring a reactive phenotype termed astrogliosis (Osborn et al. 2016; González-Reyes et al. 2017; J. Rodríguez et al. 2016; Parpura and Verkhratsky 2014). Importantly, the course of the disease graded by Braak stage is directly correlated with astrogliosis, measured by the glial fibrillary acid protein (GFAP) increase (the method usually employed for measuring astrogliosis) (Serrano-Pozo et al. 2011; Simpson et al. 2010). Therefore, astrogliosis seems to progress with the disease suggesting that astrocyte alteration could be used as a biomarker of disease development.

However, apart from astrogliosis, astrocytes can also undergo atrophy in the early stage of the AD and in specific brain areas such as entorhinal cortex. This conclusion has been illustrated by a diminution in GFAP staining observed in 3xTg-AD (triple transgenic mice of the AD) (Yeh et al. 2011). A question that remains in discussion is if astrocytes experience cell death in AD. Lie et al. proposed that only a low percentage of astrocytes dye (W. P. Li et al. 1997) whereas other authors have found apoptotic markers in the majority of astrocytes nearby amyloid plaques (Kobayashi et al. 2004; Smale et al. 1995).

Regardless of this, as it was said before, astrogliosis is a feature of AD and is characterized by an increase in the GFAP and in the expression of other cytoskeletal proteins. This alteration of the protein expression reflects the hypertrophy of the cell body and the processes nearby amyloid plaques (Osborn et al. 2016; González-Reyes et al. 2017; J. Rodríguez et al. 2016; Parpura and Verkhratsky 2014).

Hence, considering the involvement of astrogliosis in the course of AD and since Aβ is one of the principal hallmarks of the disease, the potential relationship between astrocytes and Aβ has been investigated. It has been demonstrated that astrocyte processes surround senile plaques and it can penetrate them (Kamphuis et al. 2014) although they do not migrate into the plaques (Galea et al. 2015). In addition, astrocytes also participate in the Aβ clearance through ApoE (as it has been mentioned in 1.4.1.) and in the phagocytosis of presynaptic dystrophies (Gomez-Arboledas et al. 2018).

Among the varied alterations found in astrocytes in AD, it has been found that their genetic profile is also modified, indicating that their main functions can be impaired. For instance, cholesterol metabolism genes are downregulated in contrast to immune response genes that are upregulated (Orre et al. 2014). As a result of this upregulation, the astrocytes release cytokines, interleukins and TNF that are suggested to be increasing the neuroinflammation process related to AD (Heneka et al. 2015). Another astrocyte physiological functions that could be altered in AD is the control of oxidative stress since GSH is depleted in astrocytes stimulated with Aβ (Abramov 2004).

The regulation of synaptic processes by astrocytes such as the inhibition of GABA transmission (Ortinski et al. 2010) and other neurotransmitters (Robel and Sontheimer 2015) has also been described altered in AD. In addition, calcium signalling is dysregulated in AD

in both, neurons and astrocytes (LaFerla 2002). Focusing on astrocytes and taking into account the crucial functions that calcium regulates, the principal finding was performed through *in vivo* calcium recordings of AD mouse models where authors have found an astrocytic hyperactivity marked by an increase in the frequency of calcium oscillations (Delekate et al. 2014; Takano et al. 2007; Kuchibhotla et al. 2009). In addition, these oscillations were found independent of neuronal activity, synchronized (Kuchibhotla et al. 2009) and due to the activation of purinergic receptors (Shigetomi et al. 2018; Delekate et al. 2014). The purinergic receptor that accomplishes such calcium oscillations is P2Y1, a metabotropic receptor that induces calcium waves but not microdomain calcium signals (Shigetomi et al. 2018). Furthermore, the basal astrocytic calcium is also elevated in an AD mouse model (Kuchibhotla et al. 2009).

In spite of that, the relationship of calcium alteration in astrocytes and amyloid plaques is controversial. One study showed that the calcium alterations appear near amyloid plaques (Delekate et al. 2014) whereas, another suggested that both events are independent of the distance (Kuchibhotla et al. 2009). Different groups pointed out that Aβ induction elicits calcium dysregulation as showed by the addition of Aβ to hippocampal slices and to cultured astrocytes (Bosson et al. 2017; Pirttimaki et al. 2013; Alberdi et al. 2013; D. Lim et al. 2013; Ambra A. Grolla et al. 2013; Haughey and Mattson 2003; L. Lee, Kosuri, and Arancio 2014). But, in cultured astrocytes, it has been shown some contrary results. For example, Haughey and Mattson have shown an increase in the amplitude and velocity for the evoked calcium waves when cells were treated with Aβ (Haughey and Mattson 2003). Other authors have found an increase in the spontaneous transients (L. Lee, Kosuri, and Arancio 2014). And others that Aβ induces per se intracellular calcium increases (D. Lim et al. 2013; Alberdi et al. 2013). Regarding the studies performed in hippocampal slices stimulated with Aβ, Bosson et al. have confirmed the independence of the phenomena from neuronal activity (Bosson et al. 2017). In addition, in another study using similar approaches this calcium dysfunction induced by Aβ causes dysregulation in synaptic transmission in CA1 neurons due to the alteration of calcium-dependent gliotransmission (Pirttimaki et al. 2013).

Although many authors have described alterations of calcium signalling in astrocytes, the mechanisms behind them are not always coincident. Apart from purinergic receptors, calcium elevations are induced by the nicotinic channel (α7nACHRs) (Pirttimaki et al. 2013; L. Lee, Kosuri, and Arancio 2014), TRPA1 channel (Bosson et al. 2017) or mGLUR5

receptor (Ambra A. Grolla et al. 2013). Interestingly, other authors have presented ER channels or calciuneurin (a calcium binding protein) as the cause of calcium alterations (Alberdi et al. 2013; A A Grolla et al. 2013; D. Lim et al. 2013).

Remarkably, only a few studies have explored the impact of ApoE4 in calcium signalling and this existing literature has been focused on the effects of extracellular human ApoE and, in some cases, added to murine cells expressing their endogenous ApoE. For example, exogenous treatment with ApoE4 to injured neurons causes higher calcium increases (L. Jiang et al. 2015). Furthermore, it has been described that ApoE4 treatment potentiates NMDA-mediated calcium responses more than a ApoE3 treatment in neurons (Qiu et al. 2003). Regarding astrocytes, only a study conducted in 1998 assessed calcium increases produced by ApoE treatment showing that it was exacerbated by ApoE4 isoform (Muller et al. 1998). This study demonstrated that the underlying mechanism of this calcium increase in cultured astrocytes was dependent of voltage-dependent calcium channels of the membrane, although there is some controversy around the expression of these channels *in vivo*. Given this lack of information, we studied how endogenous ApoE4 expression regulates calcium signalling .

It is also worth to note that mitochondrial dysfunction is an undoubted feature of the AD. This mitochondrial function failure was described by different studies. It has been found that pre-symptomatic patients in both cases, familiar (Mosconi et al. 2006) and ApoE4 carriers (as it is mentioned in 1.4.3. section) (Perkins et al. 2016) have cerebral hypometabolism. Since this hypometabolism appears in the preclinical phase of the disease, it is likely that this process contributes to the early steps that trigger the AD.

The molecular mechanisms behind mitochondrial alterations in AD have been mainly characterized in neurons. In this regard, oxidative damage has been found in neuronal mitochondria of AD human brains and also in animals models (Moreira et al. 2010). The approach to characterize oxidative damage consisted in studying mtDNA. Oxidized mtDNA has been found in parietal, temporal and frontal areas of AD subjects. Furthermore, the oxidation of mtDNA is superior as compared to nuclear one (J. Wang et al. 2005). Mitochondrial dysfunction has also been related to amyloid metabolism since the accumulation of amyloid precursor protein in mitochondria affects membrane channels, a fact that is associated with ROS increase (Devi 2006).

Regarding ApoE and mitochondria, as mentioned before, the prevalent theory is that its fragments alter mitochondrial enzymes in neurons (Chang et al. 2005), although the involvement of ApoE4 in astrocyte mitochondria is still unknown. Moreover, mitochondrial dynamics alterations have also been implicated in AD development. In neurons, the overexpression of mutated APP displaces the fusion/fission equilibrium towards fission events, promoting the increase in oxidative stress and also the reduction of ATP production (X. Wang et al. 2008). Despite astrocytic mitochondria play main roles in astrocyte physiology and pathology and, consequently, in brain homeostasis, the studies concerning their involvement in AD have been underestimated. Only a few studies have shown the transcriptional change of mitochondrial genes in astrocytes from an AD model (Ruffinatti et al. 2018) and from human AD samples where the astrocytes were collected by laser microdissection (Sekar et al. 2015). Therefore, the implication of ApoE4 in astrocytic mitochondria remains poorly studied, despite the fact that astrocyte are the principal source of ApoE. Hence, the present study also aims to study astrocytic mitochondria functions in presence of ApoE3 and ApoE4.

3. From altered mechanism to biomarker discovery

Biomarkers are measurable indicators that provide information for diagnosis or prognosis of a specific disease. The sensitivity and the specificity of a reliable biomarker should be above 80%. In addition, biomarkers should also be to distinguish between similar diseases to help in the adequacy of the therapeutic intervention (Guest 2017).

Currently, there are 2 approaches used for biomarker discovery: targeted and untargeted. In the target approximation, the feature or protein that is tested is decided before based on a specific characteristic of the disease. On the other hand, in the untargeted, the approximation is to compare the disease and healthy conditions in an unbiased manner, to obtain a list of molecules or features that are altered in the disease. This methodology discovers new biomarkers without taking into account the mechanism behind these alterations and why they are changing in the disease.

3.1 AD biomarkers

Concerning the AD, 2 kinds of biomarkers have been described depending on the techniques for their detection: those detected with imaging techniques or in fluids. Focusing on the imaging techniques the currently used are magnetic resonance imaging (MRI), the fluorodeoxyglucose- positron emission tomography (FDG-PET) and the Pittsburgh

compound B. MRI is used to measure atrophy that appears in AD and in different areas according to the stage of the disease. The FDG-PET measures the glucose consumption or CMRG, which has been described decreased in AD patients or ApoE4 carriers (Eric M Reiman et al. 2005; Guest 2017), as it has been indicated in previous sections of the introduction. Finally, the other most common technique is based on Pittsburgh compound B, which binds to Aβ and provides information about the deposition of this protein using PET technology. The implementation of these techniques in clinical setting remains a challenge since they need experts to interpret the collected data, specialized facilities and consensual guidelines among hospitals and countries (Sheikh-Bahaei et al. 2017).

On the other hand, fluid biomarkers are proteins whose concentration in CSF, blood or urine varies with the disease. CSF is the only fluid that contacts directly to the brain parenchyma; therefore, it is the best fluid to interpret the brain function. The principal proteins present in the CSF result from exocytosis processes and from the extracellular matrix (Guest 2017).

The principal CSF biomarkers of the AD used are the most common proteins affected in AD: Aβ or total and phosphorylated Tau. Concretely, the concentration of both proteins appears altered in the CSF of AD patients, specifically the form 1-42 of Aβ appears diminished in AD CSF, whereas total Tau or TauP is highly increased. However, a lack of consensus arrives when the range of concentrations has to be determined owing to the differences obtained in different studies (Guest 2017; Mattsson et al. 2013) .

Other molecules have also been proposed and validated as good AD biomarkers. As for example, mitochondrial DNA, because of its reduction in the CSF of AD but not in other neurodegenerative diseases (Podlesniy et al. 2016).

Concerning the untargeted proteomic studies contradictory or unreproducible results complicate the identification and the validation of new biomarkers (Spellman et al. 2015; G. Brinkmalm et al. 2018; Heywood et al. 2015). This discordance between different studies probably arouses by the fact that proteomic methods are composed of a wide range of techniques with different accuracy and sensitivity. Therefore, untargeted proteomic identification provides more information than targeted one but with high variability between studies. Two potential biomarkers that are identified using this approach are YLK40 and

ApoE (Craig-Schapiro et al. 2010; Perrin et al. 2011; Wildsmith et al. 2014). Interestingly, both of them are mainly astrocytic proteins. Since astrogliosis is a principal feature of AD and correlates with cognitive decline (Serrano-Pozo et al. 2011; Simpson et al. 2010) other astrocytic proteins could serve as AD biomarkers.

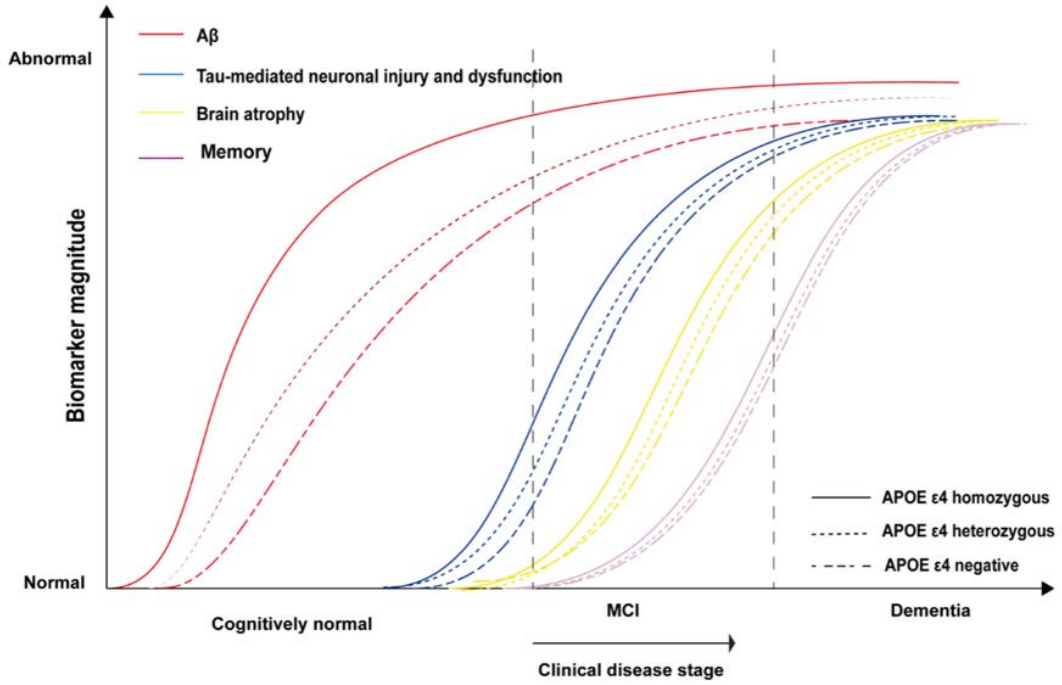

Figure I8: Hypothetical distribution of AD biomarkers depending on the stage and ApoE genotype. From Liu et al. 2016.

Regarding ApoE4 and its biomarkers associated, the study of Liu et al. evaluated the relationship between the principal biomarkers of AD and ApoE4 (Y. Liu et al. 2016). Interestingly, they adapted the hypothetical model of biomarkers created by Jack et al. to the ApoE genotype, in which they related the disease stage to the biomarkers Aβ, Tau, brain atrophy, memory impairment, among others (Jack et al. 2010). As it can be observed in the figure I8, ApoE4 is proposed to advance the appearance of biomarkers over the time. Concerning the studies of untargeted identification, mostly they are not stratified by ApoE genotype.

Therefore, we proposed the identification of molecules derived from astrocytes and related to ApoE4-induced dysfunctions in these cells as potential biomarkers of AD. This is a mixed approach since we looked for astrocytic proteins (untargeted), but also targeted, because these proteins are specific for particular dysfunction on/and organelles. We did not look for

a specific hit, but for a group of molecules that could be proposed as biomarker candidate for the early stages of AD pathology.

Working hypothesis and objectives

Our working hypothesis is that endogenous ApoE4 expression alters astrocyte functions. We focused our research on the affectation of calcium signalling as it is the basis of astrocyte excitability, and in mitochondrial functions. Both processes are dysregulated in Alzheimer's disease mouse models. Thus, our specific objectives are:

1. To decipher if the expression of human ApoE4 isoform leads to differences in astrocyte calcium signalling:
    a. To determine by calcium imaging, intracellular calcium concentrations at rest conditions and purinergic-induced calcium responses in immortalized ApoE3 and ApoE4 astrocytes.
    b. To study the calcium signalling pathways activated upon purinergic receptor stimulation in ApoE3 and ApoE4 astrocytes kept in extracellular media rich or deficient in lipoproteins.
    c. To clarify if calcium homeostasis alterations in ApoE4 astrocytes are due to the lower quantity of ApoE or owing to the structure of the ApoE4 isoform.
    d. To analyse the differences in intracellular lipid concentrations in ApoE3 and ApoE4 astrocytes by untargeted metabolomics and differential cholesterol distribution by immunocytochemistry to elucidate the mechanism by which ApoE regulates calcium signalling.
    e. To determine if oligomeric Aβ treatment exacerbates the different calcium signals between ApoE3 and ApoE4 astrocytes.

2. To determine if the expression of the human ApoE4 leads to mitochondrial dynamics alterations:
    a. To study the mitochondrial fusion and fission of ApoE3 and ApoE4 astrocytes at rest condition, and after the inhibition of mitochondrial metabolism by oligomycin.
    b. To analyse the mitochondrial motility of both cell lines at rest conditions, and the expression of proteins that participate in that movement.
    c. To examine the mitophagy and autophagy processes in ApoE3 and ApoE4 astrocytes.

3. To generate CSF biomarker candidates based on functional alterations of astrocytes.
    a. To establish which are the specific proteins of astrocytes.

b. To determine which proteins have been dysregulated in the CSF of Alzheimer's disease patients.
c. To create functional Alzheimer's signatures of astrocytes based on calcium-related proteins and mitochondrial and lysosomal compartments.

Materials and methods

1. Cell culture

1.1. ApoE mouse astrocytes

The majority of experiments were performed in immortalized derived-astrocytes from ApoE knock-in mice. In the knock-in mice, the endogenous ApoE has been replaced by a human isoform (ApoE3 or ApoE4). These cells were generated by Dr. Holztman's laboratory isolating the astrocytes from ApoE Knock-in transgenic mice. Then, astrocytes were immortalized by transfecting a plasmid that contains the SV40 T antigen and the neomycin resistance gene (Morikawa et al. 2005). The cell line is called WJE. This model proportionate 3 advantages above other models: (1) mouse ApoE is not present, and this is an advantage since it is a different ApoE that can mask the results, (2) it is not an over-expression model, so the cell is producing the physiological quantity of the protein and (3) the immortalization allows to study the specific mechanism behind the possible alterations without using a high amount of live animals

Immortalized astrocytes were routinely grown in advanced DMEM medium (12491015, Thermo Fisher Scientific) supplemented with Na^{2+} pyruvate (1mM) (11360039, Thermo Fisher Scientific), penicillin/streptomycin (100 units/mL and 100 μg/mL, respectively) (15140-122, Thermo Fisher Scientific), 10% of Fetal Bovine Serum (FBS) (1070106, Thermo Fisher Scientific) and geneticin (0.2 mg/ml) (10131027, Thermo Fisher Scientific).

Cells were cultured at 37 ºC in a 5% CO_2 humidified atmosphere air in T75 flasks and the passages were performed once per week up to passage 10. 2 mL of trypsin (T3924, Sigma Aldrich) for 5 minutes at 37 ºC were used to detach the cells. The dilution to maintain the cell line used was 1/10 . To perform the experiments astrocytes were seeded to coverslips or plates at a density from 35000 to 60000 cell/mL. Moreover, mycoplasma tests were performed twice per year being always negative.

1.2. Human induced pluripotent stem cells (iPSC)-derived astrocytes

Human iPSC-derived astrocytes were another cellular model used in our study. Cells were generated in Dr. Bu laboratory from Mayo Clinic (Zhao et al. 2017). Derived astrocytes were obtained from human skin biopsies of healthy ApoE3/3 or ApoE4/4 subjects. They were reprogramed to iPSCs and then differentiated to astrocytes thanks to that they were cultured in astrocyte medium (1801, ScienCell) supplemented with 10 ng/mL of CNTF(ciliary neurotrophic factor; 450-13, PreproTech), 10 ng/mL of BMP4 (bone morphogenetic

	ApoE genotype	Gender	Age at collection
MC0039	ε3/ε3	Female	73
MC0117	ε3/ε3	Male	71
MC0192	ε3/ε3	Female	83
MC0018	ε4/ε4	Female	63
MC0115	ε4/ε5	Male	87
MC0116	ε4/ε6	Female	83

Table M1: Human iPSC-derived astrocytes used. The ApoE genotype, the gender and the age at collection from each cell line are depicted.

protein 4; StemCell technology) and 10ng/mL of Heregulin- β (StemCell technology). After 21 days cells were frozen (table M1).

When cells were needed, they were unfrozen and seeded in PDL-coated plates (50 μg/mL in plastic or 100 μg/mL in glass) and kept in astrocyte medium supplemented with CNTF at 37 ºC in a 5% CO_2 humidified atmosphere air.

Cell passage was performed when the cells reached 80% confluence using accutase (00-4555-56 Thermo Fisher Scientific) for 7 minutes at 37 ºC to detach the cells. The dilution used for maintaining the line and for the experiments was 1 to 4.

1.3. Cell treatments

Cells were treated with different compounds depending on the analysis to be performed. The details of these treatments are summarized in table M2. All compounds were diluted in DMEM medium (41965039, Thermo Fisher Scientific) supplemented with penicillin/streptomycin, and 10% of FBS or 1x of B27 minus antioxidants (10889038, Thermo Fisher Scientific).

Name	Action mechanism	Source	Concentration	Duration
Olygomeric Aß	Cellular stress	A-42-T-1, Genic Bio	5 μM	24 hours
U18666A	Cholesterol acumulation	U3633, Sigma Aldrich	0.25 μg/ml	48 hours
Bexarotene	ABCA1 synthesis	CT-BEX, Chemietek	0.1 μM	24 hours
CS6253	ABCA1 stabilization	Johanson laboratory	10 μg/ml	5 hours
TransNed 19	NAADPR inhibitor	3954, Tocris	100 μM	20 minutes/ 48 hours
GPN (Gly-Phe ß-naphthylamide)	Catepsine C substrate, destroy lysosomal integrity	ab145914, Abcam	200 μM	20 minutes
Bafilomycin A1	V-ATPase inhibitor	1334, Tocris	2 μM	20 minutes
EGTA (Ethylene glycol-bis(2-aminoethylether)-N,N,N',N-tetraacetic acid)	Calcium chelator	E3889, Sigma Aldrich	500 μM	10 minutes
Oligomycin	ATP synthase inhibitor	04876, Sigma Aldrich	252 pM	4 hours/ 24 hours
Psck9	Promotes LDLR endocytosys	SRP6286, Sigma Aldrich	7μg/ml	24 hours
Temsirolimus	mTOR inhibitor	5264 tocris	50 nM and 100 nM	24 hours

Table M2: Treatment applied to astrocytes. Different treatments, principal action mechanism of them, source, concentration and time of treatment are depicted in the table.

1.3.1. Oligomerization of Aβ

Oligomerization procedure

(Lambert et al. 1998; W. L. Klein 2002; Dahlgren et al. 2002) was achieved from lyophilized Aβ (4014442, Bachem) which was mixed with the convenient volume of hexafluoroisopropanol (HFIP) (105228, Sigma Aldrich) until the 1 mM Aβ concentration was reached. After that, the mix was incubated for 3 hours at room temperature (RT) and left over-night for the HFIP evaporation.

The next day, DMSO was added to the solution until the concentration of Aβ reached 5 mM. Then, PBS was added until 100 μM Aβ concentration and the solution was placed in a rotatory shaker for 24 hours at 4ºC. Finally, the solution was centrifuged 10 minutes at 14,000 xg to eliminate the non-dissolve Aβ. To confirm the presence of oligomers, a Bicine western blot was performed (see section 3.2.).

1.4. Cell transfections and siRNA silencing method

Cell transfections were performed with Lipofectamine 2000 (11668019, Thermo Fisher Scientific) while silencing was accomplished by Lipofectamine RNAiMAX (13778075, Thermo Fisher Scientific). Both protocols were carried out when cells were closed to 60% confluence and the quantity of lipofectamine and DNA was set up for each plasmid or siRNA in order to reach the optimal over-expression or silencing. The plasmids and siRNAs and their conditions for the transfection are summarized in Table M2. In detail, for performing the procedure in p35 plates, lipofectamine and DNA were added separately to 150 μL of medium without FBS and antibiotics in different Eppendorf. Then, both solutions were mixed and kept at room temperature for 20 minutes to allow the formation of the micelles around DNA. Finally, the mixture was applied to the cells seeded in 800 μL of

Name	Source	Target	Type	Lipofectamine	DNA (1 ~ μg/μL)
pCMV GCEPIA 1er	Iono laboratory	ER calcium sensor protein	Plasmid	9 μL	2.5 μL
pCMV CEPIA 3mt	Iono laboratory	Mitochondrial calcium sensor protein	Plasmid	9 μL	2.5 μL
pApoE3-eGFP	Hudry laboratory	ApoE3- GFP	Plasmid	12 μL	4.5 μL
pApoE4-eGFP	Hudry laboratory	ApoE4-GFP	Plasmid	12 μL	4.5 μL
pEGFP-C1	Saura laboratory	GFP	Plasmid	12 μL	4.5 μL
ApoE siRNA	s194291, Thermo Fisher Scientific	ApoE	siRNA	4.5 μL	1 μL
neative control 1 siRNA	4390843, Thermo Fisher Scientific	Scramble	siRNA	4.5 μL	1 μL

Table M3: Plasmids and siRNAs employed. Origin and characteristics of plasmids and siRNAs used in the study. Plates of 35mm- diameter were used. The quantity of Lipofectamine and DNA is referred to that.

DMEM without FBS and antibiotics. After 5 hours, the medium was replaced by growth medium. 72 or 96 hours after the transfection or the silencing protocol, experiments were performed.

2. Cell biology methods

2.1. Intracellular calcium imaging

Calcium signalling imaging was carried out using Fura-2AM (F1221, Thermo Fisher Scientific), a calcium fluorescence indicator. Fura-2AM indicator has an acetoxymethyl (AM) ester group that allows its permeability to the cell. Once it is inside of the cell, esterases cleave the AM group and Fura2 is trapped inside the cell in its fluorescent form. Fura-2AM is a radiometric dye that upon excitation at 2 different wavelengths, at 340 nm -380 nm emits fluorescence with a peak around 510 nm. Fluorescence upon excitation at 340 nm increases proportionally to the calcium concentration, whereas fluorescence upon excitation at 380 nm decreases. Therefore, the ratio of the fluorescence obtained after excitation at 340 by 380 nm is proportional to the calcium concentration, increasing when cytosolic calcium increases and decreasing when cytosolic calcium decreases. (Devices 2013) (figure M1A).

Fura-2AM loading protocol used was as follows: seeded cells onto 1 mm glass coverslip (25 mm diameter) were incubated with 2 μM Fura-2AM for 1 hour at RT in the dark. Subsequently, coverslip was mounted on an O-ring chamber with 1 mL of medium and placed on a stage of a TE-2000U Nikon epifluorescence microscope at 37 ºC. Cells were excited at 340 and 380 nm thanks to a monochromator (Cairns, UK) and emitted fluorescence were collected every 2 seconds by the high sensitivity CCD EG-ORCA camera (Hamamatsu Photonics, Japan) in the Eclipse TE-2000U microscope with a 40x oil objective (Nikon, Japan). The images were collected through MetaFluor Software (Universal Imaging, USA).

During the recording of 5 minutes approximately, cells were stimulated with different neurotransmitters (noradrenaline (A9512, Sigma Aldrich), ATP (adenosine 5'-triphosphate, A9187, Sigma Aldrich), glutamate (G1626, Sigma Aldrich), endothelin 1(E7764, Sigma Aldrich) or acetylcholine (A6625, Sigma Aldrich) added at 10x of final concentration.

Data analysis was performed selecting individual cells (ROI: region of interest), and measuring over time the ratio of fluorescence obtained after stimulation at 340 versus the

fluorescence after stimulation at 380nm (ratio 340/380). 2 to 4 coverslips and 15 to 25 cells per coverslip were analysed for each condition. From each cytosolic calcium recording we measured the basal ratio, that is the intracellular calcium without stimulation as it is measured as the mean of the $R_{340/380}$, the peak increment after a stimulation with a neurotransmitter measured as the early increase in $R_{340/380}$ minus the basal calcium and the recovery phase measured as the percentage of the peak at 20 seconds of it. (figure M2B).

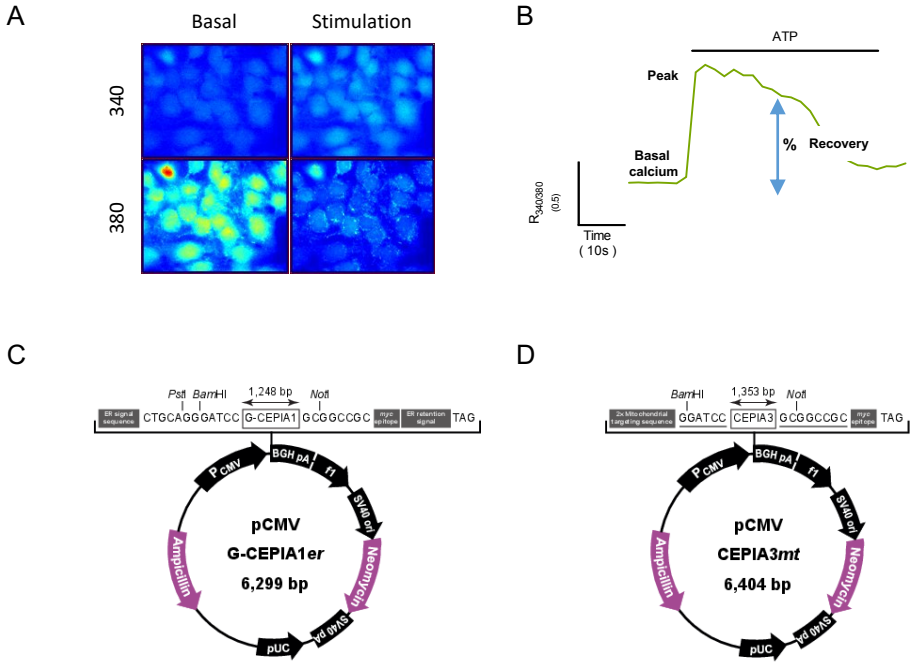

Figure M1: Calcium imaging tools. (A) Fura 2AM fluorescence in basal and after stimulation. (B) Typical calcium response of a single cell (trace) represented as the ratio 340/380 ($R_{340/380}$) versus time. Astrocytes were stimulated with 100 µM ATP. The principal parameters analysed are indicated: basal calcium (as a mean) , magnitude of the response (peak: higher early $R_{340/380}$ minus the basal calcium) and recovery (percentage of the $R_{340/380}$ left at 20 s compared to the peak). (C) Principal components of G-Cepia1er plasmid and (D) principal components of Cepia3mt plasmid.

2.2. Organellar calcium imaging

GECI (genetically encoded calcium indicators) were used to study specifically calcium inside the mitochondria and ER. The plasmids were a gift from Masamitsu Iono (J. Suzuki et al. 2014) and were transfected to the cells following the protocol described previously in section 1.4. before the calcium imaging experiments (table M3). Both plasmids had the similar sequence and hence, are called CEPIA (calcium-measuring organelle-entrapped protein indicator) and encoded for a protein with fluorescence properties proportional to the calcium concentration. Besides, the plasmids contain a specific sequence to target the calcium sensor protein to the organelle of interest. The pCMV GCEPIA1er (Addgene plasmid, #58215) measured calcium in the ER and the pCMV CEPIA3mt (Addgene plasmid, #58219)

measured the mitochondria calcium. The representation of the principal components of both plasmids is displayed in figure M1C and D.

Both fluorescence proteins are excited at 475 nm and emit fluorescence around 535 nm. The recording, stimulation and the image collecting were carried out with the same set up as intracellular calcium measurements. Fluorescence at determined time point versus initial fluorescence ($\Delta F/F_0$) were calculated to asses calcium changes in both organelles after the neurotransmitter stimulation.

2.3. Mitochondrial network imaging

Mitochondrial network visualization was accomplished with MitoTracker® Green (M7514, Thermo Fisher Scientific) staining. This mitochondrial probe is a permeable green fluorescence dye that accumulates in the matrix of active mitochondria having an excitation at 490 nm and an emission of 516nm.

200 nM of Mitotracker was added to the cells for 30 minutes at 37 ºC in a humidified atmosphere of 5% CO_2. Afterward, glass coverslips were mounted in an open-air imaging chamber at 37 ºC with 1 mL of medium and placed on the stages of an inverted epifluorescence microscope Nikon Eclipse TE2000E. 100x oil objective was used in order to have the best magnification. Images at different time points were collected with a CCD ORCA-EG monochromatic camera (Hamamatsu) controlled by MetaMorph software (6.1rU version, Universal Imaging Corporation). Images of cells were acquired to study mitochondrial fusion and fission whereas recordings of 1-minute-long were performed to monitor mitochondrial motility. 2 different image analyses were achieved according to the process subject of study: a morphometric examination of mitochondrial ultrastructure or single mitochondria tracking.

Regarding morphometric examination, a former master student, Agustín Bruzzese, developed an ImageJ plugin (called "Mitochondria quantification") that recognizes single objects of an image, in this case, mitochondria, and generates a .txt file with the area and the perimeter of each object. Cells for the analysis were selected manually having a total of one cell per picture. Therefore, each file contained all the mitochondria per one cell. Afterward, the mitochondria were classified into 3 different groups, puncta, rod and network depending on their size being the smallest puncta and the biggest network (Leonard et al. 2015). Mitochondria with an area smaller than 52 μm^2 and a perimeter smaller than 48 μm were

classified in the puncta group, mitochondria with an area from 52 μm^2 to 130 μm^2 and a perimeter from 48 μm to 119 μm were allocated in rod group and finally, mitochondria with an area larger than 130 μm^2 and perimeter larger than 119 μm to the network group. An example of the plugin analysis and the mitochondria per group is depicted in figure M2A. In addition, cells were treated with oligomycin (table M2) to promote fission and study the change of the mitochondrial ultrastructure.

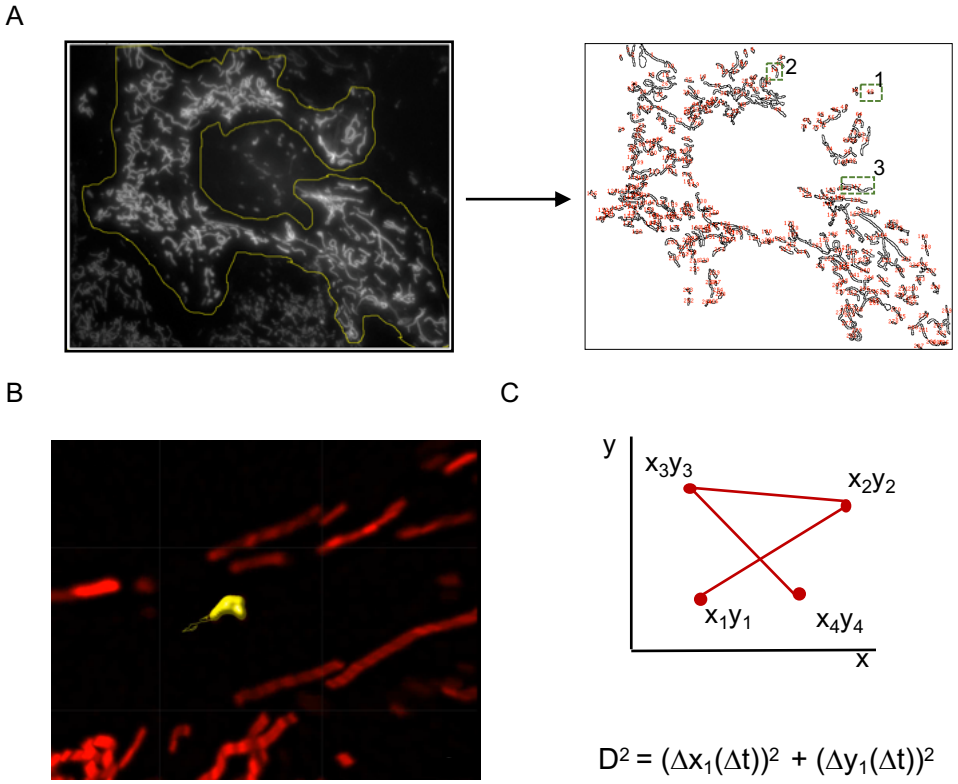

Figure M2: Mitochondrial analyses. (A)Input (left) and output (right) images before and after applied mitochondrial dynamics plugin. In numbers on output images it is depicted a puncta mitochondria (1), a rod mitochondria (2) and a network mitochondria (3). (B) Image of mitochondria (yellow) and their tracking obtained from IMARIS software. (C) Graph show a movement of a single object and the mathematical formula of D^2.

With respect to mitochondrial motility, a mitochondrial tracking analysis was accomplished by IMARIS software (Bitplane, Oxford Instrument company). Prior to that, a deconvolution (Huygens deconvolution, Scientific volume images) of video images was performed to revert the optical distortion and created clearer images. IMARIS is a software that provides the track and statistics from single objects using the surphase tool (figure M2B). A fixed threshold was set for all the videos towards comparing them. Since the mitochondrial movement was measured without any stimulation and it was in all directions, the Brownian motion was selected as the type of movement. Mitochondria were selected manually according to the following criteria: (1) only single mitochondria that can be separated from

the rest and (2) mitochondria with data in all the frames or images including those that have one gap.

The squared displacement (D^2) was the parameter chosen to compare the motility of mitochondria. D^2 is the displacement of an object from 2 positions (x_1y_1 to x_2y_2) in a time interval (Δt), which in our case was 2 seconds and it is squared to eliminate the directionality of the movement. In other words, positive as well as negatives movements were taken into account for the analysis. The mathematical formula is depicted in figure M2.

2.4. Lysosomal pH measurement

Lysosomal pH was measured in collaboration with Dr. Sánchez laboratory (University of Valladolid) using the dye LysoSensor Yellow/Blue DND-160 (L7545, Thermo Fisher Scientific). As a radiometric dye, the LysoSensor readout is independent of the dye concentration. Its excitation wavelengths are at 340 nm and 390 nm and the emission around 535 nm. Experimental parameters such as incubation time and dye concentration have been set to minimize variation and to give the best signal-to-noise ratio.

The procedure was the following. Cells were grown to 80% of confluence in black 96-well plaques (353219, Falcon) and washed with PBS. Subsequently, cells were incubated in the dark at RT for 3 minutes with 2 µM of LysoSensor Yellow/Blue in an isotonic solution (105 mM NaCl, 5mM KCl, 6mM HEPES-Acid, 4mM Na-HEPES, 5mM $NaHCO_3$, 60 mM mannitol, 5mM glucose, 0.5mM $MgCl_2$ and 1.3mM $CaCl_2$; pH adjusted to 7.4). After that, cells were rinsed 3 times in isotonic solution and then incubated with either, additional isotonic solution for pH measurement or with pH calibration buffers to perform the standard curve.

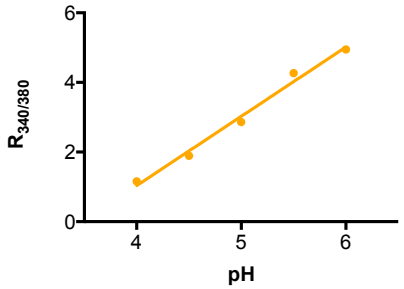

Figure M3: PH standard curve. PH standard curve of mixed culture of both cell lines in solutions at different pH. Equation of the standard curve: $y = 1.990x - 6.925$ ($R^2 = 0.98$).

With respect to the standard curve, absolute pH levels were obtained by calibrating lysosomal pH against the signal obtained with the calibration standards. Cells were incubated with 15 µM Monensin and 30 µM Nigericin (Sigma Aldrich), which are proton-cationophores that permeabilize the lysosomal membrane to Na^+ and K^+, respectively. These ionophores added

in solutions at pH 4.0, 4.5, 5.0, 5.5 and 6.0, force lysosomes to equilibrate with these pH values. Measuring the fluorescence ratio $R_{340/380}$ versus pH was used as a standard curve to calculate the lysosomal pH of different samples. Figure M3 displays the standard curve of ApoE3 and ApoE4 cells.

Fluorescence was measured with a GENios Pro Fluorometer and recorded using the XFluor4GENiosPro software package (TECAN). The final calculated pH represents the mean of 6 measurements taken strictly within the 12 min following dye removal, as LysoSensor generates lysosomal alkalization with longer incubation times.

2.5. Immunocytochemistry

Primary Antibody	Secondary	Reference	Western blot	Immunistaining
Anti-ApoE	Mouse	sc53570, Santa Cruz Biotechnology	1/250	1/400
Anti-Bip	Rabbit	3177 Cell Signalling	1/1000	
Anti- p-eIf2	Rabbit	9721, Cell Signalling	1/1000	
Anti-Ire-1α	Rabbit	3294, Cell Signalling	1/1000	
Anti-Pdi	Rabbit	3501, Cell Signalling	1/1000	
Anti-Aβ	Mouse	sig-39320, Biolegend	1/500	
Anti-Gfap	Rabbit	z 0334, Dako		1/1000
Anti-Lamp1	Rat	1D4B, Hybridoma Bank		1/200
Anti-Lc3I/II	Rabbit	ab48394, Abcam	1/200	1/200
Anti-Tfeb	Rabbit	6801,ProSci		1/400
Anti-V0D1	Mouse	ab56441, Abcam	2.5ug/ml	
Anti-V1B1 and V1B2	Rabbit	ab200839, Abcam		
Anti-Parkin	Rabbit	ab15954, Abcam	1/1000	
Anti-Tom20	Rabbit	sc11415, Santa Cruz Biotechnology	1/1000	1/1000
Anti-β-actin	Mouse	a5316, Sigma Aldrich	1:20000	
Secondary antibody	**Form**	**Source**	**Western Blot**	**Immunostaining**
Anti-rat	Donkey anti-Rat IgG	712-165-150, Jackson Immunoresearch		1/200
Alexa Fluor 488	Goat anti-Mouse IgG	A11029, Thermo Fisher Scientific		1/1000
Alexa Fluor 488	Goat anti-Rabbit IgG	A11034, Thermo Fisher Scientific		1/1000
Alexa Fluor 594	Goat anti-Rabbit IgG	A11037, Thermo Fisher Scientific		1/1000
Alexa Fluor 594	Goat anti-Mouse IgG	A11032, Thermo Fisher Scientific		1/1000
Alexa Fluor 555	Goat anti-Mouse IgG	A21424, Thermo Fisher Scientific		1/1000
Alexa Fluor 555	Goat anti-Rabbit IgG	A21429, Thermo Fisher Scientific		1/1000
Secondary Antibody, HRP	Goat anti-Mouse IgG	31430, Thermo Fisher Scientific	1/10000	
Secondary Antibody, HRP	Goat anti-Rabbit IgG	31460, Thermo Fisher Scientific	1/10000	

Cells were grown on glass coverslips into 24-well plates. Cells were treated and fixed with 4% paraformaldehyde (I5714, Electron Microscopy Science) for 15 minutes. 500 µL of different used reactives were added to the wells in each step. 3 washes of 5 minutes were carried out before adding 0,1% of Triton buffer (A16046, Alfa Aesar) to permeabilize cells in agitation. Then, 5% of NGS (normal goat serum; 16210064, Thermo Fisher

Table M4: Primary and secondary antibodies used. The antibodies are classified depending on if they are primary or secondary, and secondary for immunostaining or for Western Blot.

Scientific) were used to block the unspecific unions and primary antibody was incubated overnight at the desired concentration (table M4). Afterward, the appropriate secondary antibody (table M4) was incubated for 1 hour at RT following by 3 PBS (phosphate-buffered saline) washes of 10 minutes. Nuclear staining was accomplished by DAPI (D3571, Thermo Fisher Scientific) staining after incubation for 5 minutes (dilution of 1:20000). Coverslips were mounted on a slide with Fluoromount G (0100-01, Southern Biotech) and fixed with nail polish. Images were acquired by confocal laser scanning microscopy ZEISS LSM 700 or TE 2000E microscopy and analysed with ImageJ.

These images were analysed according to the parameter to determine. For lysosome localization, we used the IMARIS software. In that case, we identified the membrane, the nucleus and the vesicles of each cell due to "ImarisCell" tool. The Lamp1 positive staining were the vesicles which were identified owing to "spots" tool, which established spherical structures giving a dot to them. ImarisCell tool provided different parameters among the relationship between cell membrane, nucleus and vesicles or spots. We employed the distance (μm) from each vesicle to the closest point of the nucleus to study the cellular localization of the Lamp1 positive vesicles.

2.6. Cholesterol staining

Filipin III (F4767, Sigma Aldrich) is an antibiotic from Streptomyces Filipensis that is capable to bind unesterified cholesterol and emits fluorescence in the ultraviolet spectrum. The protocol described below has been adapted from Suzuki et al. and Santos et al. and setting up the appropriated concentration of Filipin for our cells (S. Suzuki et al. 2007; Copetti-Santos et al. 2015). Cells, which were grown on glass coverslips, were fixed with 500 μL of 4% paraformaldehyde for 15 minutes and washed with PBS as it is described for immunocytochemistry protocol. Afterward, coverslips were incubated with 25 μg/mL of Filipin for 30 minutes at RT in the dark. Since Filipin is cell permeant so, triton treatment is not needed. After 3 washes of PBS, glass coverslips were mounted with Fluoromount G and images were acquired by CCD ORCA-EG monochromatic camera (Hamamatsu) and the Eclipse TE-2000E (Nikon) epifluorescence microscope. 20x or de 40x oil objective was used.

2.7. Autophagic and endolysosomal vesicles quantification by transmission electron microscopy

Cells were grown in DMEM supplanted with 10% of FBS. The identification and quantification of autophagic vesicles and lipid droplets by electron microscopy were

performed in Dra. Gutierrez laboratory (University of Málaga). Cells were fixed with 4% paraformaldehyde and postfixed in 1% osmium tetroxide in 0.1 M phosphate buffer. After that, the samples were stained with uranyl acetate, dehydrated in graded acetone and embedded in Araldite (EMS, USA). The block was cut in ultrathin sections and observed with the electron microscope (JEOL JEM 1400).

First, panoramic images were acquired at 4000x to use as a map in order to avoid counting one structure twice. To quantify, consecutive non-overlapping pictures were obtained at 15000x of each cell. The distribution of the vesicles into the group of lipid droplets or autophagic vesicles was carried out manually according to the following criteria. Vesicles were identified as lipid droplets when it was an electroclear structure with a lipid monolayer without intraluminal content. On the contrary, vesicles were classified as autophagic vesicles when their structure was electroclear but with a lipid bilayer with autophagic bodies or electrodense structures with abundant vesicular content.

The final measurement was calculated as a mean of the vesicles of a specific type versus total vesicles of each cell.

3. Biochemical and Molecular Biology methods

3.1. Protein extraction and quantification

After the appropriated treatment, cells for protein extraction were lysed with RIPA buffer (50 mM Tris HCl (T3253, Sigma Aldrich) pH 7.4, 150 mM NaCl (SO02241000, Scharlau), 0.1% SDS (L3771, Sigma Aldrich), 1% Igepal (I3021, Sigma Aldrich) and 0,5% sodium Deoxycholate (D6750, Sigma Aldrich)), in which phosphatase (P5726, Sigma Aldrich) and protease (11697498001, Roche) inhibitors were added freshly. Collected cells were sonicated for 5 minutes and centrifuged to remove unbroken cells. Protein extracts were quantified with BCA kit (23225, Thermo Fisher Scientific) according to the manufacturer's protocol. In brief, this colorimetric method enables to measure the protein concentration thanks to the reduction of Cu^{2+} to Cu^{+} by protein in alkaline medium and the subsequent colorimetric reaction of Cu^{+} with bicinchoninic acids. A standard curve of BSA (bovine serum albumin) diluted in RIPA buffer was performed. Protein samples were stored at minus 20ºC.

3.2. Western blotting

Initially, samples with 15 to 35 μg protein were denatured and charged negatively by adding the appropriated volume of 4x loading buffer composed of 62.5 mM Tris HCl pH 6.8, 10%

glycerol, 2% SDS, 5% beta-mercaptoethanol and 0.01% bromophenol blue and heated at 95ºC for 5 minutes. Then, samples were loaded in polyacrylamide gels electrophoresis (PAGE) (A3579, Sigma Aldrich), which is formed by 2 layers: resolving and stacking. Stacking gel is composed of 4% polyacrylamide, 0.125 M Tris HCl, pH 6.8 and 0.1% SDS and resolving fraction by polyacrylamide whose percentage changed according to the protein weight, being bigger if the interested protein is small, 0.375 M Tris HCl pH 8.8 and 0.1% SDS. In both fractions, TEMED (T9281, Sigma Aldrich) and ammonium persulfate (A3678, Sigma Aldrich) were added to promote the polymerization of acrylamide. SDS-PAGE electrophoresis was conducted at a constant amperage (30 mA) for approximately 2 hours followed by the protein transference to a PVDF membrane (03010040001, Roche) at constant voltage (100 mV) for 1.5 hours. Electrophoresis buffer was composed of 24 mM TRIZMA base (T1503, Sigma Aldrich), 190 mM glycine (G8898, Sigma Aldrich) and 0,1% SDS while transfer buffer contained 24 mM TRIZMA base, 190 mM glycine and 20% methanol (M/40501PB17, Fisher Chemical). The membrane was blocked with 5% non-fat milk dissolved in TBS-T (Tris-buffered saline plus 0.2% tween detergent) (P1379, Sigma Aldrich) for 1 hour and the appropriated concentration of primary antibody diluted in 5 mL of TBS-T was incubated overnight at 4ºC in agitation. The next day, the membrane was washed 3 times with TBS-T followed by the incubation with an HPR (horseradish peroxidase) secondary antibody for 1 hour. Table M4 contains all the antibodies used. Finally, the membrane was developed using the chemiluminescence kit of BioRad (170-5061) by mixing 1 mL of the 2 reagents, applying to the membrane and incubated with photographic films for periods of seconds to minutes. Films were then developed automatically with film processing machine FPM-100A (Fuji Photo). Alternatively, chemiluminescence membranes were detected with a Chemidoc MP Image System (BioRad). ImageJ or Image lab software was used for the quantification of the bands.

As previously presented, a Bicine western blot was performed to confirm the correct oligomerization of Aβ. For such western blot, the electrophoresis gel was composed of a separation layer (0.4 M Trizma Base, 0.1 M H_2SO_4, 12% Acrylamide (161-0154, BioRad),0.1% SDS at pH 8.1) and a stacking layer (0.4 M BisTris (B7535, Sigma Aldrich), 0.1 M H_2SO_4, 5% Acrylamide, 0.1% SDS at pH 6.7). Ammonium persulfate and TEMED were added to promote the polymerization of the gel. The loading buffer for the Aβ sample was composed of 0.72 M BisTris, 0.32 M Bicine, 2% SDS, 100 mM DTT and 0.008% bromophenol blue. Cathode running buffer (0.2 M Bicine (B3876, Sigma Aldrich), 0.1 M NaOH, 0.25% SDS at 8.2 pH) was placed on the inner tank of the electrophoretic bucket

while in the outer tank, anode running buffer (0.2 M Tris Base, 0.05 M H_2SO_4 t 8.1 pH) was added. Electrophoresis was performed by fixing the amperes at 0.025 per gel. Transference to PVDF membrane also accounted with different buffer composition than normal western, in this case with 10 mM CAPS and 10% of methanol. Then the voltage was fixed at 100 volts for 90 minutes to accomplish the transference. Membrane block with milk and incubation with primary and secondary antibodies were performed as in normal western blot.

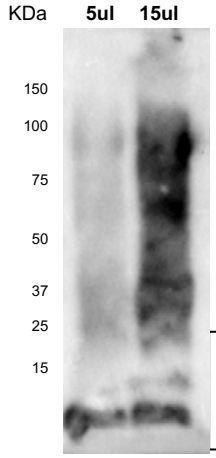

This protocol was conducted with every new oligomeric Aβ preparation. Figure M4 shows a representative western of it.

Figure M4: Representative oligomeric Aβ western blot. Special Aβ western blot carried out to assess the induction of oligomeric forms (upper part of the Western) of that protein.

3.3. Plasmid amplification and purification of ApoE3-GFP, ApoE4-GFP and CEPIA plasmids

DH5-α E.coli were transformed with the plasmid DNA through heat shock from 4ºC to 42ºC for 2 minutes. Then, bacteria were growing in 500μL of LB medium (Lysogenic broth, 12795-084, Invitrogen) for 1 hour and seeded in LB agar (00604241, Thermo Fisher Scientific) plates with the convenient antibiotic depending on the plasmid resistance over-night at 37ºC. In the case of the ApoE-GFP plasmids, the resistance was kanamycin and in the case of CEPIA plasmids, it was ampicillin. Subsequently, one colony was picked by using a pipette tip and grown in crescent volumes of LB medium, first in 5 mL and then in 300 mL with the antibiotic for approximately 24 hours at 37ºC. Once the bacteria density was the appropriated, they were lysed and the plasmid was purified with PureLink™ HiPure Plasmid Filter Maxiprep Kit (K210016, Thermo Fisher Scientific) following the manufacturer's indications. In detail, growth bacteria were resuspended in 10 mL of resuspension buffer and then,10 mL of lysis buffer was added to the resuspension that was mixed by inverting and incubated for 5 minutes at RT. Then, 10 mL of the neutralization buffer was added and the mixture was transferred to the column and washed with wash buffer. Subsequently, the plasmid was eluted by adding 15 mL of elution buffer and precipitated with 10.5 mL of isopropanol. Then DNA precipitated mixture was load in the syringe attached to a plunger keeping the DNA in the plunger. Finally, DNA was washed with ethanol and eluted with Tris-EDTA buffer. The plasmids were stored at -20 ºC.

3.4. Genomic DNA extraction and ApoE genotyping

ApoE3 and ApoE4 cells were trypsinized, collected and centrifuged at 200 xg for 5 minutes, then, the supernatant was discarded and the cellular pellet was resuspended in lysis buffer (100 mM Tris HCl pH 8.8, 5 mM EDTA, 0.2% SDS and 200 mM NaCl) supplemented with proteinase K 0.2 mg/ml. Cellular extracts were incubated for 5 hours at 55 ºC. DNA was precipitated by the addition of 500 µL of isopropanol (I9516, Sigma Aldrich) and a centrifugation of 12000 rpm for 10 minutes. The supernatant was discarded by pipetting carefully and DNA pellet was washed with 500 µL of ethanol 70% and centrifuged at 12000 rpm for 10 minutes again. DNA was dried at RT until form a translucent pellet and resuspended in 30 to 50 µL of TE (Tris EDTA buffer). It was stored at -20 ºC

Sample ApoE genotyping was performed by real-time PCR (polymerase chain reaction) (Applied Biosystems 7500 Fast Real-Time PCR system) due to the ability of the PCR to detect single variant nucleotide in a given sequence. 2 different probes (TaqMan® SNP Genotyping Assay) were used, rs429358 and rs7412 (Thermo Fisher Scientific), the first one distinguishes between the nucleotide changed of ApoE3 and ApoE4 and the second one between the nucleotide changed of ApoE2 and ApoE3. Each probe is formed by 2 different sequences that are bind to a detector, VIC or FAM, each one for one of the sequences that we want to identify, in other words, one detector bind to the sequence of ApoE3 and the other detector to the sequence of ApoE4. In addition, the probes are composed of 2 primers that amplify the polymorphic region. Therefore, the PCR mix was formed by one probe, TaqMan Genotyping Master Mix (4371353, Thermo Fisher Scientific) and genomic or plasmid DNA. The PCR program was divided into 3 stage: 1) 50ºC for 2 minutes, 2) 95ºC for 10 minutes and 3) 50 cycles of 95ºC for 15 seconds and 64ºC (rs429358 probe) or 61ºC (rs7412 probe) for 2 minutes. Finally, confirmation of the genotyping were depicted by 7500 software (Applied Biosystems).

3.5. mt-DNA extraction

Cells were grown in 35mm-diameter plates with DMEM medium supplemented with 10% FBS and antibiotics. In detail, cells were detached with 1 mL of trypsine for 5 minutes at 37 ºC and transferred to an Eppendorf tube. An extraction buffer composed of 10 mM Tris-HCl, 10 mL EDTA, 0.5% SDS and 20 µg/mL of RNAse A at pH of 8 was added to the cells and kept for 1 hour at 37 ºC. Then, 100 µg/mL proteinase K was added to the solution and incubated for 1 hour at 56 ºC. Finally, the solution was heated at 95 ºC for 10 minutes to

inactivate the proteinase K. This solution contained the mt-DNA and it was kept at -20 ºC.

3.6. RNA (ribonucleic acid) extraction and reverse transcription PCR

Cells were collected through the addition of Trizol Reagent (15596018, Thermo Fisher Scientific), using different volume depending on the size plate. 35mm-diameter plates were commonly used, so, the employed volume was 1 mL. After Trizol addition, we resuspended the cells and collected in an Eppendorf tube. Then, 0.2 mL chloroform (22711.290, AnalaR Normapur) was added and the extracts were kept 3 minutes at room temperature. Then, extracts were centrifuged at 11,500 rpm for 15 minutes at 4ºC. Centrifugation allows the formation of 3 different phases: inferior formed by phenol-chloroform, interphase formed by proteins and the superior phase, where the RNA is located. Therefore, the superior phase was isolated by pipetting carefully and 0.2 mL of isopropanol was added to promote the precipitation of RNA. RNA isolated was kept at room temperature for 10 minutes and centrifuged at 11,500 rpm for 10 minutes. Finally, RNA was washed with cold 0.5 mL of ethanol 75% and preserved at room temperature until the pellet was dry. RNA samples were resuspended in TE and kept at -80ºC.

RNA sample concentration in each sample was determined by a Nanodrop 200 spectrophotometer (Thermo Fisher Scientific). 2 μg of RNA were reverse transcripted to cDNA. The required reagents to carry out the reverse transcription PCR were 1 μM of oligo DT (SO132, Thermo Fisher Scientific), 1 μM of hexamers (SO142, Thermo Fisher Scientific), 0.5 mM dNTPs (10297018, Thermo Fisher Scientific), 0.45 mM DTT (P/N y00147, Thermo Fisher Scientific), 10 U (units) RNAse out (P/N 100000840, Thermo Fisher Scientific), 1x RT buffer and 200 U of retrotranscriptase (EP0441, Thermo Fisher Scientific). The PCR program was divided into 2 steps: 1) 65ºC for 10 minutes and 2) 25ºC for 10 minutes, 42ºC for 1 hour and 72ºC for 10 minutes. In the first step, only oligo DT, hexamers, dNTPs and the RNA sample were present and the rest were added when step 1 had finished. We kept the cDNA at -20 ºC and analysed gene expression through real-time PCR.

3.7. Gene expression and mitochondrial DNA quantification

Quantitative real-time PCR (qPCR) was used to assess gene expression and mitochondrial DNA quantification. We used 2 different approaches: the first was TaqMan assays and the second used, SYBR Green. TaqMan assay used probes with a reporter and a quencher. The reporter contains a fluorophore that is inhibited by the quencher, when the union of both is

hydrolysed after the hybridization, the reporter emits the fluorophore and fluorescence, Which is captured by the detector of 7500 Fast Real-Time PCR System. In the case of the SYBR assay, it is based on double-strand fluorescent molecules that emit fluorescence when the double strand cDNA is formed. Fluorescence is equally detected with the 7500 Fast Real-Time PCR System. In both cases, the PCR cycle in which the fluorescence peak appeared is proportional to the DNA sequence quantity. The qPCR mixes were : 1) 1 μL of TaqMan hydrolysis probe (table M5), 10 μL of Taqman™ Universal Master Mix II, with UNG(4440039, Thermo Fisher Scientific), 5 μL of RNase, DNase free water (10977035, Thermo Fisher Scientific) and 4 μL of sample for TaqMan protocol and 2) 0.4 μM of each primer (Table M5) 5 μL of SYBR mix (4367659, Thermo Fisher Scientific), the convenient RNase, DNase free water and 2.5 μL of sample for SYBR green protocol. Proper sample dilution was adjusted for each probe and is depicted in the table M5. TaqMan primers were purchased from Thermo Fisher Scientific and primers for SYBR were designed according to the sequence of the gene to be detected or guided by published probes (table M5). qPCR cycles were the following: (1) a holding stage of 50 ºC for 2 minutes initial, then 10 minutes

Gene	Reference	Sequence (5'->3')	Primers for Sybr	TaqMan®	Sample dilution
Tpc2	Desingned	5'-GCTGAGCCTTGCTTGTGAGG-3'; 5'-ACACTTCAGGGTCTTCTTCATCA-3'	+		1/5
Tpc1	Desingned	5'-CTGGGAGAGATGAATTATCAAGAG-3'; 5'-GTTGTGTACGAAGAGGTAGG-3'	+		1/25
Trpml	Mm00522550_m1			+	1/5
V1C1	Mm00445925 m1			+	1/5
V1A	Mm01343719_m1			+	1/5
Mfn1	Mm00612599_m1			+	1/5
Mfn2	Mm00500120 _m1			+	1/5
Opa1	Mm01349707_g1			+	1/25
Drp1	Mm01342903 m1			+	1/25
Fis1	Mm00481580_m1			+	1/50
Pink1	Mm00550827			+	1/5
Rhot1	Mm01304158			+	1/25
Trak1	Mm00613053			+	1/10
Trak2	Mm00549615_m1			+	1/25
ApoE	Hs00171168_m1			+	1/50
TBP	Mm00446973_m1			+	1/25 or 1/50
TBP	Desingned	5'-CAAATGCTTCATAAATCTCTGCT-3';5'-AGTTCAGTAGCTATGAGCCA-3'	+		1/25
18s	Mm03928990			+	1/250
GAPDH	Desingned	5'-AAGCTCATTTCCTGGTATGAC-3'; 5'-TGGTCCAGGGTTTCTTACTC-3'	+		1/25 or 1/50
GAPDH	Mm9999915_g1			+	1/25 or 1/50
mt DNA 115	(Podlesniy et al. 2013)	5'-CTAGCCACACCCCCACGGGA-3'; 5'-CGTATGACCGCGGTGGCTGG-3'	+		0.34 μg/mL
mt DNA 699	(Podlesniy et al. 2013)	5'-CTAGCCACACCCCCACGGGA-3; 5'-CGGGCGGTGTGTGCGTACTT-3'	+		0.34 μg/mL

Table M5: Primers for Syber Green and TaqMan probes for real time qPCR.

at 95 ºC and 40 cycles of 95 ºC for 15 seconds and 60 ºC for 1 minute for TaqMan protocol and (2) similar protocol for SYBR assay but adding an extra stage of the melting curve composed of 15 seconds at 95 ºC, 1 minute at 60 ºC, 30 seconds at 95 ºC and 15 seconds at 60 ºC. Data analysis was performed using Cq value and the average of the gene efficiency provided by LinReg PCR software. First, we normalized the Cq to the control subtracting its value and then we calculated the $1+\text{eficience}^{\Lambda Cq}$ of each gene analysed. Not RT (sample without retrotranscriptase) and blank were used as a negative control. Expression data were normalized with housekeeping genes (Gapdh, TBP or 18s) or performing a geometric mean of these genes according to the geNorm algorithm (Vandesompele et al. 2002).

3.8. Lactate and ATP quantification

To detect lactate secreted to the extracellular medium, cells were grown in a 24-well plate. When they were confluent, the medium was replaced by Krebs buffer (KH) (113 mM NaCl, 25 mM $NaHCO_3$, 4.7 mM KCl, 1.2 mM Mg_2SO_4, 10 mM Hepes (acid), 10 mM glucose and 1.3 mM CaCl at pH of 7.4) and incubated for 2 hours. Secreted lactate was measured by Lactate Assay Kit (MAK064, Sigma Aldrich) according to the manufacturer's instructions. This kit is based on an enzymatic reaction that results in a colorimetric compound (570 nm) that is proportional to lactate concentration. The mix reaction was formed 46 µL of lactate assay buffer, 2 µL of lactate enzyme mix and 2 µL of lactate probe that was added to each 50 µL of the medium sample and incubated for 30 minutes at room temperature. Lactate concentration was determined according to lactate standard curve performed with known concentrations of lactate diluted in lactate assay buffer. Data were normalized by the protein concentration collected and digested with RIPA buffer and quantified using BCA kit.

ATP production of ApoE3 and ApoE4 cells was measured by ATPlite Luminescence Assay Kit (6016943, PerkinElmer). ATP interacts with D- luciferin and luciferase producing luminescence. Cells were grown in 24-well plates for 3 to 5 days until they reached 80% of confluence, and then, the medium was changed by DMEM supplemented with 10% FBS. The next day, the medium was discarded and 100 µL of PBS was added to the cells after washing them twice with 500 µL of PBS. Then, 50 µL of lysis buffer was added to lyse the cells and they were agitated at 700 rpm for 5 minutes. The lysed cells were mixed with 50 µL substrate solution and agitated at 700 rpm for other 5 minutes. Finally, the cellular extracts were kept in the dark for 10 minutes and measured in the luminometer (Biotek). ATP quantification was normalized by protein concentration measured directly in the cellular

extracts by BCA assay.

3.9. Lysosomal isolation

Lysosomal isolation requires of large amounts of cells, thus, 4 confluent 25x25 cm plates were used for each condition. This procedure was carried out in the laboratory of Dr. Miquel Vila (Vall d' Hebron). Firstly, astrocytes were removed from the plate with a scrapper, transferred to a falcon and centrifuged 5 minutes at 800 xg and at 4ºC. The pellet was resuspended in 1 mL of 0,25 M sucrose with protease inhibitors and then placed on the cavitation chamber, remaining the cells at 2.5 atmospheres for 6 minutes. Subsequently, 2 homogenizations took place: Teflon- crystal and crystal-crystal homogenization. These last steps contribute to the cytoplasmic membrane lysis without affecting organellar membrane. The homogenized preparation was centrifuged at 25000 xg for 15 minutes at 4ºC and 2 fractions were obtained, pellet (containing DNA, membranes, nucleus and heavy mitochondria) and supernatant (containing the small organelles and cytoplasm). The supernatant was centrifuged at 17000 xg for 10 minutes at 4ºC allowing the separation of lysosomes and small mitochondria that were found in the pellet. Pellet was resuspended in 0,25 M sucrose and 2 metrizamide gradients were prepared: (1) 35%,17% and 6% metrizamide and (2) 24%, 17% and 5% of metrizamide. In the first gradient, lysosomes appear in the interphase between 17% and 6% after the centrifugation at 200000 rpm for 35 minutes at 4 ºC. The second gradient was composed of 24% (obtained from lysosomal and mitochondrial enrich fraction plus metrizamide), 17% and 5%. The lysosomes were found in the interphase of 17% to 5% after the centrifugation at 200000 rpm for 35 minutes at 4 ºC. Finally, lysosome fraction was centrifuged at 37000 xg for 15 minutes at 4 ºC and resuspended in 0,25 M sucrose. Temperature shock was used to induce lysosome lysis, and through similar centrifugation as the previous step, membrane and lysosomal content were separated.

4. Metabolomic studies

An untargeted metabolomic assay was performed by Dr. Ariza laboratory from the University of Huelva. The extraction of metabolites from the ApoE3 and ApoE4 samples was carried out by the addition of 200 µL $CHCl_3$:MeOH in a relation of 1 to 2 with 0.1% of formic acid to promote the ionization of molecules. Then, samples were vortexed for 5 minutes and centrifuged at 4000 rpm for 3 minutes to discard suspension solids. Samples were analysed with mass spectrometry. This technique was applied employing the QSTAR

XL hybrid system (Applied Biosystems, Foster City, CA, USA), which is a triple quadrupole-time of flight with an electrospray source. The sample induction flux was 15 μL/min through the infusion integrated pump. The resulted spectra were acquired in positive ionization in a range of m/z from 50 to 1100 uma. The ionization parameters were: voltage ion spray 3300 volts, decluttering potential of 60 volts and focusing potential of 250 volts. To the spectra acquisition, nitrogen was used as collision gas. Markerview™ and SIMCA-P™ software were used to reduce the results into a two-dimensional matrix of peak spectra and intensity of peaks and for the statistical analysis. We obtained around 2000 pics of each cell line and the comparison of each one in both conditions was achieved through Partial Least Squares-discriminant analysis (PLS-DA). The value obtained from this analysis is variable important of the projection (VIP) that identifies metabolites that discriminate the ApoE3 to the ApoE4 condition.

The identification of the peaks was performed comparing their accurate mass with those available in metabolomics databases (HMDB, METLIN, KEGG and LIPIDMAPS) (González-Domínguez, García-Barrera, and Gómez-Ariza 2014).

5. Statistics

The different n or sample size was determined at least by 3 different cell passages. A parametric unpaired T-test was applied for the comparison of a variable in 2 different conditions or cell types whereas one-way analysis of variance (ANOVA) with a Turkey's posthoc test was used in the case of comparing more conditions. The software employed was GraphPad Prism 6 and the data were represented as mean ± SEM (standard error of the mean). P-value < than 0.05 was considered significant (* p-value < 0.05, ** p-value < 0.01, ***p-value < 0.001 and ****p-value < 0.0001)

Results

Chapter 1: Calcium signalling alterations triggered by ApoE4 expression.

Calcium signalling is the basis of astrocyte excitability, and hence, it is responsible for many essential processes such as gliotransmission or vascular dilatation and blood flux of the brain. Moreover, it is altered in animal models of AD. For all these reasons, we investigated the contribution of ApoE4 expression to calcium homeostasis in astrocytes.

1.1. Characterization of calcium signalling in ApoE3 and ApoE4 astrocytes.

To study calcium signalling, we employed Fura 2AM, a radiometric calcium dye. The ratio of the fluorescence of Fura2 is proportional to the cytosolic calcium concentration (see materials and methods, section 2.1.). To analyse the calcium homeostasis in detail, we quantified basal calcium, which refers to intracellular calcium at rest conditions before stimulations, and 2 parameters of neurotransmitter-induced calcium responses: (1) the peak, which is the maximum increment elicited by the stimulation that takes places after a few seconds of the stimulus, and (2) the recovery phase, which is the plateau of the response after the peak. We compared these 3 parameters between ApoE3 and ApoE4 astrocytes paying special attention in the peak since it is the most universally used parameter to study calcium signals, whereas the recovery phase is less informative.

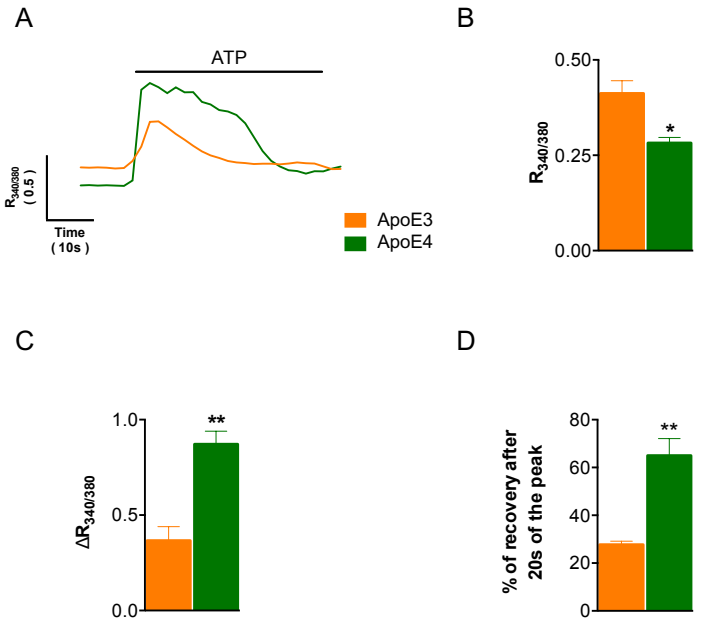

Figure R1: Calcium signalling in ApoE3 and ApoE4 astrocytes. (A) Representative calcium responses of ApoE3 (orange) and ApoE4 (green) astrocytes upon 100 µM ATP stimulation. Graph shows $R_{340/380}$ versus time (s). (B) Quantification of the intracellular calcium concentration in a non-stimulated condition. (C) Quantification of the 100 µM ATP-elicited cytosolic calcium increase (peak). (D) Quantification of the recovery after 20 seconds from the ATP peak taking into account the basal as 0% and the peak as 100%. Quantifications of several cells of 4 independent experiments. A parametric unpaired T-test was applied in all the sections.*$p<0.05$, **$p<0.01$

We stimulated these cells with ATP because purinergic receptor-elicited calcium signals are of high importance for astrocyte physiology, and since the activation of purinergic receptors has been proposed as a causative mechanism of astrocyte calcium hyperactivity in AD animal models (Delekate

et al. 2014). We used 100 μM of ATP since elicits maximal calcium responses in astrocytes (Barceló-Torns et al. 2011).

Figure R1A depicts the calcium representative traces from one ApoE3 and one ApoE4 astrocyte upon 100 μM ATP stimulation. Interestingly, both traces are totally different. As previously said, we analysed the 3 parameters: basal calcium (figure R1B), calcium peak after stimulation (figure R1C) and recovery phase after stimulation (figure R1D).

Firstly, the basal calcium measured as the Fura2 ratio of ApoE3 cells is 0.41 ± 0.03 whereas the one in ApoE4 cells is 0.28 ± 0.01 (Figure R1B). Therefore, the cytosolic calcium in non-stimulated conditions is higher in ApoE3 than in ApoE4 cells.

Secondly, ATP stimulation increased the cytosolic calcium of ApoE4 (increase of 0.87 ± 0.06 in Fura2 ratio) and ApoE3 cells (increase of 0.36 ± 0.07 in Fura2 ratio). Hence, ATP elicits a higher cytosolic calcium increase in ApoE4 astrocytes than in ApoE3 cells (figure R1C).

Thirdly, to calculate the recovery phase, we first normalized each response by considering the peak value of the ratio as 100%, and the minim value of the basal calcium ratio as 0%. Then, we measured the percentage of response after 20 seconds of the peak. With this analysis, we determined that ATP-triggered responses of ApoE4 cells have a more sustained plateau than ApoE3 astrocytes (percentage at 20 s of the peak 27.67 ± 1.51% in ApoE3 cells compared to 64.93 ± 1.17% in ApoE4 ones) (Figure R1D).

In conclusion, cytosolic calcium is lower at non-stimulated conditions, but ATP triggers higher and longer calcium responses in ApoE4 astrocytes, as compared to ApoE3 cells.

To study if the described alterations of calcium responses in ApoE4 astrocytes apply only to purinergic receptors or, conversely, they are general to other receptors, we stimulated the cells with other neurotransmitters. We used 10 μM of noradrenaline (NA) (figure R2A) and 100 μM acetylcholine (Ach) (figure R2B), which increase cytosolic calcium through the activation of G-protein coupled receptors.

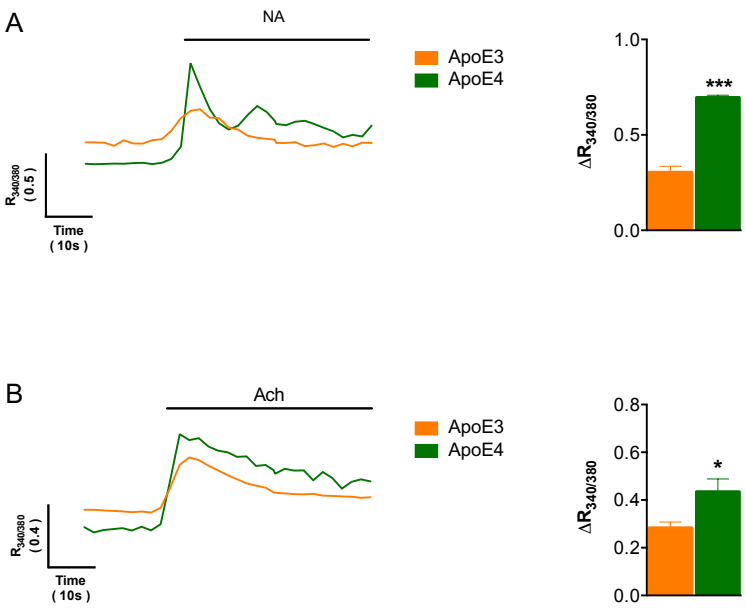

Figure R2: Calcium responses elicited by NA and Ach in ApoE3 and ApoE4 astrocytes. (A) Representative cytosolic calcium traces of single ApoE3 and ApoE4 cells after 10 µM of noradrenaline (NA) stimulation (left) and quantification of the peak of the response from several cells from 3 independent experiments (right). (B) Representative cytosolic calcium traces of single ApoE3 and ApoE4 cells after 100 µM of acetylcholine (Ach) stimulation (left) and quantification of the peak of the response of several cells from 4 independent experiments (right).Parametric unpaired T-test was applied to both analysis.*p<0.05, ***p<0.001

The cytosolic calcium peak of ApoE4 cells upon NA stimulation measured as the variation of the Fura2 ratio is 0.69 ± 0.01, whereas that increase in ApoE3 cells is 0.30 ± 0.03 (figure R2A). In addition, the recovery phase after NA stimulation, shows tended to be longer in ApoE4 cells than in ApoE3 (p-value of 0.07) with a percentage of response at the 20s from the peak of 18.31 ± 6.04% and 36.87 ± 5.02% in ApoE3 and ApoE4 astrocytes, respectively.

With respect to muscarinic stimulation, the Ach-elicited cytosolic calcium peak in ApoE4 cells is 0.43 ± 0.05, while the elicited peak in ApoE3 cells is 0.28 ± 0.02 (figure R2B). As previously, the recovery phase after Ach stimulation appears to be longer in ApoE4 cells than in ApoE3 astrocytes, with percentages of responses at the 20s of 51.06 ± 5.42% and 35.04 ± 5.83%, respectively.

Hence, both transmitters achieve a higher cytosolic calcium increases and it seems that also show longer recovery phase in ApoE4 cells. Consequently, the high cytosolic calcium increases and the more extended recovery phase are a general alteration of the calcium signalling in ApoE4 astrocytes.

1.2. Analysis of calcium signalling pathways in ApoE3 and ApoE4 astrocytes.

Calcium responses are achieved by the mobilization of calcium from organelles and the extracellular calcium entry. To understand the differences in calcium homeostasis in ApoE4 cells, we carried out a detailed study of the different calcium signalling pathways.

1.2.1. Calcium uptake by mitochondria

We first studied the calcium uptake by the mitochondria. To this end, cells were transfected with CEPIA-3mt plasmid, which codifies for a fluorescence calcium sensor protein targeting the mitochondria. Thus, we could measure the calcium concentration directly inside the mitochondria. After cell stimulation with 100 μM ATP, the quantification of the calcium uptake by the mitochondria (figure R3) measured as the variation of the ratio F/F_0 in ApoE4 cells is 0.91 ± 0.07, compared to the variation of the ratio in ApoE3 cells that is 0.56 ± 0.06. This result is in agreement with the higher ATP-mediated calcium responses in ApoE4 cells, as mitochondria buffering capacity increases with higher cytosolic calcium. Therefore, ApoE4 cell mitochondria uptake more calcium than ApoE3 cell mitochondria demonstrating that the higher ATP-elicited calcium responses in ApoE4 are not due to alterations in the mitochondrial calcium uptake.

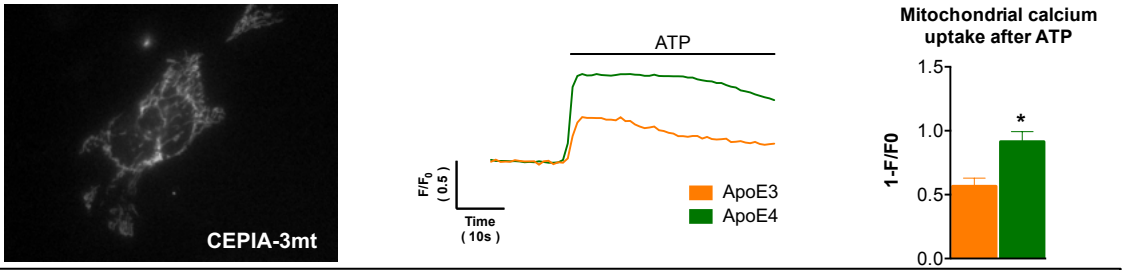

Figure R3: Mitochondrial calcium uptake mediated by ATP stimulation. ApoE3 and ApoE4 cells transfected with CEPIA-3mt (left panel), representative traces of the mitochondrial calcium of a single astrocyte after ATP stimulation (central panel), and quantification of the mitochondrial calcium uptake of cells from 3 independent experiments (right panel). Parametric unpaired T-test was applied. *p<0.05

1.2.2. Calcium release from the ER

Next, we examined the intracellular calcium mobilization. First, we studied the calcium release from the ER since it is regarded as the main source of cytosolic calcium in astrocytes.

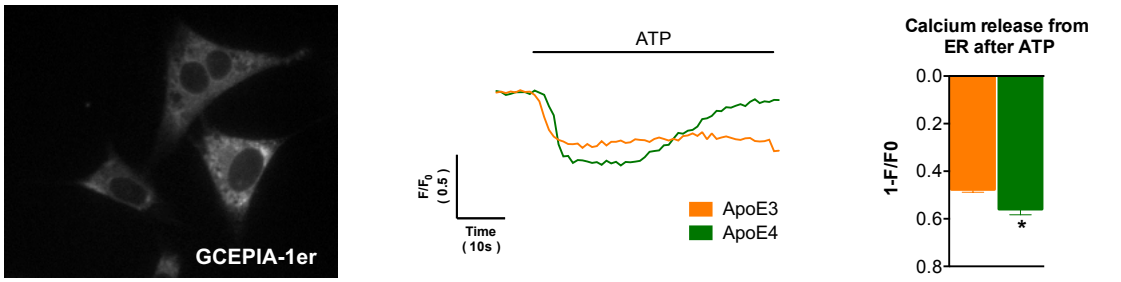

Figure R4: Calcium release from the ER mediated by ATP stimulation. Representative images of cells transfected with GCEPIA-1er (left panel), representative traces of the ER calcium of a single ApoE3 and ApoE4 cells after being stimulated by ATP (central panel), and quantification of the calcium release from the ER of several cells from 5 independent experiments (right panel). Parametric unpaired T-test was applied. *p<0.05

To this purpose, we used a ER calcium reporter similar to the one used for studying the calcium inside the mitochondria, GCEPIA-1er.

The quantification of the ER calcium release (figure R4) elicited by 100 μM ATP illustrates a higher calcium release from the ER in ApoE4 cells compared to ApoE3 astrocytes (the variation of the ratio F/F_0 is 0.55 ± 0.01 in ApoE4 astrocytes and 0.47 ± 0.01 in ApoE3 astrocytes) (figure R4). However, we believe that the difference in ER calcium release between ApoE3 and ApoE4 astrocytes does not completely explain the differences in cytosolic calcium responses between both cell lines.

1.2.3. Calcium mobilization from lysosomes

As lysosomes have been shown to be main calcium stores for ATP-mediated responses in astrocytes (Barceló-Torns et al. 2011), we analysed their calcium mobilization upon expression of ApoE3 and ApoE4 isoforms. Since there are not specific probes to study directly lysosomal calcium, we analysed its mobilization measuring cytosolic responses after the inhibition of lysosomal calcium entry and release. Figure R5A shows the inhibitors employed for the lysosomal study.

First, we used Ned-19 that inhibits lysosomal calcium release triggered by NAADP (figure R5A). After the treatment with this inhibitor we measured the basal calcium and then, cells were stimulated with ATP, quantifying the cytosolic calcium peak and the recovery phase (figure R5B). Concerning the intracellular cytosolic calcium of non-stimulated cells after the Ned-19 treatment, the basal calcium is similar to the DMSO-treated cells (DMSO was used as vehicle of Ned-19). In particular, the basal calcium of ApoE3 cells that were treated with Ned-19 is 0.36 ± 0.007, versus the basal calcium of DMSO-treated cells that is 0.35 ± 0.01. The basal calcium of ApoE4 treated cells is 0.28 ± 0.01 compared to the one from DMSO-treated cells that is 0.27 ± 0.02. Therefore, lysosomal calcium release does not alter basal calcium in any cell line and, consequently, a higher increase in the calcium release though NAADP receptors is not the cause of the decrease in basal calcium in ApoE4 cells.

Focusing on the cytosolic calcium peak and, comparing the calcium responses elicited by ATP in each cell type with its control, in both cases, the cytosolic calcium peak is reduced with the treatment. Nevertheless, the magnitude of the inhibition is different depending on the cells, being higher in the case of ApoE4 cells. Specifically, the percentage of inhibition

of the cytosolic calcium peak in Ned-19-treated ApoE3 cells is around 45% while this parameter is around 55% in Ned-19-treated ApoE4 cells. Interestingly, in the presence of Ned-19, ATP-elicited cytosolic responses of both cell lines have the same peak magnitude. Altogether, this indicates that the principal difference in the ATP-stimulated calcium peak in both cell lines is due to the lysosomal calcium release (figure R5B).

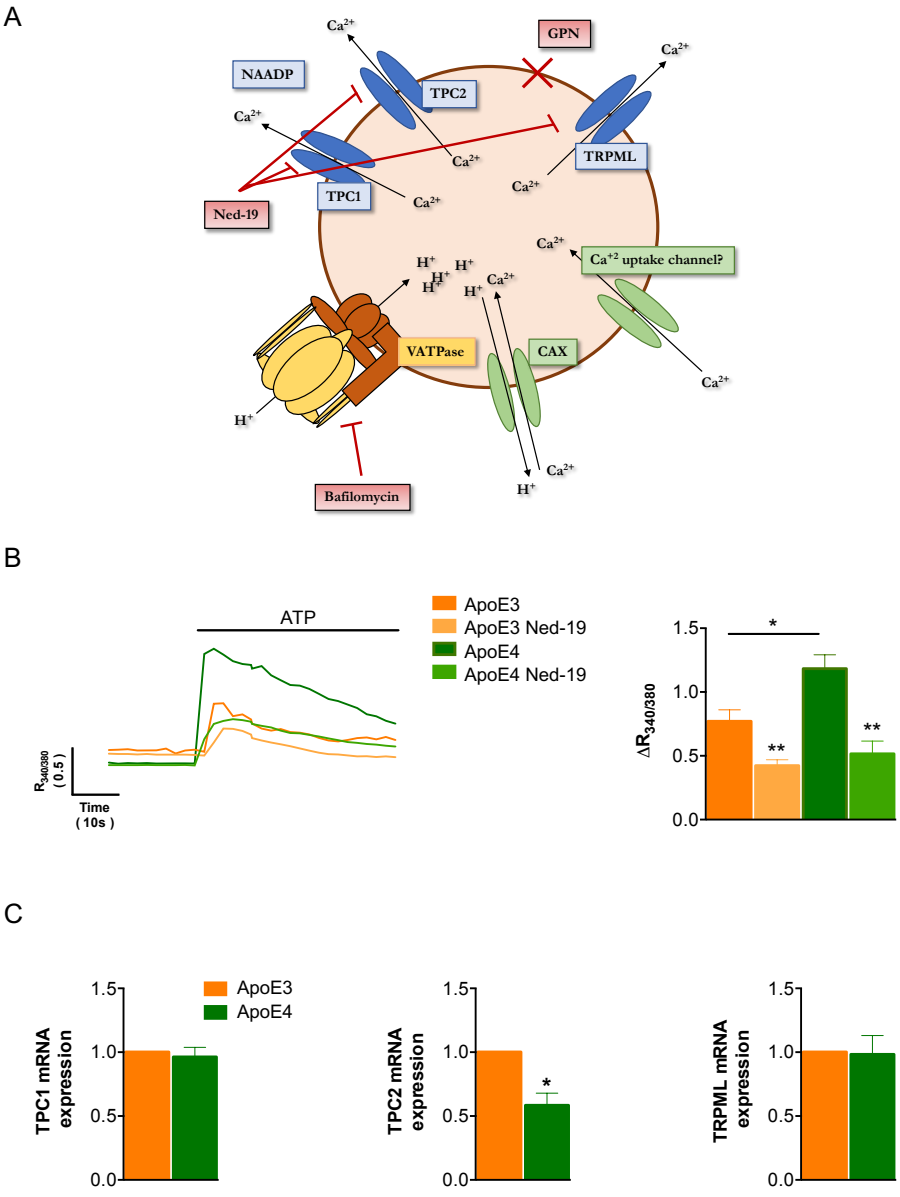

Figure R5: Lysosomal calcium release in ApoE3 and ApoE4 astrocytes. (A) Images of main calcium related channels and receptors of the lysosome (in green channels that uptake calcium and in blue that release calcium) In red, drugs that inhibit these pathways.(B) Representative traces and quantification of ATP-induced cytosolic calcium responses of cells from 3 independent experiments treated with DMSO as a vehicle or 100 µM Ned-19 for 20 min. (C) Quantification of mRNA expression through real time PCR of Tpc1(TBP) and Tpc2 (Gapdh) from 3 independent experiments and TRPML (18s and Gapdh) from 4 independent experiments. One way ANOVA was applied in section B and unpaired parametric T-test in section C. *p<0.05, **p<0.01

With respect to the recovery phase after the ATP-elicited cytosolic calcium peak, the plateau of Ned-19-treated ApoE3 and ApoE4 cells is similar to the plateaus of DMSO-treated cells. It is 38.74 ± 0.86% of the response peak at 20 seconds in Ned-19 treated ApoE3 cells compared to the plateau of cells treated with DMSO (41.63 ± 4.08%). In the case of ApoE4 astrocytes, the plateau of Ned-19-treated cells is 72.04 ± 3.35% of the peak compared to the plateau of DMSO-treated cells (72.16 ± 1.91%). Hence, the lysosomal calcium release is not the cause of the slower recovery phase of the ATP-triggered calcium responses in ApoE4 astrocytes.

A higher calcium release from lysosomes can be due to several factors such as differential expression or different regulation of NAADP receptors or higher calcium stored at the lysosomes. To examine the first option, we analysed the mRNA expression of the putative NAADP receptors: TPC1, TPC2 and TRPML by real-time qPCR. The results were normalized to the expression of these proteins in ApoE3 cells (value equal to 1). TPC1 and TRPML channels show no difference in mRNA expression between both cell lines (expression values of both closet to 1) (figure R5C) whereas the expression of TPC2 is 0.58 ± 0.09 in ApoE4 astrocytes (figure R5C). Therefore, we can conclude that the higher calcium release in ApoE4 astrocytes is not due to higher expression of NAADP receptors, on the contrary, in these cells, there is less expression of TPC2 channels, maybe because of a compensatory mechanism to limit the lysosomal calcium release after the agonist stimulation.

Subsequently, we investigated if the higher calcium release from the lysosomes in ApoE4 astrocytes could be explained by higher calcium content in the lysosomes. We stimulated the cells with GPN, a peptide that hydrolyses lysosomes with active cathepsin C (figure R5A). Hence, hydrolysed lysosomes release their content to the cytosol, and its quantification allows to approximate the calcium content stored in the lysosomes (X. Z. Zhong et al. 2017). Therefore, as an indirect and relative measurement of

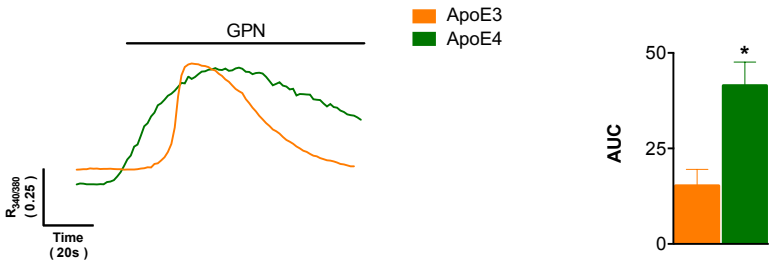

Figure R6: Lysosomal calcium content of ApoE3 and ApoE4 astrocytes. Representative traces of a single cell and quantification of the area under the curve (AUC) of intracellular calcium after lysing the lysosomes with 200 µM GPN. Unpaired parametric T-test was applied. *p<0.05

lysosomal calcium content, we measured the area under the curve (AUC) of the cytosolic calcium increase after GPN stimulation of 3 independent experiments (figure R6). 200 µM GPN elicited an AUC of 41.42 ± 6.19 in ApoE4 cells and of 15.21 ± 4.32 in ApoE3 cells. Therefore, this result indicates that the concentration of lysosomal calcium is higher in ApoE4 cells than in ApoE3 ones.

The mechanism by which lysosomes uptake calcium from the cytosol, as it is explained in the introduction, is supposed to be indirectly through the V-ATPase, that pumps protons in the lysosome. Then, the CAX protein exchanges protons for calcium ions from the cytosol. To inhibit this pathway, we used 2 µM Bafilomycin A1, which inhibits the V-ATPase activity (figure R5A).

First, we calculated the intracellular calcium in non-stimulated condition. The one in ApoE4 cells treated with Bafilomycin or the mean of the Fura2 ratio is 0.40 ± 0.05, a value that is higher than in DMSO-treated ApoE4 cells (p-value: 0.08) suggesting that the lower basal calcium in ApoE4 cells results from an increase in the uptake of lysosomal calcium. The

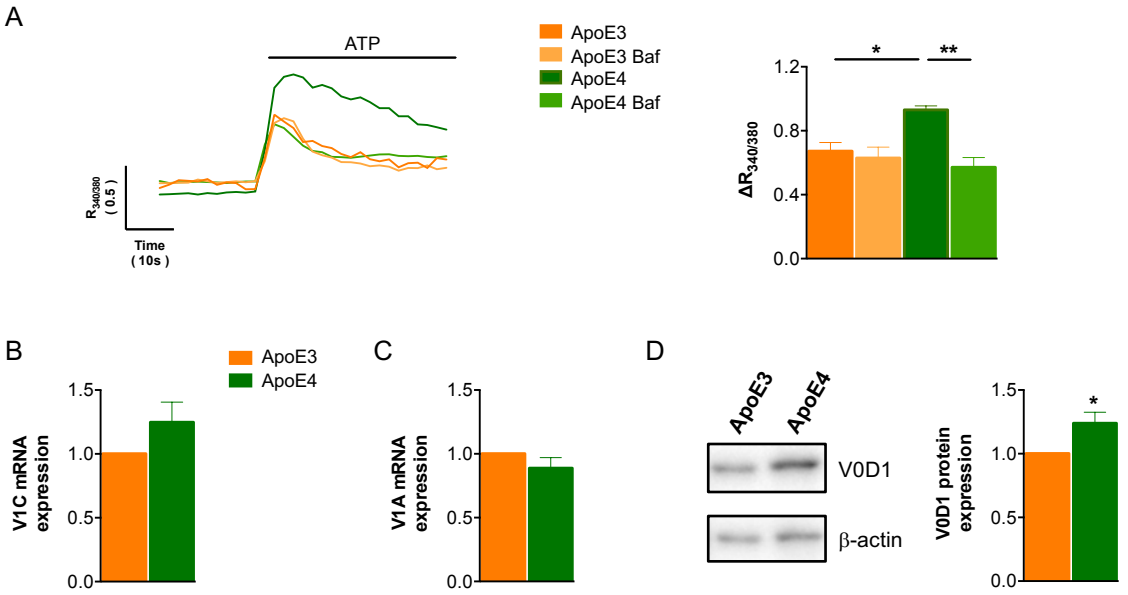

Figure R7: Lysosomal calcium uptake of ApoE3 and ApoE4 astrocytes. (A) Representative traces of a single cells and quantification of cytosolic calcium peak of cells from 3 independent experiments treated with DMSO or 2 µM Bafilomycin A1 for 20 min. (B) Quantification of mRNA expression through real time PCR of V-ATPase subunit V1C (18s and Gapdh) from 6 independent experiments and (C) V1A (18s and Gapdh) from 3 independent experiments. (D) Quantification of protein expression through western blot of V-ATPase subunit V0D1 (β-actin) from 4 independent experiments. One way ANOVA was applied in section A and unpaired parametric T-test was applied in sections B, C and D. *p<0.05, **p<0.01

trend observed in basal calcium in ApoE3 cells treated with the drug or with the vehicle is similar.

Concerning ATP-elicited cytosolic peak, Bafilomycin treatment does not inhibit it in ApoE3 cells, where the Fura2 variation is around 0.6 in Bafilomycin-treated and in DMSO-treated condition (figure R7A), contrary to what it is shown in the cytosolic calcium peak after Ned-19 treatment. This discrepancy is probably due to: (1) lysosomes are not a leaky calcium stores, so Bafilomycin does not empty them of calcium unless first they release it, or (2) Bafilomycin is enough to achieve maximal ATP-elicited lysosomal calcium release due to a low lysosomal calcium content. On the other hand, Bafilomycin treatment inhibits the lysosomal calcium release after the ATP stimulation in ApoE4 astrocytes (the variation of Fura2 ratio is 0.57 ± 0.06 in Bafilomycin-treated cells compared to 0.92 ± 0.02 of DMSO-treated cells), revealing that the higher cytosolic responses elicited by ATP are due to a higher calcium uptake and release of lysosomes in these particular cells. With respect to the recovery phase from the ATP-elicited calcium responses after Bafilomycin treatment, neither the recovery phase of ApoE3 nor of ApoE4 cells is altered with the treatment.

Altogether, ApoE3 cells uptake less calcium to the lysosomes than ApoE4 astrocytes, a fact that affects both, basal calcium that is higher and the lysosomal calcium release elicited by ATP.

To elucidate why there is a higher V-ATPase activity (that indirectly controls lysosomal calcium uptake) in ApoE4 cells, we analysed the expression of this pump. V-ATPase is formed by different subunits grouped into 2 domains, V0 (that is inserted in the lysosomal membrane) and V1 (that faces the cytosol). We measured the expression of 2 subunits of the V1 (V1C and V1A) through qPCR (figure R7B and C) and one from V0 (V0D1) through western blot (figure R7D). The results were normalized to the expression of these proteins in ApoE3 cells (value equal to 1). V1C seems to be more expressed in ApoE4 cells, although the difference is not significant (1.24 ± 0.15 expression in ApoE4 cells compared to ApoE3 expression; p-value: 0.14) and V1A is similarly expressed in both cell lines (value around 1), whereas V0D1 is significantly more expressed in ApoE4 cells (1.24 ± 0.08 compared to ApoE3 cell expression; p-value: 0.03). Therefore, not all the subunits are upregulated in ApoE4 cells.

To sum up, the lower basal calcium and the higher ATP-elicited calcium increase in ApoE4 cells are due to a high lysosomal calcium concentration. This depends on the V-ATPase indirectly calcium uptake. With respect to ApoE3 cells, the lower ATP-elicited cytosolic calcium responses are due to lower ER calcium release and especially lower lysosomal calcium release owing to a lower V-ATPase activity, a fact that is also causing the higher basal calcium in non-stimulated ApoE3 cells.

1.2.3.1. pH of lysosomes

The higher V-ATPase activity in ApoE4 cells when compared to ApoE3 cells could lead to a lower pH of the lysosomes, which in turn, could influence lysosomal functions, including regulation of calcium mobilization. For instance, the activation of TPCs and TRPML channels has been related to the pH of lysosomes (X.-P. Dong et al. 2008; Pitt et al. 2010; Schieder et al. 2010) being the TRPML potentiated at low pH in macrophages (X.-P. Dong et al. 2008). Thus, since the variations of lysosomal pH could also be involved in the lysosomal calcium release we examined this process in ApoE3 and ApoE4 cells. This measurement was performed in Dr. Sánchez laboratory by fluorimetry and using pH sensor lysosensor (Valladolid). These results show that the lysosomal pH of ApoE3 cells is 4.51 ± 0.009 whereas the lysosomal pH of ApoE4 astrocytes is 4.65 ± 0.009 (figure R8). Although significant, we consider this difference minimal, by contrast to that the magnitude of different calcium concentration and release after stimulation is large.

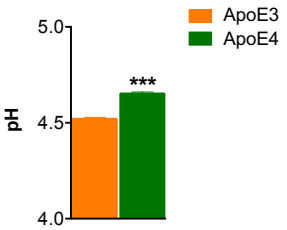

Figure R8: pH of Lysosomes in ApoE3 and ApoE4 cells. pH quantification using Lysosensor from 3 independent experiments. Unpaired parametric T-test was applied. ***p<0.001

Taking together, all our results suggest that in ApoE4 astrocytes there are higher V-ATPase activity and calcium proton exchanger CAX activities. Thus, the result is an increased exchange of protons for calcium, and hence, the pH is maintained unchanged whereas the calcium inside lysosomes is increased.

1.2.4. Extracellular calcium entry

Finally, we studied the contribution of extracellular calcium entry to the ATP-triggered calcium responses. To this purpose, we added, to the medium, EGTA that chelates the calcium. Sectional experiments presented previously have been performed in DMEM supplemented with 10% of FBS, although, due to the high calcium concentration of this medium, we employed a saline medium (KH) supplemented with 10% of FBS, where the calcium ions can be chelate by 1 mM of EGTA for 5 minutes.

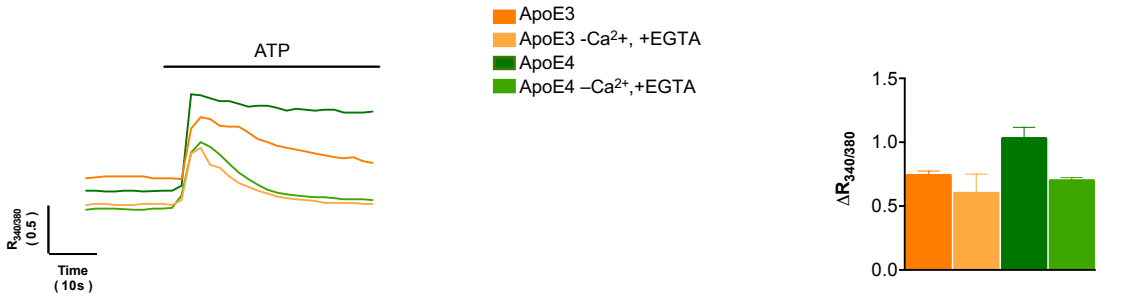

Figure R9: Extracellular calcium entry of ApoE3 and ApoE4 astrocyte. Representative traces and quantification of the peak from 3 independent experiments of the 100 µM ATP-triggered cytosolic calcium responses of cells in KH medium supplemented with 10% of FBS with or without calcium and 1 mM of EGTA for 5 minutes. One way ANOVA was applied.

The quantification of the 100 µM ATP-triggered cytosolic calcium peak shows that calcium responses in this new medium are equal to the ones reported in DMEM supplemented with 10% FBS. Moreover, EGTA inhibition of the cytosolic peak after stimulation in ApoE3 cells is low, around 19%, and not statistically significant. This indicates that the ATP-elicited responses in ApoE3 cells are almost not contributed by the extracellular calcium entry. In ApoE4 cells, the inhibition of the ATP-elicited cytosolic calcium peak is around 32% and again, not statistically significant (figure R9). Therefore, the contribution of calcium entry to the cytosol after the ATP stimulation is lower than calcium release from lysosomes in both cell lines. In addition, we cannot exclude that EGTA slightly affects ER calcium release and thus, the contribution of the extracellular calcium entry can be even less.

In both cell lines, the recovery phase and the basal calcium are diminished after the EGTA treatment, as it has been reported for many different cell types, probably, because of the efflux of calcium from the cell to the extracellular space.

1.3. Analysis of the causes that trigger different calcium responses in ApoE4 astrocytes.

1.3.1. Study of the effect of different ApoE quantity

Next, we examined the mechanisms by which ApoE4 alters V-ATPase complex causing calcium dysregulations. As it has been mentioned in the introduction, ApoE4 individuals express lower quantity of the protein than ApoE3 ones (Talwar et al. 2016). For this reason, we firstly assessed the expression of ApoE in both cell lines by qPCR and by western blot (figure R10).

qPCR showed that ApoE mRNA levels are significantly lower in ApoE4 cells than in ApoE3 cells (0.25 ± 0.08 versus ApoE3 value) (figure 10A). Western blot analysis further confirmed these results, showing a lower ApoE protein expression in ApoE4 cells compared to ApoE3 (figure 10B).

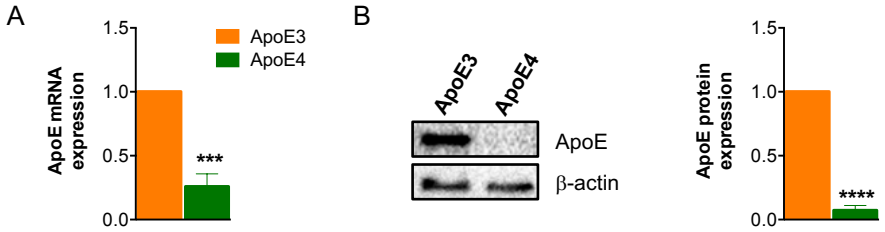

Figure R10: ApoE expression in ApoE3 and ApoE4 cells. (A) ApoE mRNA expression relative to Gapdh and 18s in ApoE3 and ApoE4 astrocytes quantified by qPCR from 3 independent experiments. (B) ApoE protein expression relative to β-actin of ApoE3 and ApoE4 cells quantified by western blot from 3 independent experiments. Unpaired parametric T-test was applied. ***p<0.001, ****p<0.0001

Therefore, we modulated the quantity of ApoE in ApoE3 and ApoE4 cells to understand if the amount of ApoE influences calcium signalling or, on the contrary, the dysregulation is caused by the ApoE4 isoform. We used 2 strategies for this purpose: (1) to decrease the levels of ApoE in ApoE3 cells, and (2) to increase the levels of ApoE in ApoE4 cells.

On the one hand, to decrease the amount of ApoE in ApoE3 astrocytes, a siRNA of ApoE was employed. After 72h of ApoE siRNA transfection, the expression of ApoE in ApoE3 astrocytes was reduced (figure R11A). At this time point, we measured the basal calcium. We found that is not affected by the reduction of ApoE in ApoE3 cells. Specifically, the cells transfected with the siRNA display a Fura2 ratio of 0.39 ± 0.02, similar to the lipofectamine (Fura2 ratio of 0.37 ± 0.02) or scramble (Fura2 ratio of 0.35 ± 0.01) transfected condition. We then stimulated the cells with 100 μM of ATP and we recorded the cytosolic calcium

responses (figure R11B). The quantification of ATP-triggered cytosolic calcium peak shows no differences after ApoE silencing since the increase in Fura2 ratio is 0.33 ± 0.10, which is similar to the peak of the ApoE3 cells transfected with a scramble siRNA (0.40 ± 0.05) or with lipofectamine without any siRNA (0.33 ± 0.13) (figure R11C). Hence, the diminution of the ApoE amount in ApoE3 cells does not lead to any difference with respect to the cytosolic calcium increase upon ATP stimulation.

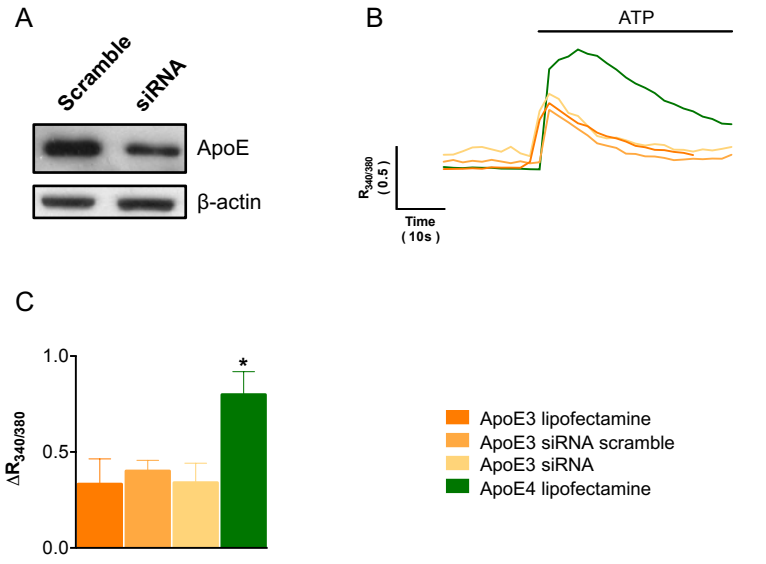

Figure R11: Modulation of the ApoE quantity in ApoE3 cells. (A) Representative ApoE western blot of ApoE3 cells transfected with siRNA scramble or ApoE siRNA. (B) Representative ATP-induced calcium responses of single ApoE3 astrocytes (transfected with lipofectamine, scramble or ApoE siRNA) and ApoE4 cell with lipofectamine only. (C) Quantification of the cytosolic calcium peak after ATP stimulation of 4 independent experiments. One way ANOVA was applied. *p<0.05

On the other hand, we transfected ApoE4 cells with the ApoE4-GFP plasmid to increase the ApoE amount. This plasmid codifies for a sequence of GFP that is bound to the sequence of ApoE, allowing us to know which cells are transfected and which are not. First, we set up the conditions of the transfection by immunocytochemistry (figure R12A) and we corroborated that the GFP signal did not interfere with the Fura2 fluorescence. Once we had the correct concentration of lipofectamine and plasmid, we transfected the cell for 72 h and we monitored calcium considering only the cells stained with GFP fluorescence (those with higher ApoE expression). In this case, the basal calcium quantification showed a similar Fura2 ratio (around 0.24) in ApoE4 cells transfected with both plasmids, GFP and ApoE4-GFP. Therefore, the quantity of ApoE4 in ApoE4 cells does not affect basal calcium. Concerning the 100 μM ATP-triggered calcium peak of ApoE4 cells, this parameter was normalized to the cytosolic calcium increment of ApoE3 cells GFP-transfected and presented as percentage. Thus, the peak after the stimulation of ApoE3 cell is 100%. The reason of that was that the efficiency of the transfection was not homogeneous. For the same reason, we applied the statistics to single cells and not to the independent days of experiments (figure R12C). The ATP-induced calcium peak of ApoE4 cells transfected with the ApoE4 plasmid

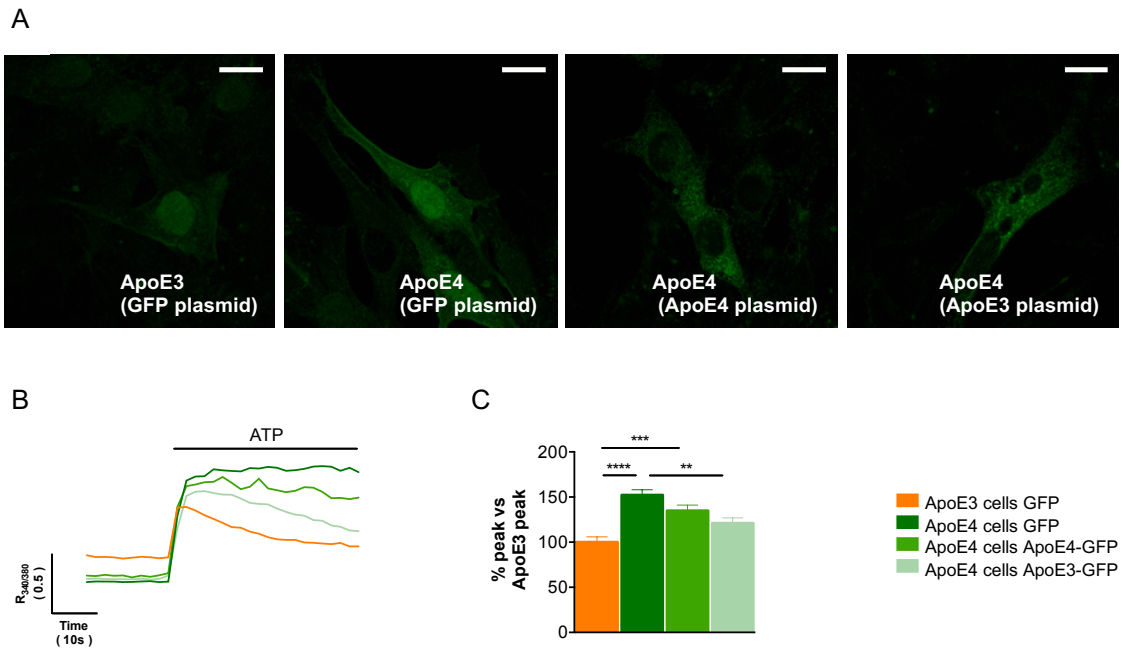

Figure R12: Calcium signalling after modulation of ApoE expression in ApoE4 cells. (A) Representative images from immunocytochemistry of GFP plasmid transfection in ApoE3 cells and GFP, ApoE3-GFP and ApoE4-GFP plasmid transfection in ApoE4 cells. Scale bar represents 15 μm (B) Representative traces of 100 μM ATP-elicited calcium responses of ApoE3 single cell transfected with GFP and ApoE4 single cells transfected with GFP, ApoE4-GFP and ApoE3-GFP. (C) Quantification of the cytosolic calcium peak after ATP stimulation normalizing all the conditions to calcium responses in ApoE3 cells transfected with GFP. Only GFP fluorescent cells were analysed. (at least N=30 from 4 independent experiments). One way ANOVA was applied. **p<0.01, ***p<0.001, ****p<0.0001.

is 135 ± 6.18%, compared to the one of the ApoE4 cells transfected with GFP plasmid that is 152.2 ± 5.89% (figure R12B and C). ATP-elicited cytosolic calcium peak decreases when ApoE4 cells are transfected with ApoE4 plasmid, although this decrease is not significant, indicating that the augment of ApoE4 does not interfere with this process.

In addition, the recovery phase after the stimulation of ApoE4 cells transfected with ApoE4 is equal to the GFP-transfected cells. In particular, the response after 20 seconds of the peak is 85 ± 3.77% in ApoE4 cells ApoE4-GFP-transfected compared to the GFP-transfected cells that is 81.01 ± 2.49%.

Overall, our results show that neither the reduction of ApoE in ApoE3 cells, nor the upregulation of ApoE4 in ApoE4 cells alters the cytosolic calcium increase upon ATP stimulation. Therefore, the lower quantity of ApoE in ApoE4 cells is not the cause of the differences in calcium homeostasis.

1.3.2. Study of the ApoE isoform

To explore if there is a lack of function of the isoform ApoE4, we transfected ApoE4 astrocytes with a ApoE3-GFP plasmid (figure R12). Concerning basal calcium, the results are similar to the transfection with ApoE4-GFP being the Fura2 ratio around 0.24 in ApoE4 cells transfected with ApoE3-GFP or with GFP. Thus, ApoE3 presence in ApoE4 cells does not change basal calcium. Interestingly, this transfection yielded to a partial reduction of the ATP-mediated calcium peak. As it is mention before, the peak values were normalized to ApoE3 cells transfected with GFP. In particular, it is shown an ATP-triggered cytosolic calcium peak of 121.1 ± 5.84% compared to the percentage of the ATP-mediated calcium increment in ApoE4 cells transfected with GFP plasmid that is 152.2 ± 5.89 (figure R12B and C). This suggests that the expression of ApoE3 isoform rather than the augment of the ApoE quantity, could partially restore the differences of ATP-induced calcium peak.

However, the recovery phase after the ATP stimulation is similar between the ApoE4 cells transfected with ApoE3-GFP and with GFP, being the percentage of response at 20 seconds of the peak of 84.26 ± 4.92 compared to 81.01 ± 2.49% of GFP-transfected cells.

1.3.3. Study of ApoE lipidation

As it has been mentioned previously, the difference between ApoE3 and ApoE4 isoform is a single amino acid change. This change implies in ApoE4 a different domain conformation (Yamazaki et al. 2016) and a reduced ability to bind lipids or to be lipidated (Mahley and Huang 2012). As our results show that the differences on calcium signalling between ApoE3 and ApoE4 astrocytes are mainly due to the isoform type and not to the quantity of protein, we tested if a different lipidation state between the isoforms could be responsible for the calcium homeostasis alterations.

The binding of ApoE to lipids is achieved by the membrane receptor ABCA1. To modulate the lipid binding of ApoE we used 2 different approaches. The first one was to treat the cells with Bexarotene, an inductor of ABCA1 (Zhao et al. 2014) and ApoE (Cramer et al. 2012) synthesis already tested in clinical trials against ApoE4 related pathology (Ghosal et al. 2016). The second one relied on the treatment with the peptide CS-6253 (CS) to increase the ApoE lipidation. This peptide induces the stabilization of ABCA1 receptor and it has also been demonstrated that improves ApoE4 pathology in a mouse model (Boehm-Cagan and

Michaelson 2014). Then, ApoE3 and ApoE4 cells were treated with each treatment individually and with the combination of both (figure R13).

Doses and period of both treatments were defined based on previous data. In the case of Bexarotene (Bx) in a previous study conducted in the same cell lines employed 0.1μM for 24 hours (Zhao et al. 2014) whereas the condition for CS (5 hours of 10mg/mL of CS) were based on previous data from Dr. Jon Johansson (Artery therapeutics), who provided us the peptide, that they showed an increase in the cholesterol efflux.

After these treatments, basal calcium and 100 μM ATP-induced calcium responses were studied. Our results showed that the lipidation status does not change basal calcium since the Fura2 ratio is around 0.40 in the case of ApoE3 cells in all the conditions, and 0.26 in the case of ApoE4 astrocytes in all the conditions. Regarding the cytosolic calcium increase upon the stimulation with ATP, we also found similar increases of the Fura2 ratio between treatment and non-treatment conditions. Specifically, the peak increase measured as the variation of the Fura2 ratio is 0.34 ± 0.03 in control ApoE3 astrocytes, 0.35 ± 0.08 in cells

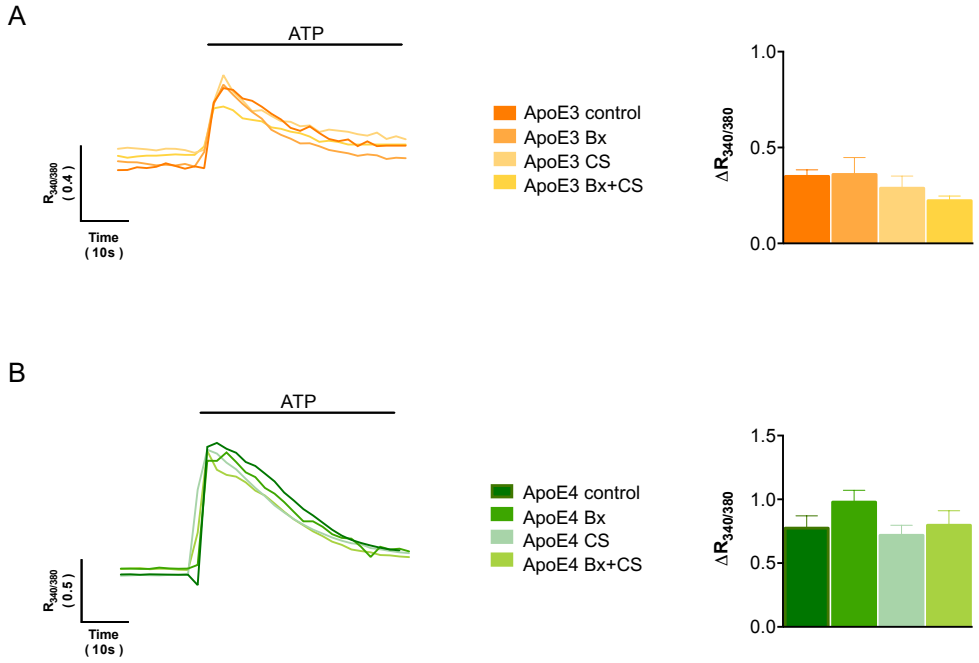

Figure R13: ATP-mediated calcium responses after ABCA1 upregulation and stabilization. (A) Representative 100 μM ATP-induced calcium traces of a single ApoE3 cells treated or not with 0.1 μM of Bx for 24h or 5h with 10mg/mL of CS or both together and quantification of these cytosolic increases. (B) Representative cytosolic calcium traces and quantification of the cytosolic increase upon cell stimulation with ATP in ApoE4 cells treated or not with 0.1uM of Bx for 24h or 5 hours with 10mg/mL of CS or both together. In all the experiments the quantification was performed from several cells of at least 3 independent experiments. One way ANOVA was applied.

treated with Bx, 0.28 ± 0.06 with CS treatment and 0.22 ± 0.02 if both compounds were applied (figure R13A). A similar conclusion is obtained in ApoE4 cells, where none of the treatments affects ATP-elicited cytosolic calcium peak. In particular, ApoE4 cells treated with Bx display an ATP-elicited calcium peak of 0.97 ± 0.09, 0.71 ± 0.07 with CS and 0.79 ± 0.11 with the combination of both treatments. In non-treated ApoE4 astrocytes, ATP elicits an increase of 0.77 ± 0.09 (figure R13B).

Therefore, our results demonstrate that the lipidation status of ApoE does not modulate basal calcium or ATP-induced calcium increases.

1.3.4. Analysis of lysosomal localization of ApoE

We next explored if the ApoE is localized in the lysosomes and, hence, if it is interacting directly with the V-ATPase. To assess the presence of endogenous ApoE in the ApoE3 lysosomes, we performed a colocalization assay by immunocytochemistry using Lamp1 (lysosomal marker) and ApoE in ApoE3 cells (figure R14A). To study the colocalization in

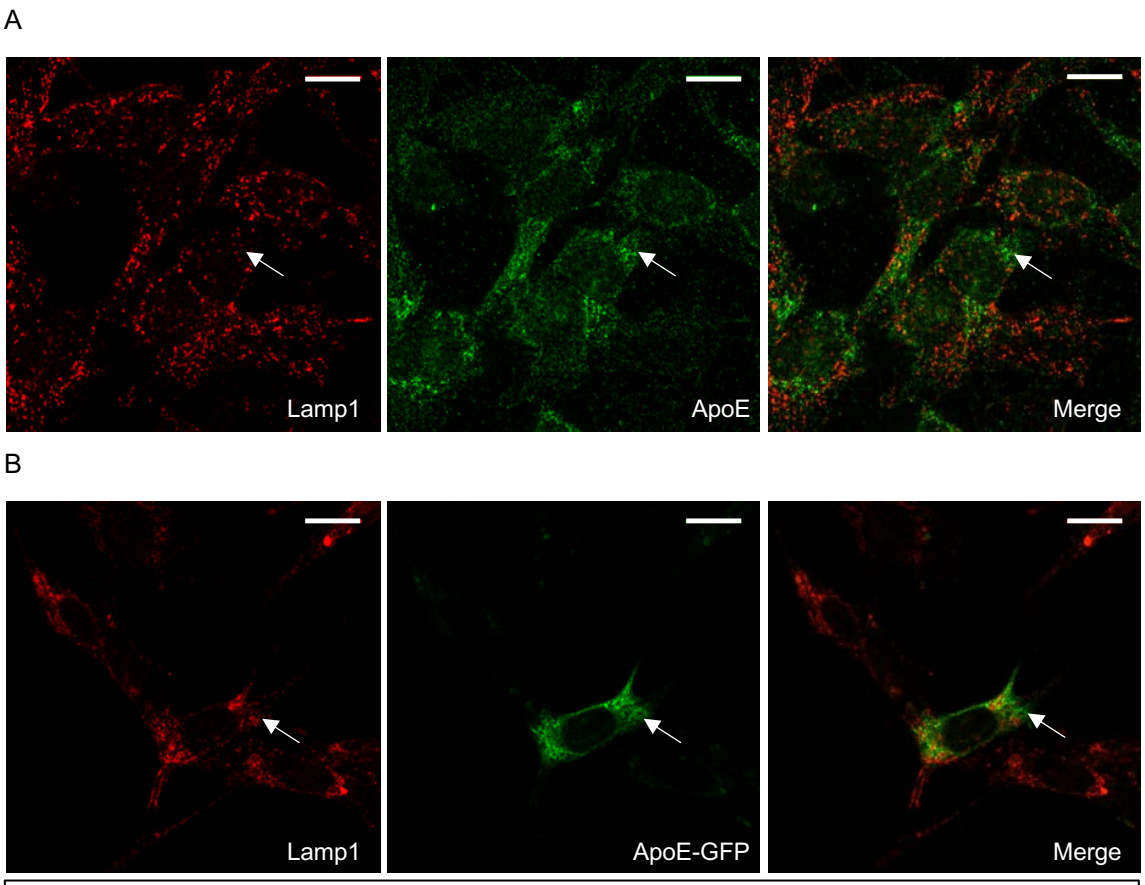

Figure R14: ApoE presence in the lysosomes. (A) Representative images of the Lamp1 and ApoE immunocytochemistry in ApoE3 cells. (B) Representative images of the Lamp1 immunocytochemistry and ApoE-GFP fluorescence in ApoE4 cells. White arrows represent area with high ApoE staining. Scale bar represents 15 μm.

ApoE4 cells, we performed a Lamp1 immunocytochemistry after the ApoE4-GFP transfection of ApoE4 cells (figure R14B).

As depicted in figure R14, the colocalization of both proteins is very low in both cell lines, since regions of high fluorescence of ApoE does not correlate with Lamp1 staining (white arrows). Therefore, we can conclude that ApoE is not predominantly present in the lysosomes and is probably affecting lysosomes in an indirect manner.

1.3.5. Study of the lipid profile of ApoE3 and ApoE4 astrocytes

ApoE mediates extracellular lipid transport and the ApoE4 isoform does not perform this function as properly as the ApoE3 does (Mahley and Huang 2012). The extracellular transport of lipids may affect lipid membrane composition that it has been described as an influent factor of the activity of channels or receptors (Tillman and Cascio 2003; A. G. Lee 2006). Taking into account these observations, a plausible hypothesis is that ApoE isoforms may differentially affect the lipid membrane composition of the astrocytes and specifically the one of the lysosomes affecting V-ATPase activity. To test this hypothesis, we performed 2 lipid studies in collaboration with Dr. Jose Luis Gómez Ariza from the University of Huelva: one analysing lipid differences in the whole cell and the other for only in lysosomal membrane lipids.

The technique used was an untargeted metabolome of hydrophobic compounds of ApoE3 and ApoE4 astrocytes, where we found most of the lipids. Once the metabolome was carried out, a partial list squares-discriminant analysis (PLS-DA) was applied to the data. PLS-DA is a mathematical analysis formed by different algorithms that allow to identify which

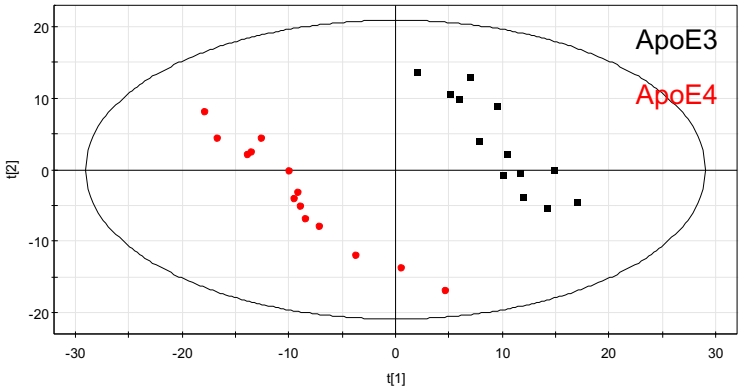

Predictive parameters	Values
R^2Y	0.995
Q^2	0.841

Figure R15: PLS-DA analysis to obtain the metabolites that discriminate ApoE3 from ApoE4 astrocytes. Graph of the PLS-DA analysis. The table contains the predictive parameters of the model. R^2Y allows to confirm that the discrimination of the factor axes was well-performed. Q^2 cumulated index determine the predictive quality of the model. Both parameters have to be close to 1. These results were performed in Huelva University by Dr. Gómez Ariza group.

metabolites are the most suitable to represent the difference between ApoE3 and ApoE4 astrocytes. In other words, the metabolites that are changed between both cell lines. As addressed in figure R15, ApoE3 and ApoE4 cells are easily differentiated based on their metabolites. Furthermore, the predictive quality of the model (Q^2) and the parameter that shows the good discrimination of the variables (R^2Y) are close to 1, meaning that the prediction and the discrimination are optimal (figure R15). Therefore, there are important differences between both cell lines regarding their profile of metabolites.

The identification of metabolites was carried out based on their experimental accurate mass (m/z) by comparing this variable to available metabolomics databases

Metabolite	m/z	VIP	Change
PC(18:3/22:4)	864.494	1.92	↓
PC(18:2/20:4)	810.468	1.85	↑
PC(18:3/22:5)	862.514	1.84	↓
PC(16:0/16:0)	734.475	1.36	↑
PC(18:2/18:0)	808.454	1.32	↑
PC(16:1/16:0)	732.57	1.24	↑
PC(16:0/18:2)	758.596	1.12	↑
PC(18:2/22:4)	866.529	1.07	↓
PC(16:0/22:6)	828.475	1.06	↑
PC(18:0/22:6)	856.567	1	↑
PS(22:6/22:6)	880.557	1.63	↓
PS(22:6/22:6)	902.575	1.12	↓
PL	924.583	2.19	↓
PL	922.596	1.85	↑
PL	898.567	1.66	↓
PL	896.552	1.35	↓
PL	908.593	1.31	↓
PL	890.593	1.29	↓
PL	904.57	1.26	↓
PL	888.581	1.12	↓
PL	938.459	1.09	↓
PL	870.538	1.06	↓
PL	940.512	1.05	↑
LPC(18:0)	524.293	1.82	↓
LPC(22:6)	590.266	1.74	↓
LPC(18:3)	540.372	1.5	↓
LPC(18:1)	522.3	1.43	↓
LPC(20:4)	566.397	1.34	↓
LPC(18:0)	546.393	1.26	↓
LPC(18:1)	544.378	1.21	↓
LPL	536.269	2.43	↓
LPL	586.333	1.07	↓
Decanoyl-carnitine	316.284	1.41	↑
Oleyl-carnitine	426.378	1.32	↑
Miritoyl-carnitine	372.408	1.22	↑
Valine	118.046	2.05	↑
Choline	104.096	1.82	↑
Glutamate	148.054	1.43	↑
Acetylcholine	146.053	1.25	↑
Tyrosine	182.162	1.12	↑
Alanine	900.285	1.04	↓

Table R1: Identification of principal metabolites that change between ApoE4 cells compared to ApoE3. The table contains the name of the metabolites, their mass (m)/ charge (z), the variable VIP and the direction of the change. ApoE4 astrocyte values above those in ApoE3 astrocyte values were compared to determine the qualitative fold change. Phosphatidylcholine (PC), phoaphatidylserine (PS), phospholipid (PL), lyso phosphatidylcholine (LPC), lysophospholipids (LPL)

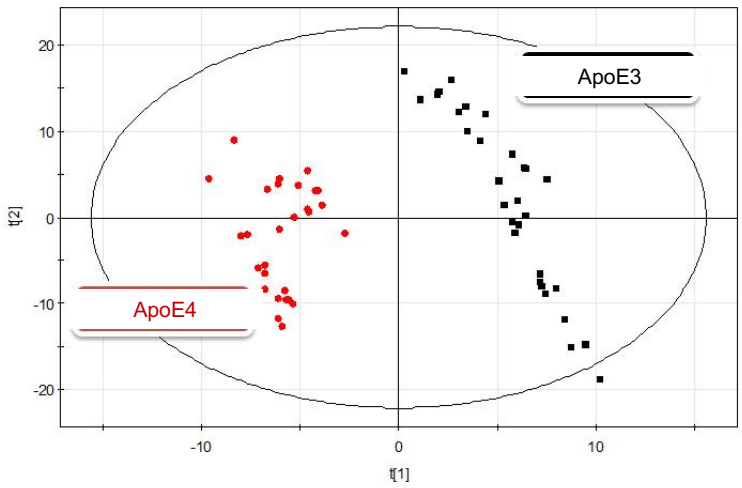

Figure R16: PLS-DA analysis to obtain the lysosomal membrane metabolites that discriminate ApoE3 from ApoE4 astrocytes. Graph of the PLS-DA analysis. These results were performed in Huelva University by Dr. Gómez Ariza group.

(METLIN, LIPIDMAPS, KEGG and HMDB). In addition, the identification was confirmed through the fragmentation pattern of each species reported in the literature. The results are displayed in table R1. VIP summarizes the contribution of each metabolite to the discrimination model. More concretely, a bigger VIP represents that this metabolite contributes more to the discrimination from both cell lines. Values below one are considered as a no difference between them (Chong and Jun 2005).

Metabolite	m/z	VIP	FC (E4/E3)
PC(16:0/16:0)	756.560	1.09	0.77
PC(16:0/18:0)	784.568	1.56	1.57
PC(16:0/18:1)	782.543	1.24	0.65
PC(16:0/18:3)	778.550	1.22	1.33
PC(18:0/18:0)	828.570	2.18	1.12
PC(18:0/22:5)	836.579	1.61	1.09
PC(18:0/22:6)	856.593	1.05	0.89
PC(18:1/22:6)	832.588	1.04	1.10
PC(18:2/18:0)	808.610	1.46	0.99
PC(18:2/18:1)	806.558	1.33	1.45
PE(16:0/18:0)	720.532	1.68	0.79
PE(18:1/20:4)	766.526	1.34	0.81
PE(18:1/20:5)	764.474	1.65	1.90
PE(18:1/22:6)	792.529	1.17	1.54
PE(22:5/22:4)	842.583	1.16	0.84
LPC(20:5)	564.306	1.39	0.72
LPC(22:6)	567.328	1.20	0.84
LPE(16:0)	454.304	1.26	0.74
Carnitine	162.117	1.10	1.28
Urea	61.040	1.35	1.26
Alanine	90.055	1.55	1.37
Choline	104.105	1.10	1.57
Glutamate	148.007	1.10	1.58

The identify metabolites are grouped depending on their properties in table R1. We found differences between both cell lines in 4 groups of compounds: phospholipids (PLs) in particular phosphatidylcholines (PCs) and phosphatidylserines (PSs) but also non-identified PLs, lysophospholipids (LPLs), namely

Table R2: Identification of principal metabolites that change between ApoE4 lysosomal membrane and ApoE3 one. The table contain the name of the metabolites, their mass (m)/ charge (z), the variable VIP and the fold change (FC) of ApoE4 cell lysosome above ApoE3 ones. Phosphatidylcholine (PC), phosphatidylethanolamine, lysophosphosphatidylcholine (LPC) and lysophosphoethanolamine (LPE)

lysophosphatidylcholines (LPCs) and non-identified LPLs, acylcarnitines and a miscellaneous group (table R1).

We put our attention into the first 2 groups, as they are lipids and they can be candidates to modulate V-ATPase activity but also other channels, for example from the ER. We identified twently-three PLs, of which, fourteen are increased and nine are diminished in ApoE4 than in ApoE3 astrocytes. Ten of the PLs are PCs, moreover, most of them are increased (seven from ten) in ApoE4 astrocytes. Finally, the other 2 identified PLs are PSs that are diminished. There are nine LPLs that are all diminished in ApoE4 cells, of which, 7 were identified as LPCs. Interestingly, the PC and LPC ratio has been proposed as a CSF biomarker of AD, being decreased in these patients (C. Mulder et al. 2003). However, in our case, the ratio increases since most of the PCs are increased and all of the LPCs are diminished in ApoE4 versus ApoE3 cells.

Therefore, we conclude that there is a general lipid dysregulation in ApoE4 astrocytes that could result in the alteration of calcium homeostasis, especially for the calcium mobilization from both, the ER and the lysosomes. To further study this possibility, and being aware of the particular lipid composition of the lysosomal membrane (Van Meer, Voelker, and Feigenson 2008) we performed a metabolomic assay of the lysosomal membrane. To accomplish that, we first isolated lysosomes from ApoE3 and ApoE4 astrocytes in collaboration with Dr. Miquel Vila from Vall d' Hebron Institute of Barcelona. Isolated lysosomal membranes were analysed by metabolomic assay with the same conditions and statistical analysis carried out for the whole cell study.

As in the case of the whole cell study, the application of the PLS-DA highlighted a good discrimination of the lysosomal membrane composition of both cell lines (figure R16). In other words, both lysosomal membranes could be easily differentiated based on their composition.

As in the previous analysis, VIP value was used to underline which metabolites drive the difference in both lysosomal membranes and we identified the ones that account with a VIP superior to 1 (table R2). The metabolites that we found changed are PLs (PCs and phosphatidylethanolamines (PEs)) and LPLs (LPCs and lysophosphatidylethanolamines (LPEs)), carnitine and, again, a miscellaneous group. In particular, LPLs are diminished in

ApoE4 cells being one of them a LPE (fold change(FC): 0.74) and 2 of them LPCs (FC 0.72 and 0.84). Regarding PLs, 10 are PCs (4 diminished and 6 augmented) and 5 PE (3 diminished and 2 augmented) in ApoE4 astrocytes.

Thus, the next step would be to modulate their quantity to probe if they are involved in calcium mobilization and uptake into lysosomes of the ApoE4 astrocytes.

1.3.6. Study of the cholesterol distribution in ApoE3 and ApoE4 astrocytes

We decided to study intracellular cholesterol distribution because lipoproteins composed of ApoE in the CNS mainly transport cholesterol, although it was not a hit of the metabolome discrimination. Moreover, cholesterol metabolism is dysregulated in AD astrocytes (Orre et al. 2014). To this end, Fillipin III staining was the method chosen as it binds to cellular cholesterol and emits UV light proportionally to the cholesterol bound (detailed in material and methods section).

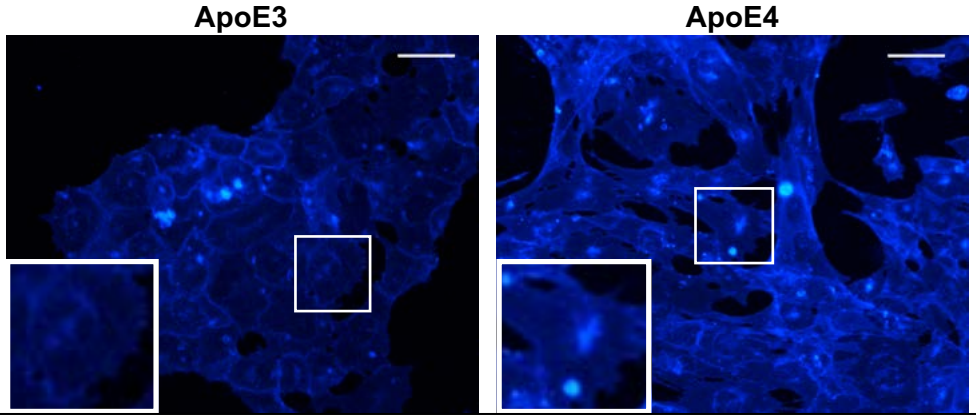

Figure R17: Cholesterol accumulation in ApoE3 and ApoE4 astrocytes. Filipin III staining of ApoE3 and ApoE4 cells. Scale bar represents 100 µm.

The analysis demonstrated a change in the distribution pattern between both cell lines (figure R17). ApoE4 astrocytes show higher cholesterol accumulations near to the nucleus and probably in the ER where cholesterol is synthetized. In ApoE3 astrocytes, these accumulations are less pronounced and cholesterol is mainly located in the plasmatic membrane. Therefore, this result demonstrates the alteration of the intracellular cholesterol in ApoE4 cells.

To investigate if that altered cholesterol accumulation in ApoE4 cells could be the cause of the different calcium concentration in ApoE4 cell lysosomes, we treated the cells with U18666A that promotes the accumulation of cholesterol in these organelles. As it is depicted

in Figure R18A, U18666A alters intracellular cholesterol accumulation in ApoE3 and ApoE4 astrocytes. However, basal calcium and 100 μM ATP-elicited calcium peaks are equal in the presence and absence of this compound in both cell lines (figure R18B). In particular, basal calcium measured as Fura2 ratio in treated ApoE3 astrocytes is 0.34 ± 0.01 compared to non-treated cells that is 0.30 ± 0.007 whereas the basal calcium in treated ApoE4 astrocytes is 0.25 ± 0.009 and in untreated 0.24 ± 0.01. Regarding the ATP-triggered calcium peak, in ApoE3 astrocytes, the increase in Fura2 ratio is 0.73 ± 0.03 and 0.86 ± 0.07 in the presence and absence of U18666A, respectively. Regarding ApoE4 cells, the elicited calcium peak measured as the variation of Fura2 after the treatment is 0.90 ± 0.02, similar to that in untreated cells that is 1.05 ± 0.09 (figure R18B).

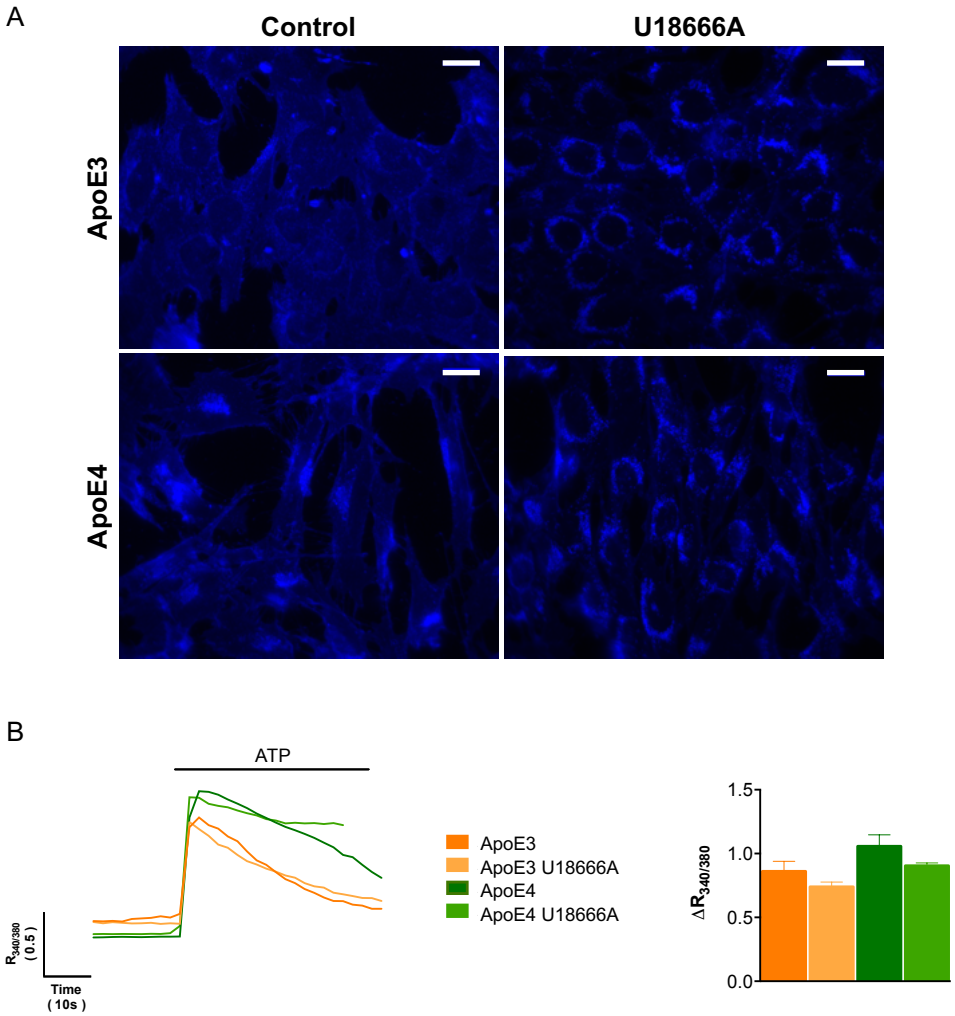

Figure R18: Accumulation of cholesterol and ATP-elicited calcium responses in ApoE3 and ApoE4 cells. (A) Representative images of cells treated or not with 0.25 μg/mL of U18666A for 48 h and stained with Filipin III. Scale bar represents 100 μm (B) Representative cytosolic calcium traces of a single cells and quantification of several cells from 3 independent experiments of the cytosolic calcium increase in cells treated or not with 0.25 μg/mL of U18666A for 48 h upon the stimulation with ATP. One way ANOVA was applied.

Hence, no significant difference is observed between treatment and control conditions in any of the cell lines, suggesting that cholesterol accumulation in ApoE4 astrocytes is not the cause of the different intracellular calcium responses in ApoE3 and ApoE4 cells.

1.3.7. Study of subcellular distribution of lysosomes in ApoE3 and ApoE4 astrocytes.

Differential lysosomal localization has been related to different lysosomal features, for instance, perinuclear lysosomes have different pH and different degradative ability than peripheral ones (Johnson et al. 2016; Pu et al. 2016). These findings could suggest that lysosomal position could regulate V-ATPase activity. For this reason, we explored lysosomal localization. We performed an immunocytochemistry of Lamp1 (a lysosomal marker) in ApoE3 and ApoE4 astrocytes and we analysed the images with IMARIS software. IMARIS allowed us to calculate the distance of each lysosome to the nucleus. We determined the number of lysosomes in distance ranges of 10 µm from the nucleus to the membrane (figure R19).

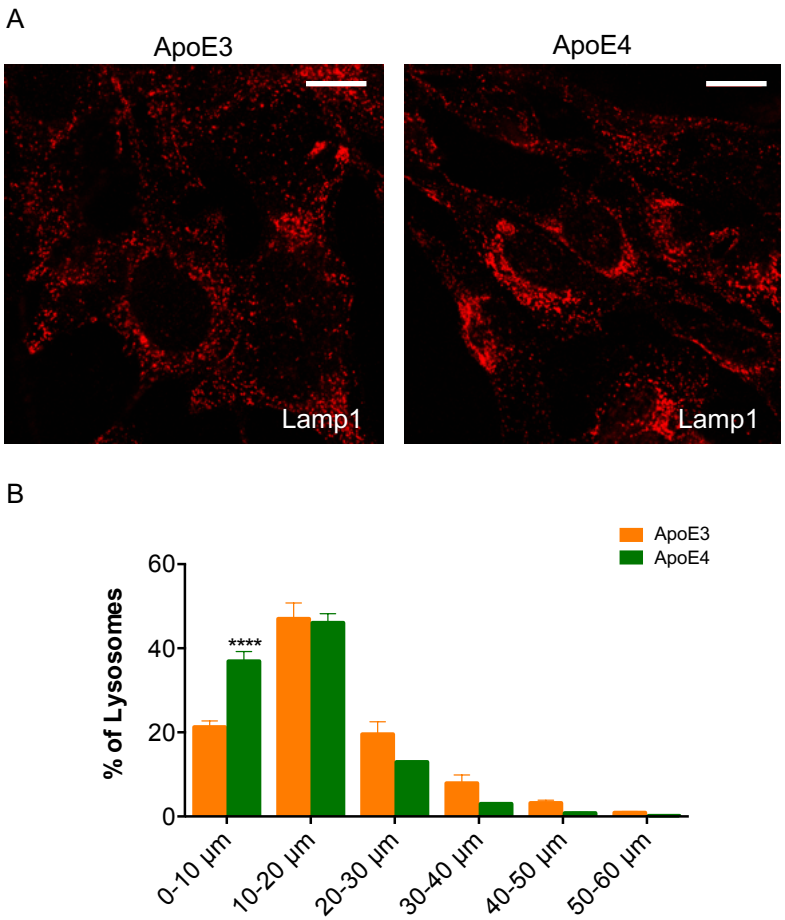

Figure R19: Pattern distribution of lysosomes in ApoE3 and ApoE4 astrocytes. (A) Representative images from Lamp1 immunofluorescence of both cell lines. Scale bar represents 15 µm. (B) Quantification of the percentage of lysosomes in the different ranges of distance being the 0 value, the nucleus in each cell. Several cells of 3 independent experiments were quantified. Unpaired parametric T-test was applied. ****p<0.0001

The results show that 36.9 ± 2.32% of lysosomes in ApoE4 astrocytes are in the first 10 μm near the nucleus, compared to the 21.29 ± 1.41% in ApoE3 cells (figure R19A and B). At longer distances from the nucleus, a higher percentage of lysosomes is observed in ApoE3 cells than in ApoE4 cells. As an example, in the range of 20 to 30 μm, the percentage of lysosomes is 19.57 ± 2.93% in ApoE3 cells compared to 12.99 ± 0.07% in ApoE4 cells. (figure R19B).

Therefore, we can conclude that the lysosomes of ApoE4 astrocytes are localized closer to the nucleus whereas the lysosomes of the ApoE3 cells are more homogeneously distributed without a major perinuclear presence. This result suggests that, in ApoE4 cells, the lysosomal trafficking could be altered. However, further experiments are needed to corroborate if lysosomal trafficking is indeed contributing to the calcium signalling differences between ApoE3 and ApoE4 cells.

1.4. Calcium signalling in ApoE3 and ApoE4 astrocytes in medium lacking lipoproteins

All the previous experiments were performed in DMEM medium, or KH medium supplemented with FBS in the case of experiments with EGTA. It is important to stress that ApoE is involved in the secretion and endocytosis of phospholipids and cholesterol through lipoproteins, whose regulation may depend on the extracellular lipoprotein concentration. Moreover, lysosomes participate in the recycling of lipoproteins, and the nutrient deprivation is known that affects their functions. Since FBS-supplemented medium has a high content of lipoproteins, we wanted to explore if the absence of lipoproteins has an impact on calcium responses upon the stimulation of 100 μM ATP in different extracellular mediums. We used DMEM supplemented with B27 or with lipoprotein-deficient FBS and Krebs medium (KH). While FBS contains high quantity of lipid or lipoproteins, B27 contains no lipoproteins and the concentration of lipids is much lower than in the FBS. In addition, we also used lipoprotein-deficient serum, in which, lipoproteins have been removed, and KH that is only composed of salts and glucose.

With respect to the basal calcium in the different mediums, the Fura2 ratio of ApoE3 cells is 0.30 ± 0.02 in DMEM supplemented with B27 compared to that in ApoE4 cells (0.22 ± 0.01). Same results were obtained after being 5 minutes in KH medium, with a higher Fura2

ratio in ApoE3 cells than in ApoE4 cells (0.29 ± 0.02 versus 0.23 ± 0.003). However, the results obtained with lipoprotein-deficient serum of the Fura2 ratio are less conclusive, being higher in ApoE3 cells (0.30 ± 0.03 in ApoE4 cells versus 0.34 ± 0.04 in ApoE3 cells) but not statistically significant.

Interestingly, 100 µM ATP-induced calcium responses in KH medium are high in both, ApoE3 and ApoE4 cells being the variation of the Fura2 ratio (peak) 1.2 ± 0.16 in ApoE3 astrocytes and 0.97 ± 0.07 in ApoE4 cells (figure 20A and F). ATP-triggered calcium peak in DMEM supplemented with lipoprotein-deficient serum shows a variation of the Fura2 ratio of 0.87 ± 0.04 in ApoE3 cells and of 0.81 ± 0.14 in ApoE4 cells (figure R20B and F). Similar results were obtained in DMEM supplemented with B27, where the quantification of ATP-mediated calcium peak through the variation of the Fura2 ratio is 0.86 ± 0.04 in ApoE3 cells and 0.83 ± 0.04 in ApoE4 astrocytes (figure R20C, D and F). Therefore, when we removed lipoproteins or lipids from the medium, ATP-induced calcium increases have a similar magnitude in ApoE3 and ApoE4 astrocytes. In other words, lipids or lipoproteins

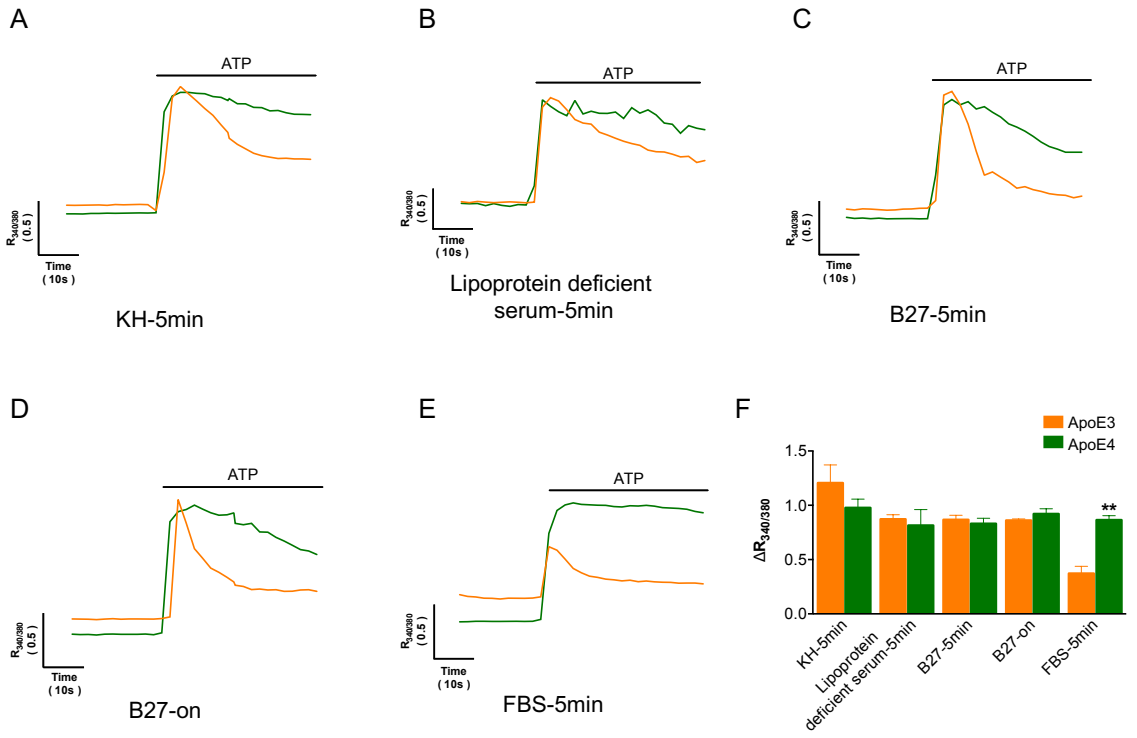

Figure R20: Calcium signalling of ApoE3 and ApoE4 cells kept in medium without lipids or lipoproteins. Representative traces of 100 µM ATP-induced calcium responses of single ApoE3 and ApoE4 cell in saline medium or Krebs medium (KH) for 2 to 5 minutes (A), DMEM medium supplemented with lipoprotein deficient serum for 2 to 5 minutes (B), DMEM medium supplemented with B27 for 2 to 5 minutes (C) and over-night (D) and DMEM medium supplemented with 10% of FBS for 5 minutes (E). (F) Quantification of the cytosolic calcium peak of several cell from at least 3 independent experiments in the different mediums. Unparied parametric T-test was applied to the data. **p<0.01

modulate ATP-elicited cytosolic calcium increases in ApoE3 cells, but not in ApoE4 astrocytes.

Focusing on the quantification of the recovery phase after the ATP stimulation, the percentage of response at 20 seconds is significantly lower in ApoE3 cells compared to ApoE4 cells in KH and DMEM supplemented with B27 medium and shows a non-statistically difference to be lower in the DMEM lipoprotein-deficient serum. Specifically, the percentage of the response at 20s in ApoE3 cells in KH medium is 36.58 ± 9.57% while in ApoE4 cells is 71.77 ± 8.09% (p-value 0.04). In DMEM B27 medium, ApoE3 cells show a percentage of 34.64 ± 3.70% and ApoE4 cells of 81.22 ± 5.55 (p-value 0.002). Finally, the percentage of response at 20s in the lipoprotein-deficient medium is higher but it is not statistically significant between ApoE3 and ApoE4 cells (51.60 ± 4.34% versus 68.37 ± 6.19%; p-value 0.06).

Therefore, these results indicate that the presence of lipoproteins only modulates the magnitude of ATP-induced calcium responses. Importantly, we discovered that this modulation is a short event that lasted from 2 to 5 minutes (figure R20). In other words, the magnitude of ATP-induced calcium increase in ApoE3 astrocytes augments already after 2 to 5 minutes of replacing DMEM 10% FBS by KH or DMEM supplemented with B27 or lipoprotein-deficient serum. On the other hand, when DMEM B27 is left overnight, ATP-mediated calcium signalling has an increase in the Fura2 ratio of 0.86 ± 0.01 in ApoE3 cells compared to 0.92 ± 0.04 in ApoE4 astrocytes, so the ATP calcium peak is high even after an extended period of ApoE3 cells being in medium without lipids or lipoproteins (figure R20D and F).

The magnitude of the ATP-triggered calcium increases in ApoE3 cells returns to be low after 5 minutes of replacing DMEM supplemented with B27 for DMEM supplemented with FBS medium, as observed by the variation of the Fura2 ratio (0.37 ± 0.06). The increase of the ATP-induced calcium responses of ApoE4 astrocytes measured as the variation of the Fura2 ratio is 0.86 ± 0.04, so it remains unchanged among the different mediums (figure R20E and F). Therefore, the time of the modulation is a few minutes indicating that there is not a channel expression change or desensitization of the purinergic receptors.

Finally, it is worth to note that we used other FBS batches to asses that the ATP-triggered cytosolic peak is diminished in all serums and it is not a peculiarity of the one that we used. The 100 μM ATP-triggered calcium peak in medium supplemented with these other FBS is 0.36 ± 0.13 in ApoE3 cells and 0.94 ± 0.006 in ApoE4 cells and 0.37 ± 0.04 in ApoE3 cells and 0.91 ± 0.05 in ApoE4 astrocytes.

Therefore, the presence of lipoproteins modulates purinergic-induced calcium responses in ApoE3 but not in ApoE4 astrocytes.

1.4.1. Mechanism of lipoprotein regulation of calcium signalling in ApoE3 astrocytes.

Which is the signalling pathway that when is potentiated or inhibited, results in higher ATP-triggered calcium peaks in ApoE3 astrocytes when the extracellular medium is poor in lipoproteins? Based on the similarity of the magnitude of calcium responses in ApoE3 and ApoE4 cells, our first hypothesis was that lysosomal V-ATPase could be modulated by lipid composition, increasing its activity and subsequently increasing the calcium concentration of lysosomes and the cytosolic calcium responses to ATP. To test the truthfulness of this hypothesis, we took advantage of the lysosomal inhibitors that we previously used but employing them in lipoprotein absent mediums. First, we treated the cells with the lysosomal calcium release inhibitor Ned-19. We quantified the peak of the calcium response after the addition of 100 μM ATP of several cells and we observed that Ned-19 diminishes the ATP-induced calcium responses in ApoE3 cells, being the Fura2 variation similar to the one observed in ApoE4 astrocytes treated (figure R21) (0.6 ± 0.03 from ApoE3 cells compared to 0.61 ± 0.07 from ApoE4 cells). Therefore, the high ATP-induced calcium signal in ApoE3 cells when extracellular lipoproteins are absent is more dependent on lysosomal calcium release than in the presence of lipoproteins.

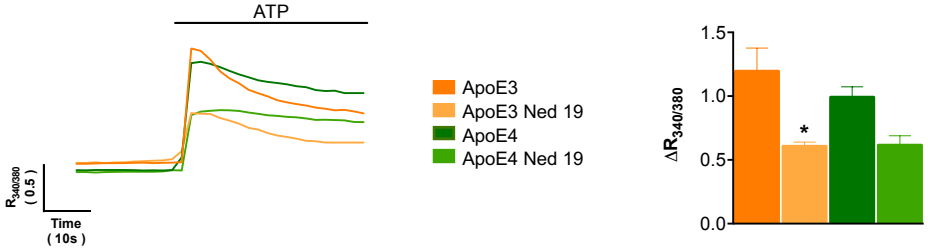

Figure R21: Lysosomal calcium mobilization kept in KH medium. Representative traces of single cells and quantification of 3 independent experiments of ATP triggered cytosolic calcium responses of cells treated with DMSO or with 100 μM Ned 19 for 20 min in KH medium. One way ANOVA was applied. *p<0.05

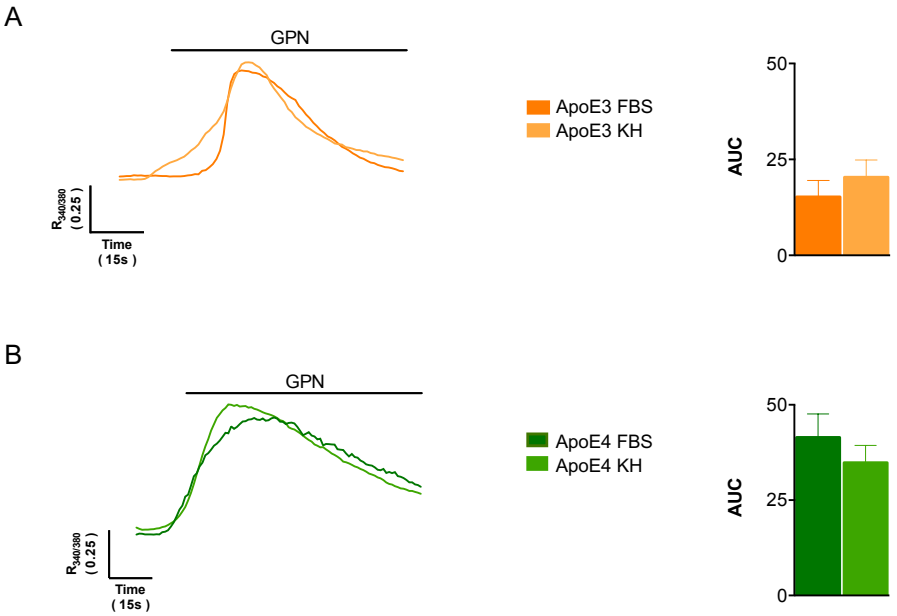

Figure R22: Quantification of lysosomal calcium content in ApoE3 and ApoE4 astrocytes in KH medium compared to DMEM medium supplemented with FBS (FBS) (figure R6). (A)Representative traces of single cells and quantification of 3 independent experiments of the area under the curve (AUC) after 200 µM GPN stimulation of ApoE3 astrocytes. (B) Representative traces of single cells and quantification of 3 independent experiments of the AUC after 200 µM GPN stimulation of ApoE4 astrocytes . The data obtained in the DMEM medium supplemented with FBS is previously presented in figure R6. One way ANOVA was applied.

Next, we assessed lysosomal calcium concentration to confirm the modulation of the V-ATPase activity due to the lipids or lipoproteins. To this end, we stimulated the cells with 200 µM GPN in KH medium and we calculated the area under the curve (AUC) defined by the intracellular calcium increase elicited by this compound. We then, compared these results with the ones previously described for GPN in DMEM supplemented with 10% FBS of both cell lines in figure R6. As shown in figure R22, in ApoE3 cells the AUC is 15.21 ± 4.32 in DMEM supplemented with FBS medium and 20.36 ± 4.47 in KH medium (figure R22A). The AUC after GPN stimulation is also similar in ApoE4 astrocytes, where is 41.41 ± 6.19 in DMEM supplemented with FBS medium compared to 34.79 ± 4.57 in KH medium (figure R22B). We concluded that the calcium concentration of the lysosomes is not affected by the lipoprotein content from the extracellular medium.

How the lack of extracellular lipoproteins upregulates purinergic-induced calcium responses in ApoE3 astrocytes if the lysosomal calcium content is independent of their concentration and there is always strong dependency on lysosomal calcium release? We may could explain it, if we take into account that lysosomal calcium release upon neurotransmitter stimulation is an initiator phenomenon amplified by other calcium signalling pathways. Therefore, we

Figure R23: ER calcium release in lipid/lipoprotein absent medium. Representative traces and quantification of 100 μM ATP-induced peak from several cells transfected with Cepia plasmid for ER. A calcium monitoring of 3 independent experiments in KH medium was performed. One way ANOVA was applied. ***p<0.001

studied if the lack of extracellular lipoproteins is triggering intracellular changes so that, lysosomal calcium release is now greatly potentiated by ER release or entry.

First, we examined the ATP-induced calcium release from the ER in the lipoprotein absent medium, KH and we compared that with the ER release in DMEM supplemented with 10% FBS (figure R23). We used the encoded calcium sensor protein of GCEPIA-1er plasmid as it has been described before. The results show that the 100 μM ATP-induced calcium release in ApoE3 cells is higher in medium without lipoproteins, but not statistically significant than in the medium with lipoproteins. In particular, the variation of the F/F_0 is 0.61 ± 0.01 in KH medium while in DMEM supplemented with FBS medium it is 0.41 ± 0.10 (p-value 0.05)(figure R23). The ATP-mediated ER calcium release of ApoE4 cells is not changed between the mediums, being the variation of the F/F_0 around 0.5 (figure R23). Therefore, the purinergic-induced ER calcium release is slightly higher in the absence of lipoproteins in ApoE3 cells and equal in ApoE4 astrocytes.

Next, we explored the extracellular calcium entry induced by ATP stimulation. Knowing that in DMEM medium with FBS this is not a principal mechanism in none of the ApoE cells, we tested if in KH medium this changes. As previously indicated, we used a KH medium without calcium added and with EGTA to chelate the possible calcium ions of the medium. As extracellular calcium is low, we were able to use lower EGTA concentrations: 0.5 mM to not deplete calcium from the ER. Regarding basal calcium, there is a slightly decrease in the Fura2 ratio in both cell lines probably due to the calcium gradient. Interestingly, we observed that the ATP-induced cytosolic calcium peak in ApoE3 cells is highly dependent on the extracellular calcium entrance. Specifically, the Fura2 ratio variation is 0.33 ± 0.05 in KH medium without calcium and with EGTA compared to 1.04 ± 0.1 in standard KH medium (figure R24). Thus, there is 65% of inhibition in the absence of calcium, a higher percentage than the one previously described for ApoE3 cells kept in KH with 10% FBS medium, which

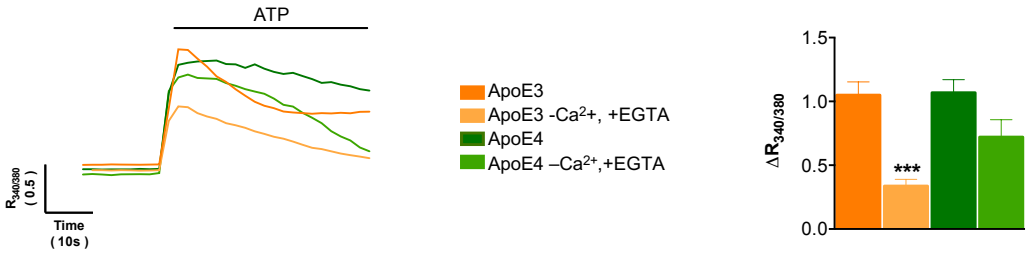

Figure R24: Extracellular calcium entry in lipid/lipoprotein absent medium. Representative traces and quantification of the peak from 6 independent experiments of the 100 µM cytosolic calcium responses in cells in KH medium with calcium or without calcium and 500 µM of EGTA for 10 minutes. One way ANOVA was applied. ***p<0.001

is 19% (figure R9). It can be concluded that in the absence of lipoproteins the extracellular calcium entry is potentiated as a part of the ATP calcium responses in ApoE3 astrocytes. Probably, this modulation is secondary to the high ER and lysosomal calcium release.

By contrast, extracellular calcium entry induced by ATP in ApoE4 astrocytes is regardless of the absence or presence of extracellular lipoproteins. In the KH medium, cytosolic calcium peak is not significantly inhibited by the absence of extracellular calcium. In particular, the variation of Fura2 ratio after the ATP stimulation is 0.72 ± 0.13 in calcium-free medium with the presence of EGTA compared to 1.06 ± 0.1 in standard KH medium. This inhibition is similar to the one obtained in the KH with 10% FBS, 28% and 32%, respectively (figure R9 and R24).

With respect to the recovery phase, in ApoE3 cells with or without extracellular calcium is similar, around 53%. The recovery phase of ApoE4 cells without calcium is faster since the percentage of response at 20 seconds is 53.48 ± 5.35 without calcium and 74.03 ± 4.04 with calcium. Probably, this is due to the gradient of calcium ions that travel through the membrane due to the absence of extracellular calcium. It can also be due to the inactivation of the SOCE being the recovery phase shorter in the medium without calcium. This result highlights that there is an extracellular entrance of calcium in ApoE4 astrocytes, although it seems important for the phase of recovery and not for the peak.

Taking all the results together, the modulation of ATP-induced calcium responses by lipoproteins in ApoE3 astrocytes depends mainly on calcium mobilization from lysosomes and extracellular calcium entrance. Most likely, calcium mobilization from lysosomes is the triggering mechanism. So that, lysosomal calcium released in ApoE3 cells potentiates more the calcium release from the ER and the extracellular calcium entrance in the absence of lipoproteins than in their presence.

1.4.2. Analysis of the potential cause of calcium signalling modulation

Knowing that the lipoprotein trafficking could be regulated by the presence or absence of these entities, and is impaired in ApoE4 cells, a plausible hypothesis of the lipoprotein modulation in ApoE3 but not in ApoE4 astrocytes could be that ApoE and lipoprotein trafficking regulate calcium signals, a process impaired in ApoE4 astrocytes. To explore this hypothesis, we inhibited endocytosis of ApoE containing lipoproteins with Psck9. This peptide promotes the endocytosis and degradation of ApoE receptor LDLR (Liang et al. 2012). Hence, Psck9 treatment turns into diminished plasmatic LDLR and thus, less lipoproteins are uptake by cells. Among all the ApoE receptors, we selected LDLR since it has been described downregulated in astrocytes from an AD model (Orre et al. 2014). We treated the cells for 24 hours to ensure the degradation of the receptor. Preliminary data recently obtained by us in a lipoprotein-rich medium (DMEM supplemented with 10% FBS), have shown a slightly augment of 100 µM ATP-elicited cytosolic calcium responses in ApoE3 cells (the variation of Fura2 ratio is 0.26 ± 0.06 in control situation and 0.45 ± 0.07 after the treatment) In ApoE4 astrocytes, there are no changes in purinergic-induced calcium responses (variation of Fura2 ratio of 1.01 ± 0.003 in control situation and 1.14 ± 0.06 after the Psck9 treatment).

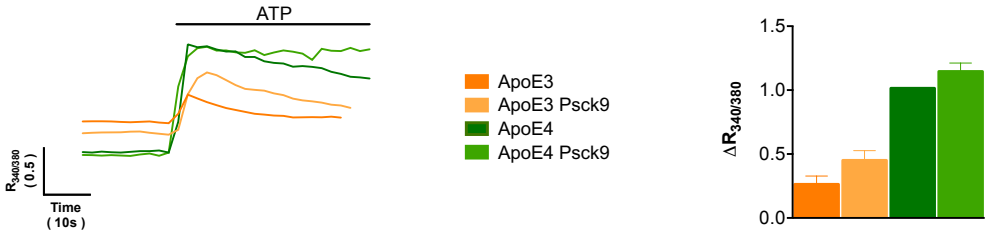

Figure R25 :Inhibition of the lipoprotein endocytosis in ApoE3 and ApoE4 cells. Representative traces of single cells and quantification of the cytosolic calcium peak after 100 µM ATP stimulation of cells treated or not with 7 µg/mL of Psck9 recombinant protein for 24 hours of several cells from 2 independent experiments. One way ANOVA was applied. Preliminary data.

Thus, the modulation of cytosolic calcium increase in ApoE3 cells might be caused by lipoprotein trafficking: when there is no lipoprotein uptake, calcium responses are higher than when there is. ApoE4 astrocytes might have a deficient lipoprotein uptake and therefore, there is no regulation of their purinergic-elicited calcium signals. However, further investigation has to be carried out to confirm these results.

1.5. ATP-mediated calcium signalling in presence of oligomeric Aβ

Finally, we tested if oligomeric Aβ (oAβ) treatment affects the cytosolic calcium increase upon ATP, since it is one of the principal hallmarks of AD and it causes calcium hyperexcitability in AD models (Bosson et al. 2017; Pirttimaki et al. 2013; Alberdi et al. 2013; D. Lim et al. 2013; Ambra A. Grolla et al. 2013; A A Grolla et al. 2013; Haughey and Mattson 2003; L. Lee, Kosuri, and Arancio 2014).

The oligomeric Aβ was obtained through the oligomerization of synthetic Aβ 1-42 monomers. We treated the ApoE3 and ApoE4 astrocytes with synthetic oligomeric Aβ for 24 hours and we monitored the basal calcium and the calcium responses upon 100 µM ATP stimulation. The quantification of the basal calcium after the oAβ treatment did not show any disturbance of intracellular calcium. In ApoE3 treated cells the Fura2 ratio is 0.47 ± 0.01 versus non-treated cells that is 0.43 ± 0.08. The basal calcium of oAβ-treated ApoE4 astrocytes is 0.28 ± 0.02 compared to the basal from non-treated cells that is 0.27 ± 0.01. Concerning the ATP-elicited calcium increase, in ApoE3 cells treated with Aβ, the Fura2 ratio increases 0.36 ± 0.20 after purinergic stimulation in the range to that observed in not treated cells (0.46 ± 0.04). In ApoE4 cells, the variation of the Fura2 ratio in presence of oAβ after the ATP stimulation is 1 ± 0.02 compared to the variation of 0.98 ± 0.09 in absence of oAβ (figure R26).

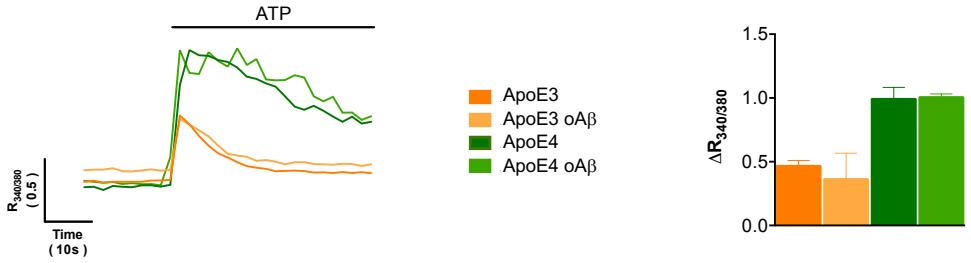

Figure R26: 100 µM ATP-triggered cytosolic calcium responses in presence of oligomeric Aβ (oAβ). Representative traces and quantification of the ATP-induced cytosolic calcium peak of cells that were treated 24 hours with 5 µM of oligomeric Aβ from 2 independent experiments. One way ANOVA was applied to the data.

Furthermore, the recovery phase after 20 seconds of the ATP-induced calcium responses is similar between oAβ-treated cells and untreated cells. In ApoE3 cells, this percentage is 16.17 ± 2.12% compared to 26.93 ± 5.33% in the control situation. In ApoE4 cells, the percentage

of response from treated cells is 57.08 ± 8.78% compared to 63.33 ± 4.4% from non-treated cells

Therefore, we do not observe any change of purinergic-elicited calcium responses in ApoE3 or ApoE4 cells in the presence or absence of oAβ, indicating that it does not exacerbate the cytosolic calcium difference between cultured ApoE3 and ApoE4 astrocytes.

1.6. Summary of the main demonstrations found regarding calcium responses upon ATP in ApoE3 and ApoE4 cells.

The principal alterations found in ApoE-expressing astrocytes are summarized in figure R27. Specifically, we found that the hyperactivation of V-ATPase increases the lysosomal calcium concentration in ApoE4 astrocytes, promoting higher ATP-induced calcium signals than in ApoE3 cells. The activity of the V-ATPase does not cause lysosomal acidification, but there is more calcium load. This fact suggests that the proton calcium exchanger of the lysosome is also hyper-activated. In addition, calcium mobilization from the ER is also higher in ApoE4 cells than in ApoE3 ones.

In the absence of lipoproteins, the amplitude of cytosolic calcium responses mediated by ATP in ApoE3 astrocytes is higher than in the presence of lipoproteins. The responses are augmented due to a higher calcium mobilization from lysosomes that might potentiate calcium release from ER and especially by extracellular calcium entrance. Preliminary experiments suggest that the lack of lipoprotein endocytosis could result in the potentiation of these different calcium signalling pathways.

Finally, in ApoE4 astrocytes, neither extracellular calcium entry nor ER calcium release is potentiated by extracellular lipoproteins and hence, purinergic calcium responses are not changed due to the lack of extracellular lipoproteins.

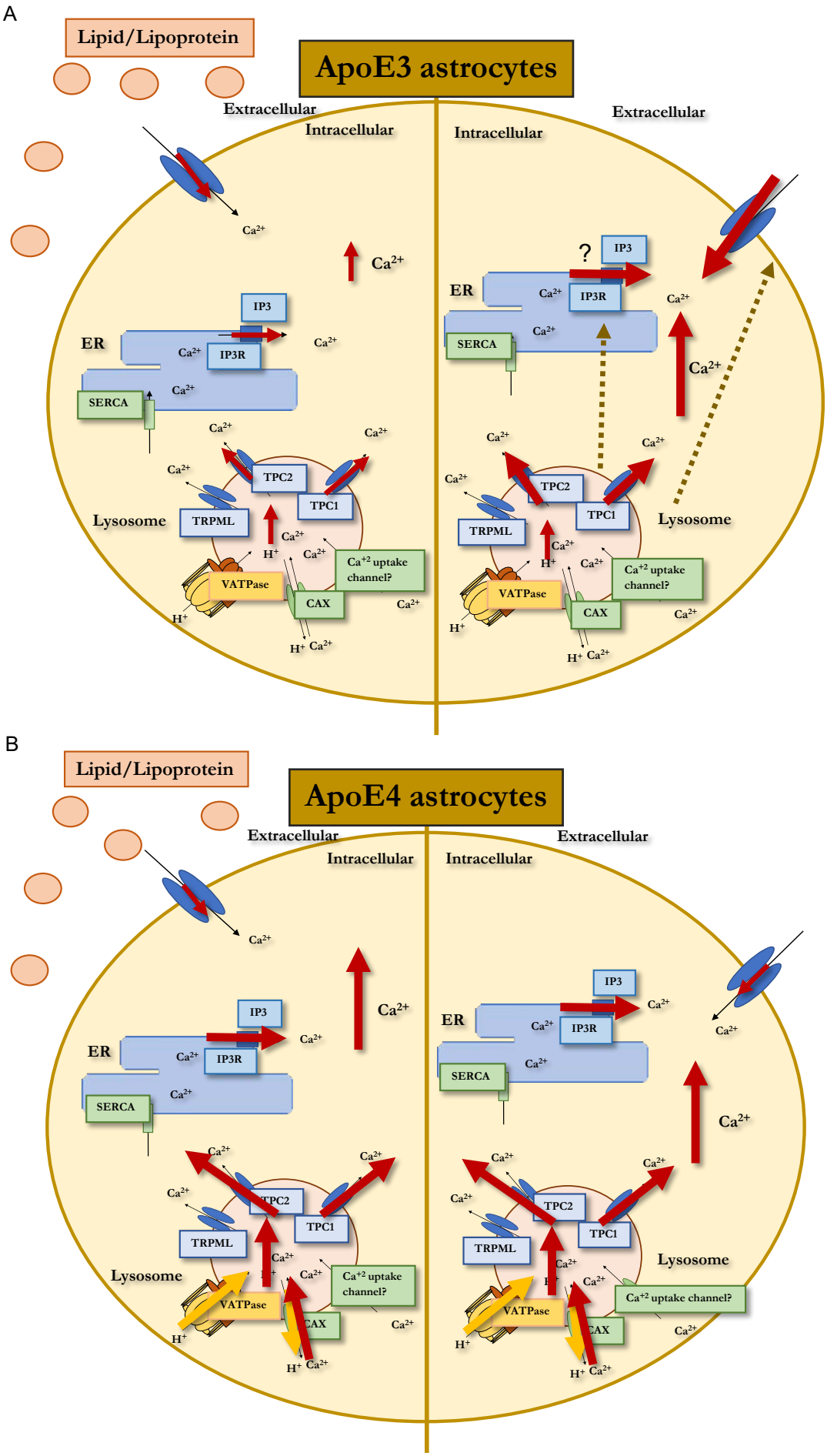
A
Lipid/Lipoprotein
ApoE3 astrocytes
Extracellular
Intracellular
Extracellular
Intracellular
Ca2+
Ca2+
IP3
ER
Ca2+
IP3R
Ca2+
SERCA
Ca2+
Ca2+
Ca2+
TPC2
TPC1
Ca2+
Ca2+
Lysosome
TRPML
Ca2+
H+
Ca2+
Ca+2 uptake channel?
VATPase
CAX
Ca2+
H+
H+ Ca2+
?
IP3
ER
Ca2+
IP3R
Ca2+
SERCA
Ca2+
Ca2+
Ca2+
Ca2+
TPC2
TPC1
Ca2+
Lysosome
Ca2+
TRPML
Ca2+
H+
Ca2+
Ca+2 uptake channel?
VATPase
CAX
Ca2+
H+
H+ Ca2+
B
Lipid/Lipoprotein
ApoE4 astrocytes
Extracellular
Intracellular
Extracellular
Intracellular
Ca2+
Ca2+
IP3
ER
Ca2+
IP3R
Ca2+
SERCA
Ca2+
Ca2+
Ca2+
Ca2+
TPC2
TPC1
Ca2+
Ca2+
Lysosome
TRPML
Ca2+
H+
Ca2+
Ca+2 uptake channel?
VATPase
CAX
Ca2+
H+
H+ Ca2+
IP3
ER
Ca2+
IP3R
Ca2+
SERCA
Ca2+
Ca2+
Ca2+
Ca2+
TPC2
TPC1
Ca2+
Ca2+
Lysosome
TRPML
Ca2+
H+
Ca2+
Ca+2 uptake channel?
VATPase
CAX
Ca2+
H+
H+ Ca2+

Figure R27: Image summarizing the principal alterations found in ApoE astrocytes. (A) ApoE3 cells alterations and (B) ApoE4 cells alterations. Red arrows show calcium, yellow arrows show protons and brown arrows show the interrelationship between calcium signalling pathways. The size of the red arrows indicates quantity of calcium.

1.7. Validation of calcium results in human brain sections and in human ApoE3/3 and ApoE4/4 iPSCs-derived astrocytes

All the experiments were performed using the immortalized astrocytes from a mouse model that express the human isoforms of ApoE. As happen with all the models, they have advantages and disadvantages. The principal advantages are that allow us to study molecular and cellular mechanisms and to obtain a great quantity of samples in a short period. The principal disadvantages are that is a mouse model and that the process of immortalization could affect astrocyte functions. For these reasons, we intend to validate the principal results in other models.

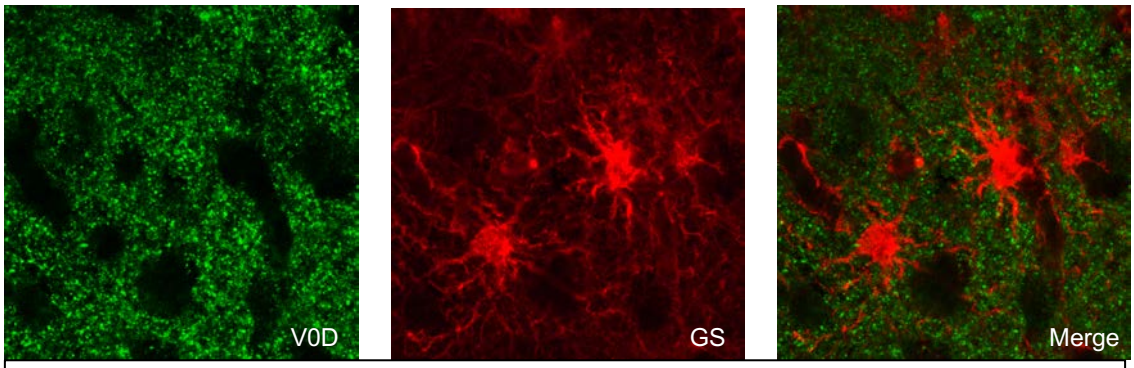

Figure R28: Representative images from V0D, Glutamine synthetase (GS) and merge of both. Immunohistochemistry of paraffin embed section of patient ApoE3 /ApoE4 Braak stage V-VI.

We used paraffin-embedded sections from Alzheimer's disease patients and astrocytes derived from human iPSC. With the paraffin-embedded sections, we cannot study calcium signalling although we wanted test the expression of the V-ATPase subunit, V0D1 since it is upregulated in ApoE4 astrocytes. These experiments were performed at the University of Málaga by the group of Dra. Antonia Gutierrez. An ApoE3/ApoE4 patient brain section was stained with V0D and glutamine synthetase (astrocyte marker) antibodies. As it is depicted in figure R28, the V0D staining is detected in the neuropil. However, distinguishing the neuropil from the astrocytes processes is extremely difficult. We tried to perform 3D reconstructions with IMARIS software although it was not possible to identify which V0D staining was from astrocytes or from the rest of the cells.

To validate calcium signalling results, we selected human iPSC-derived astrocytes generated by Dr.Bu laboratory from Mayo Clinic (USA). They generated 6 lines of human derived

astrocytes, 3 of them from ApoE3/ ApoE3 healthy individuals, (MC0039, MC0117 and MC0192) and the other 3 from ApoE4/ ApoE4 healthy individuals (MC0018, MC0115 and MC0116) (Zhao et al. 2017).

We received the astrocytes after 21 days of differentiation, we kept them growing for other 2 weeks and we characterized the principal astrocyte markers and the expression of ApoE. Unfortunately, we found that they almost not express GFAP (figure R29A) or GS (figure

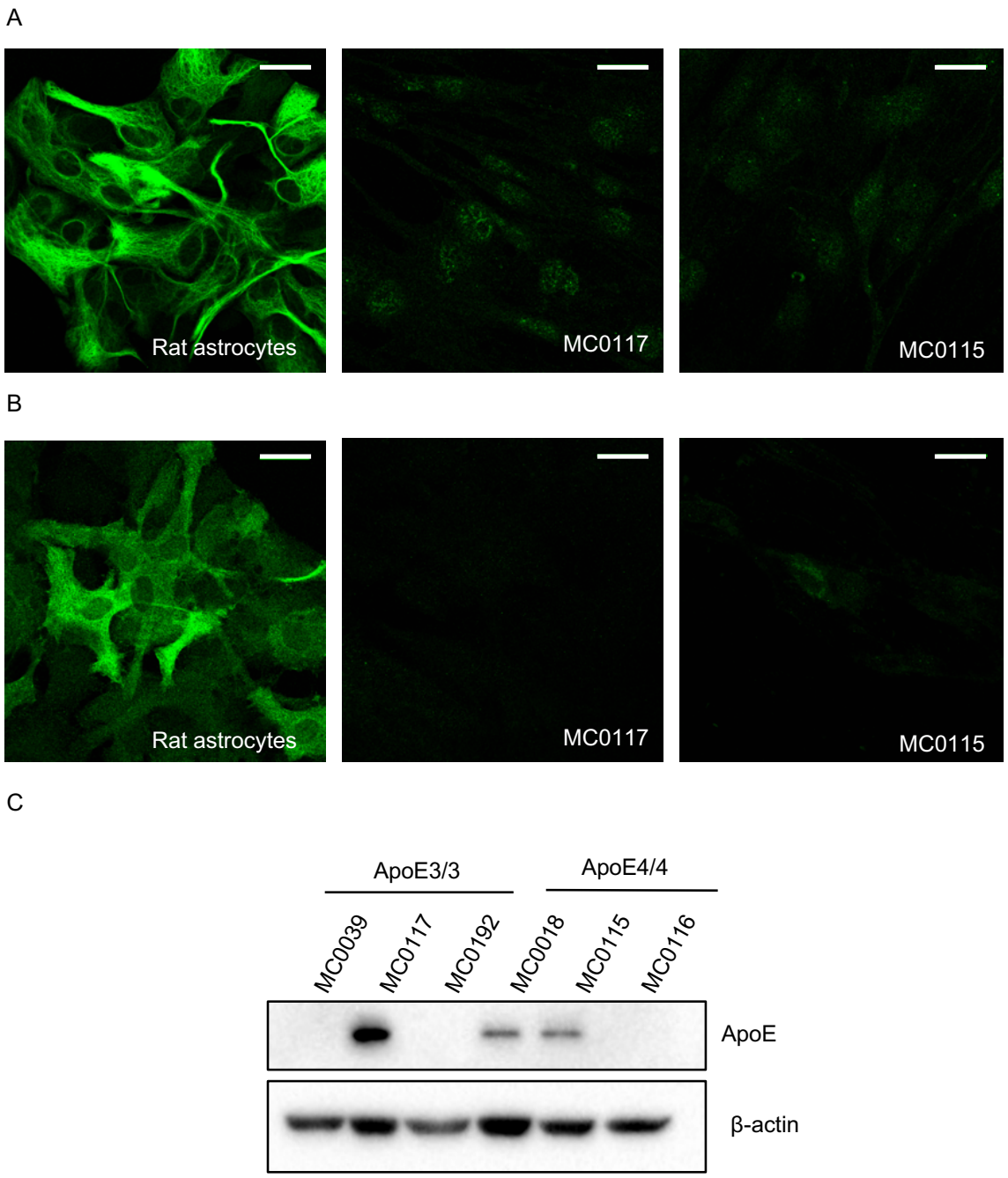

Figure R29: Astrocyte markers expression and ApoE expression in human derived astrocytes. (A) Representative images from GFAP immunocytochemistry of rat astrocytes, MC0117 and MC0115 astrocytes. (B) Representative images from GS immunocytochemistry of rat astrocytes, MC0117 and MC0115 astrocytes. (C) ApoE expression by western blot of the different human derived astrocytes.

R29B), the typical astrocytic markers of cultured astrocytes. Besides, an ApoE western blot highlighted that the expression of this protein is heterogeneous between the different cell lines (figure R29C). We need to re-evaluate the differentiation process to be able to obtain mature human astrocytes expressing ApoE3 and ApoE4.

Chapter 2: Mitochondrial alterations triggered by ApoE4 expression.

The hypometabolism of the brain is a main feature of the ApoE4 individuals even before the onset of the AD (Perkins et al. 2016). This hypometabolism is probably related to a diminution of specific mitochondrial enzymes in brain samples. In addition, alteration of mitochondrial dynamics has been described in AD pathogenesis (Zhu et al. 2013) although these studies have been focused on neuronal mitochondria. Therefore, in this chapter, we analysed if ApoE4 expression alters mitochondrial dynamics in astrocytes, specifically, the fusion/fission events, the mitophagy and the motility.

2.1. Mitochondrial fusion and fission events in ApoE3 and ApoE4 astrocytes.

Mitochondria are dynamic organelles that perform fusion/fission events to maintain a healthy network (see the introduction, section 2.3.). The predominant alteration found in AD is an increase in the fission events of neuronal mitochondria (Zhu et al. 2013; X. Wang et al. 2009). Therefore, we hypothesized that ApoE4 could potentiate this process in astrocytes.

To investigate the mitochondrial fission, we stained the mitochondria of living ApoE3 and ApoE4 astrocytes with Mitotracker green and we acquired different images. The analysis of these images was performed with an ImageJ plugin and mitochondria were categorized in 3 groups taking into account their area and perimeter: puncta (or small), rods (or middle) and network (or big ones).

In non-stimulated condition, the distribution of mitochondria in puncta, rods and network is similar between the ApoE3 and ApoE4 astrocytes (figure R31). To promote the fission process we treated the cells with 252 pM of Oligomycin for 4 hours (figure R30). Oligomycin is an antibiotic that inhibits F_0 subunit from the mitochondrial ATP-synthase. ATP-synthase transports the protons generated by the electron chain from the intermembrane space to the matrix synthetizing ATP from ADP. Hence, its inhibition affects mitochondrial membrane potential that promotes mitochondrial fission (Leonard et al. 2015). Besides, we also studied the recovery after the Oligomycin treatment keeping the cells 4 hours without the drug. Figure R30 depicts the treatment protocol for the fission analysis.

As shown in figure R31, ApoE3 cell mitochondria present fragmentation upon Oligomycin treatment and this process is reversible since they can recover the mitochondrial length after

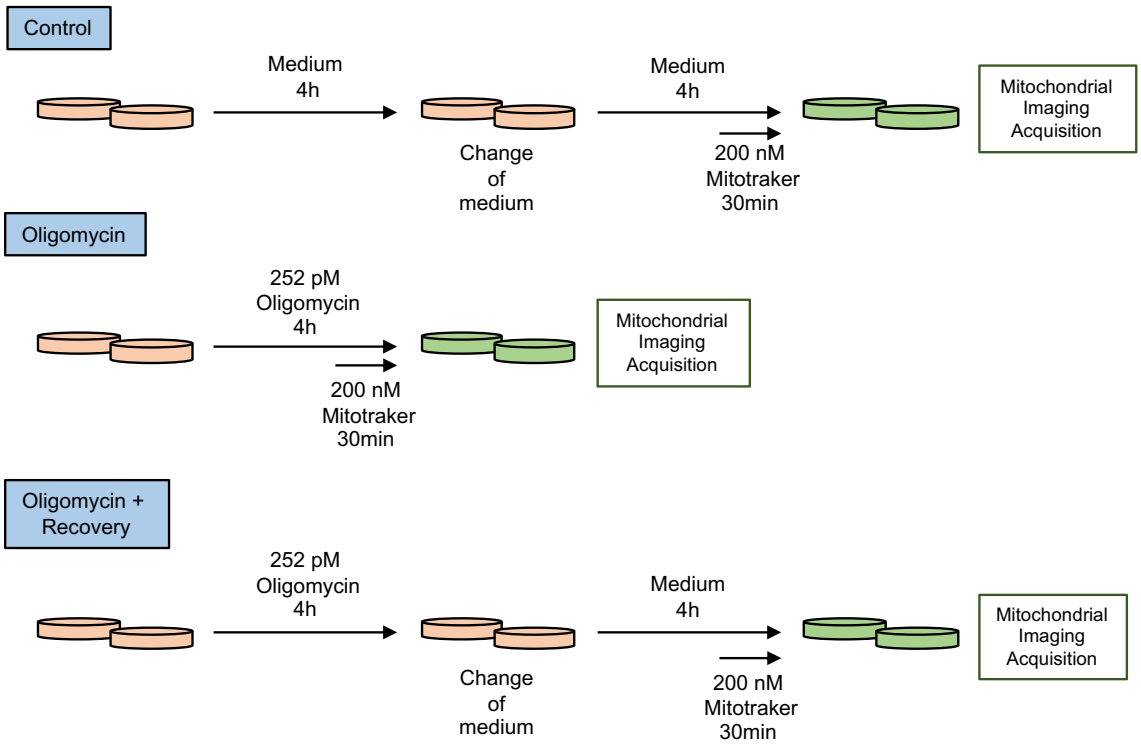

Figure R30: Protocol treatment for mitochondrial fusion/fission analysis.

4 hours of its removal (figure R31A, B and C). Specifically, the mitochondrial size quantification shows that the percentage of mitochondria in the group of puncta in control situation is 54.82 ± 1.7% whereas, with the treatment, the percentage increases until 58.64 ± 0.7 and diminishes again until 54.52 ± 1.32 after the recovery (figure R31B). Regarding the rod mitochondria, the percentages in the 3 conditions are around 35% (figure R31B). Interestingly, the significant difference between the 3 conditions is especially observed in the group of network mitochondria, in which, the percentage of mitochondria diminishes from 9.05 ± 0.93% to 6.39 ± 0.52% after the oligomycin treatment and reverses to 9.69 ± 0.65% after the 4-hours recovery. Representative images are shown in figure R31A and the quantification of at least 5 independent experiments in R31B and C.

On the contrary, ApoE4 astrocytes do not show any mitochondria fragmentation with Oligomycin treatment (Figure R31A). In detail, the percentages of mitochondria per groups in the control condition are around 51% puncta, 38% rod and 10% network. After the oligomycin treatment, the percentages are maintained being around 51% puncta, 38% rod and 10% network. The recovery phase does not promote fusion in ApoE4 astrocytes being

again the percentage similar to the percentages in control and oligomycin treatment (figure

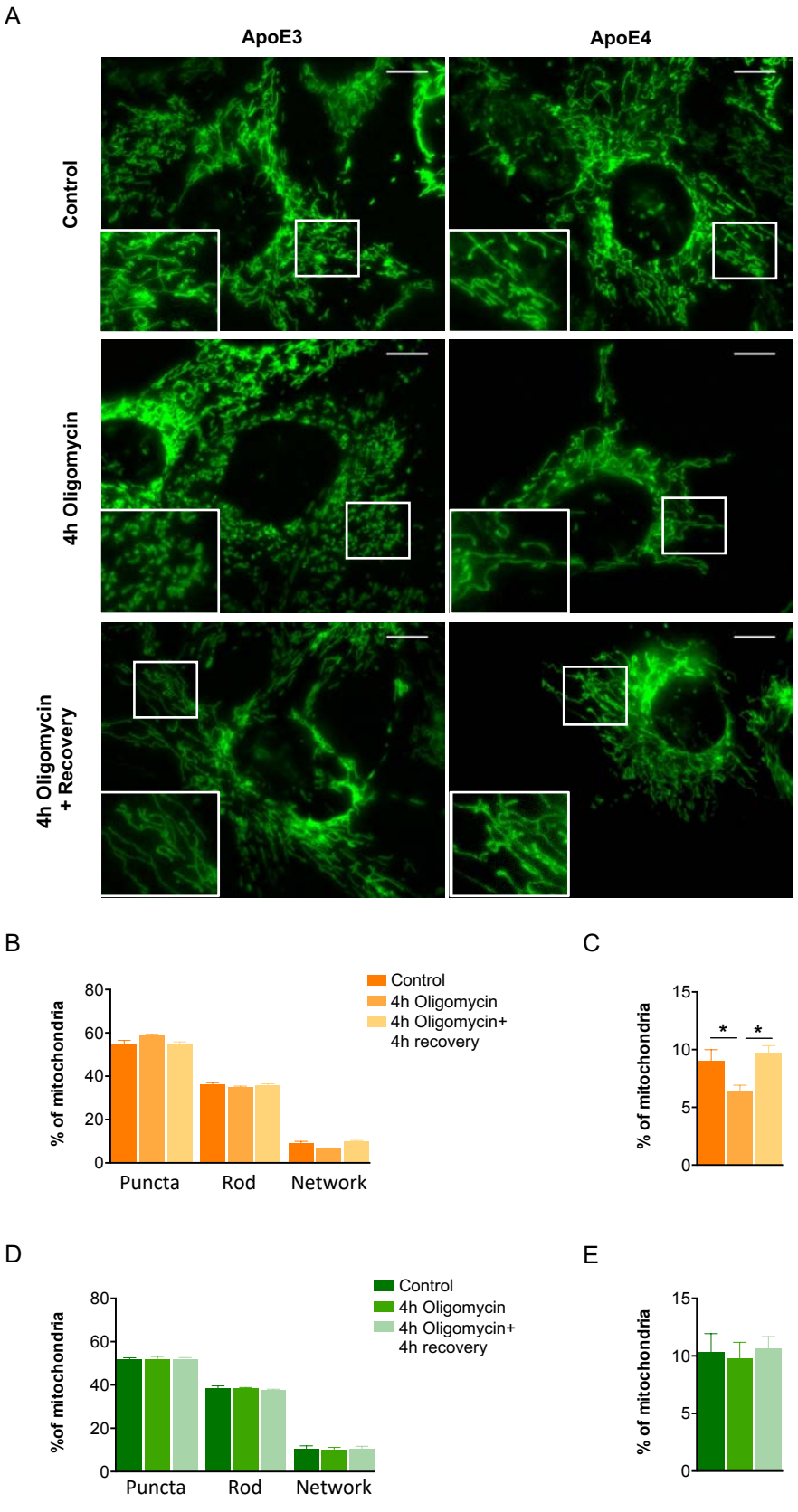

Figure R31: Mitochondria dynamics of ApoE3 and ApoE4 astrocytes. (A) Representative images from astrocytes that were stained with Mitotracker green and are untreated or treated with 0.2 ng/mL (252 pM) oligomycin for 4h followed or not by a recovery phase in which, Oligomycin was removed and cells were left with medium for 4h. The scale bar represent 10 μm and the origin for the magnification is in the white square. (B) Classification and quantification of mitochondria grouped by size : puncta, rod, and network of ApoE3 astrocytes. (C) Percentage of network mitochondria from ApoE3 cells in all the conditions. (D) Classification and quantification of mitochondria grouped by size : puncta, rod and network of ApoE4 astrocytes. (E) Percentage of network mitochondria from ApoE4 cells in all the conditions. The quantification was carried out of several cells by at least 5 independent experiments. One way ANOVA was applied. *$p < 0.05$

R31A, D and E). Representative images are shown in figure R31A and quantification of at least 5 independent experiments in R31D and E. Therefore, ApoE3 astrocytes display mitochondrial fission and fusion, whereas ApoE4 cells do not.

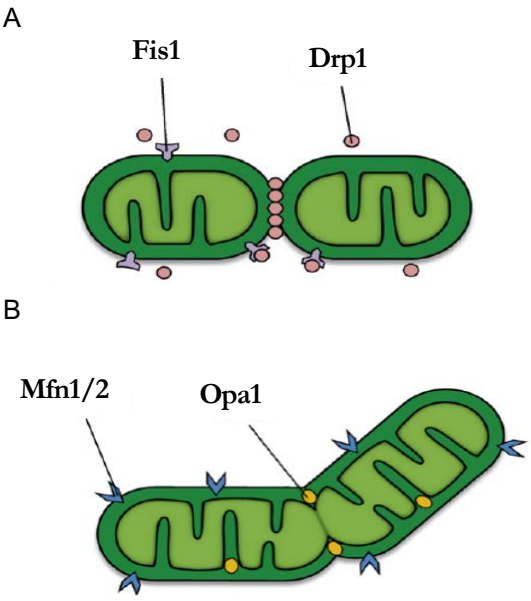

Figure R32: Principal proteins that participate in mitochondrial fusion and fission events. (A) Fis1 recruit Drp1 that promotes the division of one mitochondrion into 2 (fission). (B) Opa1 performs the fusion of the inner mitochondrial membrane whereas Mfn1 and Mfn2 achieve fusion of the outer membrane. Modified from Kuzmicic et al. 2011.

The alteration of the fragmentation promoted by ApoE4 could be due to dysregulation in the mitochondrial fusion, as if it is hyperactivated, mitochondria would be permanent fused. Although, it could also be due to alterations in mitochondrial fission, as if it is hypoactivated, mitochondria could not fragmentize. To understand the mechanism, we studied the expression of the key molecules involved in both events, fusion and fission (figure R32) (Kuzmicic et al. 2011).

In respect to fission events, we studied the expression of DRP1 and Fis1 by real-time PCR (figure R32A) since they are key proteins that control mitochondrial fission. Normalizing the results to the expression of these proteins in ApoE3 cells (value equal to 1) the expression of Drp1 in ApoE4 cells is 0.97 ± 0.14 (figure R33A), whereas the expression of Fis1 in ApoE4 cells is 1.08 ± 0.16 (figure R33B). Thus, the expression of both proteins is similar between ApoE3 and ApoE4 astrocytes, at least at the RNA level.

Regarding fusion events, we assessed again by real-time qPCR the expression of Mfn1, Mfn2 and Opa1 (figure R32B). The expression of the 3 proteins is similar in both cell lines, although Mfn2 expression shows a tendency to be upregulated in ApoE4 astrocytes. Normalizing all the protein expressions to their expressions in ApoE3 cells (being 1), in ApoE4 cells we find values of 0.99 ± 0.21, (figure R33C) , 1.32 ± 0.205 (figure R33D) and 0.90 ± 0.12 (figure R33E) for Mfn1, Mfn2 and Opa1 expression, respectively.

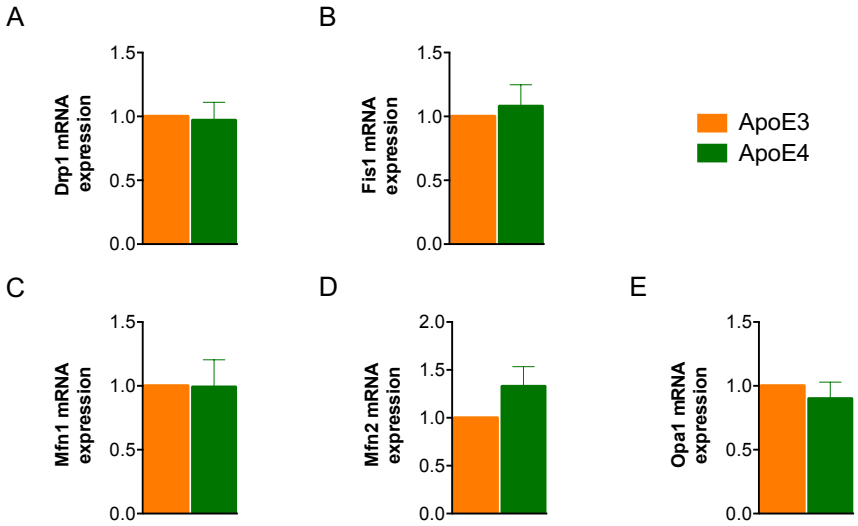

Figure R33: Expression of proteins involved in mitochondrial dynamics. Quantification of the expression of Drp1 (A), Fis1 (B), Mfn1 (C), Mfn2 (D) and Opa1 (E) by qPCR. Expression was normalized related to 18s and Gapdh expression and relative to ApoE3 cell expression of each N. At least 4 independent experiments were quantified. Unpaired parametric T-test was applied.

Therefore, none of the molecules studied in mitochondrial fission and fusion present any difference in their expression between ApoE4 and ApoE3 astrocytes at the RNA level. However, most of these proteins suffer post-translational modifications or change their location from the cytosol to mitochondria to achieve their function, so it would be interesting to study their protein expression, activation and/or locations.

2.2. Mitophagy and autophagy alterations of ApoE4 astrocytes.

As it has been explained in the introduction, mitophagy is the process by which damaged mitochondria are removed through autophagy. This process has also been related to mitochondrial dynamics since mitophagy is mainly carried out after fission events. Since we described that ApoE4 cells have an alteration in mitochondrial fission, we studied if the mitophagy and autophagy are also affected.

First, we investigated the expression of the principal molecules that trigger mitophagy: Pink1 and Parkin (figure R34). Real-time qPCR quantification showed that the expression of Pink1 is similar in both cell lines (0.79 ± 0.11 in ApoE4 cells compared to the expression in ApoE3 astrocytes) (figure R35A). Whereas, the expression of Parkin is dramatically down-regulated in ApoE4 cells (0.28 ± 0.27 normalized to the expression values in ApoE3 astrocytes) (figure R35B)

Therefore, this result suggests that ApoE4 cells could display an impairment in the mitophagy process. Thus, we asked if the general autophagy is also dysregulated. To answer this question, we studied the autophagic vesicles and the expression of a protein involved in autophagy.

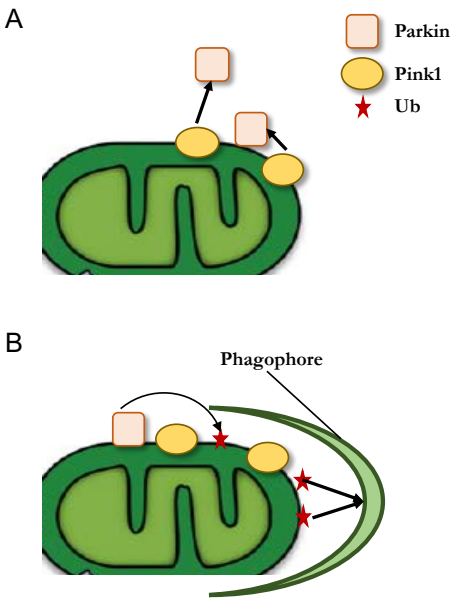

Figure R34: Principal proteins that participate in mitophagy. Pink protein recruits Parkin (A) that ubiquitinates (Ub) substrates of membrane proteins. This ubiquitination activates the formation of the phagophore (B). Modified from Kuzmicic et al. 2011.

We first evaluated the autophagic vesicles in ApoE3 and ApoE4 astrocytes by electron microscopy (Figure R36). The experiments were done by Dra. Gutierrez from the University of Málaga. Interestingly, ApoE4 cells present a higher number of autophagic vesicles compared to ApoE3 cells (yellow arrows from figure R36A). In detail, ApoE3 astrocytes have 56.16 ± 5.3% of autophagic vesicles compared to 73.95 ± 5.27% of the ApoE4 astrocytes (figure R36B). These studies also revealed differences in the number of lipid droplets between both cell lines. So that, ApoE3 cells display a higher amount of lipid droplet

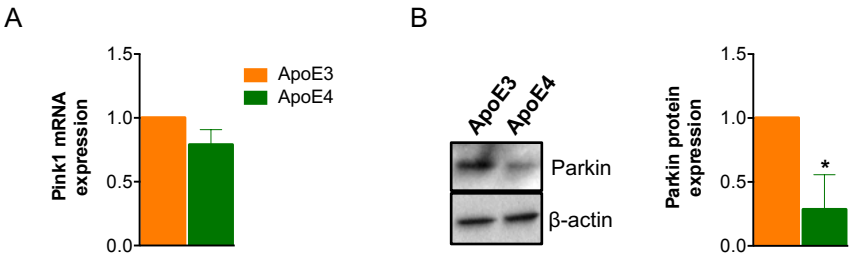

Figure R35: Pink and Parkin expression in ApoE3 and ApoE4 astrocytes. (A) Quantification of the mRNA expression of Pink1 by qPCR from 4 independent experiments. Expression was normalized with 18s and Gapdh expression. (B) Representative western of Parkin and β-actin protein expression and quantification of 4 independent western blots. Unpaired parametric T-test was applied. *p<0.05

vesicles (43.84 ± 5.3% of ApoE3 compared to 23.05 ± 5.27 of ApoE4 cells) (figure R36B) (brown arrows represents lipid droplets). The ratio of the quantifications highlighted the inverse relation of both (figure R36B). This idea is supported by the bibliography, where it has been described that there is a destruction of the lipid droplets when the autophagy is more active (H. Dong and Czaja 2011). Therefore, ApoE4 astrocytes show an accumulation of autophagic vesicles compared to ApoE3 astrocytes, and these results are in agreement with a diminution of mitophagy.

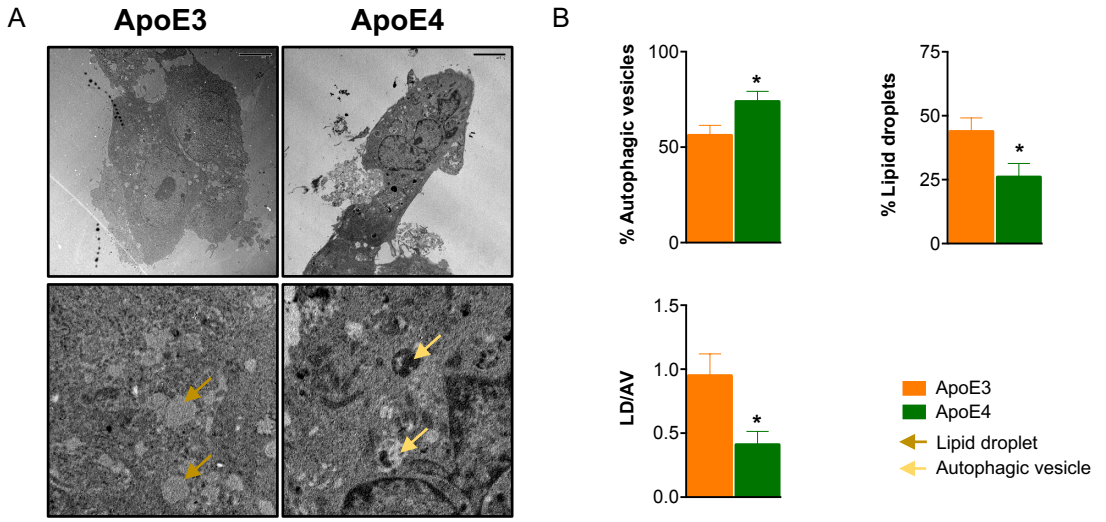

Figure R36: Autophagic vesicle and lipid droplets of ApoE3 and ApoE4 astrocytes. (A) Representative images and their magnification from electron microscopy. (B) Quantification of the vesicles from 12 ApoE3 cells and 9 ApoE4 astrocytes. The data are presented as the percentage of autophagic (AV) and lipid droplets (LD) vesicles in both cell lines and the ratio of both parameters. Parametric T-test was applied. *p<0.05

The autophagy is a very regulated process with several proteins that act in synchrony to degrade cellular components. One of the principal protein is LC3, which due to its modifications during autophagy it has been used as a marker of it. LC3 (LC3I) binds to phosphatidylethanolamine, being then LC3 II. Both forms can be identified by western blot and used to follow the autophagic process. Thus, we assessed the expression of this protein by western blot. In non-stimulated conditions, ApoE4 astrocytes show more expression of LC3I and LC3II (figure R37). Therefore, these results suggest that there is an activation of the autophagy process in ApoE4 cells in basal condition, in agreement with the findings of electron microscopy quantification.

To study the autophagic flux, we treated the cells with 50 and 100 nM Temsirolimus for 18 hours (that inhibits mTOR and activates autophagy). In ApoE3 cells, the increase in the

Temsirolimus concentration potentiates the diminution in LC3I suggesting that autophagic flux is advancing and promoting the conversion of LC3I into LC3II. Similar results were obtained in ApoE4 astrocytes (figure R37A). Therefore, it seems that both cell types can undergo the autophagic flux, although in the case of ApoE4, autophagy is activated even in non-stimulated conditions.

We also studied if the autophagic flux is affected by the presence of oAβ. We treated the cells with 5 μM oAβ for 6 and 24 hours (figure R37B). Interestingly, ApoE3 cells display a reduction in LC3I with the 24 hours-treatment whereas ApoE4 cells not, suggesting that there is no progression of the autophagic flux in presence of oAβ in these cells.

Altogether, ApoE4 astrocytes show an alteration not only in mitophagy but also in the general autophagy as it has been described by other authors (Simonovitch et al. 2016).

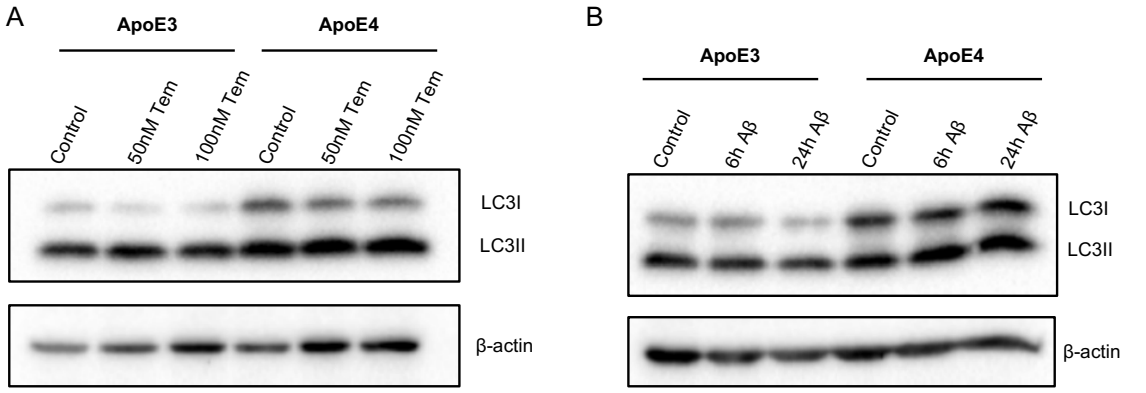

Figure R37: Autophagy in ApoE3 and ApoE4 astrocytes. Representative western blots of LC3 (A) in cells treated or not with 50nM or 100nM of Temsirolimus (Tem) for 18 hours and (B) in cells treated or not with 5μM of oAβ for 6 or 24 hours. β-actin was used to normalized the expression. Preliminary data.

2.3. Mitochondrial motility of ApoE3 and ApoE4 astrocytes.

We next analysed if the ApoE4 expression alters mitochondrial motility, essential for main cellular functions, for instance, to bring the mitochondria to places with high energy demand.

After labelling mitochondria with Mitotracker, we recorded the mitochondria of living ApoE3 and ApoE4 cells for 1 minute to explore their motility. We analysed the frames with IMARIS software obtaining a D^2 or squared displacement of each frame of the video. D^2 eliminates the directionality of the movement, taking into account the motility in all the directions (method detailed in the materials and methods section).

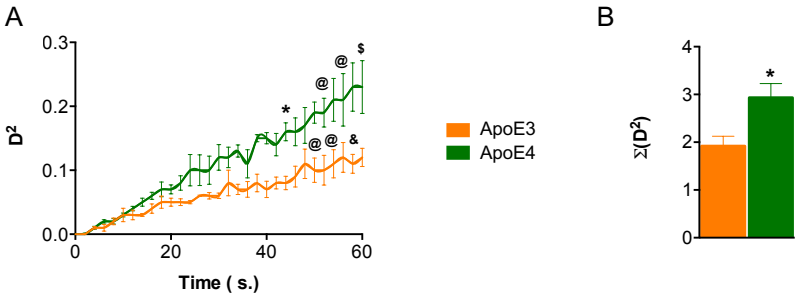

Figure R38: Mitochondrial motility of ApoE3 and ApoE4 astrocytes. (A) D^2 from astrocytic mitochondria that were stained with Mitotracker green and followed for 1 minute. (B) Mean of the addition of the D^2 from all the frames of ApoE3 and ApoE4 astrocytic mitochondria. Several mitochondria for several cells from 4 independent days were quantified. Two way ANOVA was applied in section A while parametric unpaired T-test was applied in section B. *p<0.05, @p<0.01, $p<0.001 and &p<0.0001.

Figure R38A represents the mean of the D^2 of each frame in both cell lines. The D^2 curve of ApoE4 astrocyte mitochondria is above the curve of ApoE3 cells. In particular, the time points of the frames that display significance are from 40 seconds (0.15 ± 0.008 μm^2 from ApoE4 mitochondria versus 0.07 ± 0.01 μm^2 from ApoE3 mitochondria) to the end of the recording, being the last time point measured the most clearly different (60 seconds; 0.23 ± 0.04 μm^2 from ApoE4 mitochondria versus 0.12 ± 0.01 μm^2 from ApoE3 mitochondria). This demonstrated that ApoE4 astrocyte mitochondria change their location faster than ApoE3 mitochondria. Furthermore, we observed an augment of the D^2 mean during the recording in both cell lines that is accentuated in ApoE4 cells. This suggests that light might be slightly stimulating the mitochondrial movement (figure R38A), especially in ApoE4 astrocytes. Moreover, the addition of all D^2 during all the recording also shows the increase in the mitochondrial motility in ApoE4 cells (2.93 ± 0.29 μm^2 of ApoE4 mitochondria compared to 1.91 ± 0.20 μm^2 of ApoE3 mitochondria) (figure R38B).

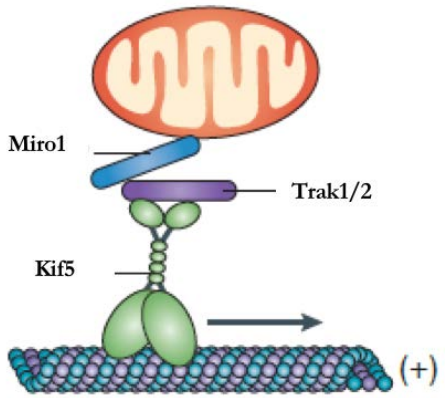

Figure R39: Principal proteins that participate in mitochondrial motility. Miro is the protein that binds to the mitochondria and Milton binds all the complex to the kinesines (Kif5). This model has been described in neurons. Modified from Sheng et al. 2012.

Overall, we can conclude that ApoE4 cell mitochondria display higher motility than ApoE3 ones. In this context, we examined the principal molecules involved in that movement. They

are Milton1 (codified by Trak1 gene), Milton2 (codified by Trak2 gene) and Miro (codified by Rhot1 gene). Their function is to anchor the mitochondria to the microtubules and promote or not their movement (figure R39). This model has been described in neurons (Sheng and Cai 2012) although Miro activity has also been found in astrocytes (Joshua G. Jackson and Robinson 2018).

The expression of Trak1 is similar in both cell lines because we detected by real-time qPCR a value of 0.96 ± 0.20 expression in ApoE4 astrocytes relative to the expression in ApoE3 cells (figure R40A). However, the expression of Trak2 shows a non-significant increment in ApoE4 astrocytes being 1.31 ± 0.25 normalized to the expression in ApoE3 cells (Figure R40B). Finally, Miro1 illustrates an upregulation in ApoE4 cells. Specifically, its expression in ApoE4 cells is 1.45 ± 0.06 compared to the expression in ApoE3 astrocytes (value equal to 1) (figure R40C).

Therefore, mitochondria from ApoE4 astrocytes present hypermotility being Miro1 and probably Trak2 the proposed candidates facilitating this increase.

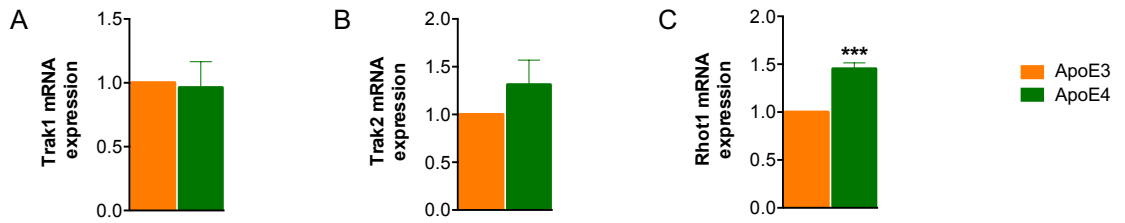

Figure R40: Expression of motility-related proteins in ApoE3 and ApoE4 astrocytes. Quantification of the mRNA expression of Trak1 (A), Trak2 (B) and Rhot1 (C) by qPCR from 4 independent experiments. Expression was normalized to the expression of 18s and Gapdh and relative to ApoE3 cell expression. Parametric unpaired T-test was applied . ***p<0.001

2.4. Mitochondrial DNA (mtDNA) assessment.

The oxidative state of the mitochondrial DNA has been studied in AD as a marker of stress. In fact, not only its oxidative state has been related to AD, but also its quantity, being diminished in the CSF of AD preclinical individuals, proposing it as a potential biomarker of this pathology (Podlesniy et al. 2013). Taking into account our results of mitochondrial dynamics alterations we analysed if mtDNA quantity is changed in ApoE4 astrocytes.

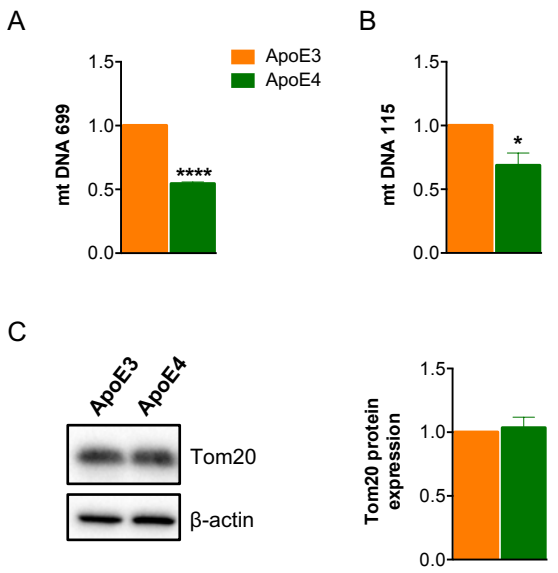

Figure R41: Quantity of mtDNA in ApoE3 and ApoE4 cells. Quantification of mitochondrial DNA by real time PCR measuring 2 fragments of mtDNA of different length, 115 (A) and 699 bp (B) from 3 independent experiments. (C) Representative western blot and quantification of 3 independent westerns from Tom20 protein. Expression data normalized by β-actin expression. Unpaired parametric T test was applied. *p<0.05, ****p<0.0001

To measure the mtDNA, we isolated this DNA from ApoE3 and ApoE4 cells and we evaluated its quantity using Real-time PCR of 2 fragments: one of 699 bp (base pair) and other of 115 bp. The primers for both fragments were selected from the study of Podlesniy et al (Podlesniy et al. 2013). The quantification demonstrated that ApoE4 cells display less quantity of both fragments. Regarding 699 fragment, ApoE4 cells show 0.54 ± 0.01, value normalized to the quantity of the fragment in ApoE3 cells (figure R41A), whereas the quantity of 115 fragment is 0.68 ± 0.09 also normalized to ApoE3 quantity (figure R41B). The use of 2 fragments with different length highlights the fact that this is a general diminution and not a deletion of a specific sequence of the mtDNA.

To understand if the reduction in the quantity is due to a reduction in the mitochondrial number or, on the contrary, it is a specific mechanism of mtDNA degradation, we quantified the expression of Tom20. Tom20 is a mitochondrial membrane protein that is constantly present in the mitochondria. The quantification of 3 independent westerns of Tom20 protein resulted in a similar expression of it between ApoE3 and ApoE4 astrocytes, thus, mitochondrial quantity or mass is similar (1.03 ± 0.08 expression in ApoE4 cells compared to 1 of ApoE3 cells) (figure R42C). These results indicate that a decrease in the mitochondrial mass in ApoE4 cells does not accompany the decrease in mtDNA. Probably, a dysfunction of the mitochondrial renewal caused by a defect in the mitophagy and/or in the fission leads to low mtDNA.

2.5. Mitochondrial metabolism in ApoE3 and ApoE4 astrocytes.

Since mitochondria dynamics can be related to mitochondrial metabolism, we investigated if the mitochondrial metabolism is altered in ApoE4 astrocytes. For that, we measured 2 molecules, ATP and lactate.

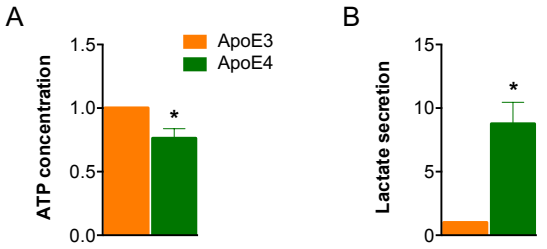

Figure R42: Lactate and ATP measurement. (A) Quantification of ATP measurement of ApoE3 and ApoE4 cells of 3 independent experiments (B) Quantification of lactate secretion for 2 hours of ApoE3 and ApoE4 astrocytes in KH medium of 3 independent experiments. Measurements were normalized by protein quantity. Parametric unpaired T-test was applied. *p<0.05

Firstly, we measured ATP concentration of the cells in a nutrient rich medium (DMEM supplemented with 10% of FBS). The ATP concentration in ApoE4 cells is 0.76 ± 0.07 compared to the ApoE3 cell ATP concentration (figure R42A). Thus, there is a reduction in the ATP concentration in ApoE4 cells.

Secondly, astrocytes also produce lactate as a principal pathway since they have the anaerobic glycolysis constitutively active, not only in the deprivation of oxygen or due to mitochondrial defects such as in other cells. We measured the secretion of lactate for 2 hours in both cell lines, and the results are very clear, ApoE4 cells secrete almost 9 times more lactate than ApoE3 cells (8.76 ± 1.6 compared to ApoE3 cell secretion) (figure R42B).

Taking all together, ApoE4 cells show lower ATP quantity and more lactate secretion than ApoE3 ones. Therefore, anaerobic glycolysis is potentiated in ApoE4 astrocytes, although, overall, there is less intracellular ATP in these cells. Anaerobic glycolysis is carried out in the cytoplasm, so ApoE4 might have an alteration of oxidative mitochondrial metabolism that probably promotes the increase in that anaerobic glycolysis in ApoE4 cells as a compensatory mechanism. Supporting this idea, the metabolic assay of the whole cells also shows that acylcarnitines are increased in ApoE4 astrocytes, as they are precursors of mitochondrial fatty oxidation, it seems that they might be accumulated due to a mitochondrial metabolism alteration. However, it cannot be discarded that the lower quantity of ATP could be due to an increase in its consumption.

Overall, our results indicate that ApoE4 astrocytes suffer mitochondrial dysfunctions. In particular, ApoE4 astrocytes do not achieve fission, have a decrease in a mitophagy-related

protein, accumulation of autophagy and increased mitochondrial motility, probably related to the increased in Miro1 expression. However, still remained unknown if the alteration in mitophagy is promoting the fission defect, or on the contrary, the mitophagy decrease is a consequence of the lack of capability to fission the mitochondria. As a probable consequence of the different mitochondrial dynamic alterations, ApoE4 astrocytes have a reduction in mtDNA content.

Chapter 3: Dysfunctional astrocyte signature as CSF AD biomarker.

Two approaches exist for CSF biomarker discovery: targeted and untargeted. In the targeted approach, the proteins related to AD pathogenesis are identified in the CSF, for instance, Aβ, whereas in the untargeted, the proteins of the CSF are identified by massive proteomic analyses. Thus, the second approach does not take into account the alterations or mechanisms that allow them to be a biomarker. Furthermore, this approach results in a huge quantity of molecules that also differ among different studies. Therefore, we proposed to use astrocytic proteins representing astrocyte dysfunction in AD. This would be in between both approaches, because we identified proteins that we know are astrocyte-specific and based on their dysfunction in AD (targeted) but looking at all the proteins from the CSF that are qualified as astrocytes (untargeted).

Concerning AD CSF biomarkers, the field is focused on single molecule detection and there are no groups of proteins that represent cellular dysfunctions in the disease. Thus, we wanted to create an astrocytic specific signature. Astrocytes are suggested to be contributors to the disease although most of the studies still underestimate them. An example related to CSF biomarker is the mitochondrial DNA. As it has been mention in the introduction, a decrease in mtDNA in the CSF has been proposed as a biomarker of preclinical stages of the AD (Podlesniy et al. 2013). In addition, this reduction is specific to AD as compared with another neurodegenerative disease such as Creutzfeldt-Jakob disease (Podlesniy et al. 2016). However, Podlesniy et al. proposed that this decrease might be due to neuronal alterations since they observed diminution of mtDNA in cultured neurons. Interestingly, we observed the same in ApoE4 astrocytes. Therefore, we believe that astrocytes could be contributing, with other cells, to the decreased mtDNA in the CSF.

Since we experimentally demonstrated that ApoE4 astrocytes have alterations in the calcium signalling, lysosomal (as calcium stores and as components of the autophagic process) and mitochondrial functions, we focused our functional signature on these alterations. Our primary purpose was to create a list of CSF biomarker candidates to identify CSF astrocytic signature related to ApoE4 pathology. We reason that since ApoE4 is expressed throughout the life, it would contribute to astrocytic dysfunction in the early stages of the AD. Thus, performing a CSF signature based on ApoE4-elicited dysfunction would help in the early identification of individuals at high-risk. However, most of the proteomic available CSF data are not stratified by ApoE genotype. Since the functions that we found altered in ApoE4 astrocytes have been widely related to the AD (LaFerla 2002; Moreira et al. 2010; Zare-

Shahabadi et al. 2015), we started our analysis by identifying an astrocytic AD signature of the CSF. After that, we will examine this signature in the context of the ApoE genotype when possible (figure R43).

Altogether, we have created an astrocytic signature of AD based on the alterations of calcium signalling, lysosomal and mitochondrial functions that we have found in astrocytes. We used

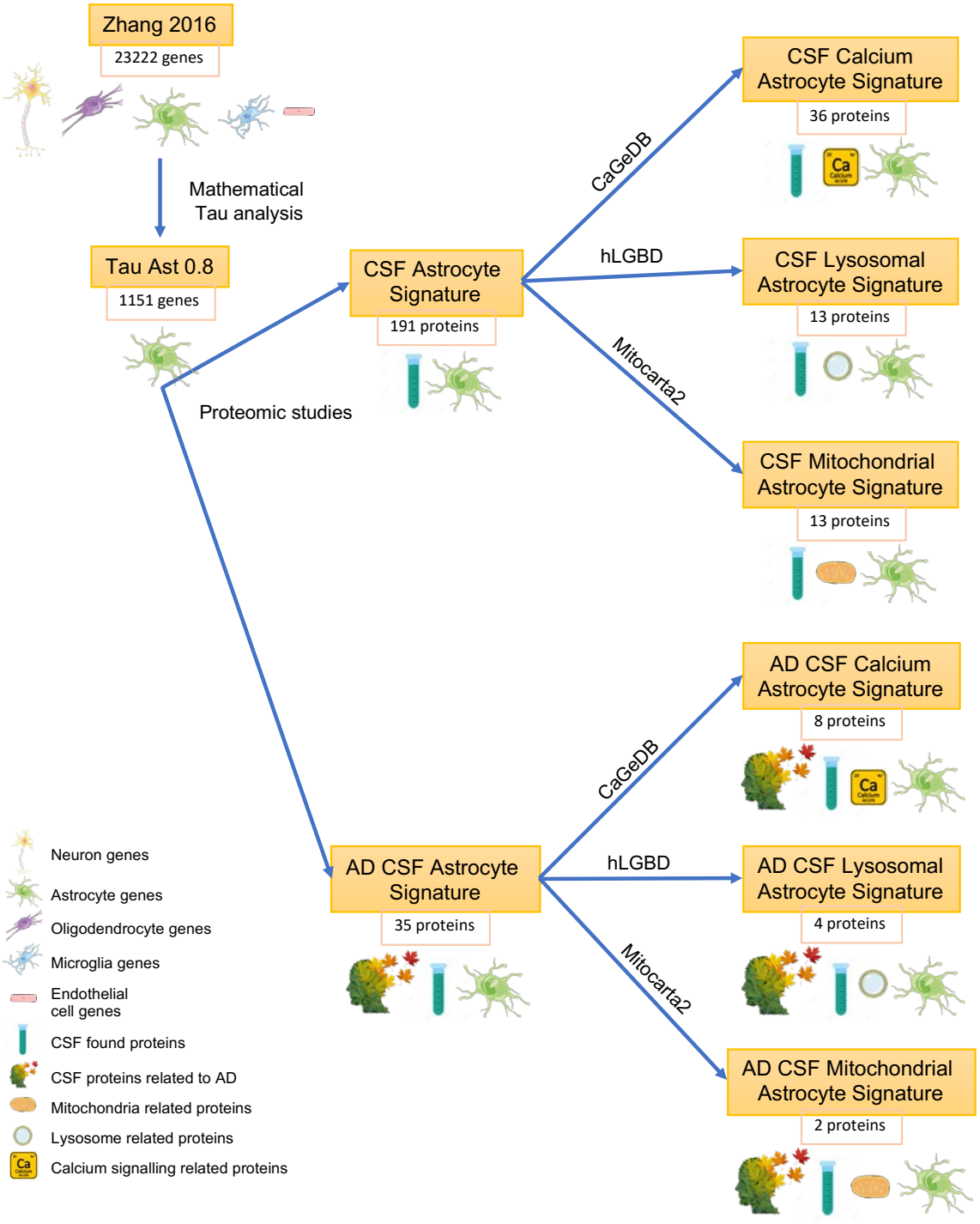

Figure R43: Workflow for the biomarker discovery. Graphical summary of the followed procedure.

public databases to the perform the analysis. Figure R43 depicts the workflow that we have employed for the candidate biomarker discovery.

3.1. Identification of astrocytic specific genes

First, to create the astrocytic signature, we had to establish which are the specific astrocytic genes. To do that, we employed the database produced by the research group of Dr. Barres that we called "Zhang 2016", according to its publication (Y. Zhang et al. 2016) (Annex I). These authors isolated the different cell types from human brain by immunopanning and extracted their RNA. They, thus, obtained data from human astrocytes, neurons, microglia, oligodendrocytes and endothelial cells. Then, they analysed the gene expression by RNA-seq obtaining 23222 differentially expressed genes for all the cell types.

Using the expression data of the different cells provided by "Zhang 2016" database, we performed a mathematical test of cell specificity of each gene in collaboration with Dr. Wood (Georgia Institute of Technology (Atlanta)). Among the different mathematical tests that exist, we chose Tau since it has been demonstrated as the most robust method on its capacity to distinguish the specific genes for a tissue (Kryuchkova-Mostacci and Robinson-Rechavi 2017) (figure R44). Tau is employed as a tissue specificity index, but we took advantage of it to distinguish the specific genes of each cell type. The main advantage of this method is that takes into account the expression of each gene in all the other cells providing a specificity number of a gene for each cell type. The mathematical formula is:

$$\tau = \frac{\sum_{i=1}^{n}(1-\hat{x}_i)}{n-1};\ \hat{x}_i = \frac{x_i}{\max\limits_{1\le i\le n}(x_i)}.$$

where τ is Tau, n is the number of cell types and x_i is the expression of the gene in cell i. When this number is close to 1, it means that this gene is specific of this cell type, by contrast, a value closer to 0 means that this gene is ubiquitously expressed.

We considered genes with Tau above 0.8 as the ones specific for each cell type based on the study of Kryuchkova et al. (Kryuchkova-Mostacci and Robinson-Rechavi 2017) (figure R44). Therefore, after applying this test, we obtained a list of 1151 specific genes for astrocytes. We called this dataset "Tau Ast 0.8".(Annex I).

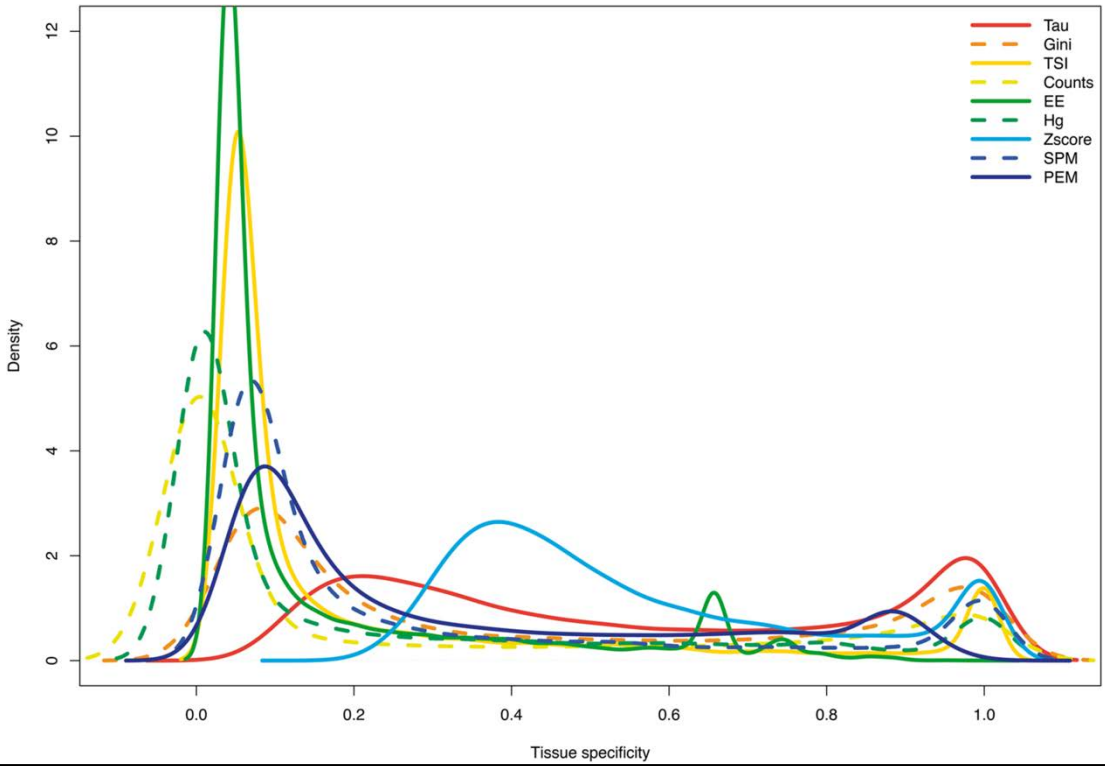

Figure R44: Distribution of the different tissue-specificity parameters with data for human RNA-seq of 27 tissues from Kryuchkova et al. 9 different tissue specific index have been used to classified the specificity of each gene. Each line represent the distribution of the genes as density of genes according to their specificity calculated based on the different indexes, in other words the gene density in all the possible values of each index. Graph created with density function from R. In red Tau analysis.

3.2. General astrocyte signature of AD

The next step was to know which of the genes in the dataset "Tau Ast 0.8" table codify for proteins that appear in CSF and are altered in the CSF of AD patients. To do that, we first created a database with CSF proteomes that we called "Proteomic studies". This table is composed of the proteomic results from 2 databases, 1 article of proteomic data from healthy CSF and 28 research articles, in which, they compared AD CSF to healthy CSF with different methodologies. Then, in this database we have proteins found in the CSF and from them, the ones that change in the CSF of AD individuals (Annex I).

The references of the proteomic table are Schutzer et al. 2010; Zetterberg 2017; Guldbrandsen et al. 2017; Pannee et al. 2013, 2016; Korecka et al. 2014; McAvoy et al. 2014; Barthélemy et al. 2016; Martínez-Morillo et al. 2014; Rezeli et al. 2015; Oeckl et al. 2014; A. Brinkmalm et al. 2014; Öhrfelt et al. 2016; Sjödin et al. 2016; Heslegrave et al. 2016; Hendrickson et al. 2015; Wijte et al. 2012; Kvartsberg et al. 2015; Bruggink et al. 2015; Rogeberg et al. 2015; Rudinskiy et al. 2016; Di Domenico et al. 2016; Hölttä et al. 2015;

Khoonsari et al. 2016; Ringman et al. 2012; Heywood et al. 2015; Spellman et al. 2015; Wildsmith et al. 2014; G. Brinkmalm et al. 2018; Remnestål et al. 2016; Paterson et al. 2016.

Gene	Accesion number	Proteomic studies	
		Found	Changed
APOE	P02649	++++++++++	+++++++
CHI3L1	P36222	++++++++	+++++
CST3	P01034	++++++++	+++
CLU	P10909	+++++++	++
PTGDS	P41222	++++++	++++
CPE	P16870	+++++	++
LSAMP	Q13449	+++++	++
NCAN	O14594	+++++	+
C4A	P0C0L4	++++	++
FBLN1	P23142	++++	++
S100B	P04271	++++	++
C5	P01031	++++	+
GFAP	P14136	++++	+
KLKB1	P03952	++++	+
NEO1	Q92859	++++	+
PAPLN	O95428	++++	+
SERPINA3	P01011	++++	+
SPON1	Q9HCB6	++++	+
NRCAM	Q92823	++++	
KAL1	P29622	+++	++
NRXN1	P58400	+++	++
DKK3	Q9UBP4	+++	+
EFEMP1	Q12805	+++	+
LTBP1	Q14766	+++	+
PTPRZ1	P23471	+++	+
SCG3	Q8WXD2	+++	+
PRDX1	Q06830	+++	
SPARCL1	Q14515	+++	
C12orf49	Q9H741	++	+
C1S	P09871	++	+
CKB	P12277	++	+
DDAH1	O94760	++	+
GFRA1	P56159	++	+
HP	P00738	++	+
ITM2C	Q9NQX7	++	+
LDHB	P07195	++	+
MT3	P25713	++	+
SDC2	P34741	++	+
AGT	P01019	++	
ALDOC	P09972	++	
BCAN	Q96GW7	++	
C1QTNF3	Q9BXJ4	++	
CACHD1	Q5VU97	++	
CADM1	Q9BY67	++	
CAT	P04040	++	
DAG1	Q14118	++	
ENO1	P06733	++	
FABP7	O15540	++	
FGFR2	P21802	++	
MEGF10	Q96KG7	++	
PLTP	P55058	++	
PRCP	P42785	++	
PRDX6	P30041	++	
PSAT1	Q9Y617	++	
SORCS2	Q96PQ0	++	
SRPX	P78539	++	
TGFB2	P61812	++	
ACP6	Q9NPH0	+	
AEBP1	Q8IUX7	+	
AK1	P00568	+	
ALDH1A1	P00352	+	
ALDH4A1	P30038	+	
ALDH5A1	P51649	+	
ANGPTL1	O95841	+	
ANTXR1	Q9H6X2	+	
APC	P25054	+	
AQP1	P29972	+	
ASPH	Q12797	+	
ASTN1	O14525	+	
ATP1A2	P50993	+	
ATP1B2	P14415	+	
BMP7	P18075	+	
C14orf37	Q86TY3	+	
C16orf89	Q6UX73	+	
C1R	P00736	+	
CA12	O43570	+	
CALCA	P06881	+	
CALCB	P10092	+	
CD109	Q6YHK3	+	
CDH2	P19022	+	
CDH20	Q9HBT6	+	
CDH4	P55283	+	
CHI3L2	Q15782	+	
CHRDL1	Q9BU40	+	
CHST1	O43916	+	
CHST10	O43529	+	
CNTFR	P26992	+	
COL16A1	Q07092	+	
COL28A1	Q2UY09	+	
COL6A1	P12109	+	
CPNE6	O95741	+	
CRELD2	Q6UXH1	+	
CSPG5	O95196	+	
CTSH	P09668	+	
DBC1	O60477	+	
DDR1	Q08345	+	
DDR2	Q16832	+	
DNAH7	Q8WXX0	+	
DNASE2	O00115	+	
ECHDC2	Q86YB7	+	
EDNRB	P24530	+	
EGFR	P00533	+	
EMID1	Q96A84	+	
ENO3	P13929	+	
EPHB1	P54762	+	
ETFA	P13804	+	
EZR	P15311	+	
FAH	P16930	+	
FAM198B	Q6UWH4	+	
FAM5B	Q5VTR2	+	
FAS	P25445	+	
FGFR3	P22607	+	
FIBIN	Q8TAL6	+	
FLRT2	O43155	+	
FREM2	Q5SZK8	+	
FSTL1	Q12841	+	
FZD7	O75084	+	
GJA1	P17302	+	
GLUL	P15104	+	
GOLIM4	O00461	+	
GPC5	P78333	+	
GPR37L1	O60883	+	
GSTM1	P09488	+	
HEPACAM	Q14CZ8	+	
HPR	P00739	+	
HRSP12	P52758	+	
HS2ST1	Q7LGA3	+	
IGSF1	Q8N6C5	+	
IGSF11	Q5DX21	+	
ITGA7	Q13683	+	
ITGB8	P26012	+	
KIAA0319	Q5VV43	+	
LFNG	Q8NES3	+	
LGI1	O95970	+	
LIFR	P42702	+	
LRIG1	Q96JA1	+	
LRP1B	Q9NZR2	+	
MASP1	P48740	+	
MCCC2	Q9HCC0	+	
ME1	P48163	+	
MMP28	Q9H239	+	
MRO	Q9BYG7	+	
MST1	P26927	+	
MSTN	O14793	+	
MYBPC1	Q00872	+	
MYLK	Q15746	+	
NDRG2	Q9UN36	+	
NOTCH2	Q04721	+	
NTM	Q9P121	+	
NTRK2	Q16620	+	
NTRK3	Q16288	+	
NUDT3	O95989	+	
OAF	Q86UD1	+	
OLFM2	O95897	+	
PARD3B	Q8TEW8	+	
PCSK5	Q92824	+	
PGM1	P36871	+	
PLXNB1	O43157	+	
PON1	P27169	+	
PON3	Q15166	+	
PPP1R1B	Q9UD71	+	
PTN	P21246	+	
PTPLAD1	Q9P035	+	
PTPRF	P10586	+	
PYGM	P11217	+	
RAB30	Q15771	+	
RGMA	Q96B86	+	
SCN4B	Q8IWT1	+	
SCRG1	O75711	+	
SDC4	P31431	+	
SELENBP1	Q13228	+	
SEMA4A	Q9H3S1	+	
SEMA4B	Q9NPR2	+	
SERPINE2	P07093	+	
SIRPA	P78324	+	
SLC14A1	Q13336	+	
SLC1A2	P43004	+	
SLC39A12	Q504Y0	+	
SLC4A4	Q9Y6R1	+	
SLC9A3R1	O14745	+	
SLITRK2	Q9H156	+	
SORBS1	Q9BX66	+	
TCF7L2	Q9NQB0	+	
TEX15	Q9BXT5	+	
TGFBR3	Q03167	+	
TKT	P29401	+	
TMEM132C	Q8N3T6	+	
TNIK	Q9UKE5	+	
TPP1	O14773	+	
VIM	P08670	+	
ZBTB20	Q9HC78	+	

Table R3: Astrocytic proteins that appear in CSF. The "+" indicates the studies where a protein has been found and if its quantity is changed in the AD CSF. Proteins are ranked by the number of times that they appear in proteomic studies.

Before comparing both databases ("Tau Ast 0.8" and "Proteomic studies") we needed to normalize them since we could not compare genes with proteins, and because of the different nomenclature. We converted each gene and protein name to an accession number based on UniProt database (https://www.uniprot.org). This platform accounts for all the known human proteome, describing for each protein, its name, gene, localization and a brief function among other information. To simplify the information, in the table of "proteomic studies" it is only shown the accession number that corresponds to each identified protein. Besides, it is detailed all the proteins identified in each study or database that composed the proteomic studies dataset ("found") and the ones whose quantity is altered in the CSF of AD patients ("changed"). Proteins whose quantity is increased in AD are in green colour and proteins whose quantity is decreased, in red colour (Annex I).

To confirm that "Tau Ast 0.8" table and "proteomic studies" table could be compared we determined the coincidence of the proteins from "proteomic studies" table to "Zhang 2016" database. Around 93% of proteins from "proteomic studies" appear in "Zhang 2016".

191 proteins in "Tau Ast 0.8" were established as specific for astrocytes and were found in the CSF ("proteomic studies" dataset). Table R3 contains these proteins, the number of times that have been identified in the proteomic studies and ,of them, in how many studies have determined it as related to the CSF of the AD patients. Interestingly, 3 proteins that have been found in more than 3 proteomic studies are not changed in AD. These proteins are NRCAM (neural cell adhesion molecule 1), PRDX1 (peroxiredoxin 1) and SPARCL1 (SPARC like 1). Therefore, these proteins might represent the healthy CSF signature of astrocytes compared to the AD CSF signature.

Until here, our criterion to select candidates was proteins that are astrocyte specific and appear in the CSF of at least in one study. Trying to improve the probability of finding a protein in the CSF, we asked if a higher brain expression of a protein means a higher probability to find this protein in the CSF. To solve this question, we used the gene expression data of human cortex from "Zhang 2016" database. We compared this expression with the number of times

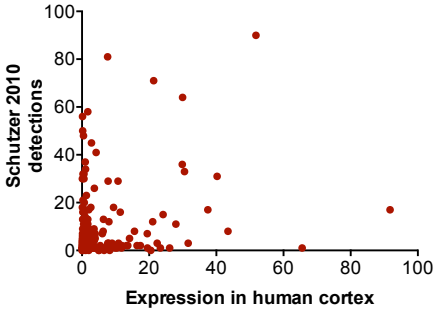

Figure R45: Astrocytic proteins that appear in CSF plotted according their expression and their detections in the CSF. 2 of the proteins were excluded for the analysis due to their extreme expression values.

that peptides from each protein were detected in one of the most compressive analysis of the healthy CSF, "Schutzer 2010"(Schutzer et al. 2010). This study is considered as one of the most complete databases from healthy human CSF. Figure R45 shows all the proteins plotted according to their expression in the human cortex and their number of detections in "Schutzer 2010" proteome. To confirm that there is no correlation between both parameters we calculated the Pearson coefficient, which 0 means no correlation and 1 means correlation. We obtained a coefficient of 0.24, confirming the absence of correlation between the expression of a protein in brain and its presence in the CSF. Therefore, we excluded the brain expression as a criterion for candidate identification and we focused on the proteomics studies.

From the 191 proteins that can be found in the CSF, 35 have been related to the AD and can be considered as a biomarker candidate. To find the candidates with high probability and improve the validation process, we represented these proteins in Figure R46 according to the number of times that appear in proteomic studies and the times that their quantity in these studies is altered in AD (figure R46). Therefore, we can consider the number of times that has been positively associated as an AD biomarker or not. 5 of the 35 proteins seems to be better candidates since they appear separated from the rest in the graph. They are apolipoprotein E (APOE), prostaglandin D2 synthase (PTGDS), cystatin C (CST3) clusterin (CLU), chitinase 3 (CHI3L1 or YLK40). From them, the 2 with high probability are APOE and CHI3L1, which have been already proposed as potential AD CSF biomarker (Craig-Schapiro et al. 2010; Perrin et al. 2011; Wildsmith et al. 2014). From the other 3, the most appropriated one would be PTGDS since it has a high score of detection (4 of 6 studies consider it related to the AD). Finally, CST3 is found in 8 studies and only changed in 3, and CLU is found in 7 and only related to the AD in 2.

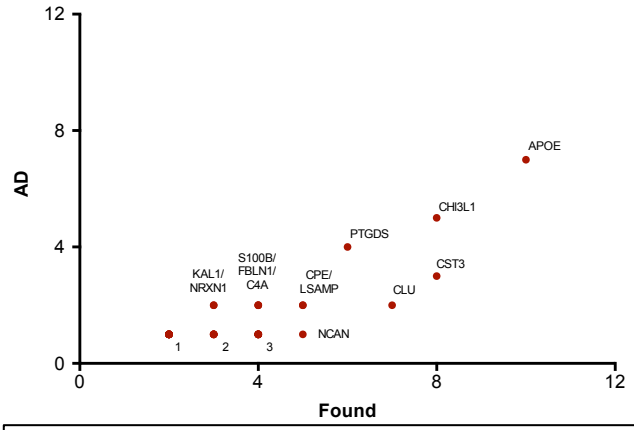

Figure R46: AD CSF astrocytic candidates for biomarkers. Representation of the astrocytic proteins that has been found changed in AD CSF proteome. The x axes correspond to the number of studies of which a protein appears, and the y axes the number of times that is altered in AD. Values of each protein in table R3. (1) GFRA1, LDHB, C1S, C12orf49, HP, ITM2C, DDAH1, CKB, SDC2 and MT3; (2) PTPRZ1, DKK3, SCG3, LTBP1 and EFEMP1; (3) NEO1, C5, SERPINA3, KLKB1, PAPLN and SPON1.

Essentially, at this point, we have an AD CSF astrocytic signature. To incorporate the alterations of the organelles that we described in astrocytes to propose a functional AD signature, we compared the CSF astrocyte signature with different databases from mitochondria (MitoCarta2), lysosome (hLGBD) and calcium related proteins (CaGeBD).

3.3. Calcium-related astrocyte signature of AD

First, we investigated which astrocytic proteins could be related to calcium signalling ,and at the same time, be a CSF biomarker. We used Calcium Genes Database (CaGeDB). This database consists of all the genes that are related in calcium signalling or calcium binding. To generate it, they used Gene Ontology terms associated with calcium and they extracted and classified the genes, employing Ensembl and NCBI Gene databases. The database is composed of 1808 calcium associated genes (http://cagedb.uhlenlab.org, (Hörtenhuber et al. 2017)) (Annex 1). As in the case of "proteomic studies" table, we needed to normalize the names of the database giving them accession numbers of UniProt and compared to "Zhang 2016". 94.95% of the genes from CaGeDB database are found in "Zhang 2016". Therefore, we continued with the assessment of candidates.

Of the 191 CSF specific astrocytic proteins, 36 are coincident with the proteins present in the CaGeDB database (table R4). The top proteins according to the times that are found in the different proteomic studies and, according to our analysis, are more probable to find in the CSF, are APOE, neurocan (NCAN), fibulin 1 (FBLN1), S100B, EFG containing fibulin

Calcium related			
Gene	Accession number	Proteomic studies	
		Found	Changed
APOE	P02649	++++++++++	+++++++
NCAN	O14594	+++++	+
FBLN1	P23142	++++	++
S100B	P04271	++++	++
EFEMP1	Q12805	+++	+
NRXN1	P58400	+++	++
LTBP1	Q14766	+++	+
SPARCL1	Q14515	+++	
C1S	P09871	++	+
AGT	P01019	++	
DAG1	Q14118	++	
CACHD1	Q5VU97	++	
MASP1	P48740	+	
PON1	P27169	+	
EGFR	P00533	+	
CDH4	P55283	+	
EDNRB	P24530	+	
ATP1A2	P50993	+	
GJA1	P17302	+	
C1R	P00736	+	
AEBP1	Q8IUX7	+	
NOTCH2	Q04721	+	
CDH20	Q9HBT6	+	
FSTL1	Q12841	+	
CALCA	P06881	+	
DNAH7	Q8WXX0	+	
TCF7L2	Q9NQB0	+	
FAS	P25445	+	
CDH2	P19022	+	
CPNE6	O95741	+	
CRELD2	Q6UXH1	+	
ASPH	Q12797	+	
LRP1B	Q9NZR2	+	
EZR	P15311	+	
CALCB	P10092	+	
MYLK	Q15746	+	

Table R4: CSF astrocytic candidate for biomarker based on calcium signalling. Astrocytic proteins based on calcium signalling that would be appeared in the CSF ranked based on the time found in a proteomic study.

extracellular matrix protein 1 (EFEMP1), neurexin1 (NRXN1), latent transforming growth factor beta binding protein 1 (LTBP1) and Sparc like 1 (SPARCL1).

Based on our results in cultured astrocyte, the interesting proteins are the ones regulated by intracellular calcium, and from all the calcium-related, only NRXN1 and S100B belong to this group. The other molecules are constituents of the extracellular matrix and are regulated by extracellular calcium. However, we also discarded NRXN1 as it has been mainly described in neurons. The Tau analysis give to that protein an index of 0.81, near of the threshold that we fixed. On the other hand, ApoE also appears in that classification due to that it is a secreted protein (pathway controlled by calcium signalling in some cell types) (table R4).

We then focused on how many proteins of the 35 found and changed in AD are related to calcium signalling. The group is reduced, only 8 proteins (figure 47) and from them, the ones that appear changed in more studies are the ApoE, FBLN1, S100B and NRXN1. Since FBLN1 is an extracellular protein and NRX1 a neuronal protein, we excluded them. Therefore, again, ApoE and S100B are proposed as a components of the astrocytic AD signature.

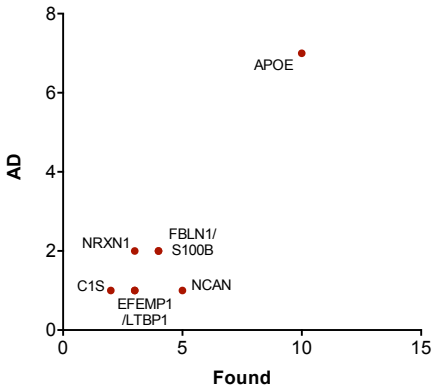

Figure R47: AD CSF astrocytic candidates for biomarkers based on calcium signalling. Representation of the astrocytic proteins that has been found changed in AD CSF proteome. The x axes correspond to the number of studies in which a protein appears and the y axes the number of times that is altered in AD. Values of each protein are in table R3.

3.4. Lysosomal-related astrocyte signature of AD

Since lysosomal alterations cause the dysregulation of the calcium signalling, and lysosomes participate in autophagy in ApoE4 astrocytes, we studied which of the proteins of "Tau Ast 0.8" table are lysosomal. To do that, we used the human Lysosome Genes Database (hLGDB). As its name indicates, it contains the human genes that codify for lysosomal proteins. The creators of this database acquired information of different sources such articles and other databases as Reactome, Gene Ontology, KEGG or UniProt to construct a comprehensive list of 435 lysosomal genes (http://lysosome.unipg.it/ (Brozzi et al. 2013)). As in the other cases, we normalized the database genes by UniProt accession number and

Lysosomal			
Gene	Accesion number	Proteomic studies	
		Found	Changed
CST3	P01034	++++++++	+++
CLU	P10909	+++++++	++
PTGDS	P41222	++++++	++++
PRCP	P42785	++	
ITM2C	Q9NQX7	++	+
PRDX6	P30041	++	
CAT	P04040	++	
TPP1	O14773	+	
GJA1	P17302	+	
FGFR3	P22607	+	
COL6A1	P12109	+	
DNASE2	O00115	+	
CTSH	P09668	+	

Table R5: CSF astrocytic candidate for lysosome based biomarker proteins. Astrocytic proteins related to lysosomal compartment that would be appeared in the CSF, ranked based on the number of times found in a proteomic study.

we compared the percentage of genes from it with "Zhang 2016". The 97.47% of genes from hLGDB are found in Zhang 2016, having the highest coincidence between databases observed in our study.

Using hLGDB, we found that 13 proteins of "Tau Ast 0.8" dataset are lysosomal or secreted by lysosomes (table R5). Of them, the first, according to the number of times that are found in a proteomic study, are cystatin C (CST3), clusterin (CLU) and prostaglandin D2 synthetase (PTGDS) (table R5).

After filtering the proteins with the ones changed in AD, we found that only 4 could contribute to the AD signature. (figure R48). These proteins are PTGDS, CST3, CLU and integral membrane protein 2C (ITM2C). From them, the protein that is changed in more studies is PTGDS (3 out 8), followed by CLU and CST3. Clusterin has been related to AD since it is an extracellular chaperone that promotes the Aβ clearance (Nelson, Sagare, and Zlokovic 2017) and PTDGS and CST3 are related to protein processing but in the case of CST3, its activity is extracellular (GeneCards website). The last lysosomal candidate is ITM2C that is a negative regulator of Aβ production (GeneCards webpage). Thus, even with the lowest score, as it has only been found in one study, due to its function, it is a good potential component of the signature. Although, none

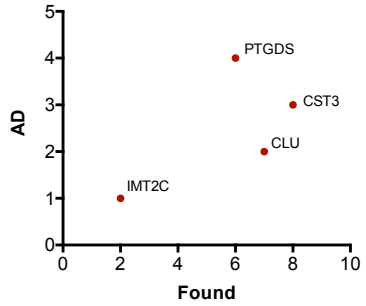

Figure R48: AD CSF astrocytic candidate for lysosome based biomarker proteins Representation of the astrocytic proteins that has been found changed in AD CSF proteome. The x axes correspond to the number of studies of which a protein appears and the y axes the number of times that is altered in AD. Values of each protein in table R3.

of these lysosomal proteins are related directly to the lysosomal functions that we found altered in ApoE4 astrocytes, we believe that they could be indirectly affected by the endolysosomal system and reflect its dysregulation changing their quantity. Thus, we considered these 4 proteins as part of the AD astrocytic signature.

3.5. Mitochondrial related astrocyte signature of AD

Finally, we looked at the signature of mitochondria using the MitoCarta2. This database englobes all the proteins that are localized at the mitochondria, thus, it is composed of proteins codified by nuclear and mitochondrial DNA. We employed the human dataset that is constituted by 1158 human mitochondrial proteins (https://www.broadinstitute.org/files/shared/metabolism/mitocarta/human.mitocarta2.0.html) (Calvo, Clauser, and Mootha 2016). Before extracting the mitochondrial proteins to determine the astrocyte signature, we normalized the protein names as previously presented (accession number of UniProt) and we tested the compatibility of the databases. 94.99% of the proteins from MitoCarta appeared in "Zhang 2016". Since the most of the proteins are found in "Zhang 2016", we proceeded with the establishment of the biomarker signature.

Mitochondrial			
Gene	Accesion number	Proteomic studies	
		Found	Changed
DDAH1	O94760	++	+
LDHB	P07195	++	+
PRDX6	P30041	++	
CAT	P04040	++	
TKT	P29401	+	
HRSP12	P52758	+	
ALDH4A1	P30038	+	
MCCC2	Q9HCC0	+	
ECHDC2	Q86YB7	+	
ME1	P48163	+	
ACP6	Q9NPH0	+	
ETFA	P13804	+	
ALDH5A1	P51649	+	

Comparing the number of times obtained from each protein with the rest of the tables, in this case, the majority of proteins have lower numbers. Therefore, it seems that the mitochondrial component is less represented in the CSF as compared to lysosomal-related proteins, for example.

Table R6: CSF astrocytic candidate for biomarker based on mitochondrial proteins. Astrocytic proteins related to mitochondrial function that would be appeared in CSF.

Filtering these proteins with the AD database, only 2 of them are suggested as good biomarker candidates according to our criteria, dimethylarginine dimethylaminohydrolase 1 (DDAH1) and lactate dehydrogenase B (LDHB) (table R6) but with a low score. They are only found in 2 studies and from them, are only changed in one in the CSF proteome of AD patients. However, none of these proteins are related to the mitochondrial processes altered in ApoE4 astrocytes. If mitochondria of ApoE4 astrocytes were totally damaged, we could propose that these proteins could be part of the signature due to the massive mitochondrial affectation, but since they can function normally in some aspects, for example, uptaking calcium we decided to discard them. Moreover, LDHB is also a cytosolic protein, so we cannot ensure that could reflect mitochondrial dysfunctions.

3.6. Summary of the biomarker candidates proposed

We proposed an astrocytic signature of the AD based on lysosomal and calcium signalling dysregulation for the early identification of AD. This signature is composed of ApoE, S100B, PTGDS, CST3, CLU and ITM2C. The candidates to form the signature are predominantly found increased in the AD CSF except ITM2C that is found in lower quantity in the AD condition. Now, an important part of the study, will be to validate this signature by proteomic studies or ELISA assays and to evaluate its specificity and sensitivity as a good biomarker.

Annex I

Data used for the identification of the biomarkers are available in an Excel file under request. Contact to raquelarramona@gmail.com. This format has been chosen due to the huge quantity of proteins from some databases that make difficult attaching them printed. The first sheet of the file contains the information that can be found in the rest of the sheets.

Discussion

ApoE4 has been recognized as the primary genetic risk factor of the sporadic form of the AD. The research about it has been focused on neurons and amyloid β metabolism, although this molecule is mainly secreted by astrocytes as part of lipoproteins. Astrocytes are altered during the development of the AD, whereas their contribution to the pathogenesis remains not fully understood. Taking into account both ideas, in this study we wanted to elucidate the relationship between the expression of ApoE4 in astrocytes and their functions to understand why ApoE4 is a genetic risk factor of the AD. Mainly, we discovered that 2 of the central astrocyte processes, previously related to the AD, are dysregulated in ApoE4 astrocytes: calcium signalling and mitochondrial functions, pointing to ApoE4 as the leading cause in astrocytes for the first time. Therefore, the expression of endogenous ApoE4 is enough to alter astrocyte functions related to AD pathology and hence might contribute to the causes or/and development of the AD.

1. ApoE4 expression dysregulates calcium signalling in astrocytes

Alterations in astrocyte calcium signalling have been described in different biological models of the AD models: cell cultures, slices and live animals (detailed in the introduction) (Pirttimaki et al. 2013; L. Lee, Kosuri, and Arancio 2014; Bosson et al. 2017; Ambra A. Grolla et al. 2013; Alberdi et al. 2013). However, none of them described ApoE or ApoE4 as a factor with the ability to affect calcium signalling. We described for the first time that the expression of ApoE4 modifies calcium homeostasis in astrocytes. Interestingly, ApoE4 alters not only intracellular calcium at rest conditions but also ATP-elicited calcium responses which are elicited by different calcium sources of the calcium pathways and not regulated by extracellular lipid or lipoproteins.

V-ATPase hyperactivity in ApoE4 astrocytes

We have described lower basal calcium in ApoE4 cells, as a consequence of the increased V-ATPase activity. This greater activity is maintained in lipoprotein deficient. A priori, this result is contrary to what is found in the bibliography. For example, neurons that are stimulated with exogenous ApoE3 or ApoE4 showed increased basal calcium with the ApoE4 isoform (L. Jiang et al. 2015). In another study on astrocytes, an increase in basal calcium was also demonstrated when the cells were treated with ApoE4 (Muller et al. 1998). However, in both studies, the ApoE is added exogenously, and whether basal calcium is chronically changed is not measured. Therefore, our results are the first to describe the fact that endogenous ApoE affects basal calcium.

We also described a greater magnitude of ATP-induced calcium responses (peak) in ApoE4 versus ApoE3 astrocytes kept in a medium rich in lipoproteins, due to an increase in the release of lysosomal calcium, which in turn, it is also higher in ApoE4 than in ApoE3 astrocytes. In addition, we have observed a slight increase in the release of calcium from the ER and extracellular calcium entry in these cells, the latter being less important to the ATP-induced calcium peak. The lysosomal calcium release has been shown as the initial event of agonist-induced calcium signals in many cell types (Churchill and Galione 2001; Galione 2015). It can then be amplified by calcium release from the ER and extracellular entry. The latter is triggered by the activation of purinergic ionotropic receptors, a decrease in calcium stored in the ER (SOCE) (Rosado 2016) or by a decrease in lysosomal calcium (Brailoiu and Brailoiu 2016). For that reason, we believe that the greater lysosomal calcium release in ApoE4 cells compared to ApoE3 could be the cause of the higher ER calcium release and extracellular calcium entry. The use of the lysosomal calcium release inhibitor, Ned-19, supported this idea since, in its presence, the difference in the magnitude of ATP-elicited calcium responses between ApoE3 and ApoE4 cells disappears.

Furthermore, we found the specific mechanism through which the lysosomes in ApoE4 astrocytes release more calcium after ATP stimulation: increased activity of the lysosomal V-ATPase pump. This conclusion is supported by experiments with Bafilomycin A1 treatment, a specific inhibitor of this complex. The intracellular cytosolic calcium in non-stimulated conditions of ApoE4 treated astrocytes is similar to the level of the ones in ApoE3 non-treated cells. Thus, there is a higher activity of V-ATPase in ApoE4 astrocytes, resulting in higher calcium inside lysosomes and lower cytoplasmic calcium in control situation. Besides, one of the 3 subunits tested by western blot or qPCR, V0D1, is augmented in these cells. This result was confirmed in the study of Nuriel et al. (Nuriel et al. 2017), where they found, apart from V0D1, 8 other upregulated subunits of V-ATPase in the entorhinal cortex of the ApoE4 mouse model, although they did not distinguish between cell types. Prasad and Rao also measured the expression of V-ATPase subunits, and they found contrary results: a general downregulation of them in human ApoE4/4 brain tissue, although V0D1 is not among the identified subunits that change their expression, and a downregulation of V0A1 in ApoE4 human fibroblast and mouse astrocytes (Prasad and Rao 2018). Looking at our results, from the 3 subunits tested, only one increases, so not all the subunits are changed in the same direction. It seems that there is variability in the expression of V-ATPase subunits

suggesting that its activity is modulated by other factors different from the upregulation or downregulation expression of all its subunits.

V-ATPase hyperactivity has also been related to another neurodegenerative disease, familiar frontotemporal lobar degeneration. Klein et al. have shown that the normalization of the V-ATPase activity by a deletion of a gene that is related to the disease rescues the behavioural deficits observed in a mouse model of the pathology (Z. A. Klein et al. 2017). This suggests that V-ATPase plays a role in the behavioural defects that appear in the disease.

The principal function of the V-ATPase is to promote the proton entrance to the lysosomes (and endolysosomes) to maintain the acidic pH. When we measured the pH of the ApoE4 astrocytes, we expected to find more acidic lysosomes than in the ApoE3 lysosomes due to the V-ATPase activity; however we found no difference between them or even a very small increase in the alkalinisation in ApoE4 ones. This alkalinisation of the lysosomes in ApoE4 astrocytes has also been described by Prasad and Rao (Prasad and Rao 2018). They measured the lysosomes separately from the endosomes, whose pH, they discovered, is more acidic in the ApoE4 astrocytes. Thus, this decompensation of the vesicle pH affected the protein clearance (Prasad and Rao 2018).

We found that there is similar or high pH in ApoE4 astrocytes and high V-ATPase activity, which seem to be contradictory unless there is upregulated mechanism to extrude protons out of the lysosome again. And in fact, there is an exchange of calcium-protons, and the overloading of calcium in ApoE4 astrocytes supports its higher activity. The molecular identity of this calcium-proton exchanger, which is called CAX, has been discovered in the last years in mammals (Melchionda et al. 2016).

Apart from the magnitude of the response, we have observed a slower recovery phase after the stimulation with ATP in ApoE4 astrocytes compared to that in ApoE3. The recovery phase is accomplished by SOCE and uptaking mechanisms carried out by different pumps, especially ATPases such as SERCA or PMCA. Since we illustrated a diminution in the ATP production of ApoE4 astrocytes, this could be a plausible cause of a reduction in the activity of the pumps and hence a more prolonged recovery phase of calcium signals. However, we described hyperactivity of V-ATPase, a complex that also depends on ATP. Thus, this suggests that the quantity of ATP is not limited, at least at the basal condition when there is

no high ATP demand. It could be possible that after purinergic receptor activation the requirement of ATP would be higher and insufficient, being affecting the ATPase activities. We cannot answer this question but we know that the V-ATPase is hyperactive so probably other factors are affecting pumps that control the recapture of calcium. In erythrocytes, a diminution in phosphatidylserine caused the reduction of ATP affinity to PMCA, so this pump works slowly (Bruce 2018; Rossi and Rega 1989). We have demonstrated by our lipid characterization that ApoE4 astrocytes show a lower amount of phosphatidylserine, hence the activity of PMCA could be compromised.

Lipids regulate calcium channels and pumps

Lipids can modulate channel activity by acting directly on the channels or by changing their environment because different lipid composition affects membrane properties. For instance, it modulates fluidity, bilayer thickness, lateral pressure or surface, which results in channel activity regulation (Tillman and Cascio 2003). Our metabolomics assays of whole astrocytes and lysosome membranes showed that the lipid profile between ApoE3 and ApoE4 cells is different. Therefore, we suggest that the ApoE4 expression in astrocytes results in membranes with different lipid composition which may alter calcium homeostasis. Specifically, we have demonstrated that phosphatidylcholine and phosphatidylethanolamine are present in different quantities in lysosomal membranes of ApoE3 and ApoE4 cells. Interestingly, it has been shown that both molecules affect the lateral pressure of the membrane due to their polar charges and phosphatidylethanolamine redistributes this pressure when it is present (Cantor 1999). Thus, both molecules can be affecting the lysosomal channels or pumps through lateral pressure changes of the membranes. Moreover, Grasso et al. found that different lipid diets given to rats alter the coupling of V-ATPase domains required for its activity in urothelial cells (Grasso, Scalambro, and Calderón 2011). Therefore, the specific lipid distribution of lysosomes in ApoE4 cells is probably also affecting the pump activity. In addition, lipids can also regulate lysosomal calcium release; for example, Churamani et al. explained that phosphatidylcholine increases this calcium release in sea urchin eggs (Churamani et al. 2006). ApoE4 astrocytes present augmented 6 different phosphatidylcholine compared to ApoE3 cells, suggesting that lysosomal calcium release could also be potentiated by the lipid composition.

Apart from the lipids previously mentioned, there are other lipids that can also play an active role in the regulation of lysosomal calcium mechanisms. Regarding the V-ATPase,

phosphatidylinositol 3,5- bisphosphate has been demonstrated as a stabilizing factor for its coupling, increasing its activity (S. C. Li et al. 2014). Moreover, Prasinou et al. explained that ApoE3 cells had differences in their saturation of fatty acids, the quantity of polyunsaturated fatty acids being lower than in ApoE4 cells (Prasinou et al. 2017). An in-depth study would be of interest to find out whether lipid dysregulation in ApoE4 astrocytes causes the V-ATPase hyperactivity as our results suggest. In summary, the endogenous expression of ApoE results in lipid alterations and calcium signalling dysregulations.

ApoE regulation interference of calcium signalling through lipids seems a plausible theory. We have discarded that ApoE4 alterations of lysosomal calcium are mediated mainly through a direct interaction between the ApoE and V-ATPase. It has been described that another apolipoprotein, ApoD, can change lysosomal features directly by its presence in the lysosomes. This apolipoprotein is necessary for controlling the pH of lysosomes after stress conditions (Pascua-Maestro et al. 2017). However, according to our results, ApoE colocalized poorly with the lysosomes while ApoD is present, suggesting, in our case, an indirect regulation of the V-ATPase activity.

Besides, we have concluded that the alteration of ATP-elicited calcium responses related to lysosomal calcium content depends on the isoform of ApoE rather than on the lower ApoE protein content that we observe in ApoE4 astrocytes.

Overall, the ApoE4 isoform might be promoting alterations in the lipid content or transport that would affect the V-ATPase and lysosomal calcium, which would increase the purinergic-elicited calcium responses.

Modulation of ApoE3 astrocyte calcium responses.

Importantly we discovered that lipoproteins modulate ATP-induced calcium responses in ApoE3 cells, but not in ApoE4 astrocytes. Specifically, there is an increase in the magnitude of ATP-elicited calcium responses. The mechanism is not mediated by changes of lysosomal calcium content. However, the increase in its release seems to be amplified by calcium release from the ER and especially by extracellular calcium entry. Thus, extracellular calcium entry becomes of great importance in the purinergic-elicited calcium signals in ApoE3 astrocytes kept in lipoprotein-poor mediums whereas it does not have a high contribution when ApoE3 cells are in lipoprotein-rich mediums. We observed that this modulation appeared a few

minutes after removing or adding the lipoproteins to the medium, so the modulation is not due to change of gene expression or specifically up- or downregulation of purinergic receptors. There are different possible explanations for this lipoprotein-based regulation:

1) Direct regulation or activation from calcium channels by some lipids. As it has been mentioned before, the lipids could modulate not only lysosomal channels but also most of the calcium channels of the cell. For example, Shirakawa et al. demonstrated that sphingosine 1 phosphate, binds to a G-coupled receptor and leads to extracellular calcium influx through the TRPC6 channel (Shirakawa et al. 2017). Other examples are the work of Estacion et al. where phosphatidylinositol-4,5-biphosphate modulates drosophila TRP activation (Estacion, Sinkins, and Schilling 2001) or the works of Choquette et al. and Gamper and Shapiro in which the PMCA pump is also affected by this lipid (Choquette et al. 1984) among others (Gamper and Shapiro 2007). Therefore, it is not surprising that the extracellular medium, rich in lipids and lipoproteins, modulates ATP-induced cytosolic calcium responses. However, this is the first time that it is described in the context of the expression of different ApoE alleles. Therefore, somehow lipids or lipoproteins could be altering the plasmatic membrane channels of ApoE3 astrocytes.

2) Better coupling of calcium signalling pathways when lipoproteins are present in the medium. SOCE, in which depletion of calcium from intracellular organelles triggers extracellular calcium entry, was first described and has been mainly characterized after the calcium depletion of the ER. The principal players are STIM (protein in the ER) and Orai1 (plasmatic membrane channel). STIM senses the quantity of calcium and contacts with the Orai1 channel physically promoting calcium influx to the cell (Islam 2012). The mechanism of SOCE induced by lysosomes is not well characterized, but it has been shown in primary cultured neurons, where lysosomal calcium release promotes the influx of calcium through N-type calcium channels from the membrane (Hui et al. 2015). Moreover, STIM protein has been reported to be present in lysosomes from platelets (Zbidi et al. 2011). In addition, it has been found that SOCE is mediated by TPC2, Stim and Orai1 in human cells, since in conditions of calcium depletion TPC2 interacts with Stim and Orai1 and its silencing decreases the extracellular influx of calcium (López et al. 2012). In our case, we have observed extracellular calcium entry dependent on lysosomes either directly or

through calcium release from the ER. We have not demonstrated the cause of a better interaction of calcium signalling pathways in the absence of lipoproteins in ApoE3 astrocytes, however it could be due to the lack of endocytosis of lipoproteins, as its inhibition with Psck9 increases calcium responses. Other possibilities have also to be taken into account. The lipid dependence of SOCE activity has been demonstrated as the absence of cholesterol increases the stabilization of STIM and Orai (Pacheco et al. 2016) or the phosphatidylinositol bisphosphate presence affects the SOCE differentially based on the species of study (Calloway et al. 2011). So, the presence of extracellular phospholipids and cholesterol (that are forming the lipoproteins) could directly modulates calcium entry.

Therefore, ApoE3 lysosomes in medium deficient in lipoproteins might activate the influx of extracellular calcium owing to a regulation of SOCE by extracellular lipids or thanks to the high ER release induced by the high lysosomal release that would increase SOCE or a regulation of SOCE directly by lysosomal calcium release Concerning ApoE4 astrocytes, we determined that the expression of TPC2 is downregulated. Therefore, if there is less amount of TPC2 in ApoE4 cells, possibly the acidic SOCE is diminished or absent, and that would be an explanation of why ApoE4 cells exhibited similar calcium responses among the mediums. Other possibility could be related to lysosomal localization. Our results show that lysosomes in ApoE3 cells are redistributed all along the cell, in opposite to the lysosomes of ApoE4 astrocytes which a high percentage is localized around the nucleus. Therefore, the more nuclear localization of lysosomes in ApoE4 astrocytes could prevent the better coupling between organelles. Regarding mitochondria, we know that it could uptake calcium, since we have demonstrated that ApoE4 cells have an increase in that uptake, discarding the mitochondria as the cause of the higher magnitude of the ATP-elicited responses or the slow recovery phase.

Consequences of calcium dysregulations in ApoE4 astrocytes

In a general view, we have described a lack of modulation of calcium signalling in ApoE4 astrocytes that might affect the adaptation to environmental changes and conferring susceptibility to pathology. For example, if one of the normal functions of astrocytes is to modulate long-term potentiation (a plasticity process that is involved in memory) through the release of calcium-dependent D-serine (Henneberger et al. 2010), in the case of ApoE4 astrocytes, that could be impaired, increasing its release and affecting the long-term

potentiation. Another process related to calcium signalling in astrocytes is the control of blood flux to the brain due to the release of vasoactive substances after cytosolic calcium increases (MacVicar and Newman 2015). As a result, alterations in calcium signalling would affect blood vessel contraction and subsequently, oxygen and nutrient delivery to the brain would be impaired.

The main transmitter used in this thesis to stimulate calcium signalling in astrocytes is ATP. ATP stimulation of astrocytes has been implicated in processes such as gliotransmission since it has been shown that ATP stimulates the glutamate release in astrocyte cultures (Jeremic et al. 2001). Purinergic receptor activation in astrocytes has also been related with the neuronal survival, although the results are not consistent. Fujita et al. explained that ATP stimulation of hippocampal astrocytes cultured with neurons promotes neuronal survival after oxidative stress (Fujita, Tozaki-Saitoh, and Inoue 2009) whereas Gandelman et al. showed that ATP stimulation of spinal cord cultured astrocytes induces toxic effects in motoneurons that lead to their cell death (Gandelman et al. 2010). The ATP concentration, the calcium signalling derived pathway activated and the differences of astrocytes from different brain regions probably explain the final effect of ATP stimulation of astrocytes. Overall, the alterations of purinergic receptor-induced calcium signals by ApoE4 expression can lead to different outcomes in different brain regions or/and under different conditions

In this sense, in the context of the AD, the purinergic P2Y1 receptor has been proposed as the cause of calcium hyperactivity in astrocytes from an AD mouse model (Delekate et al. 2014). Furthermore, this hyperexcitability is associated with Aβ plaques, suggesting that they could be promoting it. However, in our hand, oligomeric Aβ treatment does not alter calcium signalling in the conditions tested in cultured astrocytes, neither cytosolic calcium peak, nor recovery phase or basal calcium. The results are in contrast to other studies, where Aβ promotes calcium dysregulations in slices and in cultured cells (Bosson et al. 2017; Pirttimaki et al. 2013; Alberdi et al. 2013; D. Lim et al. 2013; Ambra A. Grolla et al. 2013; A A Grolla et al. 2013; Haughey and Mattson 2003; L. Lee, Kosuri, and Arancio 2014). However, treatment of oligomeric Aβ in astrocyte cultures has limitations since different laboratories have found different calcium alterations (see introduction). The causes of these controversies could be the treatment conditions of Aβ (concerning time and concentration) or the oligomers that make up the oAβ solution. Nevertheless, as we demonstrated that ApoE4 alters purinergic-elicited calcium signals, we can conclude that ApoE4 expression can

exacerbate the calcium hyperactivity mediated by purinergic receptors in the pathogenesis of Aβ. Importantly, our results have shown that ApoE4 is a factor that has to be taken into account in the study of calcium signals in astrocytes of AD models.

In addition, ApoE4 could be affecting Aβ pathogenesis through indirect pathways related to lysosomal alterations and clearance. For instance, it has been described that the endolysosomal system suffers traffic jams that lead to the accumulation of Aβ in cells, pointing to intracellular Aβ toxicity also as an AD hallmark (Small et al. 2017). Based on our results of the close nuclear localization of lysosomes in ApoE4 cells and on the fact that enlargement of endolysosomal compartments has been described in preclinical stages of the AD from ApoE4 individuals (Cataldo et al. 2000), ApoE could dysregulate the endolysosomal pathway by itself, which would promote intracellular Aβ accumulation and toxicity. The other example about how lysosomal alteration caused by ApoE4 would be impairing Aβ pathogenesis is through Aβ clearance. This has been demonstrated by Prasad et Rao. In their study, astrocytes that express ApoE4 are defective in the elimination of Aβ due to altered endolysosomal pH. The regulation of the lysosomal pH regulates the LRP1 recycling and promotes the correct clearance (Prasad and Rao 2018). Overall, ApoE4 might be conferring susceptibility or exacerbating the Aβ pathogenesis.

Concerning the endolysosomal pathway alteration described in ApoE4 astrocytes, Chung et al. described that ApoE4 astrocytes depicted deficiencies in the pruning of synapsis in the brain (Chung et al. 2016), a process that is mediated by the endolysosomal compartment. Thus, the endolysosomal trafficking alteration could be impairing not only Aβ clearance or toxicity but also synaptic pruning. In addition, we also found alterations in the autophagic process, ApoE4 astrocytes have an accumulation of autophagic vesicles. Bibliography suggests that autophagy is not totally complete in these cells. Specifically, the flux of the autophagy has been illustrated as impaired in ApoE4 astrocytes after different autophagic stimulations (Simonovitch et al. 2016). Since the last steps of autophagy correspond to the fusion with the lysosome, it seems that the signalling alteration found in ApoE4 lysosomes could be affecting the final steps of autophagy.

Interestingly, the other principal hallmark of the AD, Tau, has recently been related directly to ApoE4. A mouse model expressing ApoE4 and the mutated tau, showed brain atrophy

compared to its controls. Thus, ApoE4 presence exacerbates the dysfunctions associated with Tau pathology (Shi et al. 2017). Therefore, we would like to explore whether the mechanism by which ApoE4 is impairing Tau pathology could be related to the calcium dysregulations that we have found.

Finally, lysosomal calcium release dysregulation has also been described in other diseases, like Niemann-Pick type C (Lloyd-Evans et al. 2008). This disease is characterized by an abnormal accumulation of lipids in the lysosomes, one of them the sphingosine decreases the lysosomal calcium release (Lloyd-Evans et al. 2008). As has been described previously, in AD lysosomal dysfunctions are also found. Niemann-Pick disease is the example of how lysosomal dysfunction leads to lysosomal calcium dysregulation that contributes to the pathology.

The next step: calcium *in vivo* or *ex vivo*

Furthermore, an exhaustive study is needed to examine the calcium signalling in ApoE3 and ApoE4 mouse models. As is presented in the introduction, astrocytes are complex cells with very thin processes, a fact that is not represented in the cell culture models. Moreover, the calcium signalling from the processes and the soma could be independent and probably regulates different aspects of astrocyte function (Alexei Verkhratsky and Nedergaard 2018). Therefore, a complete study of the calcium signalling in the ApoE mouse model *in vivo* or *ex vivo* in slices would confirm our results in cultures, provide new insights into the consequences of calcium dysregulations caused by ApoE4 isoform and would integrate that dysregulation in the context of the whole cerebral circuit.

Therapy based on ApoE4 alterations:

The proper treatment to correct calcium dysregulations might be to convert the ApoE4 isoform into the ApoE3 one since we have obtained a partial reduction in the cytosolic calcium responses using ApoE3 overexpression in ApoE4 astrocytes. To do that, there are the small-molecule structure correctors, GIND25 and PH002 which change the structure of ApoE4 to an ApoE3-like. Brodbeck et al. showed the improvement of both molecules against the intracellular trafficking impairment caused by the structure of ApoE4 in Neuro2A cells and primary mouse neurons (Brodbeck et al. 2011). In addition, the efficacy of PH002 has recently been probed in ApoE4 human iPSC-derived neurons where the molecule ameliorates the detrimental effects (tau phosphorylation and neuron degeneration) derived

from ApoE4 (C. Wang et al. 2018). Another interesting approach to take into account is to reverse the pathological alterations produced by the ApoE4 expression. An example is the study of Prasad and Rao, who, as has been mentioned before, described an alteration in the endolysosome pH that leads to defects in Aβ clearance and discovered that the alteration in the pH is due to a downregulation of a sodium/proton exchanger (NHE6). Interestingly, by using HDAC4 (histone deacetylase 4) inhibitor, the expression of the exchanger and the endosome pH are normalized and the Aβ clearance is improved (Prasad and Rao 2018). Therefore, highlighting the dysregulations induced by ApoE4 in astrocytes and reversing it would also be a suitable treatment for ApoE4 derivate alterations.

2. ApoE4 expression causes mitochondrial alteration in astrocytes

Mitochondrial fusion/fission in ApoE4 astrocytes

The expression of ApoE4 in astrocytes also causes mitochondrial alterations. We have observed for the first time that ApoE4 expression in astrocytes causes defects in the fission of mitochondria upon inhibition of oxidative phosphorylation. This fission arrest has recently been addressed in different mouse models of familiar form of AD such as the APP, APP/PS1 and 3xtgAD models and in human AD brains(L. Zhang et al. 2016). In human AD brains, this arrest has been found especially located in the hippocampus, one of the principal areas affected by AD and in charge of memory. In addition, this impairment in mitochondrial fission has been illustrated in aged monkeys (Morozov et al. 2017). Our results provide the first evidence of this phenomenon in astrocytes and also its dependence on ApoE4. Other studies suggest that the alteration of the mitochondrial dynamics in AD is due to an increase in the fission rather than an arrest. For example, Cho et al. demonstrated that Aβ treatment causes hyperactivation of DRP1 in neurons (Cho et al. 2009) although in human fibroblast from AD patients the alteration found is a diminution in DRP1 (X. Wang et al. 2008) which could be varied between the cell type or between the area of the brain.

We also measured the expression of the different proteins involved in fusion and fission events. All of them (Drp1, Fis1, Mfn1, Mfn2 and Opa1) show a similar expression in ApoE3 and ApoE4 astrocytes. Since we measured the mRNA expression, we cannot affirm whether these proteins are differently activated. For example, Drp1 suffers different post-translational modifications that allow the protein to localize in the mitochondria (Meyer, Leuthner, and Luz 2017). We measured the expression as a first approximation since ApoE3 and ApoE4 have also been found as transcription factors that control gene expression

(Theendakara et al. 2016). However and due to the similar expression of the proteins, the next step would be to study their modifications and the GTPase activity to unravel whether it is altered in ApoE4 astrocytes.

Mitophagy in ApoE4 astrocytes

Mitophagy is the cellular process to eliminate damaged mitochondria and is preceded by fission events (Hamacher-Brady and Brady 2016). In our study, the expression of Parkin is downregulated in ApoE4 astrocytes. This suggested that there is impairment of mitophagy in these cells although this has to be confirmed experimentally. Parkin has been related to another neurodegenerative disease, Parkinson disease, although overexpression of this protein in APP/PS1 AD mouse model improves synaptic plasticity and behavioural defects (Hong et al. 2014) suggesting that its defect is also contributing to AD. In addition, this Parkin depletion takes place in human AD brain homogenates, being the decrease in Parkin progressively exacerbated according to the Barak stage of the pathology. Furthermore, similar results were obtained in hAPP transgenic mice (Ye et al. 2015). Thus, the reduction of Parkin in ApoE4 astrocytes recapitulates what is demonstrated in human and mouse AD and supports that the expression of ApoE4 isoform can potentiate this trait of the pathology.

We believe that there is a cause-consequence relationship between fission arrest and mitophagy inhibition. We observed the arrest of fission upon inhibition of ATP synthesis (Oligomycin treatment) without any change of the mitochondrial morphology between both cell lines in basal conditions. On the contrary, the decrease in Parkin is observed already in basal conditions. Thus, that means, that it could be the cause of the fission arrest. The basis of this hypothesis is that parkin ubiquitinates proteins of the outer mitochondrial membrane such as mitofusins, promoting their degradation (Narendra, Walker, and Youle 2012) and promoting fission. Therefore, reduction of Parkin could trigger the inhibition of the mitochondrial fission in ApoE4 astrocytes. Increasing the expression of Parkin for example by a plasmid transfection can help to confirm this hypothesis. Another possible explanation is that the inhibition of fission promotes the degradation of Parkin since fission is required for starting mitophagy (Twig et al. 2008). In addition, since we and others (Simonovitch et al. 2016) have demonstrated an alteration in the autophagy flux in ApoE4 astrocytes, Parkin reduction could be due to retrograde signalling as a compensatory mechanism to stop the increased autophagy. This idea is supported by the fact that the activation of autophagy induces the elongation of mitochondria through retraining DRP1 in the cytosol (Gomes,

Benedetto, and Scorrano 2011). Thus, mitochondrial fission would be inhibited in ApoE4 astrocytes and consequently also the mitophagy.

Mitochondrial motility and the mitochondrial metabolism of ApoE4 astrocytes

ApoE4 astrocyte mitochondria move more than ApoE3 ones. There are higher mRNA levels of Miro and a tendency also of increased Trak2 mRNA in ApoE4 versus ApoE3 astrocytes. We have discovered that ApoE4 astrocytes presented increased lactate release, a decrease in ATP production and upregulation of acylcarnitine content. Astrocytes mainly metabolize glucose through anaerobic respiration instead of mitochondrial pyruvate oxidation. It has been suggested that lactate is then released and used by neurons (Bélanger, Allaman, and Magistretti 2011) although it is not universally accepted (Mason 2017). However, astrocytes do have mitochondrial metabolism as they have an active TCA thanks to amino acid metabolism and fatty acids βoxidation (Eraso-Pichot et al. 2018). Mitochondrial energy production is related to fission events since its inhibition promotes a decrease in the mitochondrial respiration (Parone et al. 2008). Thus, we believe that the mitochondrial aerobic respiration might be impaired in ApoE4 cells. This would be in agreement with the accumulation of acylcarnitines in ApoE4 astrocytes, as acylcarnitines are the precursors of fatty-acid oxidation. In this scenario, the impairment of mitochondrial respiration will lead to an increase rate of anaerobic glycolysis to restore the ATP levels, increasing the lactate secretion. Moreover, the compromised mitochondrial metabolism that might be caused by fission arrest would produce less ATP, a fact that has been related to an increase in the motility of mitochondria to supply the requirement of energy around the cell (Sheng and Cai 2012).

However, the idea of the hyperactivated glycolysis of astrocytes is contrary to the diminution of the glucose consumption seen in individuals with ApoE4 allele and AD patients (Perkins et al. 2016; Mosconi et al. 2006). A possible explanation is that we measured the metabolites in basal conditions and metabolism is adapted to different conditions being able to change for example after stimulation. For instance, ApoE4 astrocytes would not increase their metabolism after stimulation whereas ApoE3 astrocytes would. Therefore, the glucose consumption would be higher in ApoE3 individuals as compared to ApoE4 ones. Another possible explanation is that the hypometabolism might be caused by other cellular types different of astrocytes.

How does ApoE4 cause mitochondrial dysfunction?

A principal question to be answered is how ApoE4 causes these dysregulations of mitochondrial dynamics. It is known that in neurons the toxic fragments of ApoE4 affect the electron chain, impairing the mitochondrial function, although these fragments have never been associated with mitochondrial dynamics, neither has this alteration been found in astrocytes (Chen et al. 2011). However, we know that ApoE4 has a direct action on neuronal mitochondria so we cannot discard that ApoE4 in astrocytes might localize in the mitochondria interfering directly their functions.

Indirectly, ApoE4 could be altering mitochondrial dynamics through the different lipid compositions in the mitochondrial membrane. We have reported a general change of the lipid distribution between ApoE3 and ApoE4 astrocytes. One of the principal lipids studied as a factor that regulates mitochondrial functions is cardiolipin (Frohman 2015). Cardiolipin regulates both process fission and fusion since its presence increases Opa1 dimerization necessary for its activity (Ban et al. 2010; DeVay et al. 2009) and acts on Drp1 protein stimulating its GTPase activity (Macdonald et al. 2014; Montessuit et al. 2010). We did not find this lipid in our lipid measurement although the lipid assay reflected all the cell lipids and since cardiolipin is present specifically in the mitochondria, maybe the increase or decrease in ApoE4 astrocytes could not be detected since the amount of other lipids is much superior. In general, phospholipids can also generate a negative curvature of the mitochondrial membrane affecting the process of fusion and fission (Frohman 2015). Interestingly, the protein phosphatidylserine decarboxylase that converts phosphatidylserine, phospholipid altered in ApoE4 astrocytes, in phosphatidylethanolamine has been implicated in dynamics event changes. Specifically, a reduction in that enzyme promotes fission (Chan and McQuibban 2012). Thus, in the case of ApoE4 astrocytes, an increase in the activity of this enzyme could be promoting the fission arrest and decreasing phosphatidylserine levels. Other lipids such as PCs that are changed in the ApoE4 astrocytes have also been implicated in the regulation of dynamic proteins, such as Drp1 (Q. Zhang et al. 2014). Therefore, we have proposed that ApoE4 dysregulation of mitochondrial lipids could be altering mitochondrial dynamics of ApoE4 astrocytes.

Consequences of mitochondrial alterations

Based on the study of Parone et al. we believe that the low mitochondrial DNA and the low ATP production might be the consequence of the fission arrest in ApoE4 astrocytes. They

downregulated DRP1 protein and consequently, reduced mitochondrial fission and mitochondrial DNA in HeLa cells (Parone et al. 2008). Apart from mtDNA and ATP alterations, they found an increase in the ROS production, a process that would be interesting to study in ApoE4 astrocytes.

How would these mitochondrial alterations be altering specific astrocytic function? Astrocytes contain small mitochondria in the thin processes (Genda et al. 2011; J. G. Jackson et al. 2014), suggesting that these mitochondria need proper fission to fit in there. Since we have established that ApoE4 astrocytes suffer an arrest of that fission, the delivery of the mitochondria to the thin processes would be altered, changing the calcium buffering and the energy supply to the astrocyte processes. Furthermore, an effect of the mislocalization would be the alteration in the calcium buffering. This has been proposed by Hoekstra et al., who described that the lack of calcium buffering due to a mislocalization of mitochondria, reduces the glutamate uptake of astrocytes, promoting the excitotoxicity of neurons (Hoekstra et al. 2014), a fact related to AD pathology.

Concerning the mitochondrial motility dysregulations in ApoE4 astrocytes, they could also be altering the mitochondrial transference. Recently, it has been discovered that mitochondria are transferred from astrocytes to neurons after damage (Hayakawa et al. 2016). The mechanism behind this intercellular transport is not fully understood, although Miro1 enhances the mitochondrial transference between epithelial and mesothelial cells (Ahmad et al. 2014). Our results show that ApoE4 astrocytes display an upregulation of Miro1, thus, ApoE4 astrocytes might be transferring mitochondria to nearby neurons widespread their damaged mitochondria to neurons. In addition, it has been described that the transference also takes place in the opposite direction, from neurons to astrocytes. This allows astrocytes to degrade damaged neuronal mitochondria by a process called transmitophagy (Davis et al. 2014). Due to the impairment of mitophagy in ApoE4 astrocytes, this process of transmitophagy is probably affected in ApoE4 individuals.

Validation in human models

An important part of the study was to validate our results in other models. One of the models that we used was human iPSC-derived astrocytes. Recently, a few articles have been published using these cellular models to study AD-related alteration in astrocytes (Jones et al. 2017; Zhao et al. 2017; Lin et al. 2018). Lin et al. took advantage of Crisp Cas9 to edit the

ApoE3 gene to an ApoE4 in human iPSC. They compared alteration of neurons, astrocytes and microglia. As for astrocytes, they showed altered lipid metabolism and cholesterol accumulation (Lin et al. 2018) supporting our results. Zhao et al. used 6 different human fibroblasts from 3 ApoE3/3 and 3 ApoE4/4 individuals to generate the astrocytes. They found that ApoE4 astrocytes do not support neurons in terms of survival and synaptogenesis as well as ApoE3 ones and the ApoE4 isoform is less lipidated (Zhao et al. 2017). In our study, we used human-derived astrocytes from this laboratory. However, we could not validate our results since they failed to express typical astrocytic markers suggesting a defective differentiation process. This is a quite common problem when differentiating human iPSC to astrocytes. Lundin et al. compared different human astrocyte models, including iPSC-derived astrocytes, by transcriptomic and functional assays to characterize them. They found that astrocyte models are highly diverse in their expression pattern (Lundin et al. 2018). Thus, further investigation is needed to elaborate protocols for astrocyte differentiation and characterization to improve these models.

2. Biomarker discovery: Functional astrocytic CSF signature in AD

The final part of this thesis bases the CSF biomarker discovery on the dysregulations obtained in ApoE4 astrocytes, but from a broad point of view, focuses on AD regardless of genotype because most of the proteomic data are not stratified by ApoE genotype. Thus, we obtained a functional signature of the astrocyte alteration in AD. The aim is that this targeted identification based on dysfunctions can contribute to the success of candidate establishment, since the candidates provided will reflect the disease onset or progression by a direct relationship with cellular dysfunction and pathogenesis. An example of functional signatures is the CSF signature of synaptic proteins that have recently been found related to MCI and AD, suggesting these molecules as potential candidates in the earliest stages of AD disease (Duits et al. 2018). Furthermore, astrocyte-derived biomarkers have been used in the context of traumatic brain injury (TBI). Halford et al. performed a proteomic assay comparing CSF from healthy individuals to CSF from TBI patients and filtered the result with a list of astrocytes-enriched proteins. They described aldolase, glutamine synthetase, brain lipid binding protein and astrocytic phosphoprotein 15 as biomarkers for TBI (Halford et al. 2017). Our study of astrocytic CSF biomarkers is part of this new area of the field, where not only is a unique protein proposed as a candidate, but also several proteins describe the alterations and the cellular type affected in the disease, in our case AD.

In detailed, we proposed an astrocyte signature composed of 6 candidates, related to calcium signalling and to lysosomal function. The proteins are S100B, ApoE, PTGDS, CST3, CLU, and ITM2C. Therefore, our astrocytic signature is based on the compartments and processes that are affected in the AD astrocytes, but also in ApoE4 astrocytes: calcium signalling, lysosomes. This kind of approach allows us to take into account the compartmentalization of the disease, that affects different organelles in a specific manner.

Regarding the CSF candidates that are related to calcium signalling, they are ApoE and S100B. Concerning S100B, it might not be specific for AD since it has been described as a potential candidate for traumatic brain injury (TBI) (Goyal et al. 2013), but the specificity will be provided by its combination with the other hits of our analysis. Concerning the candidates that are related with lysosome functions, we proposed 4: Clusterin, PTGDS, CST3 and ITM2C. 3 of them also have been related as a biomarker for other diseases, for example Clusterin, which is also altered in other neurodegenerative diseases (Prikrylova Vranova et al. 2016). In the case of prostaglandin D2 synthetase (PTGDS), it has been linked to meningioma (Kim et al. 2012) and regarding cystatin C (CST3) to amyotrophic lateral sclerosis (Tsuji-Akimoto et al. 2009). Nevertheless, integral membrane protein 2C has been only related to the AD (Hölttä et al. 2015).

Most of the molecules that we identify as possible AD candidates are also proposed candidates for other diseases. However, we defend that the combination of all of them might improve the power of the signature as successful biomarkers. It would even be interesting to take into account the proteins that are detected in the CSF of healthy individuals and not in the CSF of AD patients, for instance, aldolase. The absence of these proteins in the CSF would also be useful and would complement the AD signature.

One of the limitations found in the CSF biomarker assessment of candidates is the variability of the different databases concerning nomenclature of the proteins or genes among the studies. A normalization had to be done prior to the comparison to solve this problem. The other significant limitation of the study that has to be taken into account, is that we based our identification of the astrocytic proteins in astrocytes from healthy individuals. However, the expression of these proteins during the disease could be due to other cell types. Therefore, we should compare our candidates with a database that assesses the expression of the proteins in all the cell types in AD, which at the moment, does not exist.

4.Concluding remarks

In conclusion, we demonstrated that the endogenous expression of ApoE4 in astrocytes causes alterations in the calcium signalling related to lysosomal dysregulations and in the mitochondrial functions in astrocytes. These alterations are probably added to the ones produced by Aβ, which finally lead to the onset and progression of AD. Interestingly, alterations in calcium signalling and mitochondria functions have been proposed as main contributors to AD although, this is the first time that endogenous ApoE4 in astrocytes is proposed as the leading cause of these alterations. In addition, we take benefit of these alterations to identify a group of astrocytic proteins present in the CSF, and we propose this astrocytic signature as a candidate biomarker for the detection of AD.

Conclusions

- ApoE4 expression alters calcium homeostasis in astrocytes. Specifically:
    - The lysosomal V-ATPase is hyperactivated in ApoE4 astrocytes promoting lower basal calcium and higher lysosomal calcium loading but nearly equal lysosomal pH compared to ApoE3 astrocytes.
    - Purinergic receptor activation results in calcium responses of higher magnitude in ApoE4 than in ApoE3 astrocytes. There is an increased calcium release from the lysosomes and the ER and increased uptake of calcium by the mitochondria compared to ApoE3 cells. Extracellular calcium entry is not a major pathway in either cell types. Differences in the calcium responses between ApoE3 and ApoE4 astrocytes are not mainly because of different ApoE expression level, different lipidation of ApoE or a lysosomal localization of ApoE. However, they could be a result of different lipid composition since there are clear differences in the lipid content of both cell types.
- ApoE3 expressing astrocytes show different purinergic-elicited calcium responses, but not intracellular calcium concentration at rest conditions, depending if extracellular media is rich or poor in lipoproteins. In particular:
    - In lipoprotein deficient mediums, lysosomal luminal calcium content does not change, but there is higher calcium release from lysosomes, as process amplified by extracellular calcium entry.
    - The regulation of purinergic calcium responses in astrocytes by lipoproteins is relatively fast (less than 5 minutes) and preserved over time (at least up to 48 hours).
- The presence of lipoproteins in the extracellular media does not modify calcium homeostasis in ApoE4 astrocytes.
- 24 hours' incubation with oligomeric Aβ treatment does not alter the basal calcium nor ATP-induced calcium responses.
- The ApoE4 astrocytes display mitochondrial alterations. Specifically, compared to ApoE3 astrocytes:
    - Mitochondria in ApoE4 astrocytes are not able to fission in response to oligomycin treatment, despite the fact that there are no changes in mRNA expression of Drp1, Fis1, Mfn1, Mfn2 and Opa1.
    - Mitochondria in ApoE4 astrocytes have increased motility being Miro1 expression upregulated.

  - Mitophagy could be reduced as there is lower Parkin expression and autophagic vesicles are incremented.
  - Mitochondrial DNA is reduced in ApoE4 astrocytes but not mitochondrial quantity assessed through Tom20 expression.
- ApoE4 cells depict increased lactate secretion and reduced ATP concentration compared to ApoE3 astrocytes demonstrating metabolic alterations induced by ApoE4.
- We propose a group of astrocytic proteins related to calcium signalling and lysosome present in the CSF as a potential biomarker for AD. This is a functional astrocytic signature composed of: ApoE, S100B, prostaglandin D2 synthetase, clusterin, cystatin 3 and integral membrane protein 2C.

Agradecimientos

Con estos agradecimientos cierro una gran etapa. Debería comenzar por las principales personas que me han guiado en este camino que son Roser y Elena, pero si me lo permiten, nombraré primero a mis padres y a mi marido que después de mí, son los que más han invertido en esta tesis. Mis padres, siempre me habéis apoyado para que pudiera hacer cualquier cosa que quisiera, me habéis enseñado que no importa donde nazcas, si el pueblo tiene 10 o 10.000.000 habitantes, cada persona puede elegir su camino. Creo que pensabais que con este trabajo me haría rica, pero como habéis podido comprobar, no. Así que, viendo que nunca os podré devolver todo lo que habéis invertido en mí, quiero agradeceros todo el trabajo, todo el dinero y todo el apoyo que me habéis dado durante los últimos 10 años dedicándoos esta tesis especialmente a vosotros. Ojalá algún día yo consiga inspirar a mis hijos para que lleguen donde quieran, como vosotros habéis hecho conmigo. Marido, o cary, como te conocen en el lab, tu sabes de primera mano lo que es la ciencia de verdad. Las alegrías de los experimentos positivos y las frustraciones de los experimentos que no dejan conclusiones claras o que son dos semanas de trabajo que no sirven para nada por causas imposibles de conocer. Gracias por aguantarme en todo momento, y en especial, estos últimos meses. Creo que ya sabes que sin tu apoyo durante estos casi 4 años probablemente hoy no estaría escribiendo estas palabras. Creo que en este tiempo, los dos hemos crecido profesionalmente y también creo que en parte ha sido por el apoyo que nos damos el uno al otro. Mil gracias y te querré siempre.

Roser, Elena creo que os complementáis muy bien como jefas. He aprendido mucho de vosotras estos años. Roser gracias por tu apoyo siempre, por las grandes ideas que tienes y también por enseñarme todos los entresijos de la señalización del calcio. Elena, gracias por enseñarme la importancia de la buena escritura y del inglés correcto, para que no se desvíe la atención de lo importante, la ciencia. También gracias por enseñarme a llevar simples experimentos a grandes ideas. Gracias a las dos, por enseñarme que no hay laboratorio pequeño y que tal vez con más dificultades, pero podemos competir con laboratorios cuyo presupuesto probablemente sea 10 veces el nuestro. Espero que os podáis sentir orgullosas de esta tesis como yo me siento. Siempre os agradeceré haberme dado la oportunidad de llevar a cabo este doctorado.

Ahora llega otro párrafo de los importantes, Arantxa y Abel, os puedo definir como amigos pero esa definición se quedaría corta, somos familia. Desde prácticamente el primer mes hemos sido inseparables y nos hemos entendido tan bien, que no sé si esto me volverá a

ocurrir de nuevo. Hemos tenido tantos momentos juntos de toda clase, es una amistad de 4 años pero es como si fueran 20 y no solo a causa de que pasáramos juntos prácticamente todo el día en el lab sino por todo el apoyo, el cariño y las risas que me habéis dado. A Arantxa, te agradezco tu disposición inmediata para ayudar, la cual he podido disfrutar, tu invención de palabras que tantas veces me ha hecho reír y sobretodo, que desde que te conocí, has sido un apoyo gigante y espero haberte demostrado que es reciproco. A Abel, he aprendido mucho contigo, especialmente por nuestras largas conversaciones de ciencia pero también de política, porque aunque a veces tuviéramos puntos de vista opuestos siempre disfrutaba de ellas. Creo que nunca encontraré compañeros mejores.

Otras personas que han colaborado activamente en este trabajo son los estudiantes. La primera Carmen, que la pobre le ha tocado hacer las cosas más interesantes de cada proyecto, que si la FAO con Abel, que si contar espinas y lipid droplets con Arantxa, que si ayudarme a convertir los vídeos de movilidad mitocondrial…. No sé cómo nos has aguantado tanto, quizá sea porque siempre fuiste una más del trío Abel Arantxa Raquel. Gracias por todo y me alegro muchísimo de haber compartido contigo este tiempo. En cuanto a Cristina y Agus, sin vosotros el capítulo de mitocondria no existiría, muchas gracias por iniciar esos bonitos resultados. No me puedo olvidar de otros estudiantes como Blanca, que también me ha soportado estos últimos meses y siento no haberte dedicado la atención que te merecías. No me olvido tampoco de Cesc, Marina, Julia, y Nuria, gracias a vosotros también.

Estos años también he conocido a una gran amiga, Laura, que ya son 5 años de amistad, gracias por tu apoyo siempre y por escucharme, y por esas charlas en la sala de calcio, por las canciones y porque tenemos pendiente otra quedada, quizás otro concierto de Bustamante… en fin, espero que esta amistad sea para siempre. No me puedo olvidar tampoco de Dolo, Míriam, Elena y Arnaldo, gracias también por vuestro apoyo y por esos cafés en verano después de comer (Dolo felicidades por tu cumpleaños de nuevo, la tesis hizo que no te felicitara pero aquí queda para siempre!).

Cerrando el capítulo de gente maravillosa que he conocido gracias a la tesis no me quiero olvidar de Carlos, Paula, Pau, Nora, Eli, Paola, Lola, Ana … hemos compartido menos tiempo juntos pero ha sido suficiente para quedarme con ganas de conoceros más.

Quiero agradecer especialmente también a Cris, Nuria y Mar, por darnos un poco de su sabiduría que tantas veces me ha ayudado tanto para aislar astrocitos, como para analizar imágenes o como para cortar cerebros. Especialmente también agradecer a Cris el apoyo psicológico y personal que das en cultivos!

Con tantos papeleos de envíos que he hecho en esta tesis, también agradezco a Vanesa su ayuda y también al resto de administrativos que facilitan el trabajo.

También a Carla, que me ha estado ayudando con el inglés, por fin dejo de preguntarte dudas! Pero también gracias por tus consejos y tus ánimos, me han ayudado mucho!

Casi terminando, quiero nombrar a dos personas que me han impulsado a hacer el doctorado y que siempre me han ayudado a subir mi autoestima. Gracias Víctor y Theodora, sin vuestro empuje creo que me habría rendido antes de empezar. Gracias por compartir conmigo vuestra gran sabiduría.

No me quiero olvidar tampoco de mi hermano, que estos años nos han unido mucho y te agradezco que, aunque siempre nos hayamos querido muchísimo, ahora tenemos una gran confianza gracias a ti. Siempre has sido un apoyo para mí y estos 4 años más.

Antes de terminar querría hacer una mención especial, me gustaría agradecer a 3 personas ya no se encuentran con nosotros pero que fueron claves para que yo eligiera este camino. A ti María, verte sufrir tanto tiempo en esa cama me hizo dirigir mis esfuerzos hacia la investigación de las enfermedades neurodegenerativas y siento que no se cumplieran tus palabras de que algún día yo te curaría. A Guillermina, porque te fuiste solo hace dos meses pero siempre me apoyaste y me animaste junto con yayo. Y por último a Vidallé, creo que no ha habido nadie que se haya alegrado tanto por cualquier logro que conseguía en el camino académico y profesional como tú, siempre sintiéndose orgulloso de mí. Realmente os echo mucho de menos.

Por último y sin más penas, no me quiero olvidar de Bagui, Boira y Kylo que me han acompañado en cada palabra de esta tesis.

Bibliography

Abbott, Alison, and Elie Dolgin. 2016. "Failed Alzheimer's Trial Does Not Kill Leading Theory of Disease." *Nature*. https://doi.org/10.1038/nature.2016.21045.

Abramov, Andrey Y. 2004. "-Amyloid Peptides Induce Mitochondrial Dysfunction and Oxidative Stress in Astrocytes and Death of Neurons through Activation of NADPH Oxidase." *Journal of Neuroscience* 24 (2):565–75. https://doi.org/10.1523/JNEUROSCI.4042-03.2004.

Agarwal, Amit, Pei Hsun Wu, Ethan G. Hughes, Masahiro Fukaya, Max A. Tischfield, Abraham J. Langseth, Denis Wirtz, and Dwight E. Bergles. 2017. "Transient Opening of the Mitochondrial Permeability Transition Pore Induces Microdomain Calcium Transients in Astrocyte Processes." *Neuron* 93 (3):587–605.e7. https://doi.org/10.1016/j.neuron.2016.12.034.

Ahmad, Tanveer, Shravani Mukherjee, Bijay Pattnaik, Manish Kumar, Suchita Singh, Rakhshinda Rehman, Brijendra K Tiwari, et al. 2014. "Miro1 Regulates Intercellular Mitochondrial Transport & Enhances Mesenchymal Stem Cell Rescue Efficacy." *EMBO Journal* 33 (9):994–1010. https://doi.org/10.1002/embj.201386030.

Alberdi, Elena, Ane Wyssenbach, María Alberdi, Mª V. Sánchez-Gómez, Fabio Cavaliere, José J. Rodríguez, Alexei Verkhratsky, and Carlos Matute. 2013. "Ca2+-Dependent Endoplasmic Reticulum Stress Correlates with Astrogliosis in Oligomeric Amyloid β-Treated Astrocytes and in a Model of Alzheimer's Disease." *Aging Cell* 12 (2):292–302. https://doi.org/10.1111/acel.12054.

Allbritton, Nancy L, Tobias Meyer, and Lubert Stryer. 1992. "Range of Messenger Action of Calcium Ion and Inositol 1,4,5-Trisphosphate." *Science* 258 (5089):1812–15. https://doi.org/10.1126/science.1465619.

Anderson, Christopher M., Jennifer P. Bergher, and Raymond A. Swanson. 2003. "ATP-Induced ATP Release from Astrocytes." *Journal of Neurochemistry* 88 (1):246–56. https://doi.org/10.1111/j.1471-4159.2004.02204.x.

Antes, Ran, Raaya Ezra-Elia, Dov Weinberger, Arie Solomon, Ron Ofri, and Daniel M. Michaelson. 2013. "ApoE4 Induces Synaptic and ERG Impairments in the Retina of Young Targeted Replacement ApoE4 Mice." *PLoS ONE* 8 (5). Molecular Neurodegeneration:1. https://doi.org/10.1371/journal.pone.0064949.

Araque, Alfonso, Giorgio Carmignoto, Philip G. Haydon, Stéphane H.R. Oliet, Richard Robitaille, and Andrea Volterra. 2014. "Gliotransmitters Travel in Time and Space." *Neuron*. https://doi.org/10.1016/j.neuron.2014.02.007.

Aston, Daniel, Rebecca A. Capel, Kerrie L. Ford, Helen C. Christian, Gary R. Mirams, Eva A. Rog-Zielinska, Peter Kohl, Antony Galione, Rebecca A.B. Burton, and Derek A. Terrar. 2017. "High Resolution Structural Evidence Suggests the Sarcoplasmic Reticulum Forms Microdomains with Acidic Stores (Lysosomes) in the Heart." *Scientific Reports* 7 (1):40620. https://doi.org/10.1038/srep40620.

Baker, Michael J, Catherine S Palmer, and Diana Stojanovski. 2014. "Mitochondrial Protein Quality

Control in Health and Disease." *British Journal of Pharmacology*. https://doi.org/10.1111/bph.12430.

Bales, K R, T Verina, D J Cummins, Y Du, R C Dodel, J Saura, C E Fishman, et al. 1999. "Apolipoprotein E Is Essential for Amyloid Deposition in the APPV717F Transgenic Mouse Model of Alzheimer's Disease." *Proceedings of the National Academy of Sciences* 96 (26):15233–38. https://doi.org/10.1073/pnas.96.26.15233.

Bales, Kelly R, Tatyana Verina, Richard C Dodel, Yansheng Du, Larry Altstiel, Mark Bender, Paul Hyslop, et al. 1997. "Lack of Apolipoprotein E Dramatically Reduces Amyloid β-Peptide Deposition." *Nature Genetics*. https://doi.org/10.1038/ng1197-263.

Ban, Tadato, Jürgen A.W. Heymann, Zhiyin Song, Jenny E. Hinshaw, David C. Chan, Ban Tadato, Jürgen A.W. Heymann, Zhiyin Song, Jenny E. Hinshaw, and David C. Chan. 2010. "OPA1 Disease Alleles Causing Dominant Optic Atrophy Have Defects in Cardiolipin-Stimulated GTP Hydrolysis and Membrane Tubulation." *Human Molecular Genetics* 19 (11):2113–22. https://doi.org/10.1093/hmg/ddq088.

Barceló-Torns, Miquel, Alexander M. Lewis, Albert Gubern, David Barneda, Duncan Bloor-Young, Fernado Picatoste, Grant C. Churchill, Enrique Claro, and Roser Masgrau. 2011. "NAADP Mediates ATP-Induced Ca2+ Signals in Astrocytes." *FEBS Letters* 585 (14):2300–2306. https://doi.org/10.1016/j.febslet.2011.05.062.

Barthélemy, Nicolas R., Audrey Gabelle, Christophe Hirtz, François Fenaille, Nicolas Sergeant, Susanna Schraen-Maschke, Jérôme Vialaret, et al. 2016. "Differential Mass Spectrometry Profiles of Tau Protein in the Cerebrospinal Fluid of Patients with Alzheimer's Disease, Progressive Supranuclear Palsy, and Dementia with Lewy Bodies." Edited by Henrik Zetterberg. *Journal of Alzheimer's Disease* 51 (4):1033–43. https://doi.org/10.3233/JAD-150962.

Bazargani, Narges, and David Attwell. 2016. "Astrocyte Calcium Signaling: The Third Wave." *Nature Neuroscience*. https://doi.org/10.1038/nn.4201.

Beck, Andreas, Robin Zur Nieden, Hans Peter Schneider, and Joachim W Deitmer. 2004. "Calcium Release from Intracellular Stores in Rodent Astrocytes and Neurons in Situ." *Cell Calcium* 35 (1):47–58. https://doi.org/10.1016/S0143-4160(03)00171-4.

Bélanger, Mireille, Igor Allaman, and Pierre J. Magistretti. 2011. "Brain Energy Metabolism: Focus on Astrocyte-Neuron Metabolic Cooperation." *Cell Metabolism*. https://doi.org/10.1016/j.cmet.2011.08.016.

Bernardinelli, Yann, Dominique Muller, and Irina Nikonenko. 2014. "Astrocyte-Synapse Structural Plasticity." *Neural Plasticity*. https://doi.org/10.1155/2014/232105.

Bezzi, Paola, Vidar Gundersen, José Luis Galbete, Gerald Seifert, Christian Steinhäuser, Ethel Pilati, and Andrea Volterra. 2004. "Astrocytes Contain a Vesicular Compartment That Is Competent for Regulated Exocytosis of Glutamate." *Nature Neuroscience* 7 (6):613–20. https://doi.org/10.1038/nn1246.

Bezzi, Paola, and Andrea Volterra. 2001. "A Neuron-Glia Signalling Network in the Active Brain." *Current Opinion in Neurobiology*. https://doi.org/10.1016/S0959-4388(00)00223-3.

Bien-Ly, N., A. K. Gillespie, D. Walker, S. Y. Yoon, and Y. Huang. 2012. "Reducing Human Apolipoprotein E Levels Attenuates Age-Dependent A Accumulation in Mutant Human Amyloid Precursor Protein Transgenic Mice." *Journal of Neuroscience* 32 (14):4803–11. https://doi.org/10.1523/JNEUROSCI.0033-12.2012.

Bindocci, Erika, Iaroslav Savtchouk, Nicolas Liaudet, Denise Becker, Giovanni Carriero, and Andrea Volterra. 2017. "Neuroscience: Three-Dimensional Ca2+ Imaging Advances Understanding of Astrocyte Biology." *Science* 356 (6339):eaai8185. https://doi.org/10.1126/science.aai8185.

Bliek, Alexander M. van der, Qinfang Shen, and Sumihiro Kawajiri. 2013. "Mechanisms of Mitochondrial Fission and Fusion." *Cold Spring Harbor Perspectives in Biology* 5 (6):a011072–a011072. https://doi.org/10.1101/cshperspect.a011072.

Boehm-Cagan, A., and D. M. Michaelson. 2014. "Reversal of ApoE4-Driven Brain Pathology and Behavioral Deficits by Bexarotene." *Journal of Neuroscience* 34 (21):7293–7301. https://doi.org/10.1523/JNEUROSCI.5198-13.2014.

Bosson, Anthony, Adrien Paumier, Sylvie Boisseau, Muriel Jacquier-Sarlin, Alain Buisson, and Mireille Albrieux. 2017. "TRPA1 Channels Promote Astrocytic Ca2+ Hyperactivity and Synaptic Dysfunction Mediated by Oligomeric Forms of Amyloid-β Peptide." *Molecular Neurodegeneration* 12 (1):53. https://doi.org/10.1186/s13024-017-0194-8.

Brailoiu, G. Cristina, and Eugen Brailoiu. 2016. "Modulation of Calcium Entry by the Endo-Lysosomal System." In *Advances in Experimental Medicine and Biology*, 898:423–47. https://doi.org/10.1007/978-3-319-26974-0_18.

Brandon, Jason A., Brandon C. Farmer, Holden C. Williams, and Lance A. Johnson. 2018. "APOE and Alzheimer's Disease: Neuroimaging of Metabolic and Cerebrovascular Dysfunction." *Frontiers in Aging Neuroscience* 10 (June). https://doi.org/10.3389/fnagi.2018.00180.

Brinkmalm, Ann, Gunnar Brinkmalm, William G Honer, Lutz Frölich, Lucrezia Hausner, Lennart Minthon, Oskar Hansson, et al. 2014. "SNAP-25 Is a Promising Novel Cerebrospinal Fluid Biomarker for Synapse Degeneration in Alzheimer's Disease." *Molecular Neurodegeneration* 9 (1):53. https://doi.org/10.1186/1750-1326-9-53.

Brinkmalm, Gunnar, Simon Sjödin, Anja Hviid Simonsen, Steen Gregers Hasselbalch, Henrik Zetterberg, Ann Brinkmalm, and Kaj Blennow. 2018. "A Parallel Reaction Monitoring Mass Spectrometric Method for Analysis of Potential CSF Biomarkers for Alzheimer's Disease." *PROTEOMICS - Clinical Applications* 12 (1):1700131. https://doi.org/10.1002/prca.201700131.

Brodbeck, Jens, Jim McGuire, Zhaoping Liu, Anke Meyer-Franke, Maureen E. Balestra, Dah Eun Jeong, Mike Pleiss, et al. 2011. "Structure-Dependent Impairment of Intracellular Apolipoprotein E4 Trafficking and Its Detrimental Effects Are Rescued by Small-Molecule

Structure Correctors." *Journal of Biological Chemistry* 286 (19):17217–26. https://doi.org/10.1074/jbc.M110.217380.

Brozzi, Alessandro, Lorena Urbanelli, Pierre Luc Germain, Alessandro Magini, and Carla Emiliani. 2013. "HLGDB: A Database of Human Lysosomal Genes and Their Regulation." *Database* 2013 (January). https://doi.org/10.1093/database/bat024.

Bruce, Jason I.E. 2018. "Metabolic Regulation of the PMCA: Role in Cell Death and Survival." *Cell Calcium*. https://doi.org/10.1016/j.ceca.2017.06.001.

Bruggink, Kim A., H. Bea Kuiperij, Jolein Gloerich, Irene Otte-Höller, Annemieke J.M. Rozemuller, Jurgen A.H.R. Claassen, Benno Küsters, and Marcel M. Verbeek. 2015. "Dickkopf-Related Protein 3 Is a Potential Aβ-Associated Protein in Alzheimer's Disease." *Journal of Neurochemistry* 134 (6):1152–62. https://doi.org/10.1111/jnc.13216.

Calegari, Federico, Silvia Coco, Elena Taverna, Monique Bassetti, Claudia Verderio, Nicoletta Corradi, Michela Matteoli, and Patrizia Rosa. 1999. "A Regulated Secretory Pathway in Cultured Hippocampal Astrocytes." *Journal of Biological Chemistry* 274 (32):22539–47. https://doi.org/10.1074/jbc.274.32.22539.

Calloway, N., T. Owens, K. Corwith, W. Rodgers, D. Holowka, and B. Baird. 2011. "Stimulated Association of STIM1 and Orai1 Is Regulated by the Balance of PtdIns(4,5)P2 between Distinct Membrane Pools." *Journal of Cell Science* 124 (15):2602–10. https://doi.org/10.1242/jcs.084178.

Calvo, Sarah E., Karl R. Clauser, and Vamsi K. Mootha. 2016. "MitoCarta2.0: An Updated Inventory of Mammalian Mitochondrial Proteins." *Nucleic Acids Research* 44 (D1):D1251–57. https://doi.org/10.1093/nar/gkv1003.

Cantor, Robert S. 1999. "Lipid Composition and the Lateral Pressure Profile in Bilayers." *Biophysical Journal* 76 (5):2625–39. https://doi.org/10.1016/S0006-3495(99)77415-1.

Cao, Jiqing, Farida El Gaamouch, James S. Meabon, Kole D. Meeker, Li Zhu, Margaret B. Zhong, John Bendik, et al. 2017. "ApoE4-Associated Phospholipid Dysregulation Contributes to Development of Tau Hyper-Phosphorylation after Traumatic Brain Injury." *Scientific Reports* 7 (1). Springer US:1–12. https://doi.org/10.1038/s41598-017-11654-7.

Carbonell, Felix, Alex P Zijdenbos, Donald G. Mclaren, Yasser Iturria-Medina, and Barry J Bedell. 2016. "Modulation of Glucose Metabolism and Metabolic Connectivity by β-Amyloid." *Journal of Cerebral Blood Flow and Metabolism* 36 (12):2058–71. https://doi.org/10.1177/0271678X16654492.

Castellano, Joseph M., Jungsu Kim, Floy R. Stewart, Hong Jiang, Ronald B. DeMattos, Bruce W. Patterson, Anne M. Fagan, et al. 2011. "Human ApoE Isoforms Differentially Regulate Brain Amyloid-β Peptide Clearance." *Science Translational Medicine* 3 (89):89ra57-89ra57. https://doi.org/10.1126/scitranslmed.3002156.

Cataldo, Anne M, Corrinne M Peterhoff, Juan C Troncoso, Teresa Gomez-Isla, Bradley T Hyman, and Ralph A Nixon. 2000. "Endocytic Pathway Abnormalities Precede Amyloid β Deposition

in Sporadic Alzheimer's Disease and down Syndrome: Differential Effects of APOE Genotype and Presenilin Mutations." *American Journal of Pathology* 157 (1):277–86. https://doi.org/10.1016/S0002-9440(10)64538-5.

Cerf, Emilie, Adelin Gustot, Erik Goormaghtigh, J.-M. Ruysschaert, and Vincent Raussens. 2011. "High Ability of Apolipoprotein E4 to Stabilize Amyloid- Peptide Oligomers, the Pathological Entities Responsible for Alzheimer's Disease." *The FASEB Journal* 25 (5):1585–95. https://doi.org/10.1096/fj.10-175976.

Chan, Eliana Y. L., and G. Angus McQuibban. 2012. "Phosphatidylserine Decarboxylase 1 (Psd1) Promotes Mitochondrial Fusion by Regulating the Biophysical Properties of the Mitochondrial Membrane and Alternative Topogenesis of Mitochondrial Genome Maintenance Protein 1 (Mgm1)." *Journal of Biological Chemistry* 287 (48):40131–39. https://doi.org/10.1074/jbc.M112.399428.

Chang, S., T. r. Ma, R. D. Miranda, M. E. Balestra, R. W. Mahley, and Y. Huang. 2005. "Lipid- and Receptor-Binding Regions of Apolipoprotein E4 Fragments Act in Concert to Cause Mitochondrial Dysfunction and Neurotoxicity." *Proceedings of the National Academy of Sciences* 102 (51):18694–99. https://doi.org/10.1073/pnas.0508254102.

Charles, Andrew. 1998. "Intercellular Calcium Waves in Glia." *GLIA* 24 (1):39–49. https://doi.org/10.1002/(SICI)1098-1136(199809)24:1<39::AID-GLIA5>3.0.CO;2-W.

Chen, Hung Kai, Zhong Sheng Ji, Sara E. Dodson, Rene D. Miranda, Charles I. Rosenblum, Ian J. Reynolds, Stephen B. Freedman, Karl H. Weisgraber, Yadong Huang, and Robert W. Mahley. 2011. "Apolipoprotein E4 Domain Interaction Mediates Detrimental Effects on Mitochondria and Is a Potential Therapeutic Target for Alzheimer Disease." *Journal of Biological Chemistry* 286 (7):5215–21. https://doi.org/10.1074/jbc.M110.151084.

Cho, Dong-Hyung, Tomohiro Nakamura, Jianguo Fang, Piotr Cieplak, Adam Godzik, Zezong Gu, and Stuart A. Lipton. 2009. "S-Nitrosylation of Drp1 Mediates β-Amyloid-Related Mitochondrial Fission and Neuronal Injury." *Science* 324 (5923):102–5. https://doi.org/10.1126/science.1171091.

Choi, Sung S., Hong J. Lee, Inja Lim, Jun Ichi Satoh, and Seung U. Kim. 2014. "Human Astrocytes: Secretome Profiles of Cytokines and Chemokines." Edited by Cesar V. Borlongan. *PLoS ONE* 9 (4):e92325. https://doi.org/10.1371/journal.pone.0092325.

Chong, Il-Gyo, and Chi-Hyuck Jun. 2005. "Performance of Some Variable Selection Methods When Multicollinearity Is Present." *Chemometrics and Intelligent Laboratory Systems* 78 (1–2):103–12. https://doi.org/10.1016/j.chemolab.2004.12.011.

Choquette, Debra, Gabriele Hakim, Adelaida G Filoteo, Gordon A Plishker, J Robert Bostwick, and John T Penniston. 1984. "Regulation of Plasma Membrane Ca2+ ATPases by Lipids of the Phosphatidylinositol Cycle." *Biochemical and Biophysical Research Communications* 125 (3):908–15. https://doi.org/10.1016/0006-291X(84)91369-X.

Chung, Won-suk, Philip B Verghese, Chandrani Chakraborty, Julia Joung, Bradley T Hyman, Jason

D Ulrich, David M. Holtzman, and Ben A. Barres. 2016. "Novel Allele-Dependent Role for APOE in Controlling the Rate of Synapse Pruning by Astrocytes." *Proceedings of the National Academy of Sciences* 113 (36):10186–91. https://doi.org/10.1073/pnas.1609896113.

Churamani, Dev, George D. Dickinson, Mathias Ziegler, and Sandip Patel. 2006. "Time Sensing by NAADP Receptors." *Biochemical Journal* 397 (2):313–20. https://doi.org/10.1042/BJ20060179.

Churchill, G. C., and A. Galione. 2001. "NAADP Induces Ca2+ Oscillations via a Two-Pool Mechanism by Priming IP3- and CADPR-Sensitive Ca2+ Stores." *EMBO Journal* 20 (11):2666–71. https://doi.org/10.1093/emboj/20.11.2666.

Cooper, GM. 2000. *The Cell: A Molecular Approach. 2nd Edition*. 2nd editio. Sunderland (MA): Sinauer Associates.

Copetti-Santos, Daniela, Vitoria Moraes, Dácio Franco Weiler, Alexandre Silva De Mello, Fernanda De Souza MacHado, Jéssica Pereira Marinho, Cassiana Siebert, et al. 2015. "U18666A Treatment Results in Cholesterol Accumulation, Reduced Na+, K+-ATPase Activity, and Increased Oxidative Stress in Rat Cortical Astrocytes." *Lipids* 50 (10). Springer Berlin Heidelberg:937–44. https://doi.org/10.1007/s11745-015-4062-4.

Corder, E H, A M Saunders, W J Strittmatter, D E Schmechel, P C Gaskell, G W Small, A D Roses, J L Haines, and M A Pericak-Vance. 1993. "Gene Dose of Apolipoprotein E Type 4 Allele and the Risk of Alzheimer's Disease in Late Onset Families." *Science* 261 (5123):921–23. https://doi.org/10.1126/science.8346443.

Cornell-Bell, Ann H., Steven M. Finkbeiner, Mak S. Cooper, and Stephen J. Smith. 1990. "Glutamate Induces Calcium Waves in Cultured Astrocytes: Long-Range Glial Signaling." *Science* 247 (4941):470–73. https://doi.org/10.1126/science.1967852.

Craig-Schapiro, Rebecca, Richard J. Perrin, Catherine M. Roe, Chengjie Xiong, Deborah Carter, Nigel J. Cairns, Mark A. Mintun, et al. 2010. "YKL-40: A Novel Prognostic Fluid Biomarker for Preclinical Alzheimer's Disease." *Biological Psychiatry* 68 (10):903–12. https://doi.org/10.1016/j.biopsych.2010.08.025.

Cramer, Paige E, John R Cirrito, Daniel W Wesson, C Y Daniel Lee, J Colleen Karlo, Adriana E Zinn, Brad T Casali, et al. 2012. "ApoE-Directed Therapeutics Rapidly Clear -Amyloid and Reverse Deficits in AD Mouse Models." *Science* 335 (6075):1503–6. https://doi.org/10.1126/science.1217697.

Dahlgren, Karie N., Arlene M. Manelli, W. Blaine Stine, Lorinda K. Baker, Grant A. Krafft, and Mary Jo Ladu. 2002. "Oligomeric and Fibrillar Species of Amyloid-β Peptides Differentially Affect Neuronal Viability." *Journal of Biological Chemistry* 277 (35):32046–53. https://doi.org/10.1074/jbc.M201750200.

Dani, John W., Alex Chernjavsky, and Stephen J. Smith. 1992. "Neuronal Activity Triggers Calcium Waves in Hippocampal Astrocyte Networks." *Neuron* 8 (3):429–40. https://doi.org/10.1016/0896-6273(92)90271-E.

Davis, Chung-ha O., Keun-Young Kim, Eric A. Bushong, Elizabeth A. Mills, Daniela Boassa, Tiffany Shih, Mira Kinebuchi, et al. 2014. "Transcellular Degradation of Axonal Mitochondria." *Proceedings of the National Academy of Sciences* 111 (26):9633–38. https://doi.org/10.1073/pnas.1404651111.

Delekate, Andrea, Martina Füchtemeier, Toni Schumacher, Cordula Ulbrich, Marco Foddis, and Gabor C. Petzold. 2014. "Metabotropic P2Y1 Receptor Signalling Mediates Astrocytic Hyperactivity in Vivo in an Alzheimer's Disease Mouse Model." *Nature Communications* 5. https://doi.org/10.1038/ncomms6422.

DeVay, Rachel M., Lenin Dominguez-Ramirez, Laura L. Lackner, Suzanne Hoppins, Henning Stahlberg, and Jodi Nunnari. 2009. "Coassembly of Mgm1 Isoforms Requires Cardiolipin and Mediates Mitochondrial Inner Membrane Fusion." *Journal of Cell Biology* 186 (6):793–803. https://doi.org/10.1083/jcb.200906098.

Devi, Latha. 2006. "Accumulation of Amyloid Precursor Protein in the Mitochondrial Import Channels of Human Alzheimer's Disease Brain Is Associated with Mitochondrial Dysfunction." *Journal of Neuroscience* 26 (35):9057–68. https://doi.org/10.1523/JNEUROSCI.1469-06.2006.

Devices, Molecular. 2013. "Fura-2 QBT ™ Calcium Kit." *Molecular Devices*, no. July:1–16.

Ding, Fengfei, John O'Donnell, Alexander S. Thrane, Douglas Zeppenfeld, Hongyi Kang, Lulu Xie, Fushun Wang, and Maiken Nedergaard. 2013. "A1-Adrenergic Receptors Mediate Coordinated Ca2+signaling of Cortical Astrocytes in Awake, Behaving Mice." *Cell Calcium* 54 (6):387–94. https://doi.org/10.1016/j.ceca.2013.09.001.

Domenico, Fabio Di, Gilda Pupo, Esther Giraldo, Mari-Carmen Badìa, Paloma Monllor, Ana Lloret, Maria Eugenia Schininà, et al. 2016. "Oxidative Signature of Cerebrospinal Fluid from Mild Cognitive Impairment and Alzheimer Disease Patients." *Free Radical Biology & Medicine* 91 (February):1–9. https://doi.org/10.1016/j.freeradbiomed.2015.12.004.

Dong, Hanqing, and Mark J. Czaja. 2011. "Regulation of Lipid Droplets by Autophagy." *Trends in Endocrinology and Metabolism*. https://doi.org/10.1016/j.tem.2011.02.003.

Dong, Xian-Ping, Xiping Cheng, Eric Mills, Markus Delling, Fudi Wang, Tino Kurz, and Haoxing Xu. 2008. "The Type IV Mucolipidosis-Associated Protein TRPML1 Is an Endolysosomal Iron Release Channel." *Nature* 455 (September). Macmillan Publishers Limited. All rights reserved:992.

Dooren, Tom Van, David Muyllaert, Peter Borghgraef, Annelies Cresens, Herman Devijver, Ingrid Van Der Auwera, Stefaan Wera, Ilse Dewachter, and Fred Van Leuven. 2006. "Neuronal or Glial Expression of Human Apolipoprotein E4 Affects Parenchymal and Vascular Amyloid Pathology Differentially in Different Brain Regions of Double- and Triple-Transgenic Mice." *American Journal of Pathology* 168 (1):245–60. https://doi.org/10.2353/ajpath.2006.050752.

Duits, Flora H., Gunnar Brinkmalm, Charlotte E. Teunissen, Ann Brinkmalm, Philip Scheltens, Wiesje M. Van der Flier, Henrik Zetterberg, and Kaj Blennow. 2018. "Synaptic Proteins in

CSF as Potential Novel Biomarkers for Prognosis in Prodromal Alzheimer's Disease." *Alzheimer's Research & Therapy* 10 (1):5. https://doi.org/10.1186/s13195-017-0335-x.

Eiyama, Akinori, and Koji Okamoto. 2015. "PINK1/Parkin-Mediated Mitophagy in Mammalian Cells." *Current Opinion in Cell Biology*. https://doi.org/10.1016/j.ceb.2015.01.002.

Eraso-Pichot, Abel, Marina Brasó-Vives, Arantxa Golbano, Carmen Menacho, Enrique Claro, Elena Galea, and Roser Masgrau. 2018. "GSEA of Mouse and Human Mitochondriomes Reveals Fatty Acid Oxidation in Astrocytes." *GLIA* 66 (8):1724–35. https://doi.org/10.1002/glia.23330.

Estacion, Mark, William G. Sinkins, and William P. Schilling. 2001. "Regulation of Drosophila Transient Receptor Potential-like (TrpL) Channels by Phospholipase C-Dependent Mechanisms." *Journal of Physiology* 530 (1):1–19. https://doi.org/10.1111/j.1469-7793.2001.0001m.x.

Fan, Q W, Ichiro Iosbe, Hiroaki Asou, Katsuhiko Yanagisawa, and Makoto Michikawa. 2001. "Expression and Regulation of Apolipoprotein E Receptors in the Cells of the Central Nervous System in Culture: A Review." *J Am Aging Assoc* 24 (1):1–10. https://doi.org/10.1007/s11357-001-0001-9.

Farlow, M R, Y He, S Tekin, J Xu, R Lane, and H C Charles. 2004. "Impact of APOE in Mild Cognitive Impairment." *Neurology* 63 (10):1898–1901.

Fiacco, Todd A., and Ken D. McCarthy. 2018. "Multiple Lines of Evidence Indicate That Gliotransmission Does Not Occur under Physiological Conditions." *The Journal of Neuroscience* 38 (1):3–13. https://doi.org/10.1523/JNEUROSCI.0016-17.2017.

Filippini, N., B. J. MacIntosh, M. G. Hough, G. M. Goodwin, G. B. Frisoni, S. M. Smith, P. M. Matthews, C. F. Beckmann, and C. E. Mackay. 2009. "Distinct Patterns of Brain Activity in Young Carriers of the APOE- 4 Allele." *Proceedings of the National Academy of Sciences* 106 (17):7209–14. https://doi.org/10.1073/pnas.0811879106.

Fitz, N. F., A. A. Cronican, I. Lefterov, R. Koldamova, A. R. Price, G. Xu, Z. B. Siemienski, et al. 2013. "Comment on 'ApoE-Directed Therapeutics Rapidly Clear -Amyloid and Reverse Deficits in AD Mouse Models.'" *Science* 340 (6135):924–924.

Forgac, Michael. 2007. "Vacuolar ATPases: Rotary Proton Pumps in Physiology and Pathophysiology." *Nature Reviews Molecular Cell Biology*. https://doi.org/10.1038/nrm2272.

Frohman, Michael A. 2015. "Role of Mitochondrial Lipids in Guiding Fission and Fusion." *Journal of Molecular Medicine*. https://doi.org/10.1007/s00109-014-1237-z.

Fujita, Takumi, Hidetoshi Tozaki-Saitoh, and Kazuhide Inoue. 2009. "P2Y 1 Receptor Signaling Enhances Neuroprotection by Astrocytes against Oxidative Stress via IL-6 Release in Hippocampal Cultures." *Glia* 57 (3):244–57. https://doi.org/10.1002/glia.20749.

Galea, Elena, Will Morrison, Eloise Hudry, Michal Arbel-Ornath, Brian J. Bacskai, Teresa Gómez-Isla, H. Eugene Stanley, and Bradley T. Hyman. 2015. "Topological Analyses in APP/PS1 Mice Reveal That Astrocytes Do Not Migrate to Amyloid-β Plaques." *Proceedings of the National*

Academy of Sciences, December, 201516779. https://doi.org/10.1073/pnas.1516779112.

Galione, Antony. 2011. "NAADP Receptors." *Cold Spring Harbor Perspectives in Biology*. https://doi.org/10.1101/cshperspect.a004036.

———. 2015. "A Primer of NAADP-Mediated Ca2+ Signalling: From Sea Urchin Eggs to Mammalian Cells." *Cell Calcium* 58 (1):27–47. https://doi.org/10.1016/j.ceca.2014.09.010.

Gamper, Nikita, and Mark S Shapiro. 2007. "Regulation of Ion Transport Proteins by Membrane Phosphoinositides." *Nature Reviews Neuroscience*. Nature Publishing Group. https://doi.org/10.1038/nrn2257.

Gandelman, Mandi, Hugo Peluffo, Joseph S Beckman, Patricia Cassina, and Luis Barbeito. 2010. "Extracellular ATP and the P2X7 Receptor in Astrocyte-Mediated Motor Neuron Death: Implications for Amyotrophic Lateral Sclerosis." *Journal of Neuroinflammation* 7 (1):33. https://doi.org/10.1186/1742-2094-7-33.

Genda, E. N., J. G. Jackson, A. L. Sheldon, S. F. Locke, T. M. Greco, J. C. O'Donnell, L. A. Spruce, et al. 2011. "Co-Compartmentalization of the Astroglial Glutamate Transporter, GLT-1, with Glycolytic Enzymes and Mitochondria." *Journal of Neuroscience* 31 (50):18275–88. https://doi.org/10.1523/JNEUROSCI.3305-11.2011.

Gerasimenko, J. V. 2006. "NAADP, CADPR and IP3 All Release Ca2+ from the Endoplasmic Reticulum and an Acidic Store in the Secretory Granule Area." *Journal of Cell Science* 119 (2):226–38. https://doi.org/10.1242/jcs.02721.

Ghosal, Kaushik, Michael Haag, Philip B. Verghese, Tim West, Tim Veenstra, Joel B. Braunstein, Randall J. Bateman, David M. Holtzman, and Gary E. Landreth. 2016. "A Randomized Controlled Study to Evaluate the Effect of Bexarotene on Amyloid-β and Apolipoprotein E Metabolism in Healthy Subjects." *Alzheimer's and Dementia: Translational Research and Clinical Interventions* 2 (2):110–20. https://doi.org/10.1016/j.trci.2016.06.001.

Giau, Vo Van, Eva Bagyinszky, Seong Soo An, and SangYun Kim. 2015. "Role of Apolipoprotein E in Neurodegenerative Diseases." *Neuropsychiatric Disease and Treatment*, July, 1723. https://doi.org/10.2147/NDT.S84266.

Gomes, Ligia C., Giulietta Di Benedetto, and Luca Scorrano. 2011. "During Autophagy Mitochondria Elongate, Are Spared from Degradation and Sustain Cell Viability." *Nature Cell Biology* 13 (5):589–98. https://doi.org/10.1038/ncb2220.

Gomez-Arboledas, Angela, Jose C. Davila, Elisabeth Sanchez-Mejias, Victoria Navarro, Cristina Nuñez-Diaz, Raquel Sanchez-Varo, Maria Virtudes Sanchez-Mico, et al. 2018. "Phagocytic Clearance of Presynaptic Dystrophies by Reactive Astrocytes in Alzheimer's Disease." *GLIA* 66 (3):637–53. https://doi.org/10.1002/glia.23270.

González-Domínguez, R., T. García-Barrera, and J. L. Gómez-Ariza. 2014. "Metabolomic Study of Lipids in Serum for Biomarker Discovery in Alzheimer's Disease Using Direct Infusion Mass Spectrometry." *Journal of Pharmaceutical and Biomedical Analysis* 98 (September):321–26. https://doi.org/10.1016/j.jpba.2014.05.023.

González-Reyes, Rodrigo E., Mauricio O. Nava-Mesa, Karina Vargas-Sánchez, Daniel Ariza-Salamanca, and Laura Mora-Muñoz. 2017. "Involvement of Astrocytes in Alzheimer's Disease from a Neuroinflammatory and Oxidative Stress Perspective." *Frontiers in Molecular Neuroscience* 10 (December):1–20. https://doi.org/10.3389/fnmol.2017.00427.

Gowrishankar, Swetha, Peng Yuan, Yumei Wu, Matthew Schrag, Summer Paradise, Jaime Grutzendler, Pietro De Camilli, and Shawn M. Ferguson. 2015. "Massive Accumulation of Luminal Protease-Deficient Axonal Lysosomes at Alzheimer's Disease Amyloid Plaques." *Proceedings of the National Academy of Sciences* 112 (28):E3699–3708. https://doi.org/10.1073/pnas.1510329112.

Goyal, Akash, Michelle D. Failla, Christian Niyonkuru, Krutika Amin, Anthony Fabio, Rachel P. Berger, and Amy K. Wagner. 2013. "S100b as a Prognostic Biomarker in Outcome Prediction for Patients with Severe Traumatic Brain Injury." *Journal of Neurotrauma* 30 (11):946–57. https://doi.org/10.1089/neu.2012.2579.

Grasso, E. J., M. B. Scalambro, and R. O. Calderón. 2011. "Differential Response of the Urothelial V-ATPase Activity to the Lipid Environment." *Cell Biochemistry and Biophysics* 61 (1):157–68. https://doi.org/10.1007/s12013-011-9172-x.

Grolla, A A, J A Sim, D Lim, J J Rodriguez, A A Genazzani, and A Verkhratsky. 2013. "Amyloid-β and Alzheimer's Disease Type Pathology Differentially Affects the Calcium Signalling Toolkit in Astrocytes from Different Brain Regions." *Cell Death & Disease* 4 (5):e623–e623. https://doi.org/10.1038/cddis.2013.145.

Grolla, Ambra A., Gohar Fakhfouri, Giulia Balzaretti, Elena Marcello, Fabrizio Gardoni, Pier L. Canonico, Monica DiLuca, Armando A. Genazzani, and Dmitry Lim. 2013. "Aβ Leads to Ca^{2+} Signaling Alterations and Transcriptional Changes in Glial Cells." *Neurobiology of Aging* 34 (2):511–22. https://doi.org/10.1016/j.neurobiolaging.2012.05.005.

Guest, Paul C., ed. 2017. *Proteomic Methods in Neuropsychiatric Research*. Vol. 974. Advances in Experimental Medicine and Biology. Cham: Springer International Publishing. https://doi.org/10.1007/978-3-319-52479-5.

Guldbrandsen, Astrid, Yehia Farag, Ann Cathrine Kroksveen, Eystein Oveland, Ragnhild R. Lereim, Jill A. Opsahl, Kjell-Morten Myhr, Frode S. Berven, and Harald Barsnes. 2017. "CSF-PR 2.0: An Interactive Literature Guide to Quantitative Cerebrospinal Fluid Mass Spectrometry Data from Neurodegenerative Disorders." *Molecular & Cellular Proteomics* 16 (2):300–309. https://doi.org/10.1074/mcp.O116.064477.

Halassa, Michael M., and Philip G. Haydon. 2010. "Integrated Brain Circuits: Astrocytic Networks Modulate Neuronal Activity and Behavior." *Annual Review of Physiology* 72 (1):335–55. https://doi.org/10.1146/annurev-physiol-021909-135843.

Halford, Julia, Sean Shen, Kyohei Itamura, Jaclynn Levine, Albert C Chong, Gregg Czerwieniec, Thomas C Glenn, et al. 2017. "New Astroglial Injury-Defined Biomarkers for Neurotrauma Assessment." *Journal of Cerebral Blood Flow and Metabolism* 37 (10):3278–99.

https://doi.org/10.1177/0271678X17724681.

Hamacher-Brady, Anne, and Nathan Ryan Brady. 2016. "Mitophagy Programs: Mechanisms and Physiological Implications of Mitochondrial Targeting by Autophagy." *Cellular and Molecular Life Sciences* 73 (4):775–95. https://doi.org/10.1007/s00018-015-2087-8.

Hamanaka, H, Y Katoh-Fukui, K Suzuki, M Kobayashi, R Suzuki, Y Motegi, Y Nakahara, et al. 2000. "Altered Cholesterol Metabolism in Human Apolipoprotein E4 Knock-in Mice." *Human Molecular Genetics* 9 (3):353–61. https://doi.org/10.1093/hmg/9.3.353.

Han, Xiaoning, Michael Chen, Fushun Wang, Martha Windrem, Su Wang, Steven Shanz, Qiwu Xu, et al. 2013. "Forebrain Engraftment by Human Glial Progenitor Cells Enhances Synaptic Plasticity and Learning in Adult Mice." *Cell Stem Cell* 12 (3):342–53. https://doi.org/10.1016/j.stem.2012.12.015.

Harris, F. M., W. J. Brecht, Q. Xu, I. Tesseur, L. Kekonius, T. Wyss-Coray, J. D. Fish, et al. 2003. "Carboxyl-Terminal-Truncated Apolipoprotein E4 Causes Alzheimer's Disease-like Neurodegeneration and Behavioral Deficits in Transgenic Mice." *Proceedings of the National Academy of Sciences* 100 (19):10966–71. https://doi.org/10.1073/pnas.1434398100.

Hashimoto, Tadafumi, Alberto Serrano-Pozo, Yukiko Hori, Kenneth W Adams, Shuko Takeda, Adrian Olaf Banerji, Akinori Mitani, et al. 2012. "Apolipoprotein E, Especially Apolipoprotein E4, Increases the Oligomerization of Amyloid β Peptide." *The Journal of Neuroscience : The Official Journal of the Society for Neuroscience* 32 (43):15181–92. https://doi.org/10.1523/JNEUROSCI.1542-12.2012.

Haughey, Norman J., and Mark P. Mattson. 2003. "Alzheimer's Amyloid β-Peptide Enhances ATP/Gap Junction-Mediated Calcium-Wave Propagation in Astrocytes." *NeuroMolecular Medicine* 3 (3):173–80. https://doi.org/10.1385/NMM:3:3:173.

Hayakawa, Kazuhide, Elga Esposito, Xiaohua Wang, Yasukazu Terasaki, Yi Liu, Changhong Xing, Xunming Ji, and Eng H. Lo. 2016. "Transfer of Mitochondria from Astrocytes to Neurons after Stroke." *Nature* 535 (7613). Nature Publishing Group:551–55. https://doi.org/10.1038/nature18928.

Haydon, Philip G. 2006. "Astrocyte Control of Synaptic Transmission and Neurovascular Coupling." *Physiological Reviews* 86 (3):1009–31. https://doi.org/10.1152/physrev.00049.2005.

Heeren, Joerg, Thomas Grewal, Alexander Laatsch, Nils Becker, Franz Rinninger, Kerry Anne Rye, and Ulrike Beisiegel. 2004. "Impaired Recycling of Apolipoprotein E4 Is Associated with Intracellular Cholesterol Accumulation." *Journal of Biological Chemistry* 279 (53):55483–92. https://doi.org/10.1074/jbc.M409324200.

Hendrickson, Ronald C., Anita Y. H. Lee, Qinghua Song, Andy Liaw, Matt Wiener, Cloud P. Paweletz, Jeffrey L. Seeburger, et al. 2015. "High Resolution Discovery Proteomics Reveals Candidate Disease Progression Markers of Alzheimer's Disease in Human Cerebrospinal Fluid." Edited by Stephen D Ginsberg. *PLOS ONE* 10 (8):e0135365. https://doi.org/10.1371/journal.pone.0135365.

Heneka, Michael T, Monica J Carson, Joseph El Khoury, Gary E Landreth, Frederic Brosseron, Douglas L Feinstein, Andreas H Jacobs, et al. 2015. "Neuroinflammation in Alzheimer's Disease." *The Lancet Neurology*. https://doi.org/10.1016/S1474-4422(15)70016-5.

Henneberger, Christian, Thomas Papouin, Stéphane H R Oliet, and Dmitri A Rusakov. 2010. "Long-Term Potentiation Depends on Release of d-Serine from Astrocytes." *Nature* 463 (7278). Macmillan Publishers Limited. All rights reserved:232–36. https://doi.org/10.1038/nature08673.

Heslegrave, Amanda, Wendy Heywood, Ross Paterson, Nadia Magdalinou, Johan Svensson, Per Johansson, Annika Öhrfelt, et al. 2016. "Increased Cerebrospinal Fluid Soluble TREM2 Concentration in Alzheimer's Disease." *Molecular Neurodegeneration* 11 (1):3. https://doi.org/10.1186/s13024-016-0071-x.

Heywood, Wendy E., Daniela Galimberti, Emily Bliss, Ernestas Sirka, Ross W. Paterson, Nadia K. Magdalinou, Miryam Carecchio, et al. 2015. "Identification of Novel CSF Biomarkers for Neurodegeneration and Their Validation by a High-Throughput Multiplexed Targeted Proteomic Assay." *Molecular Neurodegeneration* 10 (1):64. https://doi.org/10.1186/s13024-015-0059-y.

Hirsch-Reinshagen, Veronica, Steven Zhou, Braydon L. Burgess, Lise Bernier, Sean A. McIsaac, Jeniffer Y. Chan, Gavin H. Tansley, Jeffrey S. Cohn, Michael R. Hayden, and Cheryl L. Wellington. 2004. "Deficiency of ABCA1 Impairs Apolipoprotein E Metabolism in Brain." *Journal of Biological Chemistry* 279 (39):41197–207. https://doi.org/10.1074/jbc.M407962200.

Hoekstra, Jake G., Travis J. Cook, Tessandra Stewart, Hayley Mattison, Max T. Dreisbach, Zachary S. Hoffer, and Jing Zhang. 2014. "Astrocytic Dynamin-like Protein 1 Regulates Neuronal Protection against Excitotoxicity in Parkinson Disease." *American Journal of Pathology* 185 (2):536–49. https://doi.org/10.1016/j.ajpath.2014.10.022.

Hölttä, Mikko, Lennart Minthon, Oskar Hansson, Jessica Holmén-Larsson, Ian Pike, Malcolm Ward, Karsten Kuhn, et al. 2015. "An Integrated Workflow for Multiplex CSF Proteomics and Peptidomics—Identification of Candidate Cerebrospinal Fluid Biomarkers of Alzheimer's Disease." *Journal of Proteome Research* 14 (2):654–63. https://doi.org/10.1021/pr501076j.

Holtzclaw, Lynne A., Siddhesh Pandhit, Dan J. Bare, Gregory A. Mignery, and James T. Russell. 2002. "Astrocytes in Adult Rat Brain Express Type 2 Inositol 1,4,5-Trisphosphate Receptors." *GLIA* 39 (1):69–84. https://doi.org/10.1002/glia.10085.

Holtzman, David M, Joachim Herz, and Guojun Bu. 2012. "Apolipoprotein E and Apolipoprotein E Receptors: Normal Biology and Roles in Alzheimer Disease." *Cold Spring Harbor Perspectives in Medicine* 2 (3):a006312. https://doi.org/10.1101/cshperspect.a006312.

Hong, X., J. Liu, G. Zhu, Y. Zhuang, H. Suo, P. Wang, D. Huang, et al. 2014. "Parkin Overexpression Ameliorates Hippocampal Long-Term Potentiation and -Amyloid Load in an Alzheimer's Disease Mouse Model." *Human Molecular Genetics* 23 (4):1056–72.

https://doi.org/10.1093/hmg/ddt501.

Hörtenhuber, Matthias, Enrique M Toledo, Erik Smedler, Ernest Arenas, Seth Malmersjö, Lauri Louhivuori, and Per Uhlén. 2017. "Mapping Genes for Calcium Signaling and Their Associated Human Genetic Disorders." Edited by John Hancock. *Bioinformatics (Oxford, England)* 33 (16):2547–54. https://doi.org/10.1093/bioinformatics/btx225.

Hu, Jin, Chia Chen Liu, Xiao Fen Chen, Yun Wu Zhang, Huaxi Xu, and Guojun Bu. 2015. "Opposing Effects of Viral Mediated Brain Expression of Apolipoprotein E2 (ApoE2) and ApoE4 on ApoE Lipidation and Aβ Metabolism in ApoE4-Targeted Replacement Mice." *Molecular Neurodegeneration* 10 (1):1–11. https://doi.org/10.1186/s13024-015-0001-3.

Huang, Y., X. Q. Liu, T. Wyss-Coray, W. J. Brecht, D. A. Sanan, and R. W. Mahley. 2001. "Apolipoprotein E Fragments Present in Alzheimer's Disease Brains Induce Neurofibrillary Tangle-like Intracellular Inclusions in Neurons." *Proceedings of the National Academy of Sciences* 98 (15):8838–43. https://doi.org/10.1073/pnas.151254698.

Huang, Y., and R. Mahley. 2014. "Apolipoprotein E: Structure and Function in Lipid Metabolism, Neurobiology, and Alzheimer's Diseases." *Neurobiology of Disease*. Elsevier Inc. https://doi.org/10.1016/j.nbd.2014.08.025.

Huang, Yadong, and Lennart Mucke. 2012. "Alzheimer Mechanisms and Therapeutic Strategies." *Cell*. https://doi.org/10.1016/j.cell.2012.02.040.

Hudry, Eloise, Jonathan Dashkoff, Alysson D Roe, Shuko Takeda, Robert M Koffie, Tadafumi Hashimoto, Maria Scheel, et al. 2013. "Gene Transfer of Human Apoe Isoforms Results in Differential Modulation of Amyloid Deposition and Neurotoxicity in Mouse Brain." *Science Translational Medicine* 5 (212):212ra161. https://doi.org/10.1126/scitranslmed.3007000.

Hui, Liang, Nicholas H. Geiger, Duncan Bloor-Young, Grant C. Churchill, Jonathan D. Geiger, and Xuesong Chen. 2015. "Release of Calcium from Endolysosomes Increases Calcium Influx through N-Type Calcium Channels: Evidence for Acidic Store-Operated Calcium Entry in Neurons." *Cell Calcium* 58 (6):617–27. https://doi.org/10.1016/j.ceca.2015.10.001.

Iadecola, Costantino, and Maiken Nedergaard. 2007. "Glial Regulation of the Cerebral Microvasculature." *Nature Neuroscience*. https://doi.org/10.1038/nn2003.

Inbar, Dafna, Haim Belinson, Hanna Rosenman, and Daniel M Michaelson. 2010. "Possible Role of Tau in Mediating Pathological Effects of ApoE4 in Vivo Prior to and Following Activation of the Amyloid Cascade." In *Neurodegenerative Diseases*, 7:16–23. https://doi.org/10.1159/000283477.

Islam, Md. Shahidul, ed. 2012. *Calcium Signaling*. Vol. 740. Advances in Experimental Medicine and Biology. Dordrecht: Springer Netherlands. https://doi.org/10.1007/978-94-007-2888-2.

J. Rodríguez, José, Arthur M. Butt, Emanuela Gardenal, Vladimir Parpura, and Alexei Verkhratsky. 2016. "Complex and Differential Glial Responses in Alzheimers Disease and Ageing." *Current Alzheimer Research* 13 (4):343–58. https://doi.org/10.2174/1567205013666160229112911.

Jack, Clifford R, David S Knopman, William J Jagust, Leslie M Shaw, Paul S Aisen, Michael W

Weiner, Ronald C Petersen, and John Q Trojanowski. 2010. "Hypothetical Model of Dynamic Biomarkers of the Alzheimer's Pathological Cascade." *The Lancet Neurology* 9 (1):119–28. https://doi.org/10.1016/S1474-4422(09)70299-6.

Jackson, J. G., J. C. O'Donnell, H. Takano, D. A. Coulter, and M. B. Robinson. 2014. "Neuronal Activity and Glutamate Uptake Decrease Mitochondrial Mobility in Astrocytes and Position Mitochondria Near Glutamate Transporters." *Journal of Neuroscience* 34 (5):1613–24. https://doi.org/10.1523/JNEUROSCI.3510-13.2014.

Jackson, J. G., and M. B. Robinson. 2015. "Reciprocal Regulation of Mitochondrial Dynamics and Calcium Signaling in Astrocyte Processes." *Journal of Neuroscience* 35 (45):15199–213. https://doi.org/10.1523/JNEUROSCI.2049-15.2015.

Jackson, Joshua G., and Michael B. Robinson. 2018. "Regulation of Mitochondrial Dynamics in Astrocytes: Mechanisms, Consequences, and Unknowns." *GLIA*. https://doi.org/10.1002/glia.23252.

Jeremic, A, K Jeftinija, J Stevanovic, A Glavaski, and S Jeftinija. 2001. "ATP Stimulates Calcium-Dependent Glutamate Release from Cultured Astrocytes." *Journal of Neurochemistry* 77 (2):664–75. https://doi.org/11299329.

Jiang, L., J. Zhong, X. Dou, C. Cheng, Z. Huang, and X. Sun. 2015. "Effects of ApoE on Intracellular Calcium Levels and Apoptosis of Neurons after Mechanical Injury." *Neuroscience* 301. IBRO:375–83. https://doi.org/10.1016/j.neuroscience.2015.06.005.

Jiang, Qingguang, C.Y. Y.Daniel Lee, Shweta Mandrekar, Brandy Wilkinson, Paige Cramer, Noam Zelcer, Karen Mann, et al. 2008. "ApoE Promotes the Proteolytic Degradation of Aβ." *Neuron* 58 (5):681–93. https://doi.org/10.1016/j.neuron.2008.04.010.

Jiang, Yongliang, Yumin Zhou, Gongyong Peng, Heshen Tian, Dan Pan, Lei Liu, Xing Yang, et al. 2018. "Two-Pore Channels Mediated Receptor-Operated Ca2+entry in Pulmonary Artery Smooth Muscle Cells in Response to Hypoxia." *International Journal of Biochemistry and Cell Biology* 97 (April):28–35. https://doi.org/10.1016/j.biocel.2018.01.012.

Johnson, Danielle E., Philip Ostrowski, Valentin Jaumouillé, and Sergio Grinstein. 2016. "The Position of Lysosomes within the Cell Determines Their Luminal PH." *The Journal of Cell Biology* 212 (6):677–92. https://doi.org/10.1083/jcb.201507112.

Jones, V. C., R. Atkinson-Dell, A. Verkhratsky, and L. Mohamet. 2017. "Aberrant IPSC-Derived Human Astrocytes in Alzheimer's Disease." *Cell Death and Disease* 8 (3). Nature Publishing Group:e2696. https://doi.org/10.1038/cddis.2017.89.

Kamphuis, Willem, Jinte Middeldorp, Lieneke Kooijman, Jacqueline A. Sluijs, Evert Jan Kooi, Martina Moeton, Michel Freriks, Mark R. Mizee, and Elly M. Hol. 2014. "Glial Fibrillary Acidic Protein Isoform Expression in Plaque Related Astrogliosis in Alzheimer's Disease." *Neurobiology of Aging* 35 (3):492–510. https://doi.org/10.1016/j.neurobiolaging.2013.09.035.

Kang, N., H. Peng, Y. Yu, P. K. Stanton, T. R. Guilarte, and J. Kang. 2013. "Astrocytes Release D-Serine by a Large Vesicle." *Neuroscience* 240 (June):243–57.

https://doi.org/10.1016/j.neuroscience.2013.02.029.

Khoonsari, Payam Emami, Anna Häggmark, Maria Lönnberg, Maria Mikus, Lena Kilander, Lars Lannfelt, Jonas Bergquist, et al. 2016. "Analysis of the Cerebrospinal Fluid Proteome in Alzheimer's Disease." Edited by Kristel Sleegers. *PLOS ONE* 11 (3):e0150672. https://doi.org/10.1371/journal.pone.0150672.

Kim, Jae Ho, Sang Kwang Lee, Yong Cheol Yoo, Nam Hyun Park, Dan Bi Park, Jong Shin Yoo, Hyun Joo An, Young Mok Park, and Kyung Gi Cho. 2012. "Proteome Analysis of Human Cerebrospinal Fluid as a Diagnostic Biomarker in Patients with Meningioma." *Medical Science Monitor* 18 (11):BR450-BR460. https://doi.org/10.12659/MSM.883538.

Kinnear, Nicholas P., Francois Xavier Boittin, Justyn M. Thomas, Antony Galione, and A. Mark Evans. 2004. "Lysosome-Sarcoplasmic Reticulum Junctions: A Trigger Zone for Calcium Signaling by Nicotinic Acid Adenine Dinucleotide Phosphate and Endothelin-1." *Journal of Biological Chemistry* 279 (52):54319–26. https://doi.org/10.1074/jbc.M406132200.

Klein, R C, B E Mace, S D Moore, and P M Sullivan. 2010. "Progressive Loss of Synaptic Integrity in Human Apolipoprotein E4 Targeted Replacement Mice and Attenuation by Apolipoprotein E2." *Neuroscience* 171 (4):1265–72. https://doi.org/10.1016/j.neuroscience.2010.10.027.

Klein, William L. 2002. "Aβ Toxicity in Alzheimer's Disease: Globular Oligomers (ADDLs) as New Vaccine and Drug Targets." *Neurochemistry International* 41 (5):345–52. https://doi.org/10.1016/S0197-0186(02)00050-5.

Klein, Zoe A., Hideyuki Takahashi, Mengxiao Ma, Massimiliano Stagi, Melissa Zhou, Tu Kiet T. Lam, and Stephen M. Strittmatter. 2017. "Loss of TMEM106B Ameliorates Lysosomal and Frontotemporal Dementia-Related Phenotypes in Progranulin-Deficient Mice." *Neuron* 95 (2):281–296.e6. https://doi.org/10.1016/j.neuron.2017.06.026.

Kobayashi, Katsuji, Masahiro Hayashi, Hiroyuki Nakano, Masao Shimazaki, Kaoru Sugimori, and Yoshifumi Koshino. 2004. "Correlation between Astrocyte Apoptosis and Alzheimer Changes in Gray Matter Lesions in Alzheimer's Disease." *Journal of Alzheimer's Disease : JAD* 6 (6):623-632; discussion 673-681.

Koch, S, N Donarski, K Goetze, M Kreckel, H J Stuerenburg, C Buhmann, and U Beisiegel. 2001. "Characterization of Four Lipoprotein Classes in Human Cerebrospinal Fluid." *Journal of Lipid Research* 42 (7):1143–51. https://doi.org/citeulike-article-id:14496854.

Kofuji, P., and E. A. Newman. 2004. "Potassium Buffering in the Central Nervous System." *Neuroscience*. https://doi.org/10.1016/j.neuroscience.2004.06.008.

Koldamova, Radosveta, Nicholas F. Fitz, and Iliya Lefterov. 2014. "ATP-Binding Cassette Transporter A1: From Metabolism to Neurodegeneration." *Neurobiology of Disease*. Elsevier Inc. https://doi.org/10.1016/j.nbd.2014.05.007.

Korecka, Magdalena, Teresa Waligorska, Michal Figurski, Jon B. Toledo, Steven E. Arnold, Murray Grossman, John Q. Trojanowski, and Leslie M. Shaw. 2014. "Qualification of a Surrogate

Matrix-Based Absolute Quantification Method for Amyloid-B42 in Human Cerebrospinal Fluid Using 2D UPLC-Tandem Mass Spectrometry." *Journal of Alzheimer's Disease* 41 (2):441–51. https://doi.org/10.3233/JAD-132489.

Kriegstein, Arnold, and Arturo Alvarez-Buylla. 2009. "The Glial Nature of Embryonic and Adult Neural Stem Cells." *Annual Review of Neuroscience* 32 (1):149–84. https://doi.org/10.1146/annurev.neuro.051508.135600.

Kryuchkova-Mostacci, Nadezda, and Marc Robinson-Rechavi. 2017. "A Benchmark of Gene Expression Tissue-Specificity Metrics." *Briefings in Bioinformatics* 18 (2):205–14. https://doi.org/10.1093/bib/bbw008.

Kuchibhotla, Kishore V., Carli R. Lattarulo, Bradley T. Hyman, and Brian J. Bacskai. 2009. "Synchronous Hyperactivity and Intercellular Calcium Waves in Astrocytes in Alzheimer Mice." *Science* 323 (5918):1211–15. https://doi.org/10.1126/science.1169096.

Kuzmicic, Jovan, Andrea Del Campo, Camila López-Crisosto, Pablo E. Morales, Christian Pennanen, Roberto Bravo-Sagua, Jonathan Hechenleitner, et al. 2011. "Dinámica Mitocondrial: Un Potencial Nuevo Blanco Terapéutico Para La Insuficiencia Cardiaca." *Revista Espanola de Cardiologia* 64 (10):916–23. https://doi.org/10.1016/j.recesp.2011.05.018.

Kvartsberg, Hlin, Flora H. Duits, Martin Ingelsson, Niels Andreasen, Annika Öhrfelt, Kerstin Andersson, Gunnar Brinkmalm, et al. 2015. "Cerebrospinal Fluid Levels of the Synaptic Protein Neurogranin Correlates with Cognitive Decline in Prodromal Alzheimer's Disease." *Alzheimer's & Dementia* 11 (10):1180–90. https://doi.org/10.1016/j.jalz.2014.10.009.

Labrousse, Arnaud M, Mauro D Zappaterra, Daniel A Rube, and Alexander M. Van der Bliek. 1999. "C. Elegans Dynamin-Related Protein DRP-1 Controls Severing of the Mitochondrial Outer Membrane." *Molecular Cell* 4 (5):815–26. https://doi.org/10.1016/S1097-2765(00)80391-3.

LaDu, Mary Jo, Michael T Falduto, Arlene M Manelli, Catherine A Reardon, Godfrey S Getz, and Donald E Frail. 1994. "Isoform-Specific Binding of Apolipoprotein E to β-Amyloid." *Journal of Biological Chemistry* 269 (38):23403–6.

LaFerla, Frank M. 2002. "Calcium Dyshomeostasis and Intracellular Signalling in Alzheimer's Disease." *Nature Reviews Neuroscience* 3 (11):862–72. https://doi.org/10.1038/nrn960.

Lafon-Cazal, Mireille, Oumeya Adjali, Nathalie Galéotti, Joël Poncet, Patrick Jouin, Vincent Homburger, Joël Bockaert, and Philippe Marin. 2003. "Proteomic Analysis of Astrocytic Secretion in the Mouse: Comparison with the Cerebrospinal Fluid Proteome." *Journal of Biological Chemistry* 278 (27):24438–48. https://doi.org/10.1074/jbc.M211980200.

Lambert, M P, A K Barlow, B A Chromy, C Edwards, R Freed, M Liosatos, T E Morgan, et al. 1998. "Diffusible, Nonfibrillar Ligands Derived from A 1-42 Are Potent Central Nervous System Neurotoxins." *Proceedings of the National Academy of Sciences* 95 (11):6448–53. https://doi.org/10.1073/pnas.95.11.6448.

Lane-Donovan, Courtney, and Joachim Herz. 2017. "ApoE, ApoE Receptors, and the Synapse in

Alzheimer's Disease." *Trends in Endocrinology and Metabolism*. Elsevier Ltd. https://doi.org/10.1016/j.tem.2016.12.001.

Lane-Donovan, Courtney, Wen Mai Wong, Murat S Durakoglugil, Catherine R Wasser, Shan Jiang, Xunde Xian, and Joachim Herz. 2016. "Genetic Restoration of Plasma ApoE Improves Cognition and Partially Restores Synaptic Defects in ApoE-Deficient Mice." *Journal of Neuroscience* 36 (39):10141–50. https://doi.org/10.1523/JNEUROSCI.1054-16.2016.

Lee, Anthony G. 2006. "Lipid Interactions with Ion Channels." *Future Lipidol* 1 (1):103–13. https://doi.org/10.2217/17460875.1.1.103.

Lee, Linda, Pallav Kosuri, and Ottavio Arancio. 2014. "Picomolar Amyloid-β Peptides Enhance Spontaneous Astrocyte Calcium Transients." *Journal of Alzheimer's Disease* 38 (1):49–62. https://doi.org/10.3233/JAD-130740.

Leonard, Anthony P., Robert B. Cameron, Jaime L. Speiser, Bethany J. Wolf, Yuri K. Peterson, Rick G. Schnellmann, Craig C. Beeson, and Bärbel Rohrer. 2015. "Quantitative Analysis of Mitochondrial Morphology and Membrane Potential in Living Cells Using High-Content Imaging, Machine Learning, and Morphological Binning." *Biochimica et Biophysica Acta* 1853 (2). Elsevier B.V.:348–60. https://doi.org/10.1016/j.bbamcr.2014.11.002.

Lesuisse, Christian, Guilian Xu, Jeffery Anderson, Molly Wong, Joanna Jankowsky, Greg Holtz, Victoria Gonzalez, et al. 2001. "Hyper-Expression of Human Apolipoprotein E4 in Astroglia and Neurons Does Not Enhance Amyloid Deposition in Transgenic Mice." *Hum Mol Genet* 10 (22):2525–37.

Li, Sheena Claire, Theodore T. Diakov, Tao Xu, Maureen Tarsio, Wandi Zhu, Sergio Couoh-Cardel, Lois S. Weisman, and Patricia M. Kane. 2014. "The Signaling Lipid PI(3,5)P2 Stabilizes V1-Vo Sector Interactions and Activates the V-ATPase." Edited by John York. *Molecular Biology of the Cell* 25 (8):1251–62. https://doi.org/10.1091/mbc.E13-10-0563.

Li, Wai Ping, Woody Y. Chan, Helen W.L. Lai, and David T. Yew. 1997. "Terminal DUTP Nick End Labeling (TUNEL) Positive Cells in the Different Regions of the Brain in Normal Aging and Alzheimer Patients." *Journal of Molecular Neuroscience* 8 (2):75–82. https://doi.org/10.1007/BF02736774.

Liang, H., J. Chaparro-Riggers, P. Strop, T. Geng, J. E. Sutton, D. Tsai, L. Bai, et al. 2012. "Proprotein Convertase Substilisin/Kexin Type 9 Antagonism Reduces Low-Density Lipoprotein Cholesterol in Statin-Treated Hypercholesterolemic Nonhuman Primates." *Journal of Pharmacology and Experimental Therapeutics* 340 (2):228–36. https://doi.org/10.1124/jpet.111.187419.

Liao, F., Y. Hori, E. Hudry, A. Q. Bauer, H. Jiang, T. E. Mahan, K. B. Lefton, et al. 2014. "Anti-ApoE Antibody Given after Plaque Onset Decreases A Accumulation and Improves Brain Function in a Mouse Model of A Amyloidosis." *Journal of Neuroscience* 34 (21):7281–92. https://doi.org/10.1523/JNEUROSCI.0646-14.2014.

Liao, Fan, Aimin Li, Monica Xiong, Nga Bien-Ly, Hong Jiang, Yin Zhang, Mary Beth Finn, et al.

2018. "Targeting of Nonlipidated, Aggregated ApoE with Antibodies Inhibits Amyloid Accumulation." *Journal of Clinical Investigation* 128 (5):2144–55. https://doi.org/10.1172/JCI96429.

Lim, Dmitry, Anand Iyer, Virginia Ronco, Ambra A. Grolla, Pier Luigi Canonico, Eleonora Aronica, and Armando A. Genazzani. 2013. "Amyloid Beta Deregulates Astroglial MGluR5-Mediated Calcium Signaling via Calcineurin and Nf-KB." *GLIA* 61 (7):1134–45. https://doi.org/10.1002/glia.22502.

Lim, Yen Ying, Pawel Kalinowski, Robert H. Pietrzak, Simon M. Laws, Samantha C. Burnham, David Ames, Victor L. Villemagne, et al. 2018. "Association of SS-Amyloid and Apolipoprotein e E4 with Memory Decline in Preclinical Alzheimer Disease." *JAMA Neurology* 75 (4):488–94. https://doi.org/10.1001/jamaneurol.2017.4325.

Lin, Yuan Ta, Jinsoo Seo, Fan Gao, Heather M. Feldman, Hsin Lan Wen, Jay Penney, Hugh P. Cam, et al. 2018. "APOE4 Causes Widespread Molecular and Cellular Alterations Associated with Alzheimer's Disease Phenotypes in Human IPSC-Derived Brain Cell Types." *Neuron* 98 (6):1141–1154.e7. https://doi.org/10.1016/j.neuron.2018.05.008.

Linton, Macrae F, Robert Gish, Susan T Hubl, Esther Bütler, Carlos Esquivel, William I. Bry, Janet K. Boyles, Mark R Wardell, and Stephen G Young. 1991. "Phenotypes of Apolipoprotein B and Apolipoprotein E after Liver Transplantation." *Journal of Clinical Investigation* 88 (1):270–81. https://doi.org/10.1172/JCI115288.

Liu, Chia Chen, Chia Chan Liu, Takahisa Kanekiyo, Huaxi Xu, and Guojun Bu. 2013. "Apolipoprotein E and Alzheimer Disease: Risk, Mechanisms and Therapy." *Nature Reviews. Neurology* 9 (2):106–18. https://doi.org/10.1038/nrneurol.2012.263.

Liu, Qiang, and Juan Zhang. 2014. "Lipid Metabolism in Alzheimer's Disease." *Neuroscience Bulletin*. https://doi.org/10.1007/s12264-013-1410-3.

Liu, Ying, Lan Tan, Hui Fu Wang, Yong Liu, Xiao Ke Hao, Chen Chen Tan, Teng Jiang, et al. 2016. "Multiple Effect of APOE Genotype on Clinical and Neuroimaging Biomarkers Across Alzheimer's Disease Spectrum." *Molecular Neurobiology* 53 (7). Molecular Neurobiology:4539–47. https://doi.org/10.1007/s12035-015-9388-7.

Lloyd-Evans, Emyr, Anthony J Morgan, Xingxuan He, David A Smith, Elena Elliot-Smith, Daniel J Sillence, Grant C Churchill, Edward H Schuchman, Antony Galione, and Frances M Platt. 2008. "Niemann-Pick Disease Type C1 Is a Sphingosine Storage Disease That Causes Deregulation of Lysosomal Calcium." *Nature Medicine* 14 (October). Nature Publishing Group:1247.

López, José J., Natalia Dionisio, Alejandro Berna-Erro, Carmen Galán, Ginés M. Salido, and Juan A. Rosado. 2012. "Two-Pore Channel 2 (TPC2) Modulates Store-Operated Ca2+entry." *Biochimica et Biophysica Acta - Molecular Cell Research* 1823 (10). Elsevier B.V.:1976–83. https://doi.org/10.1016/j.bbamcr.2012.08.002.

Loson, O. C., Zhiyin Song, Hsiuchen Chen, and David C. Chan. 2013. "Fis1, Mff, MiD49, and

MiD51 Mediate Drp1 Recruitment in Mitochondrial Fission." Edited by Donald D. Newmeyer. *Molecular Biology of the Cell* 24 (5):659–67. https://doi.org/10.1091/mbc.E12-10-0721.

Lovatt, D., U. Sonnewald, H. S. Waagepetersen, A. Schousboe, W. He, J. H.-C. Lin, X. Han, et al. 2007. "The Transcriptome and Metabolic Gene Signature of Protoplasmic Astrocytes in the Adult Murine Cortex." *Journal of Neuroscience* 27 (45):12255–66. https://doi.org/10.1523/JNEUROSCI.3404-07.2007.

Lundin, Anders, Louise Delsing, Maryam Clausen, Piero Ricchiuto, José Sanchez, Alan Sabirsh, Mei Ding, et al. 2018. "Human IPS-Derived Astroglia from a Stable Neural Precursor State Show Improved Functionality Compared with Conventional Astrocytic Models." *Stem Cell Reports* 10 (3):1030–45. https://doi.org/10.1016/j.stemcr.2018.01.021.

Luzio, J. Paul, Paul R. Pryor, and Nicholas A. Bright. 2007. "Lysosomes: Fusion and Function." *Nature Reviews Molecular Cell Biology*. https://doi.org/10.1038/nrm2217.

MacAskill, Andrew F., Johanne E. Rinholm, Alison E. Twelvetrees, I. Lorena Arancibia-Carcamo, James Muir, Asa Fransson, Pontus Aspenstrom, David Attwell, and Josef T. Kittler. 2009. "Miro1 Is a Calcium Sensor for Glutamate Receptor-Dependent Localization of Mitochondria at Synapses." *Neuron* 61 (4):541–55. https://doi.org/10.1016/j.neuron.2009.01.030.

Macdonald, Patrick J., Natalia Stepanyants, Niharika Mehrotra, Jason A. Mears, Xin Qi, Hiromi Sesaki, and Rajesh Ramachandran. 2014. "A Dimeric Equilibrium Intermediate Nucleates Drp1 Reassembly on Mitochondrial Membranes for Fission." Edited by Thomas D. Fox. *Molecular Biology of the Cell* 25 (12):1905–15. https://doi.org/10.1091/mbc.E14-02-0728.

MacVicar, Brian A, and Eric A. Newman. 2015. "Astrocyte Regulation of Blood Flow in the Brain." *Cold Spring Harbor Perspectives in Biology* 7 (5). https://doi.org/10.1101/cshperspect.a020388.

Mahley, Robert W. 2016. "Central Nervous System Lipoproteins: ApoE and Regulation of Cholesterol Metabolism." *Arteriosclerosis, Thrombosis, and Vascular Biology* 36 (7):1305–15. https://doi.org/10.1161/ATVBAHA.116.307023.

Mahley, Robert W., and Yadong Huang. 2012. "Apolipoprotein e Sets the Stage: Response to Injury Triggers Neuropathology." *Neuron* 76 (5). Elsevier Inc.:871–85. https://doi.org/10.1016/j.neuron.2012.11.020.

Mahley, Robert W, Yadong Huang, and S C Rall Jr. 1999. "Pathogenesis of Type III Hyperlipoproteinemia (Dysbetalipoproteinemia). Questions, Quandaries, and Paradoxes." *Journal of Lipid Research* 40 (11):1933–49.

Malta, C. Di, J. D. Fryer, C. Settembre, and A. Ballabio. 2012. "Astrocyte Dysfunction Triggers Neurodegeneration in a Lysosomal Storage Disorder." *Proceedings of the National Academy of Sciences* 109 (35):E2334–42. https://doi.org/10.1073/pnas.1209577109.

Marpegan, L., A. E. Swanstrom, K. Chung, T. Simon, P. G. Haydon, S. K. Khan, A. C. Liu, E. D.

Herzog, and C. Beaule. 2011. "Circadian Regulation of ATP Release in Astrocytes." *Journal of Neuroscience* 31 (23):8342–50. https://doi.org/10.1523/JNEUROSCI.6537-10.2011.

Martínez-Morillo, Eduardo, Oskar Hansson, Yuka Atagi, Guojun Bu, Lennart Minthon, Eleftherios P. Diamandis, and Henrietta M. Nielsen. 2014. "Total Apolipoprotein E Levels and Specific Isoform Composition in Cerebrospinal Fluid and Plasma from Alzheimer's Disease Patients and Controls." *Acta Neuropathologica* 127 (5):633–43. https://doi.org/10.1007/s00401-014-1266-2.

Mason, Shayne. 2017. "Lactate Shuttles in Neuroenergetics-Homeostasis, Allostasis and Beyond." *Frontiers in Neuroscience*. https://doi.org/10.3389/fnins.2017.00043.

Mattsson, Niklas, Ulf Andreasson, Staffan Persson, Maria C. Carrillo, Steven Collins, Sonia Chalbot, Neal Cutler, et al. 2013. "CSF Biomarker Variability in the Alzheimer's Association Quality Control Program." *Alzheimer's & Dementia* 9 (3):251–61. https://doi.org/10.1016/j.jalz.2013.01.010.

Mauch, D. H., K. Nägier, S Schumacher, C Göritz, E C Müller, A Otto, and F W Pfrieger. 2001. "CNS Synaptogenesis Promoted by Glia-Derived Cholesterol." *Science* 294 (5545):1354–57. https://doi.org/10.1126/science.294.5545.1354.

McAvoy, T., M. E. Lassman, D. S. Spellman, Z. Ke, B. J. Howell, O. Wong, L. Zhu, M. Tanen, A. Struyk, and O. F. Laterza. 2014. "Quantification of Tau in Cerebrospinal Fluid by Immunoaffinity Enrichment and Tandem Mass Spectrometry." *Clinical Chemistry* 60 (4):683–89. https://doi.org/10.1373/clinchem.2013.216515.

Mecca, Adam P., Nicole M. Barcelos, Shuo Wang, Anna Brück, Nabeel Nabulsi, Beata Planeta-Wilson, Jennifer Nadelmann, et al. 2018. "Cortical β-Amyloid Burden, Gray Matter, and Memory in Adults at Varying APOE E4 Risk for Alzheimer's Disease." *Neurobiology of Aging* 61 (January):207–14. https://doi.org/10.1016/j.neurobiolaging.2017.09.027.

Medina, Diego L., Simone Di Paola, Ivana Peluso, Andrea Armani, Diego De Stefani, Rossella Venditti, Sandro Montefusco, et al. 2015. "Lysosomal Calcium Signalling Regulates Autophagy through Calcineurin and TFEB." *Nature Cell Biology* 17 (3):288–99. https://doi.org/10.1038/ncb3114.

Medvedev, Nikolai, Victor Popov, Christian Henneberger, Igor Kraev, Dmitri A. Rusakov, and Michael G. Stewart. 2014. "Glia Selectively Approach Synapses on Thin Dendritic Spines." *Philosophical Transactions of the Royal Society B: Biological Sciences* 369 (1654):20140047–20140047. https://doi.org/10.1098/rstb.2014.0047.

Meer, Gerrit Van, Dennis R. Voelker, and Gerald W. Feigenson. 2008. "Membrane Lipids: Where They Are and How They Behave." *Nature Reviews Molecular Cell Biology*. https://doi.org/10.1038/nrm2330.

Melchionda, Manuela, Jon K. Pittman, Roberto Mayor, and Sandip Patel. 2016. "Ca2+/H+exchange by Acidic Organelles Regulates Cell Migration in Vivo." *Journal of Cell Biology* 212 (7):803–13. https://doi.org/10.1083/jcb.201510019.

Mellman, Ira, Renate Fuchs, and Ari Helenius. 1960. "Acidification of the Urine." *New England Journal of Medicine* 262 (1):45–45. https://doi.org/10.1056/NEJM196001072620120.

Meyer, Joel N., Tess C. Leuthner, and Anthony L. Luz. 2017. "Mitochondrial Fusion, Fission, and Mitochondrial Toxicity." *Toxicology* 391 (March). Elsevier:42–53. https://doi.org/10.1016/j.tox.2017.07.019.

Mishra, Prashant, and David C. Chan. 2016. "Metabolic Regulation of Mitochondrial Dynamics." *Journal of Cell Biology* 212 (4):379–87. https://doi.org/10.1083/jcb.201511036.

Montessuit, Sylvie, Syam Prakash Somasekharan, Oihana Terrones, Safa Lucken-Ardjomande, Sébastien Herzig, Robert Schwarzenbacher, Dietmar J. Manstein, et al. 2010. "Membrane Remodeling Induced by the Dynamin-Related Protein Drp1 Stimulates Bax Oligomerization." *Cell* 142 (6):889–901. https://doi.org/10.1016/j.cell.2010.08.017.

Moreira, Paula I., Cristina Carvalho, Xiongwei Zhu, Mark A. Smith, and George Perry. 2010. "Mitochondrial Dysfunction Is a Trigger of Alzheimer's Disease Pathophysiology." *Biochimica et Biophysica Acta - Molecular Basis of Disease*. https://doi.org/10.1016/j.bbadis.2009.10.006.

Moreno, Claudia, Alicia Sampieri, Oscar Vivas, Claudia Peña-Segura, and Luis Vaca. 2012. "STIM1 and Orai1 Mediate Thrombin-Induced Ca2+influx in Rat Cortical Astrocytes." *Cell Calcium* 52 (6):457–67. https://doi.org/10.1016/j.ceca.2012.08.004.

Morikawa, Masayuki, John D. Fryer, Patrick M. Sullivan, Erin A. Christopher, Suzanne E. Wahrle, Ronald B. DeMattos, Mark A. O'Dell, et al. 2005. "Production and Characterization of Astrocyte-Derived Human Apolipoprotein E Isoforms from Immortalized Astrocytes and Their Interactions with Amyloid-β." *Neurobiology of Disease* 19 (1–2):66–76. https://doi.org/10.1016/j.nbd.2004.11.005.

Morozov, Yury M., Dibyadeep Datta, Constantinos D. Paspalas, and Amy F.T. Arnsten. 2017. "Ultrastructural Evidence for Impaired Mitochondrial Fission in the Aged Rhesus Monkey Dorsolateral Prefrontal Cortex." *Neurobiology of Aging* 51 (March):9–18. https://doi.org/10.1016/j.neurobiolaging.2016.12.001.

Morris, John C., Catherine M. Roe, Chengjie Xiong, Anne M. Fagan, Alison M. Goate, David M. Holtzman, and Mark A. Mintun. 2010. "APOE Predicts Amyloid-Beta but Not Tau Alzheimer Pathology in Cognitively Normal Aging." *Annals of Neurology* 67 (1):122–31. https://doi.org/10.1002/ana.21843.

Morrow, Julie A, Danny M Hatters, Bin Lu, Peter Höchtl, Keith A Oberg, Bernhard Rupp, and Karl H Weisgraber. 2002. "Apolipoprotein E4 Forms a Molten Globule: A Potential Basis for Its Association with Disease." *Journal of Biological Chemistry* 277 (52):50380–85. https://doi.org/10.1074/jbc.M204898200.

Mosconi, Lisa, Sandro Sorbi, Mony J de Leon, Yi Li, Benedetta Nacmias, Paul S Myoung, Wai Tsui, et al. 2006. "Hypometabolism Exceeds Atrophy in Presymptomatic Early-Onset Familial Alzheimer's Disease." *Journal of Nuclear Medicine : Official Publication, Society of Nuclear Medicine* 47 (11):1778–86. https://doi.org/47/11/1778 [pii].

Motori, Elisa, Julien Puyal, Nicolas Toni, Alexander Ghanem, Cristina Angeloni, Marco Malaguti, Giorgio Cantelli-Forti, et al. 2013. "Inflammation-Induced Alteration of Astrocyte Mitochondrial Dynamics Requires Autophagy for Mitochondrial Network Maintenance." *Cell Metabolism* 18 (6):844–59. https://doi.org/10.1016/j.cmet.2013.11.005.

Mulder, C., L.-O. Wahlund, T. Teerlink, M. Blomberg, R. Veerhuis, G. J. van Kamp, P. Scheltens, and P. G. Scheffer. 2003. "Decreased Lysophosphatidylcholine/Phosphatidylcholine Ratio in Cerebrospinal Fluid in Alzheimer?S Disease." *Journal of Neural Transmission* 110 (8):949–55. https://doi.org/10.1007/s00702-003-0007-9.

Mulder, Sandra D., Henrietta M. Nielsen, Marinus A. Blankenstein, Piet Eikelenboom, and Robert Veerhuis. 2014. "Apolipoproteins E and J Interfere with Amyloid-Beta Uptake by Primary Human Astrocytes and Microglia in Vitro." *Glia* 62 (4):493–503. https://doi.org/10.1002/glia.22619.

Muller, W, V Meske, K Berlin, H Scharnagl, W Marz, and T G Ohm. 1998. "Apolipoprotein E Isoforms Increase Intracellular Ca2+ Differentially through a Omega-Agatoxin IVa-Sensitive Ca2+-Channel." *Brain Pathology (Zurich, Switzerland)* 8 (4):641–53.

n.d. 2017. "Brain with Alzheimer's Disease." BrightFocus Foundation. 2017.

n.d. 2010. "ALZGENE- Gene Overview of All Published AD-Association Studies for APOE_E2/3/4." Alzforum. 2010. http://www.alzgene.org/geneoverview.asp?geneid=83.

Nakamura, Toshiyuki, Atsushi Watanabe, Takahiro Fujino, Takashi Hosono, and Makoto Michikawa. 2009. "Apolipoprotein E4 (1-272) Fragment Is Associated with Mitochondrial Proteins and Affects Mitochondrial Function in Neuronal Cells." *Molecular Neurodegeneration* 4 (1). https://doi.org/10.1186/1750-1326-4-35.

Narendra, Derek, John E. Walker, and Richard Youle. 2012. "Mitochondrial Quality Control Mediated by PINK1 and Parkin: Links to Parkinsonism." *Cold Spring Harbor Perspectives in Biology* 4 (11). https://doi.org/10.1101/cshperspect.a011338.

Nelson, Amy R., Abhay P. Sagare, and Berislav V. Zlokovic. 2017. "Role of Clusterin in the Brain Vascular Clearance of Amyloid-β." *Proceedings of the National Academy of Sciences* 114 (33):8681–82. https://doi.org/10.1073/pnas.1711357114.

Neu, Scott C, Judy Pa, Walter Kukull, Duane Beekly, Amanda Kuzma, Prabhakaran Gangadharan, Li San Wang, et al. 2017. "Apolipoprotein E Genotype and Sex Risk Factors for Alzheimer Disease: A Meta-Analysis." *JAMA Neurology* 74 (10):1178–89. https://doi.org/10.1001/jamaneurol.2017.2188.

Nuriel, Tal, Katherine Y. Peng, Archana Ashok, Allissa A. Dillman, Helen Y. Figueroa, Justin Apuzzo, Jayanth Ambat, et al. 2017. "The Endosomal-Lysosomal Pathway Is Dysregulated by APOE4 Expression in Vivo." *Frontiers in Neuroscience* 11 (DEC):1–12. https://doi.org/10.3389/fnins.2017.00702.

Nyarko, Jennifer N.K., Maa O Quartey, Paul R Pennington, Ryan M Heistad, Doris Dea, Judes Poirier, Glen B Baker, and Darrell D Mousseau. 2018. "Profiles of β-Amyloid Peptides and

Key Secretases in Brain Autopsy Samples Differ with Sex and APOE E4 Status: Impact for Risk and Progression of Alzheimer Disease." *Neuroscience* 373 (March):20–36. https://doi.org/10.1016/j.neuroscience.2018.01.005.

Oberheim, N. A., T. Takano, X. Han, W. He, J. H. C. Lin, F. Wang, Q. Xu, et al. 2009. "Uniquely Hominid Features of Adult Human Astrocytes." *Journal of Neuroscience* 29 (10):3276–87. https://doi.org/10.1523/JNEUROSCI.4707-08.2009.

Oeckl, Patrick, Petra Steinacker, Christine A. F. von Arnim, Sarah Straub, Magdalena Nagl, Emily Feneberg, Jochen H. Weishaupt, Albert C. Ludolph, and Markus Otto. 2014. "Intact Protein Analysis of Ubiquitin in Cerebrospinal Fluid by Multiple Reaction Monitoring Reveals Differences in Alzheimer's Disease and Frontotemporal Lobar Degeneration." *Journal of Proteome Research* 13 (11):4518–25. https://doi.org/10.1021/pr5006058.

Öhrfelt, Annika, Ann Brinkmalm, Julien Dumurgier, Gunnar Brinkmalm, Oskar Hansson, Henrik Zetterberg, Elodie Bouaziz-Amar, Jacques Hugon, Claire Paquet, and Kaj Blennow. 2016. "The Pre-Synaptic Vesicle Protein Synaptotagmin Is a Novel Biomarker for Alzheimer's Disease." *Alzheimer's Research & Therapy* 8 (1):41. https://doi.org/10.1186/s13195-016-0208-8.

Orre, Marie, Willem Kamphuis, Lana M. Osborn, Anne H.P. Jansen, Lieneke Kooijman, Koen Bossers, and Elly M. Hol. 2014. "Isolation of Glia from Alzheimer's Mice Reveals Inflammation Anddysfunction." *Neurobiology of Aging* 35 (12):2746–60. https://doi.org/10.1016/j.neurobiolaging.2014.06.004.

Ortinski, Pavel I, Jinghui Dong, Alison Mungenast, Cuiyong Yue, Hajime Takano, Deborah J Watson, Philip G Haydon, and Douglas A Coulter. 2010. "Selective Induction of Astrocytic Gliosis Generates Deficits in Neuronal Inhibition." *Nature Neuroscience* 13 (5):584–91. https://doi.org/10.1038/nn.2535.

Osborn, Lana M., Willem Kamphuis, Wytse J. Wadman, and Elly M. Hol. 2016. "Astrogliosis: An Integral Player in the Pathogenesis of Alzheimer's Disease." *Progress in Neurobiology*. Elsevier Ltd. https://doi.org/10.1016/j.pneurobio.2016.01.001.

Pacheco, Jonathan, Laura Dominguez, A. Bohorquez-Hernandez, Alexander Asanov, and Luis Vaca. 2016. "A Cholesterol-Binding Domain in STIM1 Modulates STIM1-Orai1 Physical and Functional Interactions." *Scientific Reports* 6 (1):29634. https://doi.org/10.1038/srep29634.

Pannee, Josef, Erik Portelius, Lennart Minthon, Johan Gobom, Ulf Andreasson, Henrik Zetterberg, Oskar Hansson, and Kaj Blennow. 2016. "Reference Measurement Procedure for CSF Amyloid Beta (Aβ) 1-42 and the CSF Aβ 1-42 /Aβ 1-40 Ratio - a Cross-Validation Study against Amyloid PET." *Journal of Neurochemistry* 139 (4):651–58. https://doi.org/10.1111/jnc.13838.

Pannee, Josef, Erik Portelius, Madalina Oppermann, Alan Atkins, Martin Hornshaw, Ingrid Zegers, Peter Höjrup, et al. 2013. "A Selected Reaction Monitoring (SRM)-Based Method for Absolute Quantification of Aβ38, Aβ40, and Aβ42 in Cerebrospinal Fluid of Alzheimer's

Disease Patients and Healthy Controls." *Journal of Alzheimer's Disease* 33 (4):1021–32. https://doi.org/10.3233/JAD-2012-121471.

Parone, Philippe A., Sandrine Da Druz, Daniel Tondera, Yves Mattenberger, Dominic I. James, Pierre Maechler, François Barja, and Jean Claude Martinou. 2008. "Preventing Mitochondrial Fission Impairs Mitochondrial Function and Leads to Loss of Mitochondrial DNA." *PLoS ONE* 3 (9). https://doi.org/10.1371/journal.pone.0003257.

Parpura, Vladimir, and Alexei Verkhratsky. 2014. *Pathological Potential of Neuroglia: Possible New Targets for Medical Intervention*. Edited by Vladimir Parpura and Alexei Verkhratsky. *Pathological Potential of Neuroglia: Possible New Targets for Medical Intervention*. New York, NY: Springer New York. https://doi.org/10.1007/978-1-4939-0974-2.

Pascua-Maestro, Raquel, Sergio Diez-Hermano, Concepción Lillo, Maria D. Ganfornina, and Diego Sanchez. 2017. "Protecting Cells by Protecting Their Vulnerable Lysosomes: Identification of a New Mechanism for Preserving Lysosomal Functional Integrity upon Oxidative Stress." *PLoS Genetics* 13 (2):1–33. https://doi.org/10.1371/journal.pgen.1006603.

Patergnani, Simone, Jan M Suski, Chiara Agnoletto, Angela Bononi, Massimo Bonora, Elena De Marchi, Carlotta Giorgi, et al. 2011. "Calcium Signaling around Mitochondria Associated Membranes (MAMs)." *Cell Communication and Signaling*. https://doi.org/10.1186/1478-811X-9-19.

Paterson, R W, W E Heywood, A J Heslegrave, N K Magdalinou, U Andreasson, E Sirka, E Bliss, et al. 2016. "A Targeted Proteomic Multiplex CSF Assay Identifies Increased Malate Dehydrogenase and Other Neurodegenerative Biomarkers in Individuals with Alzheimer's Disease Pathology." *Translational Psychiatry* 6 (11):e952. https://doi.org/10.1038/tp.2016.194.

Pellerin, Luc, and Pierre J Magistretti. 2012. "Sweet Sixteen for ANLS." *Journal of Cerebral Blood Flow and Metabolism*. https://doi.org/10.1038/jcbfm.2011.149.

Pereira, Gustavo J.S., Hanako Hirata, Gian M. Fimia, Lúcia G. Do Carmo, Claudia Bincoletto, Sang W. Han, Roberta S. Stilhano, et al. 2011. "Nicotinic Acid Adenine Dinucleotide Phosphate (NAADP) Regulates Autophagy in Cultured Astrocytes." *Journal of Biological Chemistry* 286 (32):27875–81. https://doi.org/10.1074/jbc.C110.216580.

Perkins, Michelle, Andrew B. Wolf, Bernardo Chavira, Daniel Shonebarger, J. P. Meckel, Lana Leung, Lauren Ballina, et al. 2016. "Altered Energy Metabolism Pathways in the Posterior Cingulate in Young Adult Apolipoprotein e ϵ 4 Carriers." *Journal of Alzheimer's Disease* 53 (1):95–106. https://doi.org/10.3233/JAD-151205.

Perrin, Richard J., Rebecca Craig-Schapiro, James P. Malone, Aarti R. Shah, Petra Gilmore, Alan E. Davis, Catherine M. Roe, et al. 2011. "Identification and Validation of Novel Cerebrospinal Fluid Biomarkers for Staging Early Alzheimer's Disease." Edited by Mark P. Mattson. *PLoS ONE* 6 (1):e16032. https://doi.org/10.1371/journal.pone.0016032.

Pfrieger, Frank W, and Nicole Ungerer. 2011. "Cholesterol Metabolism in Neurons and

Astrocytes." *Progress in Lipid Research*. https://doi.org/10.1016/j.plipres.2011.06.002.

Pirttimaki, Tiina Maria, Neela Krushna Codadu, Alia Awni, Pandey Pratik, David Andrew Nagel, Eric James Hill, Kelly Tennyson Dineley, and H. Rheinallt Parri. 2013. "A7 Nicotinic Receptor-Mediated Astrocytic Gliotransmitter Release: Aβ Effects in a Preclinical Alzheimer's Mouse Model." Edited by Thierry Amédée. *PLoS ONE* 8 (11):e81828. https://doi.org/10.1371/journal.pone.0081828.

Pitt, Samantha J., Tim M. Funnell, Mano Sitsapesan, Elisa Venturi, Katja Rietdorf, Margarida Ruas, A. Ganesan, et al. 2010. "TPC2 Is a Novel NAADP-Sensitive Ca 2+ Release Channel, Operating as a Dual Sensor of Luminal PH and Ca 2+." *Journal of Biological Chemistry* 285 (45):35039–46. https://doi.org/10.1074/jbc.M110.156927.

Podlesniy, Petar, Joana Figueiro-Silva, Albert Llado, Anna Antonell, Raquel Sanchez-Valle, Daniel Alcolea, Alberto Lleo, Jose Luis Molinuevo, Nuria Serra, and Ramon Trullas. 2013. "Low Cerebrospinal Fluid Concentration of Mitochondrial DNA in Preclinical Alzheimer Disease." *Annals of Neurology* 74 (5):655–68. https://doi.org/10.1002/ana.23955.

Podlesniy, Petar, Franc Llorens, Ewa Golanska, Beata Sikorska, Pawel Liberski, Inga Zerr, and Ramon Trullas. 2016. "Mitochondrial DNA Differentiates Alzheimer's Disease from Creutzfeldt-Jakob Disease." *Alzheimer's and Dementia* 12 (5). Elsevier Inc.:546–55. https://doi.org/10.1016/j.jalz.2015.12.011.

Prasad, Hari, and Rajini Rao. 2018. "Amyloid Clearance Defect in ApoE4 Astrocytes Is Reversed by Epigenetic Correction of Endosomal PH." *Proceedings of the National Academy of Sciences* 115 (28):E6640–49. https://doi.org/10.1073/pnas.1801612115.

Prasinou, Paraskevi, Ioannis Dafnis, Giorgia Giacometti, Carla Ferreri, Angeliki Chroni, and Chryssostomos Chatgilialoglu. 2017. "Fatty Acid-Based Lipidomics and Membrane Remodeling Induced by ApoE3 and ApoE4 in Human Neuroblastoma Cells." *Biochimica et Biophysica Acta - Biomembranes* 1859 (10). Elsevier B.V.:1967–73. https://doi.org/10.1016/j.bbamem.2017.07.001.

Prikrylova Vranova, Hana, Eva Hényková, Jan Mareš, Michaela Kaiserová, Kateřina Menšíková, Miroslav Vaštík, Petr Hluštík, et al. 2016. "Clusterin CSF Levels in Differential Diagnosis of Neurodegenerative Disorders." *Journal of the Neurological Sciences* 361 (February):117–21. https://doi.org/10.1016/j.jns.2015.12.023.

Prince, Martin, Martin Knapp, Maëlenn Guerchet, and Maria Karagiannidou. 2016. "World Alzheimer Report 2016."

Pu, Jing, Carlos M. Guardia, Tal Keren-Kaplan, and Juan S. Bonifacino. 2016. "Mechanisms and Functions of Lysosome Positioning." *Journal of Cell Science* 129 (23):4329–39. https://doi.org/10.1242/jcs.196287.

Qiu, Z, K. A. Crutcher, B. T. Hyman, and G. W. Rebeck. 2003. "ApoE Isoforms Affect Neuronal N-Methyl-D-Aspartate Calcium Responses and Toxicity via Receptor-Mediated Processes." *Neuroscience* 122 (2):291–303. https://doi.org/10.1016/j.neuroscience.2003.08.017.

Raber, Jacob, Yadong Huang, and J. Wesson Ashford. 2004. "ApoE Genotype Accounts for the Vast Majority of AD Risk and AD Pathology." *Neurobiology of Aging*. https://doi.org/10.1016/j.neurobiolaging.2003.12.023.

Raffaello, Anna, Cristina Mammucari, Gaia Gherardi, and Rosario Rizzuto. 2016. "Calcium at the Center of Cell Signaling: Interplay between Endoplasmic Reticulum, Mitochondria, and Lysosomes." *Trends in Biochemical Sciences*. Elsevier Ltd. https://doi.org/10.1016/j.tibs.2016.09.001.

Reiman, E. M., K. Chen, X. Liu, D. Bandy, M. Yu, W. Lee, N. Ayutyanont, et al. 2009. "Fibrillar Amyloid- Burden in Cognitively Normal People at 3 Levels of Genetic Risk for Alzheimer's Disease." *Proceedings of the National Academy of Sciences* 106 (16):6820–25. https://doi.org/10.1073/pnas.0900345106.

Reiman, Eric M, Kewei Chen, Gene E Alexander, Richard J Caselli, Daniel Bandy, David Osborne, Ann M Saunders, and John Hardy. 2005. "From The Cover: Correlations between Apolipoprotein E 4 Gene Dose and Brain-Imaging Measurements of Regional Hypometabolism." *Proceedings of the National Academy of Sciences* 102 (23):8299–8302. https://doi.org/10.1073/pnas.0500579102.

Remnestål, Julia, David Just, Nicholas Mitsios, Claudia Fredolini, Jan Mulder, Jochen M Schwenk, Mathias Uhlén, et al. 2016. "CSF Profiling of the Human Brain Enriched Proteome Reveals Associations of Neuromodulin and Neurogranin to Alzheimer's Disease." *PROTEOMICS - Clinical Applications* 10 (12):1242–53. https://doi.org/10.1002/prca.201500150.

Rezeli, Melinda, Henrik Zetterberg, Kaj Blennow, Ann Brinkmalm, Thomas Laurell, Oskar Hansson, and György Marko-Varga. 2015. "Quantification of Total Apolipoprotein E and Its Specific Isoforms in Cerebrospinal Fluid and Blood in Alzheimer's Disease and Other Neurodegenerative Diseases." *EuPA Open Proteomics* 8 (September):137–43. https://doi.org/10.1016/j.euprot.2015.07.012.

Riddell, D. R., H. Zhou, K. Atchison, H. K. Warwick, P. J. Atkinson, J. Jefferson, L. Xu, et al. 2008. "Impact of Apolipoprotein E (ApoE) Polymorphism on Brain ApoE Levels." *Journal of Neuroscience* 28 (45):11445–53. https://doi.org/10.1523/JNEUROSCI.1972-08.2008.

Ringman, John M., Howard Schulman, Chris Becker, Ted Jones, Yuchen Bai, Fred Immermann, Gregory Cole, et al. 2012. "Proteomic Changes in Cerebrospinal Fluid of Presymptomatic and Affected Persons Carrying Familial Alzheimer Disease Mutations." *Archives of Neurology* 69 (1):96. https://doi.org/10.1001/archneurol.2011.642.

Robel, Stefanie, and Harald Sontheimer. 2015. "Glia as Drivers of Abnormal Neuronal Activity." *Nature Neuroscience*. https://doi.org/10.1038/nn.4184.

Rogeberg, Magnus, Ina Selseth Almdahl, Marianne Wettergreen, Lars N G Nilsson, and Tormod Fladby. 2015. "Isobaric Quantification of Cerebrospinal Fluid Amyloid-β Peptides in Alzheimer's Disease: C-Terminal Truncation Relates to Early Measures of Neurodegeneration." *Journal of Proteome Research* 14 (11):4834–43.

https://doi.org/10.1021/acs.jproteome.5b00668.

Rosado, Juan A. 2016. *Calcium Entry Pathways in Non-Excitable Cells*. Vol. 898. https://doi.org/10.1007/978-3-319-26974-0.

Rossi, J P, and A F Rega. 1989. "A Study to See Whether Phosphatidylserine, Partial Proteolysis and EGTA Substitute for Calmodulin during Activation of the Ca2+-ATPase from Red Cell Membranes by ATP." *Biochimica et Biophysica Acta* 996 (3):153–59. https://doi.org/2526658.

Rudinskiy, Nikita, Christophe Fuerer, Davide Demurtas, Sebastian Zamorano, Cyntia De Piano, Abigail G. Herrmann, Tara L. Spires-Jones, et al. 2016. "Amyloid-Beta Oligomerization Is Associated with the Generation of a Typical Peptide Fragment Fingerprint." *Alzheimer's & Dementia* 12 (9):996–1013. https://doi.org/10.1016/j.jalz.2016.03.011.

Ruffinatti, F, L Tapella, I Gregnanin, A Stevano, G Chiorino, PL Canonico, C Distasi, AA Genazzani, and D Lim. 2018. "Transcriptional Remodeling in Primary Hippocampal Astrocytes from an Alzheimer's Disease Mouse Model." *Current Alzheimer Research* 15 (June). https://doi.org/10.2174/1567205015666180613113924.

Rungta, Ravi L., Louis-Philippe Bernier, Lasse Dissing-Olesen, Christopher J. Groten, Jeffrey M. LeDue, Rebecca Ko, Sibyl Drissler, and Brian A. MacVicar. 2016. "Ca 2+ Transients in Astrocyte Fine Processes Occur via Ca 2+ Influx in the Adult Mouse Hippocampus." *Glia* 64 (12):2093–2103. https://doi.org/10.1002/glia.23042.

Russo, Claudio, Giovanna Angelini, Debora Dapino, Alessandra Piccini, Giuseppe Piombo, Gennaro Schettini, Shu Chen, et al. 1998. "Opposite Roles of Apolipoprotein E in Normal Brains and in Alzheimer's Disease." *Proceedings of the National Academy of Sciences of the United States of America* 95 (26):15598–602. https://doi.org/10.1073/pnas.95.26.15598.

Sanchez-Varo, Raquel, Laura Trujillo-Estrada, Elisabeth Sanchez-Mejias, Manuel Torres, David Baglietto-Vargas, Ines Moreno-Gonzalez, Vanessa De Castro, et al. 2012. "Abnormal Accumulation of Autophagic Vesicles Correlates with Axonal and Synaptic Pathology in Young Alzheimer's Mice Hippocampus." *Acta Neuropathologica* 123 (1):53–70. https://doi.org/10.1007/s00401-011-0896-x.

Saunders, A M, W J Strittmatter, D Schmechel, P. H. St. George-Hyslop, M A Pericak-Vance, S H Joo, B L Rosi, et al. 1993. "Association of Apolipoprotein E Allele 4 with Late-Onset Familial and Sporadic Alzheimer's Disease." *Neurology* 43 (8):1467–1467. https://doi.org/10.1212/WNL.43.8.1467.

Savtchouk, Iaroslav, and Andrea Volterra. 2018. "Gliotransmission: Beyond Black-and-White." *The Journal of Neuroscience* 38 (1):14–25. https://doi.org/10.1523/JNEUROSCI.0017-17.2017.

Schieder, Michael, Katrin Rötzer, Andrea Brüggemann, Martin Biel, and Christian A. Wahl-Schott. 2010. "Characterization of Two-Pore Channel 2 (TPCN2)-Mediated Ca 2+ Currents in Isolated Lysosomes." *Journal of Biological Chemistry* 285 (28):21219–22. https://doi.org/10.1074/jbc.C110.143123.

Schutzer, Steven E., Tao Liu, Benjamin H. Natelson, Thomas E. Angel, Athena A. Schepmoes,

Samuel O. Purvine, Kim K. Hixson, et al. 2010. "Establishing the Proteome of Normal Human Cerebrospinal Fluid." Edited by Howard E. Gendelman. *PLoS ONE* 5 (6):e10980. https://doi.org/10.1371/journal.pone.0010980.

Sekar, Shobana, Jacquelyn McDonald, Lori Cuyugan, Jessica Aldrich, Ahmet Kurdoglu, Jonathan Adkins, Geidy Serrano, et al. 2015. "Alzheimer's Disease Is Associated with Altered Expression of Genes Involved in Immune Response and Mitochondrial Processes in Astrocytes." *Neurobiology of Aging* 36 (2). Elsevier Inc:583–91. https://doi.org/10.1016/j.neurobiolaging.2014.09.027.

Serrano-Pozo, Alberto, Matthew L. Mielke, Teresa Gómez-Isla, Rebecca A. Betensky, John H. Growdon, Matthew P. Frosch, and Bradley T. Hyman. 2011. "Reactive Glia Not Only Associates with Plaques but Also Parallels Tangles in Alzheimer's Disease." *American Journal of Pathology* 179 (3):1373–84. https://doi.org/10.1016/j.ajpath.2011.05.047.

Sheikh-Bahaei, Nasim, Seyed Ahmad Sajjadi, Roido Manavaki, and Jonathan Harvey Gillard. 2017. "Imaging Biomarkers in Alzheimer's Disease: A Practical Guide for Clinicians." *Journal of Alzheimer's Disease Reports* 1 (1):71–88. https://doi.org/10.3233/ADR-170013.

Sheng, Zu Hang, and Qian Cai. 2012. "Mitochondrial Transport in Neurons: Impact on Synaptic Homeostasis and Neurodegeneration." *Nature Reviews Neuroscience*. https://doi.org/10.1038/nrn3156.

Shi, Yang, Kaoru Yamada, Shane Antony Liddelow, Scott T. Smith, Lingzhi Zhao, Wenjie Luo, Richard M. Tsai, et al. 2017. "ApoE4 Markedly Exacerbates Tau-Mediated Neurodegeneration in a Mouse Model of Tauopathy." *Nature* 549 (7673). Nature Publishing Group:523–27. https://doi.org/10.1038/nature24016.

Shigetomi, Eiji, Yukiho J. Hirayama, Kazuhiro Ikenaka, Kenji F. Tanaka, and Schuichi Koizumi. 2018. "Role of Purinergic Receptor P2Y1 in Spatiotemporal Ca 2+ Dynamics in Astrocytes." *The Journal of Neuroscience* 38 (6):2625–17. https://doi.org/10.1523/JNEUROSCI.2625-17.2017.

Shinohara, Mitsuru, Ronald C. Petersen, Dennis W. Dickson, and Guojun Bu. 2013. "Brain Regional Correlation of Amyloid-β with Synapses and Apolipoprotein e in Non-Demented Individuals: Potential Mechanisms Underlying Regional Vulnerability to Amyloid-β Accumulation." *Acta Neuropathologica* 125 (4):535–47. https://doi.org/10.1007/s00401-013-1086-9.

Shirakawa, Hisashi, Rumi Katsumoto, Shota Iida, Takahito Miyake, Takuya Higuchi, Takuya Nagashima, Kazuki Nagayasu, Takayuki Nakagawa, and Shuji Kaneko. 2017. "Sphingosine-1-Phosphate Induces Ca2+signaling and CXCL1 Release via TRPC6 Channel in Astrocytes." *GLIA* 65 (6):1005–16. https://doi.org/10.1002/glia.23141.

Simonovitch, Shira, Eran Schmukler, Alina Bespalko, Tal Iram, Dan Frenkel, David M. Holtzman, Eliezer Masliah, Danny M. Michaelson, and Ronit Pinkas-Kramarski. 2016. "Impaired Autophagy in APOE4 Astrocytes." *Journal of Alzheimer's Disease* 51 (3):915–27.

https://doi.org/10.3233/JAD-151101.

Simpson, J. E., P. G. Ince, G. Lace, G. Forster, P. J. Shaw, F. Matthews, G. Savva, C. Brayne, and S. B. Wharton. 2010. "Astrocyte Phenotype in Relation to Alzheimer-Type Pathology in the Ageing Brain." *Neurobiology of Aging* 31 (4):578–90. https://doi.org/10.1016/j.neurobiolaging.2008.05.015.

Sjödin, Simon, Annika Öhrfelt, Gunnar Brinkmalm, Henrik Zetterberg, Kaj Blennow, and Ann Brinkmalm. 2016. "Targeting LAMP2 in Human Cerebrospinal Fluid with a Combination of Immunopurification and High Resolution Parallel Reaction Monitoring Mass Spectrometry." *Clinical Proteomics* 13 (1):4. https://doi.org/10.1186/s12014-016-9104-2.

Smale, Georgeann, Nancy R. Nichols, Daniel R. Brady, Caleb E. Finch, and Walter E. Horton. 1995. "Evidence for Apoptotic Cell Death in Alzheimer's Disease." *Experimental Neurology* 133 (2):225–30. https://doi.org/10.1006/exnr.1995.1025.

Small, Scott A., Sabrina Simoes-Spassov, Richard Mayeux, and Gregory A. Petsko. 2017. "Endosomal Traffic Jams Represent a Pathogenic Hub and Therapeutic Target in Alzheimer's Disease." *Trends in Neurosciences* 40 (10):592–602. https://doi.org/10.1016/j.tins.2017.08.003.

Spellman, Daniel S., Kristin R. Wildsmith, Lee A. Honigberg, Marianne Tuefferd, David Baker, Nandini Raghavan, Angus C. Nairn, et al. 2015. "Development and Evaluation of a Multiplexed Mass Spectrometry Based Assay for Measuring Candidate Peptide Biomarkers in Alzheimer's Disease Neuroimaging Initiative (ADNI) CSF." *PROTEOMICS - Clinical Applications* 9 (7–8):715–31. https://doi.org/10.1002/prca.201400178.

Spinney, Laura. 2014. "Alzheimer's Disease: The Forgetting Gene." *Nature* 510 (7503):26–28. https://doi.org/10.1038/510026a.

Srinivasan, Rahul, Ben S Huang, Sharmila Venugopal, April D Johnston, Hua Chai, Hongkui Zeng, Peyman Golshani, and Baljit S Khakh. 2015. "Ca2+ Signaling in Astrocytes from Ip3r2−/− Mice in Brain Slices and during Startle Responses in Vivo." *Nature Neuroscience* 18 (5):708–17. https://doi.org/10.1038/nn.4001.

Staff, Mayo Clinic. 2018. "Alzheimer's Stages: How the Disease Progresses." Mayo Clinic E-Newsletter. 2018. https://www.mayoclinic.org/diseases-conditions/alzheimers-disease/in-depth/alzheimers-stages/art-20048448.

Stephen, T.-L., N. F. Higgs, D. F. Sheehan, S. Al Awabdh, G. Lopez-Domenech, I. L. Arancibia-Carcamo, and J. T. Kittler. 2015. "Miro1 Regulates Activity-Driven Positioning of Mitochondria within Astrocytic Processes Apposed to Synapses to Regulate Intracellular Calcium Signaling." *Journal of Neuroscience* 35 (48):15996–11. https://doi.org/10.1523/JNEUROSCI.2068-15.2015.

Strittmatter, Warren J, A. M. Saunders, Donald Schmechel, M. Pericak-Vance, J. Enghild, Guy S Salvesen, and Allen D Roses. 1993. "Apolipoprotein E: High-Avidity Binding to Beta-Amyloid and Increased Frequency of Type 4 Allele in Late-Onset Familial Alzheimer Disease." *Proceedings of the National Academy of Sciences* 90 (5):1977–81.

https://doi.org/10.1073/pnas.90.5.1977.

Suzuki, Junji, Kazunori Kanemaru, Kuniaki Ishii, Masamichi Ohkura, Yohei Okubo, and Masamitsu Iino. 2014. "Imaging Intraorganellar Ca2+ at Subcellular Resolution Using CEPIA." *Nature Communications* 5 (1):4153. https://doi.org/10.1038/ncomms5153.

Suzuki, S., K. Kiyosue, S. Hazama, A. Ogura, M. Kashihara, T. Hara, H. Koshimizu, and M. Kojima. 2007. "Brain-Derived Neurotrophic Factor Regulates Cholesterol Metabolism for Synapse Development." *Journal of Neuroscience* 27 (24):6417–27. https://doi.org/10.1523/JNEUROSCI.0690-07.2007.

Svennerholm, Lars, and Carl-Gerhard G Gottfries. 1994. "Membrane Lipids, Selectively Diminished in Alzheimer Brains, Suggest Synapse Loss as a Primary Event in Early-Onset Form (Type I) and Demyelination in Late-Onset Form (Type II)." *Journal of Neurochemistry* 62 (3):1039–47. https://doi.org/10.1046/j.1471-4159.1994.62031039.x.

Takano, T., X. Han, R. Deane, B. Zlokovic, and M. Nedergaard. 2007. "Two-Photon Imaging of Astrocytic Ca2+ Signaling and the Microvasculature in Experimental Mice Models of Alzheimer's Disease." *Annals of the New York Academy of Sciences* 1097 (1):40–50. https://doi.org/10.1196/annals.1379.004.

Takata, N., T. Mishima, C. Hisatsune, T. Nagai, E. Ebisui, K. Mikoshiba, and H. Hirase. 2011. "Astrocyte Calcium Signaling Transforms Cholinergic Modulation to Cortical Plasticity In Vivo." *Journal of Neuroscience* 31 (49):18155–65. https://doi.org/10.1523/JNEUROSCI.5289-11.2011.

Talwar, Puneet, Juhi Sinha, Sandeep Grover, Rachna Agarwal, Suman Kushwaha, M.V. V.Padma Srivastava, and Ritushree Kukreti. 2016. "Meta-Analysis of Apolipoprotein e Levels in the Cerebrospinal Fluid of Patients with Alzheimer's Disease." *Journal of the Neurological Sciences* 360 (January):179–87. https://doi.org/10.1016/j.jns.2015.12.004.

Tambini, Marc D, Marta Pera, Ellen Kanter, Hua Yang, Cristina Guardia-laguarta, David Holtzman, David Sulzer, Estela Area-gomez, and Eric A Schon. 2015. "ApoE 4 Upregulates the Activity of Mitochondria- Associated ER Membranes." *EMBO Reports* 17 (e201540614):1–10.

Tammineni, Prasad, Yu Young Jeong, Tuancheng Feng, Daniyal Aikal, and Qian Cai. 2017. "Impaired Axonal Retrograde Trafficking of the Retromer Complex Augments Lysosomal Deficits in Alzheimer's Disease Neurons." *Human Molecular Genetics* 26 (22):4352–66. https://doi.org/10.1093/hmg/ddx321.

Tan, Andrew R., Andrew Yi Cai, Samineh Deheshi, and Gordon L. Rintoul. 2011. "Elevated Intracellular Calcium Causes Distinct Mitochondrial Remodelling and Calcineurin-Dependent Fission in Astrocytes." *Cell Calcium* 49 (2):108–14. https://doi.org/10.1016/j.ceca.2010.12.002.

Theendakara, V., C. A. Peters-Libeu, P. Spilman, K. S. Poksay, D. E. Bredesen, and R. V. Rao.

2016. "Direct Transcriptional Effects of Apolipoprotein E." *Journal of Neuroscience* 36 (3):685–700. https://doi.org/10.1523/JNEUROSCI.3562-15.2016.

Tillman, Tommy S., and Michael Cascio. 2003. "Effects of Membrane Lipids on Ion Channel Structure and Function." *Cell Biochemistry and Biophysics*. https://doi.org/10.1385/CBB:38:2:161.

Tsuji-Akimoto, Sachiko, Ichiro Yabe, Masaaki Niino, Seiji Kikuchi, and Hidenao Sasaki. 2009. "Cystatin C in Cerebrospinal Fluid as a Biomarker of ALS." *Neuroscience Letters* 452 (1):52–55. https://doi.org/10.1016/j.neulet.2009.01.026.

Twig, Gilad, Alvaro Elorza, Anthony J.A. Molina, Hibo Mohamed, Jakob D Wikstrom, Gil Walzer, Linsey Stiles, et al. 2008. "Fission and Selective Fusion Govern Mitochondrial Segregation and Elimination by Autophagy." *EMBO Journal* 27 (2):433–46. https://doi.org/10.1038/sj.emboj.7601963.

Uchihara, Toshiki, Charles Duyckaerts, Yi He, Katsuji Kobayashi, Danielle Seilhean, Philippe Amouyel, and Jean Jacques Hauw. 1995. "ApoE Immunoreactivity and Microglial Cells in Alzheimer's Disease Brain." *Neuroscience Letters* 195 (1):5–8. https://doi.org/10.1016/0304-3940(95)11763-M.

Valla, Jon, Roy Yaari, Andrew B. Wolf, Yael Kusne, Thomas G. Beach, Alex E. Roher, Jason J. Corneveaux, Matthew J. Huentelman, Richard J. Caselli, and Eric M. Reiman. 2010. "Reduced Posterior Cingulate Mitochondrial Activity in Expired Young Adult Carriers of the APOE E4 Allele, the Major Late-Onset Alzheimer's Susceptibility Gene." *Journal of Alzheimer's Disease* 22 (1):307–13. https://doi.org/10.3233/JAD-2010-100129.

Vandesompele, Jo, Katleen De Preter, Filip Pattyn, Bruce Poppe, Nadine Van Roy, Anne De Paepe, and Frank Speleman. 2002. "Accurate Normalization of Real-Time Quantitative RT-PCR Data by Geometric Averaging of Multiple Internal Control Genes." *Genome Biology* 3 (7):RESEARCH0034. https://doi.org/10.1186/gb-2002-3-7-research0034.

Verghese, P. B., J. M. Castellano, K. Garai, Y. Wang, H. Jiang, A. Shah, G. Bu, C. Frieden, and D. M. Holtzman. 2013. "ApoE Influences Amyloid- (A) Clearance despite Minimal ApoE/A Association in Physiological Conditions." *Proceedings of the National Academy of Sciences* 110 (19):E1807–16. https://doi.org/10.1073/pnas.1220484110.

Verkhratsky, A., M. Matteoli, V. Parpura, J.-P. Mothet, and R. Zorec. 2016. "Astrocytes as Secretory Cells of the Central Nervous System: Idiosyncrasies of Vesicular Secretion." *The EMBO Journal* 35 (3):239–57. https://doi.org/10.15252/embj.201592705.

Verkhratsky, Alexei, and Maiken Nedergaard. 2018. "Physiology of Astroglia." *Physiological Reviews* 98 (1):239–389. https://doi.org/10.1152/physrev.00042.2016.

Verkhratsky, Alexei, and Vladimir Parpura. 2014. *Introduction to Neuroglia. Colloquium Series on Neuroglia in Biology and Medicine: From Physiology to Disease*. Vol. 1. https://doi.org/10.4199/C00102ED1V01Y201401NGL001.

Volterra, Andrea, Nicolas Liaudet, and Iaroslav Savtchouk. 2014. "Astrocyte Ca2+ Signalling: An

Unexpected Complexity." *Nature Reviews Neuroscience*. https://doi.org/10.1038/nrn3725.

Waagepetersen, Helle S., Gert H. Hansen, Kirsten Fenger, J. Gordon Lindsay, Gary Gibson, and Arne Schousboe. 2006. "Cellular Mitochondrial Heterogeneity in Cultured Astrocytes as Demonstrated by Immunogold Labeling of α-Ketoglutarate Dehydrogenase." *GLIA* 53 (2):225–31. https://doi.org/10.1002/glia.20276.

Wahrle, Suzanne E, Hong Jiang, Maia Parsadanian, Justin Legleiter, Xianlin Han, John D Fryer, Tomasz Kowalewski, and David M Holtzman. 2004. "ABCA1 Is Required for Normal Central Nervous System ApoE Levels and for Lipidation of Astrocyte-Secreted ApoE." *Journal of Biological Chemistry* 279 (39):40987–93. https://doi.org/10.1074/jbc.M407963200.

Wang, Chengzhong, Ramsey Najm, Qin Xu, Dah Eun Jeong, David Walker, Maureen E. Balestra, Seo Yeon Yoon, et al. 2018. "Gain of Toxic Apolipoprotein E4 Effects in Human IPSC-Derived Neurons Is Ameliorated by a Small-Molecule Structure Corrector Article." *Nature Medicine* 24 (5):647–57. https://doi.org/10.1038/s41591-018-0004-z.

Wang, J., S. Xiong, C. Xie, W. R. Markesbery, and M. A. Lovell. 2005. "Increased Oxidative Damage in Nuclear and Mitochondrial DNA in Alzheimer's Disease." *Journal of Neurochemistry* 93 (4):953–62. https://doi.org/10.1111/j.1471-4159.2005.03053.x.

Wang, X., B. Su, H.-g. Lee, X. Li, G. Perry, M. A. Smith, and X. Zhu. 2009. "Impaired Balance of Mitochondrial Fission and Fusion in Alzheimer's Disease." *Journal of Neuroscience* 29 (28):9090–9103. https://doi.org/10.1523/JNEUROSCI.1357-09.2009.

Wang, X., B. Su, S. L. Siedlak, P. I. Moreira, H. Fujioka, Y. Wang, G. Casadesus, and X. Zhu. 2008. "Amyloid- Overproduction Causes Abnormal Mitochondrial Dynamics via Differential Modulation of Mitochondrial Fission/Fusion Proteins." *Proceedings of the National Academy of Sciences* 105 (49):19318–23. https://doi.org/10.1073/pnas.0804871105.

Wang, Yipeng, Marta Martinez-Vicente, Ulrike Krüger, Susmita Kaushik, Esther Wong, Eva Maria Mandelkow, Ana Maria Cuervo, and Eckhard Mandelkow. 2009. "Tau Fragmentation, Aggregation and Clearance: The Dual Role of Lysosomal Processing." *Human Molecular Genetics* 18 (21):4153–70. https://doi.org/10.1093/hmg/ddp367.

Ward, Carl, Nuria Martinez-Lopez, Elsje G. Otten, Bernadette Carroll, Dorothea Maetzel, Rajat Singh, Sovan Sarkar, and Viktor I. Korolchuk. 2016. "Autophagy, Lipophagy and Lysosomal Lipid Storage Disorders." *Biochimica et Biophysica Acta - Molecular and Cell Biology of Lipids*. https://doi.org/10.1016/j.bbalip.2016.01.006.

Whyte, Lauren S., Adeline A. Lau, Kim M. Hemsley, John J. Hopwood, and Timothy J. Sargeant. 2017. "Endo-Lysosomal and Autophagic Dysfunction: A Driving Factor in Alzheimer's Disease?" *Journal of Neurochemistry*. https://doi.org/10.1111/jnc.13935.

Wijte, Dorien, Liam A. McDonnell, Crina I.A. Balog, Koen Bossers, André M. Deelder, Dick F. Swaab, Joost Verhaagen, and Oleg A. Mayboroda. 2012. "A Novel Peptidomics Approach to Detect Markers of Alzheimer's Disease in Cerebrospinal Fluid." *Methods* 56 (4):500–507. https://doi.org/10.1016/j.ymeth.2012.03.018.

Wildsmith, Kristin R, Stephen P Schauer, Ashley M Smith, David Arnott, Yuda Zhu, Joshua Haznedar, Surinder Kaur, W Mathews, and Lee A Honigberg. 2014. "Identification of Longitudinally Dynamic Biomarkers in Alzheimer's Disease Cerebrospinal Fluid by Targeted Proteomics." *Molecular Neurodegeneration* 9 (1):22. https://doi.org/10.1186/1750-1326-9-22.

Xiong, Jian, and Michael X. Zhu. 2016. "Regulation of Lysosomal Ion Homeostasis by Channels and Transporters." *Science China Life Sciences*. https://doi.org/10.1007/s11427-016-5090-x.

Xu, Qin, Aubrey Bernardo, David Walker, Tiffany Kanegawa, Robert W Mahley, and Yadong Huang. 2006. "Profile and Regulation of Apolipoprotein E (ApoE) Expression in the CNS in Mice with Targeting of Green Fluorescent Protein Gene to the ApoE Locus" 26 (19):4985–94. https://doi.org/10.1523/JNEUROSCI.5476-05.2006.

Yamazaki, Yu, Meghan M Painter, Guojun Bu, and Takahisa Kanekiyo. 2016. "Apolipoprotein E as a Therapeutic Target in Alzheimer's Disease: A Review of Basic Research and Clinical Evidence." *CNS Drugs* 30 (9):773–89. https://doi.org/10.1007/s40263-016-0361-4.

Ye, Xuan, Xiaqin Sun, Valentin Starovoytov, and Qian Cai. 2015. "Parkin-Mediated Mitophagy in Mutant HAPP Neurons and Alzheimer's Disease Patient Brains." *Human Molecular Genetics* 24 (10):2938–51. https://doi.org/10.1093/hmg/ddv056.

Yeh, Chia-Yu, Bhamini Vadhwana, Alexei Verkhratsky, and José J Rodríguez. 2011. "Early Astrocytic Atrophy in the Entorhinal Cortex of a Triple Transgenic Animal Model of Alzheimer's Disease." *ASN Neuro* 3 (5):AN20110025. https://doi.org/10.1042/AN20110025.

Youmans, Katherine L, Leon M Tai, Evelyn Nwabuisi-Heath, Lisa Jungbauer, Takahisa Kanekiyo, Ming Gan, Jungsu Kim, et al. 2012. "APOE4-Specific Changes in Aβ Accumulation in a New Transgenic Mouse Model of Alzheimer Disease." *Journal of Biological Chemistry* 287 (50):41774–86. https://doi.org/10.1074/jbc.M112.407957.

Yu, Chunjiang, Katherine L. Youmans, and Mary J. LaDu. 2010. "Proposed Mechanism for Lipoprotein Remodelling in the Brain." *Biochimica et Biophysica Acta - Molecular and Cell Biology of Lipids*. https://doi.org/10.1016/j.bbalip.2010.05.001.

Yu, W. H., A. Kumar, C. Peterhoff, L. Shapiro Kulnane, Y. Uchiyama, B. T. Lamb, A. M. Cuervo, and R. A. Nixon. 2004. "Autophagic Vacuoles Are Enriched in Amyloid Precursor Protein-Secretase Activities: Implications for β-Amyloid Peptide over-Production and Localization in Alzheimer's Disease." *International Journal of Biochemistry and Cell Biology* 36 (12):2531–40. https://doi.org/10.1016/j.biocel.2004.05.010.

Zare-Shahabadi, Ameneh, Eliezer Masliah, Gail V.W. Johnson, and Nima Rezaei. 2015. "Autophagy in Alzheimer's Disease." *Reviews in the Neurosciences* 26 (4):385–95. https://doi.org/10.1515/revneuro-2014-0076.

Zbidi, Hanene, Isaac Jardin, Geoffrey E. Woodard, Jose J. Lopez, Alejandro Berna-Erro, Ginés M. Salido, and Juan A. Rosado. 2011. "STIM1 and STIM2 Are Located in the Acidic Ca2+ Stores and Associates with Orai1 upon Depletion of the Acidic Stores in Human Platelets."

Journal of Biological Chemistry 286 (14):12257–70. https://doi.org/10.1074/jbc.M110.190694.

Zetterberg, Henrik. 2017. "ALZBIOMARKER." Alzforum. 2017. https://www.alzforum.org/alzbiomarker.

Zhang, Liang, Sergey Trushin, Trace A. Christensen, Benjamin V. Bachmeier, Benjamin Gateno, Andreas Schroeder, Jia Yao, et al. 2016. "Altered Brain Energetics Induces Mitochondrial Fission Arrest in Alzheimer's Disease." *Scientific Reports* 6 (January). Nature Publishing Group:1–12. https://doi.org/10.1038/srep18725.

Zhang, Qiang, Yasushi Tamura, Madhuparna Roy, Yoshihiro Adachi, Miho Iijima, and Hiromi Sesaki. 2014. "Biosynthesis and Roles of Phospholipids in Mitochondrial Fusion, Division and Mitophagy." *Cellular and Molecular Life Sciences* 71 (19):3767–78. https://doi.org/10.1007/s00018-014-1648-6.

Zhang, Ye, Steven A. Sloan, Laura E. Clarke, Christine Caneda, Colton A. Plaza, Paul D. Blumenthal, Hannes Vogel, et al. 2016. "Purification and Characterization of Progenitor and Mature Human Astrocytes Reveals Transcriptional and Functional Differences with Mouse." *Neuron* 89 (1):37–53. https://doi.org/10.1016/j.neuron.2015.11.013.

Zhang, Zhijun, Gang Chen, Wei Zhou, Aihong Song, Tao Xu, Qingming Luo, Wei Wang, Xiao Song Gu, and Shumin Duan. 2007. "Regulated ATP Release from Astrocytes through Lysosome Exocytosis." *Nature Cell Biology* 9 (8):945–53. https://doi.org/10.1038/ncb1620.

Zhao, Jing, Mary D. Davis, Yuka A. Martens, Mitsuru Shinohara, Neill R. Graff-Radford, Steven G. Younkin, Zbigniew K. Wszolek, Takahisa Kanekiyo, and Guojun Bu. 2017. "APOE E4/E4 Diminishes Neurotrophic Function of Human IPSC-Derived Astrocytes." *Human Molecular Genetics* 26 (14):2690–2700. https://doi.org/10.1093/hmg/ddx155.

Zhao, Jing, Yuan Fu, Chia Chen Liu, Mitsuru Shinohara, Henrietta M. Nielsen, Qiang Dong, Takahisa Kanekiyo, and Guojun Bu. 2014. "Retinoic Acid Isomers Facilitate Apolipoprotein e Production and Lipidation in Astrocytes through the Retinoid X Receptor/Retinoic Acid Receptor Pathway." *Journal of Biological Chemistry* 289 (16):11282–92. https://doi.org/10.1074/jbc.M113.526095.

Zhong, Ning, Gayathri Ramaswamy, and Karl H. Weisgraber. 2009. "Apolipoprotein E4 Domain Interaction Induces Endoplasmic Reticulum Stress and Impairs Astrocyte Function." *Journal of Biological Chemistry* 284 (40):27273–80. https://doi.org/10.1074/jbc.M109.014464.

Zhong, Ning, and Karl H. Weisgraber. 2009. "Understanding the Association of Apolipoprotein E4 with Alzheimer Disease: Clues from Its Structure." *Journal of Biological Chemistry*. https://doi.org/10.1074/jbc.R800009200.

Zhong, Xi Zoë, Yiming Yang, Xue Sun, and Xian-Ping Dong. 2017. "Methods for Monitoring Ca 2+ and Ion Channels in the Lysosome." *Cell Calcium* 64 (June):20–28. https://doi.org/10.1016/j.ceca.2016.12.001.

Zhu, Xiongwei, George Perry, Mark A. Smith, and Xinglong Wang. 2013. "Abnormal Mitochondrial Dynamics in the Pathogenesis of Alzheimer's Disease." Edited by George

Perry, Xiongwei Zhu, Mark A. Smith, Aaron Sorensen, and Jesús Avila. *Journal of Alzheimer's Disease : JAD* 33 Suppl 1 (s1):S253-62. https://doi.org/10.3233/JAD-2012-129005.